



City Research Online

City, University of London Institutional Repository

Citation: Takanobu, T (2021). Non-Hermitian Quantum Field Theory. (Unpublished Doctoral thesis, City, University of London)

This is the accepted version of the paper.

This version of the publication may differ from the final published version.

Permanent repository link: <https://openaccess.city.ac.uk/id/eprint/27412/>

Link to published version:

Copyright: City Research Online aims to make research outputs of City, University of London available to a wider audience. Copyright and Moral Rights remain with the author(s) and/or copyright holders. URLs from City Research Online may be freely distributed and linked to.

Reuse: Copies of full items can be used for personal research or study, educational, or not-for-profit purposes without prior permission or charge. Provided that the authors, title and full bibliographic details are credited, a hyperlink and/or URL is given for the original metadata page and the content is not changed in any way.

Non-Hermitian Quantum Field Theory

Takanobu Taira

Qualification for Doctor of Philosophy



CITY UNIVERSITY
LONDON

City, University of London
Department of Mathematics

September 2021

Contents

Contents	iii
List of Figures	vii
List of Tables	xi
Acknowledgements	xiii
Declaration	xv
Abstract	xvii
1 Introduction	1
1.1 The History of non-Hermitian Physics	1
1.1.1 Early use of non-Hermitian Hamiltonian in physics	2
1.1.2 Development of the modified inner product	4
1.1.3 Modern development of non-Hermitian physics	6
1.2 The Development of non-Hermitian Quantum Field Theory	9
1.3 Outline	10
2 Spontaneous symmetry breaking of non-Hermitian quantum field theories and breakdown of Higgs mechanism	13
2.1 The implication of spontaneous symmetry breaking in particle physics	13
2.1.1 Goldstone theorem	13
2.1.2 Higgs mechanism	17
2.1.3 Summary	19
2.2 Pseudo-Hermitian approach to spontaneously broken symmetries . .	19
2.2.1 Summary	25
2.3 Spontaneous symmetry breaking of a global Abelian group	25

2.3.1	A non-Hermitian model with n complex scalar fields	26
2.3.2	\mathcal{PT} symmetric and broken regimes	28
2.3.3	Relating field theoretic \mathcal{CPT} operator to quantum mechanical \mathcal{PT} operators	39
2.3.4	Goldstone bosons in \mathcal{CPT} -symmetric and broken regimes . .	43
2.3.5	Summary	48
2.4	Spontaneous symmetry breaking of global non-Abelian group	48
2.4.1	A \mathcal{CPT} -symmetric non-Hermitian model with global $SU(2)$ - symmetry	49
2.4.2	Physical regions	53
2.4.3	Goldstone bosons in \mathcal{CPT} symmetric and \mathcal{CPT} broken regimes	57
2.4.4	Summary	60
2.5	Spontaneous symmetry breaking of local non-Abelian group	60
2.5.1	A $SU(2)$ -model in the fundamental representation	61
2.5.2	A $SU(2)$ -symmetric model in the adjoint representation . . .	71
2.5.3	Summary	79

3 Complex topological soliton solutions with real energies in non-Hermitian quantum field theories **81**

3.1	Reality of the complex soliton solutions	81
3.2	Topological Solitons in particle physics	82
3.2.1	Soliton solution in a Hermitian model with $SU(2)$ gauge sym- metry	83
3.2.2	Soliton solution in a non-Hermitian model with $SU(2)$ gauge symmetry	87
3.2.3	The energy bound	90
3.2.4	The fourfold BPS scaling limit	92
3.2.5	Real and complex monopole solutions with real energies . . .	95
3.2.6	Summary	101
3.3	Topological solitons in $1 + 1$ dimensions	102
3.3.1	BPS solitons from self-duality and anti-self-duality	102
3.3.2	A non-Hermitian BPS theory with super-exponential kink so- lutions	105
3.3.3	A non-Hermitian coupled sine-Gordon model	110

3.3.4	Complex extended sine-Gordon model and its Hermitian partner	115
3.3.5	Summary	117
3.4	Topological solitons in nuclear physics	117
3.4.1	The Skyrme model - extensions and restrictions	118
3.4.2	Pseudo Hermitian variants of Skyrme models	120
3.4.3	Skyrme model with semi-kink and massless solutions	130
3.4.4	Skyrme model with a Bender-Boettcher type potential	132
3.4.5	Skyrme model with complex trigonometric potentials	135
3.4.6	A new Skyrme submodel with complex BPS solutions and real energy	137
3.4.7	Summary	139
4	Conclusion	141
A	The topology of the monopole solutions and Derrick's scaling ar- gument	143
A.1	Derrick's scaling argument	143
A.2	The topology of the monopole solutions	146
A.2.1	Deriving equation (3.15)	146
A.2.2	Deriving equation (3.14) from (3.13)	148
B	Type I (standard) versus type II (zero) exceptional points	153
C	General interaction term	157
D	Similarity transformation of gauge field theories	161
	Bibliography	165

List of Figures

1.1	Energy spectrum of the Hamiltonian $H = p^2 - (ix)^N$ plotted for the real parameter N , taken from [1].	7
1.2	Plot of eigenvalues $\lambda_{\pm} = \pm\sqrt{1 - z^2}$. The solid and dotted lines represents real and imaginary part.	8
2.1	Eigenvalues λ of M_1^2 as a function of ν for $c_1 = c_2 = -c_3 = 1$, at the special point $\mu = \mu_s$ and imaginary part of the special point $\text{Im}(\mu_s)$. The physical regions are bounded by vertical lines, $5/13^{1/4} < \nu^2 < 135/2\sqrt{26}$	35
2.2	Nonvanishing eigenvalues λ_i of M_2^2 as a functions of ν for $c_1 = c_2 = c_3 = 1$, $m_1 = 1$, $m_2 = 1/2$ and $m_3 = 1/5$. In the left panel we choose $\mu = 1.7$ observing that there is no physical region for which all eigenvalues are non-negative. In the right panel we choose $\mu = 3$ and have two physical regions for $\nu \in (-0.64468, -0.54490)$ and $\nu \in (0.54490, 0.64468)$	38
2.3	Nonvanishing eigenvalues λ_i of M_2^2 as a function of ν for $c_1 = -c_2 = c_3 = 1$, $m_1 = 1$, $m_2 = 1/2, m_3 = 1/5$ and $\mu = 1.7$. Singularities occur at $\nu = \nu_{\text{sing}}^{\pm} \approx \pm 0.31623$. The regimes $\nu \in (-0.50608, \nu_{\text{sing}}^-)$, $\nu \in (\nu_{\text{sing}}^+, 0.50608)$ are physical.	38
2.4	Physical regions (in orange) in parameter space bounded by exceptional and zero exceptional points as function of $(\mu^4/m_1^4, m_2^2/m_1^2)$ for the theory expanded around the SU(2)-symmetry breaking vacuum. Left panel for $c_1 = -c_2 = 1$ and right panel for $c_1 = -c_2 = -1$	56
2.5	Physical regions (in orange, blue and green) in parameter space bounded by exceptional and zero exceptional points as function of $(\mu^4/m_1^4, m_2^2/m_1^2)$ for the theory expanded around the SU(2)-symmetry invariant vacuum.	57

2.6	Regions, for which the gauge vector boson is massive (blue with mesh) versus physical regions (orange) in which the would be Goldstone boson can be identified, bounded by exceptional and zero exceptional points as texttion of $(\mu^4/m_1^4, m_2^2/m_1^2)$ for the theory expanded around the SU(2)-symmetry breaking vacuum. Left panel for $c_1 = -c_2 = 1$ and right panel for $c_1 = -c_2 = -1$. The coupling constant g must be positive.	67
3.1	Monopole, gauge and Higgs masses plotted for $m_1^2/g = -0.44, \mu/g = -0.14, e = 2, c_1 = -c_2 = -1$. The solid line represent the real part and dotted line represent the imaginary part of the masses. The dotted vertical lines indicate the boundaries of the physical regions where all the masses acquire real positive values.	97
3.2	Monopole and gauge masses plotted for $X = 1, Y = 0.8, e = 2, c_1 = -c_2 = 1$. The solid line represent the real part and dotted line represent the imaginary part of the masses.	98
3.3	Both panels are plotted for $X = 1, Y = 0.8, n = 1, e = 2$. The solid line represent the real part and dotted line represent the imaginary part of the masses. Panel (a) shows the monopole and gauge masses against $Z \geq 0$, with vertical lines indicating the location of the boundaries of three regions. The panel (b) shows three profile function $h_1(r)$ defined on each regions indicated in panel (a).	98
3.4	Both panels are plotted for $X = 1, Y = 1, n = 1, e = 2$. The solid line represent the real part and dotted line represent the imaginary part of the masses.	99
3.5	Both panels are plotted for $X = 1, Y = 1, n = 1, e = 2$. The solid line represent the real part and dotted line represent the imaginary part of the masses.	99
3.6	Both panels are plotted for $X = 1, Y = 1, n = 1, e = 2$. The solid line represent the real part and dotted line represent the imaginary part of the masses.	101

3.7	Complex BPS kink and antikink solutions of the two pairs of coupled BPS equations (3.73) and (3.74) associated to the potential (3.72) with initial values $\phi_1^{k+}(0) = \phi_2^{k+}(0) = \phi_1^{a-}(0) = \phi_2^{a-}(0) = -1/e$ and $\phi_1^{a+}(0) = \phi_2^{a+}(0) = \phi_1^{k-}(0) = \phi_2^{k-}(0) = 1/e$ for $\mu_1 = 0.2$, $\mu_2 = 0.1$, $\lambda = 0.1$	108
3.8	Real part of the potential $\mathcal{V}(\phi_1, \phi_2)$ in (3.72) as a function of $\text{Re}\phi_1$ and $\text{Re}\phi_2$ with the gradient flow of the real parts of F^+ superimposed in white. The kink-kink, kink-antikink, antikink-kink and antikink-antikink interpolate between the different types of stable and unstable vacua as specified in (3.85)	109
3.9	Complex BPS kink and antikink solutions of the pair of BPS equations (3.88) and (3.89) with initial values $\phi_1^{k+}(0) = \phi_2^{k+}(0) = \phi_2^{k-}(0) = \phi_1^{a-}(0) = \pi/2$ and $\phi_1^{a+}(0) = \phi_2^{a+}(0) = \phi_1^{k-}(0) = \phi_2^{a-}(0) = -\pi/2$ for $\lambda = 3$, $\mu = 0.5$	112
3.10	Real part of the potential $\mathcal{V}(\phi_1, \phi_2)$ as a function of $\text{Re}\phi_1$ and $\text{Re}\phi_2$ with the gradient flow of the real parts of G^+ superimposed in white. The kink solutions $\phi_1^{k+}(x)$, $\phi_2^{k+}(x)$ interpolate between the vacua $v_1^{(0,0)}$ and $v_2^{(0,1)}$ (red dots) as indicated by the red solid trajectory.	114
3.11	The $\tilde{\zeta}$ -part of the solutions of the BPS equation (3.140) for different scenarios with $n = \tilde{\lambda} = 1$, $\mu = 3/2$ and different choices for c . The different relative orderings are: panel (a) $r_\pi \leq 0 \leq r_0$ with $c = 1/2$, panel (b) $0 \leq r_\pi \leq r_0$ with $c = -1/2$, panel (c) $r_0 \leq 0 \leq r_\pi$ with $c = 1/2$ and panel (d) $0 \leq r_0 \leq r_\pi$ with $c = 7/2$. Real parts correspond to solid lines and imaginary parts to dotted ones.	124
3.12	The BPS solution $\tilde{\zeta}_{\text{BPS}}$ with $n = 1$, $c = 1/2$, $\tilde{\mu} = 3/2$, $\tilde{\lambda} = 1$, the step solution $\tilde{\zeta}_{\text{St}}$ with $n = 1$, $-c = 1/2$, $\tilde{\mu} = 3/2$, $\tilde{\lambda} = 1$, the cusp solution $\tilde{\zeta}_{\text{Cusp}}$ with $n = 1$, $c = 3/2$, $\tilde{\mu} = 3/2$, $\tilde{\lambda} = 1$, the shell solution $\tilde{\zeta}_{\text{Shell}}$ with $n = 1$, $c = 11/2$, $\tilde{\mu} = 3/2$, $\tilde{\lambda} = 1$ and the purely imaginary solution $\tilde{\zeta}_{\text{IBPS}}$ with $n = 1$, $c = 11/2$, $\tilde{\mu} = 3/2$, $\tilde{\lambda} = 1$	125
3.13	Different types of solutions to the equations of motion as defined in (3.144) - (3.143) with parameters $n = \tilde{\lambda} = 1$, $\tilde{\mu} = 3/2$ and $c = 1/2$ in panel (a), $c = -1/2$ in panel (b), $c = 3/2$ in panel (c), $c = 11/2$ in panel (d).	126

3.14	Panel (a): Purely imaginary and real compacton and semi-kink solutions (3.159) resulting from the potential $V_{SK}(\zeta)$ with parameter choices $n = \lambda = 1$, $\mu = 2$ and $c = \pm 1$ for $\gamma = \mp 1$. Panel (b): Complex solutions with zero energy resulting from the potential $V_{m0}(\zeta)$ with parameter choices $n = \lambda = 10$, $\mu = 2$ and $c = \pm 25.15$ for $\gamma = \mp 1$. Real parts correspond to solid lines and imaginary parts to dotted ones.	131
3.15	BPS solutions $\zeta_m^\pm(r)$ for a Skyrme model with a Bender-Boettcher type potential for the parameter choices $\lambda = 1$, $\mu = 2$, $n = 1$. In panels (a), (b) we have taken $c = -2$ and in panels (c), (d) we have $c = 0.2$.	133
3.16	Real energies E_{BB}^\pm of the compacton (panel a) and unbounded (panel b) BPS solutions for the cases (3.168) - (3.170) with $\lambda = 1$, $\mu = 2$, $n = 1$ and $c = 0.2$ for several values of ℓ, m .	134
3.17	Complex BPS solutions $\zeta_-^{(0)}$ for different values of n and the initial condition c for $\mathcal{L}_-^{(2)}$. Real parts as solid and imaginary parts as dotted lines.	139

List of Tables

2.1	Flow diagram showing the general procedure of pseudo-Hermitian approach	25
-----	---	----

Acknowledgements

I am eternally thankful to my supervisor Professor Andreas Fring for all his guidance and wisdom in academics and life. His interest and passion for mathematics and physics have inspired me at every 140 meetings (excluding the extra ones). Even during a mentally challenging time caused by the national lockdown, I have managed to keep my sanity with the weekly non-academic meeting.

I would also like to thank all the friends I made during this degree. Many insightful discussions with creative and knowledgeable friends has inspired me to work harder and enjoy student life.

Finally, I wish to thank my family for their spiritual and financial support sincerely. I am grateful for their unconditional love and faith towards me, and I am enormously indebted both spiritually and financially.

Declaration

I declare that this thesis has been composed solely by myself and that it has not been submitted, in whole or in part, in any previous application for a degree. Except where stated otherwise by reference or acknowledgement, the work presented is entirely my own.

Abstract

The general aim of this thesis is to investigate how some well-known features of Hermitian quantum field theory extend to a non-Hermitian setting. We analyse many different versions of bosonic field theories, where some of them have application to particle physics (standard model) and nuclear physics (Skyrme model). We establish the validity of the Goldstone theorem [2] and Englert-Brout-Higgs-Guralnik-Hagen-Kibble mechanism [3, 4, 5, 6] for the complex scalar field theory with global $U(1)$, global $SU(2)$ and local $U(1)$ symmetry with anti-linear \mathcal{CPT} symmetry [7, 8, 9], in the bounded region of the parameter space. Both are shown to hold in the \mathcal{CPT} symmetric regime, but need to be treated differently or even break down at the boundaries of these regions in parameter space, that is at different types of exceptional points corresponding to the algebraic singularity of the particle masses. Some particular type of these singularities were not previously found in the literature.

We also analyse particular non-trivial solutions of the equations of motion, including t'Hooft-Polyakov monopoles [10], kink and BPS solutions [11] and BPS Skyrmions [12]. We show that some of the solutions are complex and yet, possess finite real energy. Drawing an analogy from the non-Hermitian quantum mechanics, we develop a reality constraint on the solutions and show that the Hamiltonian and pair of solutions needs to satisfy symmetry relation simultaneously to realise the real energy. We also show for the first time, the complex t'Hooft-Polyakov monopole solution with real energy which vanishes at the exceptional point of the Higgs particles.

Chapter 1

Introduction

1.1 The History of non-Hermitian Physics

Quantum mechanics is a celebrated branch of physics that is a fundamental part of modern physics. The contemporary formulation of quantum mechanics in a closed system is based on four axioms which can be traced back to the mathematical formulation of quantum mechanics, proposed by Paul Dirac [13] in 1930 and John von Neumann [14] in 1932. Below we present the axioms of quantum mechanics generally found in standard quantum mechanics textbooks.

- (State): The quantum system is characterised by the state vector $|v\rangle$, element of the Hilbert space \mathbb{H} .
- (Observable): The physical observables such as energy, position, momentum, etc., can be represented as a self-adjoint operator acting on a Hilbert space $A : \mathbb{H} \rightarrow \mathbb{H}$. The operator A is said to be self-adjoint if

$$\langle v|Av\rangle = \langle A^\dagger v|v\rangle, \quad \forall |v\rangle \in \mathbb{H}. \quad (1.1)$$

- (Measurement): Consider an observable A with eigenvector $A|a\rangle = a|a\rangle$, where $a \in \mathbb{C}$. The probability of finding a as the result of the measurement of A in a system with state vector $|v\rangle$ is given by

$$p_v(a) = |\langle a|v\rangle|^2. \quad (1.2)$$

- (Time evolution): The time evolution of the state vector defined at a specific

time $|v(t)\rangle$ to $|v(0)\rangle$ is governed by a unitary operator

$$|v(t)\rangle = U(t, 0) |v(0)\rangle. \quad (1.3)$$

These axioms have slowly developed into their current form through the discoveries of black body radiation, the Compton effect, Planck's radiation law, etc. Therefore, without any historical context, the above axioms may seem unmotivated and unnatural. Similarly, the development of non-Hermitian physics seems unmotivated and unnatural without any historical context.

Below we attempt to give a chronological story of the non-Hermitian physics, highlighting a few notable publications that have changed the general perception and landscape of the field. Note that the summary below is not a complete representation of the history of non-Hermitian physics but a gentle introduction.

Before we proceed, let us clarify the definition of Hermiticity. The notation often used to denote the *Hermitian conjugated* operator is with the superscript \dagger on the operator A^\dagger , which is defined with the Dirac inner product

$$\langle v|Aw\rangle = \langle A^\dagger v|w\rangle, \quad |v\rangle, |w\rangle \in \mathbb{H}. \quad (1.4)$$

If an operator satisfies $\langle v|Aw\rangle = \langle v|A^\dagger w\rangle$, then it is said to be *symmetric*. We define the Hermitian operator as a *bounded symmetric operator, densely defined on the Hilbert space*. This definition is similar to the self-adjointness where the operator is *symmetric and domain of operator and its Hermitian conjugate coincide*. The ambiguity of the domain of the operator is not the main concern of this thesis. Therefore we will simply assume all operators to be bounded and densely defined on the Hilbert space unless otherwise stated.

1.1.1 Early use of non-Hermitian Hamiltonian in physics

Although it is after 1998, by the publication of [1], a certain type of non-Hermitian Hamiltonian gained popularity, non-Hermitian systems have been around in physics for a long time. Complex Hamiltonian were used in the dissipative systems as far back as 1928 [15, 16, 17], where the imaginary part of the Hamiltonian determines the width of the resonance state. In general, a resonance state is a wave function/state or solution of the Schrödinger equation with complex eigenvalues, describing particles

with finite lifetime. However, the \mathcal{PT} -symmetric and/or pseudo/quasi Hermitian Hamiltonians and the complex Hamiltonians describing dissipative systems differ fundamentally as the standard inner product is no longer positive definite for resonance states (see [18] for an alternative inner product which is positive definite for resonance state). To construct a well-defined closed non-Hermitian quantum mechanical Hamiltonian is difficult, but the reality of its spectrum was shown by Eugene Wigner in 1960 [19], which follows from the anti-linear symmetry. The operator A and the state vector $|v\rangle$ is said to *symmetric under anti-linear transformation* $\mathcal{PT} : \mathbb{H} \rightarrow \mathbb{H}$ if the operator commute with the $[A, \mathcal{PT}] = 0$ and $\mathcal{PT} |v\rangle = |v\rangle$. The anti-linear transformation is a linear transformation which complex conjugate the coefficients.

$$\mathcal{PT}(\alpha |v\rangle + \beta |w\rangle) = \alpha^* \mathcal{PT} |v\rangle + \beta^* \mathcal{PT} |w\rangle, \quad \alpha, \beta \in \mathbb{C}, \quad |v\rangle, |w\rangle \in \mathbb{H}. \quad (1.5)$$

If one assumes that the Hamiltonian is symmetric under some anti-linear symmetry \mathcal{PT} , $[H, \mathcal{PT}] = 0$ and its eigenvectors are also symmetric up to some phase $\mathcal{PT} |v_i\rangle = e^{i\theta_i} |v_i\rangle$ for $|v_i\rangle \in \mathbb{H}, \theta_i \in \mathbb{R}$ for all i . Then by following simple argument, the eigenspectrum of H is guaranteed to be real.

$$\begin{aligned} \mathcal{PT}H |v_i\rangle &= \mathcal{PT}\lambda_i |v_i\rangle = \lambda_i^* \mathcal{PT} |v_i\rangle = \lambda_i^* e^{i\theta_i} |v_i\rangle, \\ \mathcal{PT}H |v_i\rangle &= H\mathcal{PT} |v_i\rangle = H e^{i\theta_i} |v_i\rangle = \lambda_i e^{i\theta_i} |v_i\rangle. \end{aligned}$$

Although the above argument is valid for any anti-linear symmetry, the most famous example of this symmetry is the \mathcal{PT} -symmetry popularised by [1]. The theory where both Hamiltonian and its eigenvectors are \mathcal{PT} -symmetric is called the *\mathcal{PT} -symmetric theory*. The theory where only the Hamiltonian is \mathcal{PT} symmetric is said to have *spontaneously broken \mathcal{PT} -symmetry*. In this case, pair of eigenvalues can coalesces at an algebraic singularity of the eigenvalue called the *exceptional point* (see figure 1.1), beyond which the pair of eigenvalues become complex conjugate pairs (see figure 1.2). If both Hamiltonian and eigenvectors are not \mathcal{PT} -symmetric, then the theory is said to have an explicitly broken \mathcal{PT} -symmetry.

1.1.2 Development of the modified inner product

The modern way of the well-defined closed non-Hermitian quantum mechanics was first realised by Frederik Scholtz, Hendrik Geyer, and Fritz Hahne in 1992, [20]. The authors used the mathematical condition on the operator called the *quasi-Hermiticity* introduced in [21] to define the positive definite inner product. The definition of the quasi-Hermiticity is given as a condition on the bounded linear operator of the Hilbert space $A : \mathbb{H} \rightarrow \mathbb{H}$ which satisfies

- (i) $\langle v|\rho v\rangle > 0$ for all $|v\rangle \in \mathbb{H}$ and $|v\rangle \neq 0$.
- (ii) $\rho A = A^\dagger \rho$.

Where the bounded Hermitian linear operator $\rho : \mathbb{H} \rightarrow \mathbb{H}$, is often called the metric operator because the inner product defined by the operator $\langle \cdot | \cdot \rangle_\rho := \langle \cdot | \rho \cdot \rangle$, restores the Hermiticity of the operator. This result can be shown by using the condition(ii)

$$\langle v|Aw\rangle_\rho \equiv \langle v|\rho Aw\rangle = \langle v|A^\dagger \rho w\rangle = \langle Av|\rho w\rangle = \langle Av|w\rangle_\rho, \quad \forall |v\rangle, |w\rangle \in \mathbb{H}. \quad (1.6)$$

Note that the quasi-Hermiticity alone does not guarantee the real energy spectrum of the operator A (which includes the Hamiltonian). In fact, one requires two extra conditions.

- (iii) The metric operator is invertible.
- (iv) $\rho = \eta^\dagger \eta$.

The operator which satisfies only conditions (ii) and (iv) is refer to as the *pseudo-Hermitian* operator, which was first introduced in [22]. These extra conditions were considered in [20] to prove that, given a set of pseudo-Hermitian operators $\mathcal{A} = \{A_i\}$, the metric operator $\rho_{\mathcal{A}}$ which satisfies conditions (i), (ii), (iii) and (iv) for all operators of set \mathcal{A} is uniquely determined if and only if all operators of the set \mathcal{A} are irreducible on the Hilbert space \mathbb{H} . Furthermore, one can choose to restrict the number of operators $\mathcal{B} \subset \mathcal{A}$, satisfying the conditions (i) to (iv) with respect to the metric $\rho_{\mathcal{B}}$ to simplify the calculation of the metric operator. If all the operators of a subset \mathcal{B} are irreducible on the whole Hilbert space, then the new metric is proportional to the original metric $\rho_{\mathcal{B}} \propto \rho_{\mathcal{A}}$. Suppose some of the operators of a subset \mathcal{B} are reducible. In that case, the physical Hilbert space is a subset $\mathbb{H}_{\mathcal{B}} \subset \mathbb{H}$ where all the operators of \mathcal{B} are irreducible. This procedure is

analogous to the Dyson mapping first introduced by Freeman Dyson [23] used in the study of nuclear reaction [24, 25, 26], which maps the non-Hermitian operator A to Hermitian operator $\eta^{-1}A\eta$ via *Dyson map* η . The relation between the metric operator and the Dyson map is found by utilising the Hermiticity of the expression $\eta^{-1}A\eta$

$$\eta^{-1}A\eta = (\eta^{-1}A\eta)^\dagger \implies A\eta^\dagger\eta = \eta^\dagger\eta A^\dagger \implies \eta^\dagger\eta = \rho. \quad (1.7)$$

Several examples were considered to explore the non-uniqueness of the metric. A simple 2×2 complex matrix has been considered in [27, 28], where it was shown that by demanding the Hamiltonian and one other operator to be pseudo-Hermitian, the free parameter of the metric is uniquely fixed. In fact, by choosing a different set of operators to be pseudo-Hermitian, one can have a family of different physical models. An example of this result is presented in [29], where authors considered the non-Hermitian Hamiltonian $H(x, p)$ called the Swanson model, first introduced in [30]. The operators x and p are Hermitian and satisfies the Heisenberg algebra $[x, p] = i\hbar$. This model has a one-parameter family of Dyson map $\eta(z)$ which maps the Swanson model to the harmonic oscillator

$$\eta(z)H\eta^{-1}(z) \equiv h = \frac{1}{2}\mu(z)p^2 + \frac{1}{2}\nu(z)x^2, \quad (1.8)$$

where $\mu(z), \nu(z) \in \mathbb{R}$ for all $z \in [-1, 1]$. Therefore *the energy spectrum of Swanson model is equivalent to the energy spectrum of harmonic oscillator for all values of $z \in [-1, 1]$, which is real and bounded.*

However, one needs to take extra care, when establishing which operators are the observable of the non-Hermitian theory. This is because the expectation values of some observables between Hermitian and non-Hermitian theories are different depending on the values of z as the inner product is a function of this parameter. Below we list some examples.

$z = 1$	$z = 0$	$z = -1$	
$\langle H \rangle_\rho = \langle h \rangle$	$\langle H \rangle_\rho = \langle h \rangle$	$\langle H \rangle_\rho = \langle h \rangle$	(1.9)
$\langle X \rangle_\rho \equiv \langle x \rangle = \langle x \rangle_\rho$	$\langle x \rangle_\rho \neq \langle x \rangle$	$\langle x \rangle_\rho \neq \langle x \rangle$	
$\langle P \rangle_\rho \equiv \langle p \rangle \neq \langle p \rangle_\rho$	$\langle p \rangle_\rho \neq \langle p \rangle$	$\langle p \rangle_\rho = \langle p \rangle$	
$\langle N \rangle_\rho \equiv \langle n \rangle \neq \langle n \rangle_\rho$	$\langle n \rangle_\rho = \langle n \rangle$	$\langle n \rangle_\rho \neq \langle n \rangle$	

The operator n is a number operator and $X \equiv \eta^{-1}x\eta$, $P \equiv \eta^{-1}p\eta$ and $N \equiv \eta^{-1}n\eta$. In the $z = 1$ case, the operator x is an observable in both versions of the theory because the expectation value coincide with the position of the particle in the harmonic oscillator. However, the operator p is not an observable because one can show that at $z = 1$, $\langle p \rangle_\rho \neq \langle p^\dagger \rangle_\rho$. In fact the observable operator is $P \neq p$. This is because P is a self-adjoint operator in the non-Hermitian theory in sense of equation (1.1), where as p is not

$$\langle p \rangle = \langle \eta\eta^{-1}v | p | \eta\eta^{-1}v \rangle = \langle \eta^{-1}v | \eta^\dagger \eta \eta^{-1} p \eta | \eta^{-1}v \rangle = \langle \eta^{-1}p\eta \rangle_\rho. \quad (1.10)$$

Since p is an observable in the harmonic oscillator, the new operator $\eta^{-1}p\eta$ is the observable in the non-Hermitian theory. In the $z = 1$ case, the Hermitian Hamiltonian can be written in terms of observables $\eta^{-1}x\eta \equiv X = x$, $\eta^{-1}p\eta \equiv P$ as

$$\eta H \eta^{-1} = \frac{1}{2}\mu(1) (\eta P \eta^{-1})^2 + \frac{1}{2}\nu(1) X^2, \quad (1.11)$$

where $\eta P \eta^{-1}$ is a non-trivial combination of X and P (see [29] for explicit form). Therefore we see that the non-Hermitian Swanson model share the same energy spectrum with the harmonic operators but the theories obtained for different values of z are different, i.e. *different z leads to different physics*.

1.1.3 Modern development of non-Hermitian physics

In a seminal paper [1], Carl Bender and Stephan Boettcher performed a numerical and asymptotic analysis of the energy spectrum of the one-parameter family of the following non-Hermitian quantum mechanical Hamiltonian

$$H = p^2 - (ix)^N, \quad N \in \mathbb{R}, N \geq 1. \quad (1.12)$$

Where x, p are usual position and momentum operators satisfying the Heisenberg relation $[x, p] = i\hbar$. The numerical result is shown in figure 1.1. They claimed that the reality of the energy is guaranteed by the discrete anti-linear symmetry of the Hamiltonian, induced by parity (\mathcal{P}) and time-reversal (\mathcal{T}) operators transforming the position and momentum operators x and p .

$$\mathcal{PT} : x \rightarrow -x, \quad p \rightarrow p, \quad i \rightarrow -i. \quad (1.13)$$

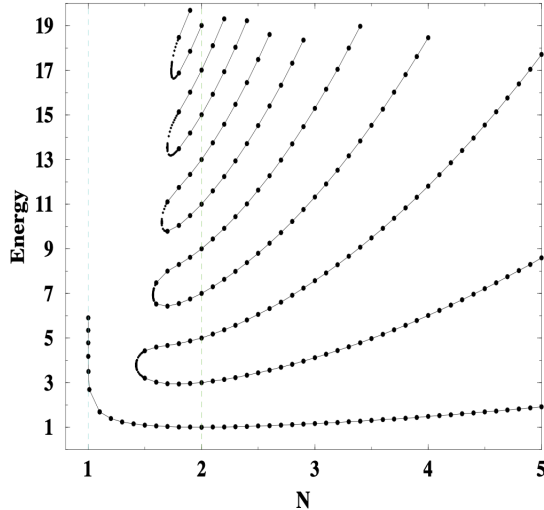


Figure 1.1: Energy spectrum of the Hamiltonian $H = p^2 - (ix)^N$ plotted for the real parameter N , taken from [1].

The mathematical proof of their claim was later presented in [31]. After the publication of [1], the analysis of non-Hermitian quantum mechanics in a closed system has become popular. However, the real and bounded energy spectrum is not enough to realise the well-defined quantum mechanics. One of the vital ingredients is the unitary time-evolution, which follows directly from the Hermiticity of the Hamiltonian. This problem was resolved by introducing a new operator \mathcal{C} [32] to define a modified inner product. The \mathcal{C} operator is defined as a sum of all eigenfunctions of the Hamiltonian. The connection to the similarity transformation discussed above was also found by Ali Mostafazadeh [33], who found that the metric operator ρ and the operator \mathcal{C} are related by

$$\mathcal{C} = \rho^{-1}\mathcal{P}. \quad (1.14)$$

From this equivalence, the non-uniqueness of the metric discussed in [20] can also be used for the \mathcal{PT} -symmetric quantum mechanics.

The eigenspectrum of the Hermitian Hamiltonian is known to avoid crossing [34]. However, the novelty of non-Hermitian Hamiltonian is the existence of the exceptional point where two or more eigenvalues coalesces, conforming the level crossing. It can be defined as an algebraic singularity of the eigenvalues of the linear operator H , depending on one-parameter z , mapping between two vector spaces where the eigenvalue is defined as the root of the characteristic equation. From

function analysis, it can be shown that the eigenvalues are analytic functions of $z \in \mathbb{C}$ except at the exceptional points (algebraic singularities). The term exceptional point was first coined by Tosio Kato [35]. A simple example is the finite-dimensional two-level system

$$H = \begin{pmatrix} 1 & iz \\ iz & -1 \end{pmatrix}, \quad \lambda_{\pm} = \pm\sqrt{1-z^2}, \quad (1.15)$$

where the parameter $z \in \mathbb{C}$ is complex and λ_{\pm} are eigenvalues. From the explicit forms of the eigenvalues, it is clear that the analytic singularities are located at $z = \pm 1$. If we restrict the parameter z on the real axis, then two eigenvalues coalesce and form a complex conjugate pair (see figure 1.2). Notice that they behave in a similar way as the energy spectrum of the Bender-Boettcher model plotted in the figure 1.1. This is a common trait seen in non-Hermitian physics where the pair

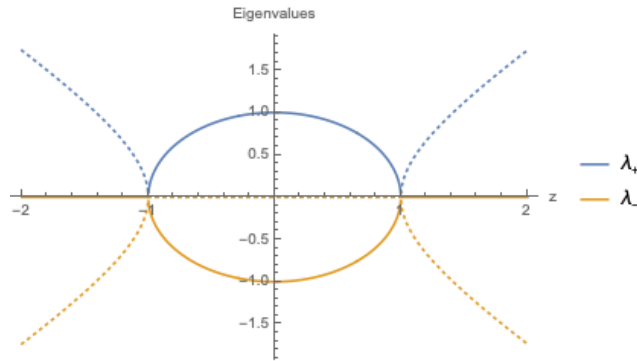


Figure 1.2: Plot of eigenvalues $\lambda_{\pm} = \pm\sqrt{1-z^2}$. The solid and dotted lines represent real and imaginary parts.

of eigenvalues coalesce at the exceptional point and split into complex conjugate pairs. However, there exist different types of exceptional points, which can be found by the generalised algebraic equation found in [36]. These higher dimensional exceptional points will not appear in the models considered in this thesis. However, we found a new type of exceptional point, which we refer to as the zero-exceptional point. A detail of this is found in the appendix B.

The exceptional point is ubiquitous in physics from molecular physics [37, 38, 39, 40, 41], laser physics [42], chaotic system [43, 44, 45, 46], fluid mechanics [47] and most notably in optics [48, 49, 50, 51, 52, 53] where the exceptional point and the branch cut structure of the square root of the eigenvalue were experimentally confirmed [48]. We will observe the effect of exceptional points throughout this thesis.

1.2 The Development of non-Hermitian Quantum Field Theory

The development of the non-Hermitian quantum field theory (QFT) in its early stage was mainly focused on building field-theoretic models based on existing quantum mechanical model. The most well studied models are complex ϕ^3 model ($i\phi^3$ model) [54, 55, 56, 57, 58, 59, 60, 61, 62, 63, 64, 65, 66] and wrong sign quartic model ($-\phi^4$ model) [54, 67, 68, 69, 70, 71, 72]. These two models are subset of the field theoretic extension of the Bender-Boettcher model (1.12) when $N = 3$ and $N = 4$, respectively. Most notably, both models are renormalisable and asymptotically free as shown in [61] and [73]. Another surprising result is that the energy spectrum of the wrong sign quartic model is bounded from below [1], despite the fact that the shape of the potential indicate instability. However, as demonstrated by the table (1.9), the key to defining a consistent non-Hermitian quantum theory is to find the similarity transformation or equivalently finding the \mathcal{C} -operator. Therefore the results found in $i\phi^3$ and $-\phi^4$ models can not predict the physical quantities unless the metric is found. Unfortunately, the definition of the \mathcal{C} -operator given above is not helpful in the quantum field theory as there are infinitely many eigenfunctions for the quantum field theoretic Hamiltonian. An alternative approach was proposed by [55] where the authors utilised the algebraic relation that the \mathcal{C} -operator needs to satisfy. The calculation of \mathcal{C} -operator or equivalently the similarity transformation was done for the several field-theoretic models such as complex ϕ^1 model [56], complex ϕ^3 model [55, 56], free Dirac model with γ_5 mass term [74], sine-Gordon and massive Thirring models [75]. The wrong sign quartic model transformation was found using the field-redefinition of the path-integral [68], using the quantum mechanical result [71]. However, the precise connection between the path-integral field redefinition and the \mathcal{C} operator (or similarity transformation) has not been explored in-depth with only one paper, exploring the connection of non-uniqueness and path-integral of Swanson model [76].

Once the \mathcal{C} operator is found, the non-Hermitian QFT can be cast into consistent theory using the argument given in the quantum mechanical case. A well-defined QFT is a key tool to analyse particle physics. The most modern physical description of the fundamental particle interaction is described by the QFT model called the standard model. The standard model can be broken down into four sectors: quantum

electrodynamics (QED), electroweak, quantum chromodynamics (QCD), and Higgs sectors. Each sector can be analysed as a separate theory. The general idea is that at the high energy limit, the four sectors combine into one theory where the interactions between each sector can not be ignored. The non-Hermitian extension of the variation, toy model or effective theories of each sector is studied by various authors. The sectors can generally be grouped into bosonic models (Higgs sector) and fermionic models (QED, QCD and electroweak sectors). A sample of the bosonic models are [77, 78, 79, 80, 81, 82, 83, 7, 9, 8, 10, 84] and fermionic models [85, 86, 87, 88, 84, 89, 90, 91, 92, 93, 94, 95, 96, 97, 98]. Some notable findings are the symmetry restoration of massive Dirac theory at exceptional point and lightness of neutrino [86], Goldstone and Higgs mechanism [78, 79, 7] and the possible breakdown of the Higgs mechanism at exceptional point [79, 9], complex t'Hooft-Polyakov monopole solution with real energy [10], dynamical mass generation [93, 95, 94], confinement [90], supersymmetry [84]. The general motivation is to extend the standard model to non-Hermitian theory to resolve some of the limitations of the standard model.

Another aspect of the non-Hermitian quantum field theory is in the theory with ghost states. The quantum mechanical state with a negative norm is referred to as a ghost state. Such a state can have a positive norm with respect to the new inner product defined via the metric operator. For this reason, the non-Hermitian field theory also has a natural extension to the theory with ghost field, such as in the Lee model [99]. An example for the Lee model can be found in [100, 101] and higher derivative theories such as Pauli-Villars theory [102] and Chern-Simon theory [103]. These results demonstrate that the problems such as ghost fields in the non-Hermitian theory is, in fact, pseudo-problem and can be removed by appropriate \mathcal{C} operator.

1.3 Outline

This thesis is divided into two parts. The first part focuses on the particle physics aspect where we discuss spontaneous symmetry breaking, Goldstone theorem and Higgs mechanism. The second part focuses on the non-trivial solutions of the equations of motion of the non-Hermitian quantum field theories. Two parts are bridged by the analysis of the t'Hooft-Polyakov monopole, a non-trivial solution to the equations of motion, which appears in the standard model. The details of each section

are as follows.

In section 2.1, we will review the Goldstone theorem and Higgs mechanism in Hermitian theories. In section 2.2, we contain the analysis of the approach we have taken to analyse non-Hermitian quantum field theory. The subsequent three sections 2.3 - 2.4 will analyse the Goldstone theorem and Higgs mechanism for non-Hermitian global $U(n)$, global $SU(n)$ and local $SU(n)$ symmetric theories. In section 2.5, we will also consider a non-Hermitian extension of the model, which is known to possess a non-trivial solution to the equations of motion called the t'Hooft-Polyakov monopole.

In section 3.1, we will review the t'Hooft-Polyakov monopole in a Hermitian theory. In section 3.2, a detailed analysis of the t'Hooft-Polyakov monopole in a non-Hermitian theory is discussed. In section 3.3, we will consider several $1 + 1$ dimensional field theories which possess a particular type of solutions called the BPS solutions. We observe a relation between the reality of the BPS soliton energies and the anti-linear symmetries of the model. The final section will apply the analysis of section 3.3 to a BPS Skyrme model, which is believed to be an approximate model of the nuclei.

Chapter 2

Spontaneous symmetry breaking of non-Hermitian quantum field theories and breakdown of Higgs mechanism

2.1 The implication of spontaneous symmetry breaking in particle physics

This short section will summarise the mechanism behind the breaking of continuous symmetry of a given quantum field theory and state one of the crucial implications to particle physics and condensed matter physics, namely the Higgs mechanism. The first part of this thesis plans to perturb further the discussion in this section and accommodate the unexplored area of the quantum field theory, made accessible via the rapid development of non-Hermitian physics in recent years.

2.1.1 Goldstone theorem

We begin with a simple quantum field theoretic Lagrangian of complex scalar fields $\phi(t, \vec{x}) \in \mathbb{C}$, which is invariant under global continuous symmetry of $U(1)$.

$$\mathcal{L} = \int_{-\infty}^{\infty} d^3x \left[\eta^{\mu\nu} \partial_\mu \phi(t, \vec{x})^* \partial_\nu \phi(t, \vec{x}) - \frac{g}{4} (v^2 - 2\phi^* \phi)^2 \right]. \quad (2.1)$$

Where $g, v \in \mathbb{R}$ are real constants and the derivative $\partial_\mu = (\partial_t, \partial_x, \partial_y, \partial_z)$ are Lorentz contracted with the metric $\eta^{\mu\nu} = \text{diag}(1, -1, -1, -1)$. Crucially this Lagrangian is invariant under $U(1)$ transformation of the complex fields

$$\begin{aligned} U(1) : \phi(t, \vec{x}) &\rightarrow e^{i\theta} \phi(t, \vec{x}), \\ \phi(t, \vec{x})^* &\rightarrow e^{-i\theta} \phi^*(t, \vec{x}) \end{aligned} \quad (2.2)$$

where $\theta \in \mathbb{R}$. Although this is a toy model to study the spontaneous symmetry breaking of $U(1)$, a similar sector appears in the standard model called the Higgs sector. The only difference is that the Higgs sector consists of two complex scalar fields. Therefore the Lagrangian having the $SU(2) \times U(1)$ symmetry, and most importantly, the symmetries are local, meaning the symmetry transformation of a field ϕ and its derivative $\partial_\mu \phi$ are different. This will be a key ingredient in the celebrated Higgs mechanism, discussed in the next subsection.

The $U(1)$ symmetry of the model (2.1) breaks down to a trivial group $\{\mathbb{I}\}$ by Taylor expanding the Lagrangian around the constant solution to the equations of motion of the theory. We will refer to such solution as a *vacuum solution*, which is found by solving the algebraic equation obtained by varying the potential of the model with the fields $\delta V(\phi) = 0$ (here, the potential does not contain the spatial derivatives of the fields). In the vicinity of the vacuum solution, the theory reduces to simple free theory with perturbation in the higher order of fields. One can then construct a Hilbert space from the vacuum state of the reduced theory. If the vacuum solutions are degenerate, one may speculate that the Hilbert spaces obtained by expanding around different vacua are different. Indeed this is the case for the quantum field theory because the tunnelling amplitude between these vacua vanishes with the infinite suppression by the infinite degree of freedom. This can be understood by discretising the field theoretic Hamiltonian $H[\phi]$ to many copies of quantum mechanical Hamiltonian by $\phi(t, \vec{x}) \rightarrow q_{\vec{x}}(t)$ where $\vec{x} \in \mathbb{Z}^d$ is a lattice point in a d -dimensional lattice. Then for a $d = 1$ dimensional case, the Hamiltonian can be written as

$$H = \sum_x H_x = \sum_{x \in \mathbb{Z}} \frac{1}{2} \frac{dq_x(t)}{dt} + \frac{1}{2} \frac{(q_x(t) - q_{x-1}(t))^2}{\delta x} + g(1 - q_x(t)^2)^2. \quad (2.3)$$

Each Hamiltonian H_x can be expanded around two position operators $q_x^{\pm 0}(t) = \pm 1$

to give two separate theories with different vacuum state $\{|+0\rangle, |-0\rangle\}$. Then one can calculate the tunnelling amplitude $\langle -|+\rangle$ of going from the vacuum $|+\rangle$ to $|-\rangle$ by WKB approximation, named after Wentzel, Kramers and Brillouin. If $\langle -|+\rangle$ is zero, then our analysis is done as the field theoretic limit (i.e. when the lattice spacing goes to zero) of the tunnelling amplitude is also zero. If the probability of tunnelling is non-zero $1 > e^{-c} > 0$, where $c > 0$, then the total probability is given by the product at every points on the lattice

$$\text{tunnelling probability} \sim \prod_{x \in \mathbb{Z}} e^{-c} = e^{-c \text{Volume}}. \quad (2.4)$$

Since $c > 0$, in the field theoretic limit where the volume of the space time is assumed to be infinite, the tunnelling probability is zero. Therefore the theories obtained by expanding around different vacua are truly different theories with reduced symmetries.

Let us denote the complex vacuum solution $\{\phi_0, \phi_0^*\}$ which simultaneously satisfies $\delta V(\phi_0, \phi_0^*)/\delta\phi = 0$, and $\delta V(\phi_0, \phi_0^*)/\delta\phi^* = 0$. In this example, the vacuum solution is a circle $\phi_0^* \phi_0 = v^2$, with radius v . This can be readily seen by rewriting the Lagrangian in terms of real components of the complex fields $\phi = (\phi^R + i\phi^I)/\sqrt{2}$, $\phi^R, \phi^I \in \mathbb{R}$,

$$\mathcal{L} = \int_{-\infty}^{\infty} d^3x \left[\frac{1}{2} \partial_\mu \Phi^T \partial^\mu \Phi - \frac{g}{4} (v^2 - \Phi^T \Phi)^2 \right] \quad (2.5)$$

where $\Phi = (\phi^R, \phi^I)$. The vacuum solution is now $\Phi^2 = (\phi_0^R)^2 + (\phi_0^I)^2 = v^2$, which is the equation of the circle with radius $|v|$. The symmetry of the Lagrangian is now the $SO(2)$ transformation $\Phi \rightarrow T\Phi$, $T \in \{T \in \text{Mat}_2(\mathbb{R}) \mid T^T T = \mathbb{I}\}$.

Before we expand the Lagrangian, we choose a simplest vacuum solution $\sqrt{2}\phi_0 = \phi_0^R = v$, $\phi_0^I = 0$. This is justified by the fact that the Lagrangian expanded around two vacua which are related by the symmetry transformation T , say $\Phi_0^1 = T\Phi_0^2$, are equivalent up to second order in the fields. To see this explicitly, let us expand the Lagrangian by denoting two new fields $\phi = \psi_1 + \phi_0^1 = \psi_2 + \phi_0^2$.

$$\begin{aligned} V(\phi) &= V(\psi_1 + \phi_0^1) = V(\psi_1 + T^{-1}\phi_0^2) = V(\mathcal{T}^{-1}(T\psi_1 + \phi_0^2)) = V(T\psi_1 + \phi_0^2) \\ &= V(\phi_0^2) + \frac{1}{2} \psi_1^T T^T H(\phi_0^2) T \psi_1 + \dots \\ V(\phi) &= V(\psi + \phi_0^2) = V(\phi_0^2) + \frac{1}{2} \psi_2^T H(\phi_0^2) \psi_2 + \dots \end{aligned} \quad (2.6)$$

Where $H(\phi_0^1)_{ij} = \delta^2 V(\phi_0^1) / \delta\psi_i \delta\psi_j$ is the Hessian matrix which in the Hermitian theory corresponds to the mass matrix of the expanded theory. Two Hessian matrices were obtained by expanding around two vacua related by the similarity transformation $H(\phi_0^2) \rightarrow T^T H(\phi_0^1) T$. This implies that the eigenvalues are unchanged. Therefore the expanded theories are equivalent up to second order after the diagonalisation of the two theories.

The Hessian matrix of the vacuum solution $\phi/\sqrt{2} = v$ is simply

$$H = \begin{pmatrix} 2gv^2 & 0 \\ 0 & 0 \end{pmatrix}. \quad (2.7)$$

Notice that the expanded theory now contains one massive field with mass $\sqrt{g}|v|$ and one massless field. This massless field is called the Goldstone field, named after Jeffrey Goldstone [2]. In fact, this can be generalised to an arbitrary Lagrangian of the following form

$$\hat{S} = \int d^4x \left[\frac{1}{2} \partial_\mu \Phi^T \partial^\mu \Phi - V(\Phi) \right]. \quad (2.8)$$

The vacuum solution is found by solving the equation

$$\left. \frac{\partial V(\Phi)}{\partial \Phi} \right|_{\Phi=\Phi_0} = 0. \quad (2.9)$$

The continuous global symmetry $\Phi \rightarrow \Phi + \delta\Phi$, i.e. $V(\Phi) = V(\Phi + \delta\Phi) = V(\Phi) + \nabla V(\Phi)^T \delta\Phi + \dots$, then implies

$$\frac{\partial V(\Phi)}{\partial \Phi_i} \delta\Phi_i(\Phi) = 0. \quad (2.10)$$

Differentiating this equation with respect to Φ_j and evaluating the result at a vacuum Φ_0 , determined by (2.9), yields

$$\left. \frac{\partial^2 V(\Phi)}{\partial \Phi_j \partial \Phi_i} \right|_{\Phi=\Phi_0} \delta\Phi_i(\Phi_0) + \left. \frac{\partial V(\Phi)}{\partial \Phi_i} \right|_{\Phi=\Phi_0} \left. \frac{\partial \delta\Phi_i(\Phi)}{\partial \Phi_j} \right|_{\Phi=\Phi_0} = 0. \quad (2.11)$$

Since the last term vanishes, due to (2.9), we are left with two options to solve (2.11). Either the vacuum is left invariant such that $\delta\Phi_i(\Phi_0) = 0$ or the vacuum breaks the global symmetry and $\delta\Phi_i(\Phi_0) \neq 0$. Denoting $(\theta_0)_i := \delta\Phi_i(\Phi_0)$ we obtain

$$\left. \frac{\partial^2 V(\Phi)}{\partial \Phi_j \partial \Phi_i} \right|_{\Phi=\Phi_0} \delta\Phi_i(\Phi_0) = (H(\Phi_0)\theta_0)_j = 0, \quad (2.12)$$

When the vacuum is left invariant by the global symmetry transformation, we have $\theta_0 = 0$ so that there is no restriction on H . However, when the vacuum breaks the global symmetry, we have $\theta_0 \neq 0$ so that θ_0 becomes an eigenvector for H with zero eigenvalue. Thus, in this case, we have a zero mass particle identified as a Goldstone boson.

In the case where the symmetry group is non-Abelian, the variation of the field can be organised as $\delta^a \Phi_i = T^a \Phi_i$, where $\{\delta^a \Phi_i\}_{a=1, \dots, N}$ are N linearly independent vectors (indexed with i) with the generators of the symmetry group $\{T^a\}_{a=1, \dots, N}$, where N is the rank of the group. For example $SU(n)$ has $n^2 - 1$ generators. The eigenvalue equation (2.12) now has N many copies with linearly independent eigenvectors $\{(\theta_0^a)_i := \delta^a \Phi_i(\Phi_0) = T^a(\Phi_0)_i\}$. Let $\{\theta_0^a\}_{a=1, \dots, M}$ be the eigenvectors with zero eigenvalues, then the expanded theory now has a reduced symmetry generated by $\{T^a\}_{a=M, \dots, N-M}$, where the corresponding eigenvectors $\theta^a = T^a \Phi_0$ are not the zero eigenvectors of the Hessian $H\theta^a \neq 0$. We will refer to such set of generators as *unbroken generators*. The number of eigenvectors with zero eigenvalues can be calculated by the following formula

$$\text{Number of Goldstone bosons} = \dim(G/H). \quad (2.13)$$

Where G is an original symmetry group and H is a set of unbroken generators.

2.1.2 Higgs mechanism

The Goldstone theorem requires the theory obtained via spontaneous symmetry breaking to contain massless particles. However, there is no massless scalar field in nature. Therefore one would like to find a way around the Goldstone theorem to remove the massless particles. In 1964, Carl Hagen, François Englert, Gerald Guralnik, Peter Higgs, Robert Brout and Tom Kibble [3, 4, 5, 6] (in alphabetical order) discovered that the degrees of freedom of massless particles are removed by changing the continuous global symmetry to continuous local symmetry. For example the continuous symmetry group $U(1)$ can be made local by letting the transformation to also depends on the space time $e^{i\theta(t, \vec{x})}$. However, this will break the symmetry of the kinetic term in the Lagrangian. This is resolved by introducing a new scalar field $A_\mu(t, \vec{x})$ and redefining the derivative to covariant derivative $D_\mu := \partial_\mu - ieA_\mu$, where $e \in \mathbb{R}$ is a constant, refer to as a charge of the field A_μ . For

example, in the quantum electrodynamics, A_μ represents the fundamental field of electron (i.e. its equations of motion satisfies the Maxwell's equations), therefore e corresponds to the electron charge. Imposing that the new scalar field transforms as $A_\mu \rightarrow A_\mu - i\partial_\mu\theta/e$, then one can show that $D_\mu\phi \rightarrow e^{i\theta}D_\mu\phi$. There is also a dynamical term of A_μ which respect this symmetry, defined by $F_{\mu\nu} := i[D_\mu, D_\nu]/e = \partial_\mu A_\nu - \partial_\nu A_\mu$. The extension to higher-order symmetry group is also possible. The transformations for $U \in SU(N)$ are

$$\phi \rightarrow U\phi, \quad D_\mu := \partial_\mu - ieA_\mu, \quad A_\mu \rightarrow UAU^{-1} + \frac{i}{e}\partial U U^{-1}. \quad (2.14)$$

Where the scalar field $A_\mu := A_\mu^a T^a$ can be decomposed in term of the generators of $SU(N)$, $\{T^a\}_{a=1, \dots, N^2-1}$. The kinetic term is still defined by $F_{\mu\nu} := i[D_\mu, D_\nu]/e$. Let us consider the local $U(1)$ symmetric Lagrangian

$$\mathcal{L} = \int d^3x \left[D_\mu\phi^* D^\mu\phi - \frac{g}{4}(v^2 - 2\phi^*\phi)^2 - \frac{1}{4}F_{\mu\nu}F^{\mu\nu} \right]. \quad (2.15)$$

After expanding around the vacuum, the potential term reduces to $-gv^2(\phi^R)^2 + \mathcal{O}(\Phi^2)$. The kinetic term will take the non-trivial form after expanding around the vacuum solution

$$\begin{aligned} |D_\mu(\phi + \phi_0)|^2 &= |\partial_\mu\phi + ieA_\mu(\phi + \phi_0)|^2 = |\partial\phi|^2 + e^2|A(\phi + \phi_0)|^2 \\ &= \frac{1}{2}(\partial\phi^R)^2 + \frac{1}{2}(\partial\phi^I)^2 \\ &\quad + e^2 A_\mu A^\mu (|\phi|^2 + |\phi_0|^2 + \phi_0^R \phi^R). \end{aligned} \quad (2.16)$$

The expanded Lagrangian now takes the form

$$\begin{aligned} \mathcal{L} &= \int d^3x \left[\frac{1}{2}(\partial_\mu\phi^R)^2 - gv^2(\phi^R)^2 - \frac{1}{4}F_{\mu\nu}F^{\mu\nu} \right. \\ &\quad \left. + \frac{1}{2}(\partial_\mu\phi^I)^2 + \frac{e^2}{2}A_\mu A^\mu [(\phi^R)^2 + (\phi^I)^2 + (\phi_0^R)^2 + 2\phi^R\phi_0^R] + \dots \right] \\ &= \int d^3x \left[\frac{1}{2}(\partial_\mu\phi^R)^2 - gv^2(\phi^R)^2 - \frac{1}{4}F_{\mu\nu}F^{\mu\nu} \right. \\ &\quad \left. + e^2v^2 \left| A_\mu + i\frac{\partial_\mu\phi^I}{ev\sqrt{2}} \right|^2 + \dots \right] \end{aligned} \quad (2.17)$$

The ellipsis in the last term includes the term with higher-order in fields. Defining the new field by $B_\mu := A_\mu + i\partial_\mu\phi^I/ev\sqrt{2}$, the degree of freedom of the massless field

ϕ^I is removed from the second order. The kinetic term of A_μ is equivalent to the kinetic term of B_μ by simply replacing A_μ with B_μ . This is because of the anti-symmetric nature of $\mu\nu$ in the kinetic term $F_{\mu\nu}F^{\mu\nu}$, where $F_{\mu\nu} = \partial_\mu A_\nu - \partial_\nu A_\mu := 2\partial_{[\mu}A_{\nu]}$. Inserting B in to $F_{\mu\nu}$, we find

$$\partial_{[\mu}B_{\nu]} = \partial_{[\mu}A_{\nu]} + \frac{i}{ev\sqrt{2}}\partial_{[\mu}\partial_{\nu]}\phi^I = \partial_{[\mu}A_{\nu]}, \quad (2.18)$$

where the square bracket in the subscript represent the anti-symmetrizer. Finally, the Lagrangian consist of two massive scalar fields $\{\phi^R, B_\mu\}$ and no more massless fields.

In the following few sections, we will investigate the Goldstone theorem and Higgs mechanism in a non-Hermitian theory with the global Abelian group in section 2.3, a non-Hermitian theory with the global non-Abelian group in section 2.4 and a non-Hermitian theory with the local non-Abelian group in section 2.5. However, in order to consistently analyse the non-Hermitian theory, we need to resort to few techniques from \mathcal{PT} symmetric quantum mechanics and non-Hermitian physics. In the next section, we will detail the pseudo-Hermitian method of the non-Hermitian quantum field theory.

2.1.3 Summary

We gave a motivation for the occurrence of spontaneous symmetry breaking in the quantum field theory and considered an example (2.1). By explicit calculation, the spontaneous symmetry breaking introduced massless particles called the Goldstone bosons, where its number is determined by the number of linearly independent broken generators. This massless degree of freedom can be removed by promoting the derivative ∂_μ to covariant derivative D_μ . The Goldstone boson is absorbed into the newly defined massive gauge field through the Higgs mechanism.

2.2 Pseudo-Hermitian approach to spontaneously broken symmetries

Throughout this section, we will use the pseudo-Hermitian approach to study the physical aspects of the non-Hermitian quantum field theory. Therefore in this section, we will layout the general idea of the methods used in next three sections which

we refer to as the pseudo-Hermitian approach. Note that the example given in this section is to demonstrate the approach, therefore any detail will be left out until the next section. The general form of the Lagrangian we consider takes the following form:

$$S_n = \int d^4x [\partial_\mu \phi^T \partial^\mu \phi^* - V(\phi)], \quad (2.19)$$

with n -component complex scalar fields $\phi = (\phi_1, \dots, \phi_n)$ and potential $V(\phi)$. The action is assumed to possess three general properties:

- i) It is invariant under a global continuous symmetry $\phi \rightarrow \phi + \delta\phi$ with $V(\phi) = V(\phi + \delta\phi)$. The symmetry is, for instance, generated by a Lie group \mathfrak{g} with Lie algebraic generators T , so that being global implies an infinitesimal change $\delta\phi = \alpha T\phi$ with α being a small parameter and $\partial_\mu(\alpha T) = 0$. In section 2.5, we will consider the local group.
- ii) It is invariant under a discrete antilinear symmetry $\phi(x_\mu) \rightarrow U\phi^*(-x_\mu)$, with U being a constant unitary matrix. These symmetries may be viewed as modified \mathcal{CPT} -symmetries. When $U \rightarrow \mathbb{I}$ the symmetry reduces to the standard \mathcal{CPT} -symmetry, where ϕ is the scalar field.
- iii) The potential $V(\phi)$ is not Hermitian, that is $V(\phi) \neq V^\dagger(\phi)$.

At first sight, such types of theories appear to be inconsistent as the two sets of equations of motion obtained by functionally varying the action S separately with respect to the fields ϕ_i and ϕ_i^* , $\delta S_n/\delta\phi_i = 0$ and $\delta S_n/\delta\phi_i^* = 0$, are in general incompatible. A specific example of this is given in equations (2.42)-(2.47) in the section 2.3.2. One may, however, overcome this problem by using a non-standard variational principle combined with keeping some non-vanishing surface terms [78, 82] or alternatively by exploiting the fact that the content of the theory is unaltered as long as the equal time commutation relations are preserved and carry out a similarity transformation that guarantees that feature [7, 75, 79]. Hence, in the latter approach, which we refer to as the "*pseudo-Hermitian approach*", one seeks a Dyson map η , named this way in analogy to its quantum mechanical counterpart [23], to transform a non-Hermitian Hamiltonian to a Hermitian Hamiltonian. Since the action S contains a Lagrangian, rather than a Hamiltonian, we need to first Legendre transform the complex Lagrangian \mathcal{L} to a non-Hermitian Hamiltonian \mathcal{H} . Next, we carry out the similarity transformation by means of a Dyson map to

obtain a Hermitian Hamiltonian \mathfrak{h} , which we then inverse Legendre transform to a real Lagrangian \mathfrak{l}

$$\mathcal{L} \xrightarrow{\text{Legendre}} \mathcal{H} \xrightarrow{\text{Dyson}} \eta \mathcal{H} \eta^{-1} = \mathfrak{h} \xrightarrow{\text{Legendre}^{-1}} \mathfrak{l}. \quad (2.20)$$

A new equivalent action obtained through this process takes the following form

$$\hat{S} = \int d^4x \mathfrak{l} = \int d^4x \left[\partial_\mu \phi I \partial^\mu \phi^* - \hat{V}(\phi) \right], \quad (2.21)$$

where the transformed potential is Hermitian, i.e. it remains invariant under complex conjugation $\hat{V}(\phi) = \hat{V}^\dagger(\phi)$. The Hermitian matrix I , which results from the similarity transformation, can give a negative sign in the kinetic term, apparently resulting in a ghost field. An explicit example of such matrix can be seen in Eq. (2.62) in section 2.3. However, the negative kinetic term disappears by diagonalising the Lagrangian using the biorthonormal basis of the non-Hermitian squared mass matrix. Therefore the apparent ghost problem in the complex theory is a pseudo-problem, which disappears once a correct similarity transformation and diagonalisation has been implemented. We post-pond a detailed discussion to the end of this section.

Another way to perform a similarity transformation was recently proposed in [83]. Instead of constructing a Dyson map with fields and their corresponding canonical momenta, the authors defined a Dyson map in terms of creation and annihilation operators of the plane-wave decomposition of the fields. This method will allow one to transform the Lagrangian without performing the Legendre transformation, which can be difficult in some models and impossible for higher-order theories.

As already indicated above, next it is in general useful to convert the complex scalar field theory into one involving only real valued fields by decomposing the n complex scalar fields into real and imaginary parts as $\phi = 1/\sqrt{2}(\varphi + i\chi)$ with $\varphi, \chi \in \mathbb{R}$. Defining then a real $2n$ -component field $\Phi = (\varphi_1, \dots, \varphi_n, \chi_1, \dots, \chi_n)$, possibly with the fields in different order to block diagonalise the mass squared matrix, the new action \hat{S} may be re-written as

$$\hat{S} = \int d^4x \left[\frac{1}{2} \partial_\mu \Phi^T \hat{I} \partial^\mu \Phi - \hat{V}(\Phi) \right]. \quad (2.22)$$

Where the two Hermitian matrices \hat{I} and I are related via rearrangement of fields.

Analysing the action in this form, the extension of Goldstone's theorem from section 2.1 to the non-Hermitian case is easily established. We follow the same calculation from equation (2.9) to (2.12). However, the Hessian matrix is no longer the mass matrix of the expanded theory because of the unconventional metric of the kinetic term. The correct mass matrix is obtained by multiplying the Hessian matrix with the metric $M := \hat{I}H$. The reason for this can be seen by rewriting the expanded Lagrangian up to second order

$$\mathcal{L} = \int d^3x \left[\frac{1}{2} \phi \hat{I} (-\square - \hat{I}H) \phi \right] = \int d^3x \left[\frac{1}{2} \phi^T \hat{I} (-\square - TDT^{-1}) \phi \right], \quad (2.23)$$

where $H(\Phi_0)$ is the Hessian of the potential $\hat{V}(\Phi)$ evaluated at the vacuum Φ_0 . We have used integration by parts and the assumption that the surface terms vanish. The mass matrix $\hat{I}H = M$ is diagonalised by matrix T . At the end of this section, we will show that by utilising the biorthonormal basis, one can always choose a matrix T such that $T^{-1} = T^T \hat{I}$. Therefore the free part of the Lagrangian can be diagonalised

$$\mathcal{L} = \int d^3x \left[\sum_i \frac{1}{2} (T^T \hat{I} \phi)_i [-\square - \lambda_i] (T^T \hat{I} \phi)_i \right], \quad (2.24)$$

where λ_i are eigenvalues of $\hat{I}H$. This Lagrangian is now a standard Hermitian quantum field theory. Therefore the rest mass of the particles are identified at the poles of the free propagator. In this case it is

$$G_i = \frac{1}{p^2 - \lambda_i}. \quad (2.25)$$

Indeed we see that the masses of the particles are eigenvalues of $\hat{I}H$. Therefore we conclude that the correct mass matrix of the theory given in equation (2.22) is $M := \hat{I}H$. Multiplying (2.12) by \hat{I} we obtain

$$\hat{I}H(\Phi_0)\theta_0 = M^2\theta_0 = 0. \quad (2.26)$$

The occurrence of the matrix \hat{I} results from the similarity transformation and is, therefore, a trace of the feature that the potential is non-Hermitian. The reformulation also has the effect that M^2 is no longer Hermitian either. We can now read off Goldstone's theorem for non-Hermitian systems from (2.12). When the vacuum is

left invariant by the global symmetry transformation, we have $\theta_0 = 0$ so that there is no restriction on M^2 . However, when the vacuum breaks the global symmetry, we have $\theta_0 \neq 0$ so that θ_0 becomes an eigenvector for M^2 with zero eigenvalue. Thus, in this case, we have a zero mass particle identified as a Goldstone boson.

Assuming that the symmetry is generated by a Lie group \mathfrak{g} , we may repeat this argument for each Lie algebraic generator T so that we obtain a Goldstone boson for each generator that when acting on the vacuum Φ_0 produces a different one. The crucial difference, when compared to the scenario with Hermitian potentials, is that here M^2 is also not Hermitian. This means that the discrete antilinear symmetries determine the physical regimes. Referring to this symmetry as \mathcal{PT} -symmetry [1, 104] in a wider sense, we may encounter \mathcal{PT} -symmetric regimes with real mass spectra, exceptional points with non-diagonalisable mass matrix, zero exceptional points, singularities and a spontaneously broken \mathcal{PT} -symmetric regime with unphysical complex conjugate masses. Similar as in [7] we distinguish here between a *standard exceptional point* where two eigenvalues coalesce and become complex, and a *zero exceptional point* at which one positive real eigenvalue coincides with a zero eigenvalue and remains real thereafter. A detail discussion of the different types of exceptional points are found in appendix B. We will see in the section 2.3.4 that the identification of the Goldstone boson is different in these regimes and in parts impossible.

Below we will also make use of the general property that the expansions around two vacua, say ϕ_0^1 and ϕ_0^2 , that are related by the symmetry transformation \mathcal{T} of the potential $V(\phi) = V(\mathcal{T}\phi)$ as $\mathcal{T}\phi_0^1 = \phi_0^2$ with $\mathcal{T}^T = \mathcal{T}^{-1}$ yield to theories with mass squared matrix possessing the same eigenvalues. This can be seen from

$$\begin{aligned}
V(\phi + \phi_0^1) &= V(\phi + \mathcal{T}^{-1}\phi_0^2) = V(\mathcal{T}^{-1}(\mathcal{T}\phi + \phi_0^2)) = V(\mathcal{T}\phi + \phi_0^2) & (2.27) \\
&= V(\phi_0^2) + \frac{1}{2}\phi^T \mathcal{T}^T H(\phi_0^2) \mathcal{T}\phi + \dots = V(\phi_0^2) + \frac{1}{2}\phi^T H(\phi_0^2)\phi + \dots \\
&= V(\phi + \phi_0^2).
\end{aligned}$$

As the kinetic term is invariant by itself, no modification of the mass squared matrix will arise from there, apart from the multiplication by \hat{I} as a result of the non-Hermitian nature. Thus we may employ the symmetry to transform the vacuum into the most convenient form for analysis without altering the physics, such as the eigenvalue spectrum of the mass matrix.

Diagonalising the Lagrangian using biorthonormal basis

Finally, we finish this section with a short discussion that establishes that the unconventional matrix I in the kinetic term disappear when the Lagrangian is properly diagonalised. Consider the corresponding action

$$\begin{aligned} S &= \frac{1}{2} \int d^4x \left(\partial_\mu \Phi^\top \hat{I} \partial^\mu \Phi - \Phi^\top H \Phi \right) + S_{\text{int}}[\Phi], \\ &= -\frac{1}{2} \int d^4x \left[\Phi^\top \hat{I} (\partial_\mu \partial^\mu + M^2) \Phi \right] + S_{\text{int}}[\Phi], \end{aligned} \quad (2.28)$$

where S_{int} contains all terms of higher order than Φ^2 . We also assumed that surface terms vanish at infinity when integrating by parts and used $\hat{I}^2 = \mathbb{I}$, $M^2 = \hat{I}H_\pm$. The identity $\hat{I}^2 = \mathbb{I}$ can easily be shown by using the property of the similarity transformation $\eta (\eta \mathcal{H} \eta^{-1}) \eta^{-1} = \mathcal{H}^\dagger$. Performing the transformation twice on the kinetic term, one can conclude that the identity is indeed true

$$\partial_\mu \Phi^T \partial^\mu \Phi \xrightarrow{\eta} \partial_\mu \Phi^T \hat{I} \partial^\mu \Phi \xrightarrow{\eta} \partial_\mu \Phi^T \hat{I}^2 \partial^\mu \Phi = \partial_\mu \Phi^T \partial^\mu \Phi \implies \hat{I}^2 = \mathbb{I}. \quad (2.29)$$

Next we diagonalise the squared mass matrix as $M^2 = T^{-1}DT$ and consider only the integrand of the first term in (2.28)

$$\Phi^\top \hat{I} (\partial_\mu \partial^\mu + M^2) \Phi = \Phi^\top \hat{I} (\partial_\mu \partial^\mu + TDT^{-1}) \Phi = \Psi^\top (\partial_\mu \partial^\mu + D) \Psi, \quad (2.30)$$

where we introduced the new field $\Psi := T^\top \hat{I} \Phi$ and used $T^{-1} = T^\top \hat{I}$.

The latter relation is derived as follows: We start by defining the right and left eigenvectors v and u of M^2 by

$$\hat{I}Hv_i = \lambda_i v_i, \quad \text{and} \quad (\hat{I}H)^\dagger u_i = \lambda_i u_i, \quad (2.31)$$

respectively. Since the similarity transformation maps non-Hermitian Hamiltonian to Hermitian Hamiltonian, we have $\hat{I}^\dagger = \hat{I}$ and $H^\dagger = H$, which implies that $\hat{I}H_\pm \hat{I}u_i = \lambda_i \hat{I}u_i$. Therefore we can express the right eigenvectors in terms of the left eigenvectors as $v_i = \hat{I}u_i$. The matrix T is composed of the column vectors of v_i , i.e. $T = (v_1, \dots)$ so that $\hat{I}T = (u_1, \dots)$. Since the left and right eigenvector form a biorthonormal basis, $v_i \cdot u_j = \delta_{ij}$, it follows that $T^\top \hat{I}T = \mathbb{I}$ and hence $T^{-1} = T^\top \hat{I}$. The new field Ψ and the old field Φ are simply related by a invertible matrix multiplication, therefore an interaction term S_{int} can also be written in terms of the new

fields. Resulting in a diagonalised Hermitian theory

$$S[\Psi] = \frac{1}{2} \int d^4x \left[\partial_\mu \Psi^T \partial^\mu \Psi - \frac{1}{2} \Psi^T D \Psi + S_{\text{int}}[T\Psi] \right]. \quad (2.32)$$

Since any square matrix with linearly independent eigenvectors are diagonalisable using biorthonormal basis [105]. The above method can apply to any squared mass matrix. However, we will encounter in next three sections that this method fails at the exceptional points.

2.2.1 Summary

	{Hamiltonian, Action, Mass matrix }
Equation (2.19)	$\{H^\dagger \neq H, S^\dagger \neq S, M^\dagger \neq M\}$
<i>Dyson map</i>	↓
Equation (2.21)	$\{\tilde{H}^\dagger = \tilde{H}, \tilde{S}^\dagger = \tilde{S}, \tilde{M}^\dagger \neq \tilde{M}\}$
<i>Biorthonormal basis</i>	↓
Equation (2.32)	$\{\tilde{\tilde{H}}^\dagger = \tilde{\tilde{H}}, \tilde{\tilde{S}}^\dagger = \tilde{\tilde{S}}, \tilde{\tilde{M}}^\dagger = \tilde{\tilde{M}}\}$

Table 2.1: Flow diagram showing the general procedure of pseudo-Hermitian approach

We have assumed three properties for our action and gave a general idea of the procedure we plan to use for the next three sections. We take the non-Hermitian theory (2.19) and perform a similarity transformation to obtain (2.21) which is a real action but its mass matrix is not Hermitian due to the matrix \mathcal{I} in the kinetic term. A true Hermitian theory is obtained in (2.32) after performing a biorthonormal diagonalisation to the non-Hermitian mass matrix. We summarise this as a flow diagram in table 2.1. Let us denote the theory as a set $\{H, S, M\}$ where each letter represents the Hamiltonian, action and the mass matrix respectively. After the theory has been transformed, we denote the new quantities by tilde on the letters.

2.3 Spontaneous symmetry breaking of a global Abelian group

This section studies the interplay between spontaneously breaking global Abelian continuous symmetries and discrete antilinear symmetries in non-Hermitian quantum field theories composed of several complex scalar fields. We analyse the model for different types of global symmetry preserving and breaking vacua. In addition, the models are symmetric under various types of discrete antilinear symmetries com-

posed of nonstandard simultaneous charge conjugations, time-reversals and parity transformations; \mathcal{CPT} . While the global symmetry governs the existence of massless Goldstone bosons, the discrete one controls the precise expression of the Goldstone bosons in terms of the original fields in the model and its physical regimes where masses of the particles stay real and positive. We will show that the Goldstone bosons emerge not only in the physical regimes but also at some boundary of the regime called *exceptional point* but not at a different type of boundary referred to as the *zero exceptional point*

2.3.1 A non-Hermitian model with n complex scalar fields

We analyse here generalisations of the model originally proposed in [78] and further studied in [79] using the pseudo-Hermitian approach discussed in the previous section. To be a suitable candidate for the investigation of the non-Hermitian version of Goldstone's theorem, the model should be not invariant under complex conjugation, possess a discrete \mathcal{CPT} -transformation symmetry, and crucially be invariant under a global continuous symmetry, see i) - iii) after equation (2.19). The actions $\mathcal{I}_n = \int d^4x [\mathcal{L}_n]$ involving the Lagrangian densities functional of the general form

$$\mathcal{L}_n = \sum_{i=1}^n (\partial_\mu \phi_i \partial^\mu \phi_i^* + c_i m_i^2 \phi_i \phi_i^*) + \sum_{i=1}^{n-1} \kappa_i \mu_i^2 (\phi_i^* \phi_{i+1} - \phi_{i+1}^* \phi_i) - \sum_{i=1}^n \frac{g_i}{4} (\phi_i \phi_i^*)^2 \quad (2.33)$$

possess all of these three properties. The parameter space is spanned by the real parameters $m_i, g_i, \mu_i \in \mathbb{R}$ and $c_i, \kappa_i = \pm 1$. The latter constants usually take the value -1 in the Hermitian theory as it corresponds to the sign of the squared rest mass of the fields. However, we keep these constants arbitrary since their values distinguish between different types of qualitative behaviour, as we shall see below. When fixing those constants to specific values, the Lagrangian \mathcal{L}_n reduces to the model discussed in [78, 79]. In order to keep matters as simple as possible in our detailed analysis, we will set here $g_i = 0$ for $i \neq 1$. However, in appendix C we argue that the interaction term may be chosen in a more complicated way with all three properties still preserved.

Functionally varying the action \mathcal{I}_n separately with respect to ϕ_i and ϕ_i^* gives

rise to the two sets of equations of motion

$$\frac{\delta \mathcal{I}_n}{\delta \phi_i} = \frac{\partial \mathcal{L}_n}{\partial \phi_i} - \partial_\mu \left[\frac{\partial \mathcal{L}_n}{\partial (\partial_\mu \phi_i)} \right] = 0, \quad \frac{\delta \mathcal{I}_n}{\delta \phi_i^*} = \frac{\partial \mathcal{L}_n}{\partial \phi_i^*} - \partial_\mu \left[\frac{\partial \mathcal{L}_n}{\partial (\partial_\mu \phi_i^*)} \right] = 0. \quad (2.34)$$

We comment below on the compatibility of these equations. Evidently, the action \mathcal{I}_n is not Hermitian when the fields are real, i.e. $\phi_i^* \neq \phi_i$ for some i . However, it is invariant under two types of \mathcal{CPT} -transformations

$$\mathcal{CPT}_1 : \phi_i(x_\mu) \rightarrow (-1)^{i+1} \phi_i^*(-x_\mu), \quad \mathcal{CPT}_2 : \phi_i(x_\mu) \rightarrow (-1)^i \phi_i^*(-x_\mu). \quad (2.35)$$

Where $i = 1, \dots, n$. As pointed out in [106] these types of symmetries are not the standard \mathcal{CPT} transformations as some of the fields are not simply conjugated and \mathcal{P} does not simply act on the argument of the fields but also acquire an additional minus sign as a factor under the transformation. A more detailed study of such types of symmetries in quantum field theoretic context is found in [106]. Alternatively one can assume that the model consist of scalar and pseudo-scalar fields. However, we will keep the \mathcal{CPT} as a generic anti-linear symmetry as we will encounter non-trivial transformation in chapter 3.

In addition, the action related to (2.33) is left invariant under the continuous global $U(1)$ -symmetry

$$\phi_i \rightarrow e^{i\alpha} \phi_i, \quad \phi_i^* \rightarrow e^{-i\alpha} \phi_i^*, \quad i = 1, \dots, n, \alpha \in \mathbb{R}, \quad (2.36)$$

when none of the fields in the theory is real, that is when $\phi_i^* \neq \phi_i$ for all i . Applying Noether's theorem and using the standard variational principle for this symmetry, one obtains

$$\delta \mathcal{L}_n = \partial_\mu \left[\sum_{i=1}^n \frac{\partial \mathcal{L}_n}{\partial (\partial_\mu \phi_i)} \delta \phi_i + \frac{\partial \mathcal{L}_n}{\partial (\partial_\mu \phi_i^*)} \delta \phi_i^* \right] + \sum_{i=1}^n \left[\frac{\delta \mathcal{I}_n}{\delta \phi_i} \delta \phi_i + \frac{\delta \mathcal{I}_n}{\delta \phi_i^*} \delta \phi_i^* \right]. \quad (2.37)$$

Thus provided the equations of motion in (2.34) hold, and $\delta \mathcal{L}_n = 0$ when using the global $U(1)$ -symmetry in the variation with $\delta \phi_j = i\alpha \phi_j$ and $\delta \phi_j^* = -i\alpha \phi_j^*$, we derive the Noether current associated to this symmetry as

$$j_\mu = i\alpha \sum_i (\phi_i \partial_\mu \phi_i^* - \phi_i^* \partial_\mu \phi_i). \quad (2.38)$$

The following two subsections show that this current is not conserved in its present form but can be transformed into a correct conserved form using the pseudo-Hermitian method. We note here that the unconserved current is also a pseudo-problem, only present in the complex theory. Such a problem will be resolved once the correct choice of similarity transformation is chosen.

2.3.2 \mathcal{PT} symmetric and broken regimes

We now discuss the model \mathcal{L}_3 in more detail with all fields being genuinely complex scalar fields, i.e. $\phi_i \neq \phi_i^*$, $i = 1, 2, 3$. Then the action for (2.33) takes on the form

$$S_3 = \int d^4x \left[\sum_{i=1}^3 \partial_\mu \phi_i \partial^\mu \phi_i^* - V_3 \right], \quad (2.39)$$

$$V_3 = - \sum_{i=1}^3 c_i m_i^2 \phi_i \phi_i^* + c_\mu \mu^2 (\phi_1^* \phi_2 - \phi_2^* \phi_1) + c_\nu \nu^2 (\phi_2 \phi_3^* - \phi_3 \phi_2^*) + \frac{g}{4} (\phi_1 \phi_1^*)^2.$$

Compared to (2.33) we have simplified here the interaction term by taking $g_1 = g$ and $g_2 = g_3 = 0$. The model contains the real parameters $m_i, \mu, \nu, g \in \mathbb{R}$ and $c_i, c_\mu, c_\nu = \pm 1$. While this action S_3 is not Hermitian, that is invariant under complex conjugation, it respects various discrete and continuous symmetries. It is invariant under two types of \mathcal{CPT} -transformations (2.35)

$$\mathcal{CPT}_{1/2} : \phi_1(x_\mu) \rightarrow \pm \phi_1^*(-x_\mu), \quad \phi_2(x_\mu) \rightarrow \mp \phi_2^*(-x_\mu), \quad \phi_3(x_\mu) \rightarrow \pm \phi_3^*(-x_\mu), \quad (2.40)$$

which are both discrete antilinear transformations. Moreover, the action (2.39) is left invariant under the continuous global $U(1)$ -symmetry (2.36), which gives rise to the Noether current (2.38)

$$j_\mu = i\alpha \sum_{i=1}^3 (\phi_i \partial_\mu \phi_i^* - \phi_i^* \partial_\mu \phi_i). \quad (2.41)$$

The Goldstone theorem suggests that after expanding the action (2.39), the resulting theory should contain either no massless fields or just one [2, 107]. As we shall see, breaking in our model the global $U(1)$ -symmetry for the vacuum will give rise to the massless Goldstone bosons in the standard fashion, albeit with some modifications and novel features for a non-Hermitian setting. The six equations of motion in (2.34)

read in this case

$$\square\phi_1 - c_1 m_1^2 \phi_1 - c_\mu \mu^2 \phi_2 + \frac{g}{2} \phi_1^2 \phi_1^* = 0, \quad (2.42)$$

$$\square\phi_2 - c_2 m_2^2 \phi_2 + c_\mu \mu^2 \phi_1 + c_\nu \nu^2 \phi_3 = 0, \quad (2.43)$$

$$\square\phi_3 - c_3 m_3^2 \phi_3 - c_\nu \nu^2 \phi_2 = 0, \quad (2.44)$$

$$\square\phi_1^* - c_1 m_1^2 \phi_1^* + c_\mu \mu^2 \phi_2^* + \frac{g}{2} \phi_1 (\phi_1^*)^2 = 0, \quad (2.45)$$

$$\square\phi_2^* - c_2 m_2^2 \phi_2^* - c_\mu \mu^2 \phi_1^* - c_\nu \nu^2 \phi_3^* = 0, \quad (2.46)$$

$$\square\phi_3^* - c_3 m_3^2 \phi_3^* + c_\nu \nu^2 \phi_2^* = 0, \quad (2.47)$$

with d'Alembert operator $\square := \partial_\mu \partial^\mu$ and metric $\text{diag}\eta = (1, -1, -1, -1)$. Here we explicitly see the incompatibility of the equations as pointed out for \mathcal{L}_2 with four scalar fields investigated in [78, 79], namely that as a consequence of the non-Hermiticity of the action the equations of motions obtained from the variation with regard to the fields ϕ_i^* , (2.42)-(2.44), are not the complex conjugates of the equations obtained from the variation with respect to the fields ϕ_i , (2.45)-(2.47). Hence, the two sets of equations appear to be incompatible, and therefore the quantum field theory related to the action (2.39) seems to be inconsistent. Without detailed calculation, we see that the current is not conserved

$$\partial_\mu j^\mu = i\alpha \sum_i (\phi_i \square \phi_i^* - \phi_i^* \square \phi_i) \neq 0 \quad (2.48)$$

because $\square\phi_i \neq \square\phi_i^*$ for all $i \in \{1, 2, 3\}$. An alternative solution to this conundrum was proposed in [78], by suggesting to omit the variation with respect to one set of fields and also taking non-vanishing surface terms into account. Here we adopt the pseudo-Hermitian approach explained in previous section. It consists of seeking a similarity transformation for the action that achieves compatibility between the two sets of equations of motion. It is easy to see that any transformation of the form $\phi_2 \rightarrow \pm i\phi_2$, $\phi_2^* \rightarrow \pm i\phi_2^*$ that leaves all the other fields invariant will achieve compatibility between the two sets of equations (2.42)-(2.44) and (2.45)-(2.47).

The analysis to achieve this is most conveniently carried out when reparameterising the complex fields in terms of real component fields. Parameterising therefore the complex scalar field as $\phi_i = 1/\sqrt{2}(\varphi_i + i\chi_i)$ with $\varphi_i, \chi_i \in \mathbb{R}$ the action S_3 in

(2.39) acquires the form

$$S_3 = \int d^4x \left[\sum_{i=1}^3 \frac{1}{2} [\partial_\mu \varphi_i \partial^\mu \varphi_i + \partial_\mu \chi_i \partial^\mu \chi_i + c_i m_i^2 (\varphi_i^2 + \chi_i^2)] \right. \\ \left. + i c_\mu \mu^2 (\varphi_1 \chi_2 - \varphi_2 \chi_1) + i c_\nu \nu^2 (\varphi_3 \chi_2 - \varphi_2 \chi_3) - \frac{g}{16} (\varphi_1^2 + \chi_1^2)^2 \right]. \quad (2.49)$$

This approach differs slightly from Philip Mannheim's approach [79], who took the component fields to be complex as well. The continuous global $U(1)$ -symmetry (2.36) of the action is realised for the real fields as $\varphi_i \rightarrow \varphi_i \cos \alpha - \chi_i \sin \alpha$, $\chi_i \rightarrow \varphi_i \sin \alpha + \chi_i \cos \alpha$, that is $\delta \varphi_i = -\alpha \chi_i$ and $\delta \chi_i = \alpha \varphi_i$ for α small. The $\mathcal{CPT}_{1/2}$ symmetries in (2.40) manifests on these fields as

$$\mathcal{CPT}_{1/2} : \varphi_{1,3}(x_\mu) \rightarrow \pm \varphi_{1,3}(-x_\mu), \quad \varphi_2(x_\mu) \rightarrow \mp \varphi_2(-x_\mu), \quad (2.50) \\ \chi_{1,3}(x_\mu) \rightarrow \pm \chi_{1,3}(-x_\mu), \quad \chi_2(x_\mu) \rightarrow \mp \chi_2(-x_\mu), \quad i \rightarrow -i.$$

In this form also the antilinear symmetry

$$\mathcal{CPT}_{3/4} : \varphi_{1,2,3}(x_\mu) \rightarrow \pm \chi_{1,2,3}(-x_\mu), \quad \chi_{1,2,3}(x_\mu) \rightarrow \pm \varphi_{1,2,3}(-x_\mu), \quad i \rightarrow -i,$$

leaves the action invariant. Let us now transform the action S_3 in the form (2.49) to an equivalent Hermitian one.

A \mathcal{CPT} equivalent action, different types of vacua

We define now the analogue to the Dyson map [23] in quantum mechanics as

$$\eta = \exp \left[\frac{\pi}{2} \int d^3x \{ \Pi_2^\varphi(\mathbf{x}, t) \varphi_2(\mathbf{x}, t) \} \right] \exp \left[\frac{\pi}{2} \int d^3x \{ \Pi_2^\chi(\mathbf{x}, t) \chi_2(\mathbf{x}, t) \} \right], \quad (2.51)$$

involving the canonical momenta $\Pi_i^\varphi = \partial_t \varphi_i$ and $\Pi_i^\chi = \partial_t \chi_i$, $i = 1, 2, 3$. Using the Baker-Campbell-Hausdorff formula we compute the adjoint actions of η on the scalar fields as

$$\eta \varphi_i \eta^{-1} = (-i)^{\delta_{2i}} \varphi_i, \quad \eta \chi_i \eta^{-1} = (-i)^{\delta_{2i}} \chi_i, \\ \eta \phi_i \eta^{-1} = (-i)^{\delta_{2i}} \phi_i, \quad \eta \phi_i^* \eta^{-1} = (-i)^{\delta_{2i}} \phi_i^*. \quad (2.52)$$

The equal time commutation relations $[\psi_j(\mathbf{x}, t), \Pi_j^{\psi_j}(\mathbf{y}, t)] = i\delta(\mathbf{x}-\mathbf{y})$, $i = 1, 2, 3$, for $\psi = \varphi, \chi$ are preserved under these transformations. Applying this transformation

using the method explained in section 2.2, equation (2.20) to (2.49), we obtain the new equivalent action

$$\hat{S}_3 = \int d^4x \left[\sum_{i=1}^3 \frac{1}{2} (-1)^{\delta_{2i}} [\partial_\mu \varphi_i \partial^\mu \varphi_i + \partial_\mu \chi_i \partial^\mu \chi_i + c_i m_i^2 (\varphi_i^2 + \chi_i^2)] \right. \\ \left. + c_\mu \mu^2 (\varphi_1 \chi_2 - \varphi_2 \chi_1) + c_\nu \nu^2 (\varphi_3 \chi_2 - \varphi_2 \chi_3) - \frac{g}{16} (\varphi_1^2 + \chi_1^2)^2 \right]. \quad (2.53)$$

The $U(1)$ -symmetry is still realised in the same way as for S_3 , but the \mathcal{CPT} -symmetries for \hat{S}_3 are now modified to

$$\widehat{\mathcal{CPT}}_{1/2} : \varphi_{1,3}(x_\mu) \rightarrow \pm \varphi_{1,3}(-x_\mu), \quad \varphi_2(x_\mu) \rightarrow \mp \varphi_2(-x_\mu), \quad (2.54)$$

$$\chi_{1,3}(x_\mu) \rightarrow \mp \chi_{1,3}(-x_\mu), \quad \chi_2(x_\mu) \rightarrow \pm \chi_2(-x_\mu),$$

$$\widehat{\mathcal{CPT}}_{3/4} : \varphi_{1,2,3}(x_\mu) \rightarrow \pm \chi_{1,2,3}(-x_\mu), \quad (2.55)$$

The equations of motion resulting from functionally varying \hat{S}_3 with respect to the real fields are

$$-\square \varphi_1 = \frac{\partial V}{\partial \varphi_1} = -c_1 m_1^2 \varphi_1 - c_\mu \mu^2 \chi_2 + \frac{g}{4} \varphi_1 (\varphi_1^2 + \chi_1^2), \quad (2.56)$$

$$-\square \chi_2 = -\frac{\partial V}{\partial \chi_2} = -c_2 m_2^2 \chi_2 + c_\mu \mu^2 \varphi_1 + c_\nu \nu^2 \varphi_3, \quad (2.57)$$

$$-\square \varphi_3 = \frac{\partial V}{\partial \varphi_3} = -c_3 m_3^2 \varphi_3 - c_\nu \nu^2 \chi_2, \quad (2.58)$$

$$-\square \chi_1 = \frac{\partial V}{\partial \chi_1} = -c_1 m_1^2 \chi_1 + c_\mu \mu^2 \varphi_2 + \frac{g}{4} \chi_1 (\varphi_1^2 + \chi_1^2), \quad (2.59)$$

$$-\square \varphi_2 = -\frac{\partial V}{\partial \varphi_2} = -c_2 m_2^2 \varphi_2 - c_\mu \mu^2 \chi_1 - c_\nu \nu^2 \chi_3, \quad (2.60)$$

$$-\square \chi_3 = \frac{\partial V}{\partial \chi_3} = -c_3 m_3^2 \chi_3 + c_\nu \nu^2 \varphi_2. \quad (2.61)$$

We may write the action $\hat{\mathcal{I}}_3$ and the corresponding equation of motions more compactly. Introducing the column vector field $\Phi = (\varphi_1, \chi_2, \varphi_3, \chi_1, \varphi_2, \chi_3)^T$, the action acquires the concise form

$$\hat{S}_3 = \frac{1}{2} \int d^4x \left[\partial_\mu \Phi^T I \partial^\mu \Phi - \Phi^T H_t \Phi - \frac{g}{8} (\Phi^T E \Phi)^2 \right]. \quad (2.62)$$

Here we employed the Hessian matrix $H_{ij}(\Phi) = \left. \frac{\partial^2 V}{\partial \Phi_i \partial \Phi_j} \right|_{\Phi}$ which for our potential V_3 reads

$$H(\Phi) = \begin{pmatrix} \frac{g}{4}(3\varphi_1^2 + \chi_1^2) - c_1 m_1^2 & -c_\mu \mu^2 & 0 & \frac{g}{2} \varphi_1 \chi_1 & 0 & 0 \\ -c_\mu \mu^2 & c_2 m_2^2 & -c_\nu \nu^2 & 0 & 0 & 0 \\ 0 & -c_\nu \nu^2 & -c_3 m_3^2 & 0 & 0 & 0 \\ \frac{g}{2} \varphi_1 \chi_1 & 0 & 0 & \frac{g}{4}(\varphi_1^2 + 3\chi_1^2) - c_1 m_1^2 & c_\mu \mu^2 & 0 \\ 0 & 0 & 0 & c_\mu \mu^2 & c_2 m_2^2 & c_\nu \nu^2 \\ 0 & 0 & 0 & 0 & c_\nu \nu^2 & -c_3 m_3^2 \end{pmatrix}. \quad (2.63)$$

In (2.62) we use $H_t = H(\Phi_1^0)$, $\Phi_1^0 = (0, 0, 0, 0, 0, 0)$ and the 6×6 -matrices I , E with $\text{diag} I = (1, -1, 1, 1, -1, 1)$ and $\text{diag} E = (1, 0, 0, 1, 0, 0)$. Note that the kinetic term of equation (2.62) is no longer positive definite, which may result in a ghost field with unbounded energy. The resolution for this is discussed in the previous section, and the explicit forms of the biorthonormal basis will be given in section 2.3.4. The equation of motion resulting from (2.62) reads

$$-\square \Phi - I H_t \Phi - \frac{g}{4} I (\Phi^T E \Phi) E \Phi = 0. \quad (2.64)$$

We find different types of vacua by solving $\delta V = 0$, amounting to setting simultaneously the right hand sides of the equations (2.56)-(2.61) to zero and solving for the fields φ_i, χ_i . Denoting the solutions by $\Phi^0 = (\varphi_1^0, \chi_2^0, \varphi_3^0, \chi_1^0, \varphi_2^0, \chi_3^0)^T$, we find the vacua

$$\Phi_1^0 = (0, 0, 0, 0, 0, 0), \quad (2.65)$$

$$\Phi_2^0 = K(0) \left(1, \frac{c_3 c_\mu m_3^2 \mu^2}{\kappa}, -\frac{c_3 c_\mu m_3^2 \mu^2}{\kappa}, 0, 0, 0 \right), \quad (2.66)$$

$$\Phi_3^0 = K(0) \left(0, 0, 0, -1, \frac{c_3 c_\mu m_3^2 \mu^2}{\kappa}, \frac{c_\nu c_\mu \nu^2 \mu^2}{\kappa} \right), \quad (2.67)$$

$$\Phi_4^0 = \left(\varphi_1^0, \frac{c_3 c_\mu m_3^2 \mu^2 \varphi_1^0}{\kappa}, -\frac{c_\nu c_\mu \nu^2 \mu^2 \varphi_1^0}{\kappa}, -K(\varphi_1^0), \frac{c_3 c_\mu m_3^2 \mu^2 K(\varphi_1^0)}{\kappa}, \frac{c_\nu c_\mu \nu^2 \mu^2 K(\varphi_1^0)}{\kappa} \right), \quad (2.68)$$

where for convenience we introduced the function and constant

$$K(x) := \pm \sqrt{\frac{4c_3 m_3^2 \mu^4}{g\kappa} + \frac{4c_1 m_1^2}{g} - x^2}, \quad \kappa := c_2 c_3 m_2^2 m_3^2 + \nu^4. \quad (2.69)$$

Notice, that in the vacuum Φ_4^0 the field φ_1^0 is generic and not fixed. When varied it interpolates between the vacua Φ_2^0 and Φ_3^0 . For $(\varphi_1^0)^2 \rightarrow 4(c_1 m_1^2 \kappa + c_3 m_3^2 \mu^4)/g\kappa$ and $\varphi_1^0 \rightarrow 0$ we obtain $\Phi_4^0 \rightarrow \Phi_2^0$ and $\Phi_4^0 \rightarrow \Phi_3^0$, respectively. We also note that

$K(0) = 0$ at the special value of the coupling $\mu = \mu_s^4 = -c_1 m_1^2 \kappa / c_3 m_3^2$ so that $\Phi_2^0(\mu_s) = \Phi_1^0$. Unlike as in [79], where the vacuum is taken to be complex, our vacua are real. Next, we probe Goldstone's theorem by computing the masses resulting by expanding around the different vacua up to second order in the fields.

The mass spectra, \mathcal{PT} -symmetry

Defining the column vector field $\Phi = \Phi^0 + \hat{\Phi}$ with vacuum component Φ^0 as defined above and $\hat{\Phi} = (\hat{\varphi}_1, \hat{\chi}_2, \hat{\varphi}_3, \hat{\chi}_1, \hat{\varphi}_2, \hat{\chi}_3)^T$, we expand the potential about the vacua (2.65)-(2.68) as

$$V(\Phi) = V(\Phi^0 + \hat{\Phi}) = V(\Phi^0) + \nabla V(\Phi^0)^T \hat{\Phi} + \frac{1}{2} \hat{\Phi}^T H(\Phi^0) \hat{\Phi} + \dots \quad (2.70)$$

The linear term is of course vanishing, as by design $\nabla V(\Phi^0) = 0$. The squared mass matrix M^2 defined in section 2.2 is

$$(M^2)_{ij} = [IH(\Phi^0)]_{ij}. \quad (2.71)$$

In general this matrix is not diagonal, but in the \mathcal{CPT} -symmetric regime we may diagonalise it using the biorthonormal basis as explained in section 2.2. We may therefore introduce the masses m_i for the fields

$$\psi := T^T I \hat{\Phi} \quad (2.72)$$

as the positive square roots of the eigenvalues of the squared mass matrix M^2 , that is $m_i = \sqrt{\lambda_i}$. Naturally, this means the fields ψ_i in the specific form (2.72) are absent when M^2 can not be diagonalised by biorthonormal basis. From linear algebra, it is known that the biorthonormal basis can characterise any n -square matrix with n linearly independent eigenvectors [105]. It is characteristic of the non-Hermitian matrix that the eigenvectors become degenerate at the exceptional point. Meaning the matrix can only be decomposed down to Jordan block form rather than to a diagonal form. As a result of this, we will see in the next subsection that the Goldstone boson can not be identified at some particular types of exceptional points.

Since the squared mass matrix M^2 is not Hermitian but may have real eigenvalues λ_i in some regime, we can employ the standard framework from \mathcal{PT} -symmetric quantum mechanics with M^2 playing the role of the non-Hermitian Hamiltonian

[1, 104]. In the next section, a detailed discussion of how the \mathcal{CPT} operator acting on a theory with infinite degrees of freedom (i.e. quantum field theory) is related to the \mathcal{PT} operator acting on a finite dimensional theory (i.e. non-Hermitian matrix).

$U(1)$ and \mathcal{CPT} invariant vacuum, absence of Goldstone bosons

We investigate now the theory expanded about the trivial vacuum Φ_1^0 in (2.65). According to our discussion at the end of the last section, the theory expanded about this vacuum is invariant under the global $U(1)$ -symmetry and all four \mathcal{CPT} -symmetries. As the dimension of the coset, G/H equals 0, the standard field theoretical arguments on Goldstone's theorem suggest that we do not expect a Goldstone boson to emerge when expanding around this vacuum. It is also clear that the number of zero eigenvalues does not increase by expanding the action around the trivial vacuum because the form of the mass matrix does not change after the expansion. However, even in this simple case, we will observe novel features of the non-Hermitian theory. Consider the squared mass matrix as defined in (2.71)

$$M_1^2 = \begin{pmatrix} -c_1 m_1^2 & -c_\mu \mu^2 & 0 & 0 & 0 & 0 \\ c_\mu \mu^2 & -c_2 m_2^2 & c_\nu \nu^2 & 0 & 0 & 0 \\ 0 & -c_\nu \nu^2 & -c_3 m_3^2 & 0 & 0 & 0 \\ 0 & 0 & 0 & -c_1 m_1^2 & c_\mu \mu^2 & 0 \\ 0 & 0 & 0 & -c_\mu \mu^2 & -c_2 m_2^2 & -c_\nu \nu^2 \\ 0 & 0 & 0 & 0 & c_\nu \nu^2 & -c_3 m_3^2 \end{pmatrix}, \quad (2.73)$$

here, we label the matrix entries by the fields in the order defined for the vector field Φ . The two blocks are simply related as $c_{\nu/\mu} \rightarrow -c_{\nu/\mu}$. We find that the eigenvalues of each block only depend on the combination $c_{\nu/\mu}^2 = 1$. Therefore without loss of generality, we will only consider one block. Any result found in one block is applied to the other block by the replacement $c_{\nu/\mu} \rightarrow -c_{\nu/\mu}$.

To simplify the eigenvalues of the 3×3 block matrix, we let one of the eigenvalue be zero. This means we require the determinant of the matrix to be zero for each block, $\det(M_1^2) = -c_3 m_3^2 \mu^4 - c_1 m_1^2 \nu^4 - c_1 c_2 c_3 m_1^2 m_2^2 m_3^2 = 0$. This allows us to simplify the eigenvalues to $\{0, \lambda_\pm\}$ where

$$\lambda_\pm = \frac{1}{2} \text{Tr}(A) \pm \frac{1}{2} \sqrt{2 \text{Tr}(A^2) - \text{Tr}(A)}. \quad (2.74)$$

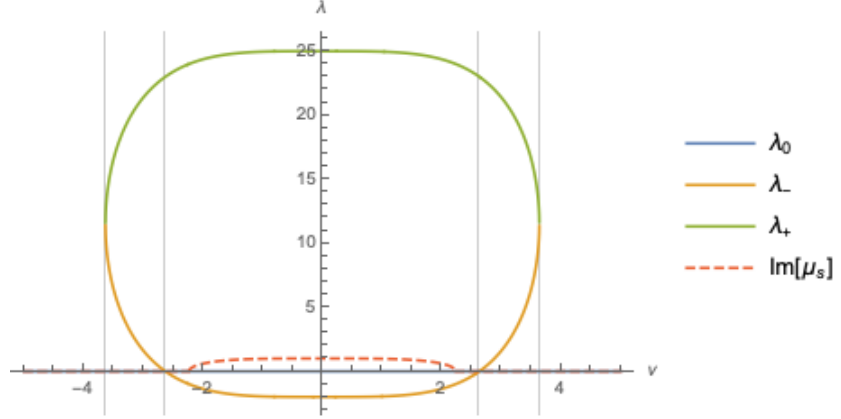


Figure 2.1: Eigenvalues λ of M_1^2 as a function of ν for $c_1 = c_2 = -c_3 = 1$, at the special point $\mu = \mu_s$ and imaginary part of the special point $\text{Im}(\mu_s)$. The physical regions are bounded by vertical lines, $5/13^{1/4} < \nu^2 < 135/2\sqrt{26}$.

The matrix A represent the 3×3 block diagonal matrix of M_1^2 . Notice that these eigenvalues take the same form as the coalescing eigenvalues shown in the introduction. In fact these eigenvalues also possesses exceptional point when $2\text{Tr}(A^2) = \text{Tr}(A)$ as one can see from figure 2.1.

By inspection, one may notice that there is a possibility for one of the eigenvalue to be zero. To see this explicitly, the equation $\det(M_1^2)(\mu_s) = 0$ has been solve for $\mu = \mu_s$ where $\mu_s = (m_1^2 m_2^2 - \nu^4 m_1^2 / m_3^2)^{1/4}$. Notice that μ_s can be seen as a function of other parameters, meaning one needs to take extra care when fixing the other parameters as it can lead to complex μ_s , which is a possibility that we omit to keep the analysis simple. The eigenvalues and the imaginary part of μ_s has been plotted in figure 2.1. We will disregard the regions where one of the eigenvalues is negative and the region where μ_s is imaginary because these regions correspond to complex masses. Then notice that in figure 2.1, there is a point where λ_- becomes zero. We note that this point is an exceptional point where two eigenvectors of λ_0 and λ_- coalesce, which reduces the rank of the square mass matrix. As we discussed in the previous section, the matrix can not be diagonalised at such a point. In fact, this point differs from the standard exceptional point as the eigenvalues are real before and after crossing the exceptional point. Such point has been dubbed *zero exceptional point*, where detail discussion can be found in appendix B. We observe here that the number of the massless particle is limited as the Lagrangian can not be diagonalised at the zero exceptional points where two eigenvalues are zero. We will see that this point will play a prominent role when the model is expanded around the $U(1)$ broken vacuum. We end the discussion of this subsection by concluding

that choosing different signs of the mass term such as $c_1 = c_2 = -c_3 = 1$ can give non trivial physical regions in the parameter space as one can see from figure 2.1. Namely that the theory is only well-defined between $5/13^{1/4} < \nu^2 < 135/2\sqrt{26}$, indicated as vertical lines in the figure 2.1.

$U(1)$ broken and \mathcal{CPT} -invariant vacua, presence of Goldstone bosons

Let us next choose another vacuum that in contrast to the previous section, breaks the global $U(1)$ -symmetry. In this case, we expect one massless Goldstone boson to appear. However, as in the previous case, there are some regions in the parameter space for which the model may possess a second massless particle. We choose now the vacuum Φ_2^0 . Notice that for $c_1 = -c_2 = c_3 = 1$ and $\mu \rightarrow \mu_s$, as defined above, the global symmetry breaking and symmetry preserving vacua coincide $\Phi_2^0 \rightarrow \Phi_1^0$, and therefore the previous discussion applies in that case. Expanding the action around this $U(1)$ -symmetry breaking vacuum for $\mu \neq \mu_s$, the corresponding squared mass matrix becomes

$$M_2^2 = \begin{pmatrix} \frac{3c_3 m_3^2 \mu^4}{\kappa} + 2c_1 m_1^2 & -c_\mu \mu^2 & 0 & 0 & 0 & 0 \\ c_\mu \mu^2 & -c_2 m_2^2 & c_\nu \nu^2 & 0 & 0 & 0 \\ 0 & -c_\nu \nu^2 & -c_3 m_3^2 & 0 & 0 & 0 \\ 0 & 0 & 0 & \frac{c_3 m_3^2 \mu^4}{\kappa} & c_\mu \mu^2 & 0 \\ 0 & 0 & 0 & -c_\mu \mu^2 & -c_2 m_2^2 & -c_\nu \nu^2 \\ 0 & 0 & 0 & 0 & c_\nu \nu^2 & -c_3 m_3^2 \end{pmatrix} \quad (2.75)$$

$$= \begin{pmatrix} A_2^2 & 0 \\ 0 & B_2^2 \end{pmatrix} \quad (2.76)$$

with $\det M_2^2 = 0$, hence indicating a zero eigenvalue. We have denoted the upper and lower 3×3 blocks as A_2^2 and B_2^2 , respectively. Let us now comment on where this Goldstone boson originates from. Both blocks in M_2^2 are of the following general 3×3 -matrix form

$$\begin{pmatrix} A & W & 0 \\ -W & B & -V \\ 0 & V & -C \end{pmatrix}, \quad (2.77)$$

whose eigenvalues are solutions to the cubic characteristic equation $\lambda^3 + r\lambda^2 + s\lambda + t = 0$ with

$$r = C - A - B, \quad s = V^2 + W^2 + AB - C(A + B), \quad t = ABC + CW^2 - AV^2. \quad (2.78)$$

Reading off the entries for the block in the lower right corner of M_2^2 as $A = c_3 m_3^2 \mu^4 / \kappa$, $B = -c_2 m_2^2$, $C = c_3 m_3^2$, $W = c_\mu \mu^2$, $V = c_\nu \nu^2$, we find that the constant term in the characteristic equation is zero, i.e. $t = 0$. Hence at least one eigenvalue becomes zero. The remaining equation is simply quadratic with solutions

$$\lambda_\pm = \frac{c_3 m_3^2 \mu^4}{2\kappa} - \frac{c_2 m_2^2 + c_3 m_3^2}{2} \pm \frac{1}{2\kappa} \sqrt{m_3^4 (\mu^4 - \mu_e^4)^2 + 4c_\nu \nu^2 \kappa^{3/2} (\mu^4 - \mu_e^4)}. \quad (2.79)$$

We introduced here the quantity $\mu_e^\pm = [\kappa(\kappa - m_3^4 + \nu^4 \pm 2c_\nu \nu^2 \sqrt{\kappa})]^{1/4} / m_3$, that signifies the value for μ at which the eigenvalues λ_+ and λ_- coincide, which is the exceptional point. For the block in the top left corner we identify $A = 3c_3 m_3^2 \mu^4 / \kappa + 2c_1 m_1^2$, $B = -c_2 m_2^2$, $C = c_3 m_3^2$, $W = -c_\mu \mu^2$ and $V = -c_\nu \nu^2$. The linear term becomes $t = -2(c_3 m_3^2 \mu^4 + c_1 m_1^2 \nu^4 + c_1 c_2 c_3 m_1^2 m_2^2 m_3^2)$, which is exactly twice the value of t obtained previously for the vacuum Φ_1^0 . For $t \neq 0$ we define with (2.78) the quantities

$$\begin{aligned} \rho &= \sqrt{-\frac{p^3}{27}}, \quad \cos \theta = -\frac{q}{2\rho}, \quad p = \frac{3s-r^2}{3}, \\ q &= \frac{2r^3}{27} - \frac{rs}{3} + t, \quad \Delta = \left(\frac{p}{3}\right)^3 + \left(\frac{q}{2}\right)^2. \end{aligned} \quad (2.80)$$

Then, provided that $p < 0$ and $\Delta \leq 0$, the remaining three eigenvalues are real and according to Cardano's formula of the form

$$\lambda_i = 2\rho^{1/3} \cos \left[\frac{\theta}{3} + \frac{2\pi}{3}(i-1) \right], \quad i = 1, 2, 3. \quad (2.81)$$

Similarly as for the vacuum Φ_1^0 the values of c_μ and c_ν are not relevant for the computation of the eigenvalues. Naturally, for these eigenvalues to be interpretable as squared masses they need to be non-negative. There are indeed some regions in the parameter space for which this holds, taking for instance $c_1 = c_3 = -c_2 = 1$, $m_1 = 1$, $m_2 = 1/2$, $m_3 = 1/5$, $\mu = 2$ and $\nu = 1/2$ we compute the six non-negative eigenvalues $(\lambda_1, \lambda_3, \lambda_2, \lambda_+, \lambda_-, 0) = (38.1493, 0.5683, 0.0639, 10.6534, 1.7471, 0)$. However, as seen in figure 2.2 these physical regions are quite isolated in the parameter space.

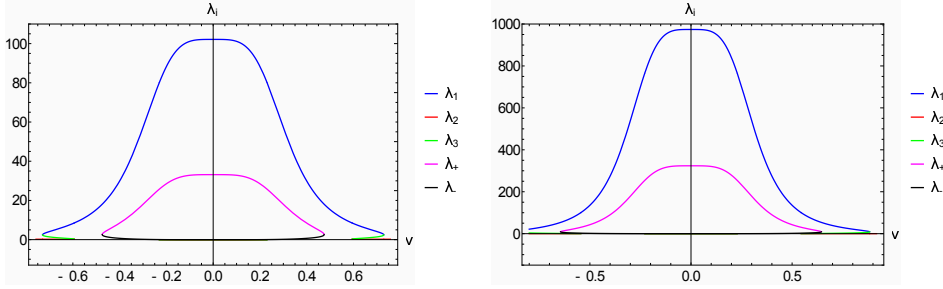


Figure 2.2: Nonvanishing eigenvalues λ_i of M_2^2 as a functions of ν for $c_1 = c_2 = c_3 = 1$, $m_1 = 1$, $m_2 = 1/2$ and $m_3 = 1/5$. In the left panel we choose $\mu = 1.7$ observing that there is no physical region for which all eigenvalues are non-negative. In the right panel we choose $\mu = 3$ and have two physical regions for $\nu \in (-0.64468, -0.54490)$ and $\nu \in (0.54490, 0.64468)$.

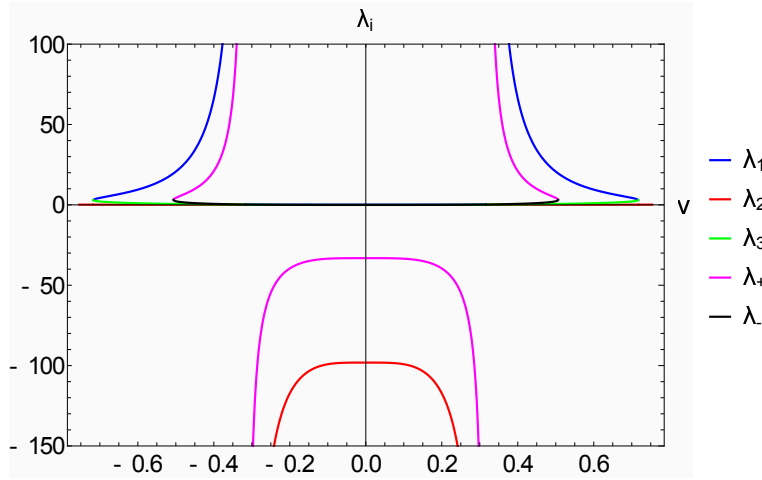


Figure 2.3: Nonvanishing eigenvalues λ_i of M_2^2 as a function of ν for $c_1 = -c_2 = c_3 = 1$, $m_1 = 1$, $m_2 = 1/2$, $m_3 = 1/5$ and $\mu = 1.7$. Singularities occur at $\nu = \nu_{\text{sing}}^{\pm} \approx \pm 0.31623$. The regimes $\nu \in (-0.50608, \nu_{\text{sing}}^-)$, $\nu \in (\nu_{\text{sing}}^+, 0.50608)$ are physical.

For the choice $c_1 = -c_3 = \pm 1$ we may also find a value for $\nu = \nu_{\text{sing}}^{\pm} = \pm \sqrt{m_2 m_3}$, for which $\kappa \rightarrow 0$ leading to singularities in the eigenvalues. Figure 2.3 depicts such a situation.

As for the case with $U(1)$ -invariant vacuum, for some specific choices of μ we can generate an additional massless particle. Since the linear term of the characteristic equation for the upper right corner is simply twice the one of the previous section, this scenario occurs for $\mu = \mu_s$. i.e $\det(A_2^2(\mu_s)) = 0$. However, as we pointed out above, for this value of μ the two vacua Φ_1^0 and Φ_2^0 coincide, so that the discussion of the previous section applies. The square mass matrix is no longer diagonalisable using a biorthonormal basis. In addition, as the two blocks are different in this case there is a second choice $\bar{\mu}_s^4 = \kappa^2 / (m_3^4 - \nu^4)$ for which $\lambda_- = 0$ found by solving $\det(B_2^2(\bar{\mu}_s)) = 0$. The non-zero eigenvalue coalesces with the zero eigenvalue at the zero-exceptional point. Hence, it appears that besides the Goldstone boson, there is

a second massless, non-Goldstone, particle present in the model. However, this is not the case as one can not identify this second massless field using the diagonalisation method explained in equation (2.30). We will show this explicitly in section 2.3.4.

Choosing instead the vacuum Φ_3^0 , the resulting mass matrix M_3^2 is similar to M_2^2 with the block in the top left corner and lower right corner exchanged accompanied by the transformation $c_{\nu/\mu} \rightarrow -c_{\nu/\mu}$, hence the previous discussion applied in this case.

Expanding instead around the vacuum Φ_4^0 the resulting mass matrix reads

$$M_4^2 = \begin{pmatrix} \frac{c_3 m_3^2 \mu^4}{\kappa} + (\varphi_1^0)^2 & -\frac{g}{2} c_\mu \mu^2 & 0 & \frac{g}{2} \varphi_1^0 \chi_1^0 & 0 & 0 \\ c_\mu \mu^2 & -c_2 m_2^2 & c_\nu \nu^2 & 0 & 0 & 0 \\ 0 & -c_\nu \nu^2 & -c_3 m_3^2 & 0 & 0 & 0 \\ \frac{g}{2} \varphi_1^0 \chi_1^0 & 0 & 0 & 2c_1 m_1^2 + \frac{3c_3 m_3^2 \mu^4}{\kappa} - \frac{g}{2} (\varphi_1^0)^2 & c_\mu \mu^2 & 0 \\ 0 & 0 & 0 & -c_\mu \mu^2 & -c_2 m_2^2 & -c_\nu \nu^2 \\ 0 & 0 & 0 & 0 & c_\nu \nu^2 & -c_3 m_3^2 \end{pmatrix}.$$

Computing the sixth order characteristic polynomial for M_4^2 we find that the dependence on the free field φ_1^0 drops out entirely. We also note that the linear term always vanishes and that therefore a Goldstone boson is present for this vacuum. We will not present here a more detailed discussion as the qualitative behaviour of the model is similar to the one discussed in detail in the previous section. The model posses various well defined physical regions. For instance, for $c_1 = -1$, $c_2 = c_3 = c_\mu = c_\nu = 1$, $m_1 = 2$, $m_2 = 1/2$, $m_3 = 1/10$, $\mu = 3/2$ and $\nu = 0.28$ we find the eigenvalues $(0, 0.0130, 0.2731, 0.7294, 4.8655, 9.0186)$ for M_4^2 . Let us now see how to explain the reality of the mass spectrum.

2.3.3 Relating field theoretic \mathcal{CPT} operator to quantum mechanical \mathcal{PT} operators

First, we clarify that the \mathcal{CPT} operator acts on the fields which have infinite degree of freedom. Where as the \mathcal{PT} operator in question acts on the non-Hermitian matrix, which is used to draw an analogy to the finite dimensional \mathcal{PT} symmetric quantum mechanics. In order to identify that connection, let us first see which properties the \mathcal{P} -operator must satisfy at the level of the action. Expressing S_3 in the form

$$S_3[\Phi] = S_3^M[\Phi] + S_3^{\text{int}}[\Phi] = \frac{1}{2} \int d^4x [\Phi^T (\square + M^2) \Phi] + S_3^{\text{int}}[\Phi], \quad (2.82)$$

with real field vector Φ , the action of the \mathcal{CPT} -operator on $S_3^M[\Phi]$ is

$$\begin{aligned} \mathcal{CPT} : S_3^M[\Phi] &\rightarrow \frac{1}{2} \int d^4x \left[\Phi^T \left[\mathcal{C}\mathcal{P}^T \mathcal{C}\mathcal{P} \square + \mathcal{C}\mathcal{P}^T (M^2)^* \mathcal{C}\mathcal{P} \right] \Phi \right], \\ &= \frac{1}{2} \int d^4x \left[\Phi^T \left[\mathcal{P}^T \mathcal{P} \square + \mathcal{P}^T (M^2)^* \mathcal{P} \right] \Phi \right] \end{aligned} \quad (2.83)$$

Where the \mathcal{T} operator conjugated the mass matrix as it is an anti-linear operator and the charge conjugation does not affect the real scalar field. Hence for this part of the action to be invariant we require the \mathcal{P} -operator to obey the two relations

$$\mathcal{P}^T \mathcal{P} = \mathbb{I}, \quad \text{and} \quad (M^2)^* \mathcal{P} = \mathcal{P} M^2. \quad (2.84)$$

This is in fact the same property \mathcal{P} needs to satisfy in the \mathcal{PT} -quantum mechanical framework. Therefore, we see that \mathcal{CPT} operator acting on a theory with infinite degree of freedom (i.e. quantum field theory) is reduced to \mathcal{PT} operator acting on a finite dimensional non-Hermitian matrix M^2 , satisfying the above relations.

Let us see how to construct \mathcal{P} when given the non-Hermitian matrix M^2 . Following the method presented in [108], we start by constructing a biorthonormal basis from the left and right eigenvectors u_n and v_n , respectively, of M^2

$$M^2 v_n = \varepsilon_n v_n, \quad (M^2)^\dagger u_n = \varepsilon_n u_n \quad (2.85)$$

satisfying

$$\langle u_n | v_n \rangle = \delta_{nm}, \quad \sum_n |u_n\rangle \langle v_n| = \sum_n |v_n\rangle \langle u_n| = \mathbb{I}. \quad (2.86)$$

The left and right eigenvectors are related by the \mathcal{P} -operator as

$$|u_n\rangle = s_n \mathcal{P} |v_n\rangle. \quad (2.87)$$

with $s_n = \pm 1$ defining the signature. Combining (2.87), (2.86) and the first relation in (2.84) we can express the \mathcal{P} -operator and its transpose in terms of the left and right eigenvectors as

$$\mathcal{P} = \sum_n s_n |u_n\rangle \langle u_n|, \quad \text{and} \quad \mathcal{P}^T = \sum_n s_n |v_n\rangle \langle v_n|. \quad (2.88)$$

The biorthonormal basis can also be used to construct an operator, often denoted

with the symbol C , that is closely related to the metric ρ used in non-Hermitian quantum mechanics

$$C = \mathcal{P}^T \rho = \sum_n s_n |v_n\rangle \langle u_n|. \quad (2.89)$$

Despite its notation, this operator is not to be confused with the charge conjugation operator \mathcal{C} employed on the level of the action. The operator C satisfies the algebraic properties [32]

$$[C, M^2] = 0, \quad [C, \mathcal{PT}] = 0, \quad C^2 = \mathbb{I}. \quad (2.90)$$

When compared to the quantum mechanical setting, the operator T^{-1} defined in the general example (2.28) in section 2.2 plays the analogue to the Dyson map η and the combination $(T^{-1})^\dagger T^{-1}$ is the analogue to the metric operator ρ . However, constructing \mathcal{P} with M^2 as a starting point does of course not guarantee that also $S_3^{\text{int}}[\Phi]$ will be invariant under \mathcal{CPT} when using this particular \mathcal{P} -operator. In fact, we shall see next that there are many solutions to the two relations in (2.84) that do not leave $S_3^{\text{int}}[\Phi]$ invariant. Thus for these \mathcal{CPT} -operators, the symmetry is broken on the level of the action. However, the mass spectra would still be real as the symmetry is preserved at the second order in the fields, and the breaking only occurs at higher order.

Explicit example

We consider now the lower right block of the squared mass matrix in (2.75) and construct a \mathcal{P} -operator in a manner as describes above. Subsequently, we verify whether the operator constructed in the manner is a parity operator that can be used in the \mathcal{CPT} -symmetry transformations that leave the quantum field theoretical actions invariant. Including the remaining part of the squared mass matrix is straightforward.

We consider the version of M_2^2 resulting from the action before carrying out the similarity transformation, with the lower right block in (2.75) given as

$$\mathcal{M} = \begin{pmatrix} \frac{c_3 m_3^2 \mu^4}{\kappa} & i c_\mu \mu^2 & 0 \\ i c_\mu \mu^2 & -c_2 m_2^2 & -i c_\nu \nu^2 \\ 0 & -i c_\nu \nu^2 & -c_3 m_3^2 \end{pmatrix}. \quad (2.91)$$

As explained in the introduction, the standard argument that explains the reality of the spectrum for this non-Hermitian matrix is simply stated: The eigenvalues of non-Hermitian \mathcal{M} are real if and only if there exists an antilinear operator \mathcal{PT} , satisfying

$$[\mathcal{M}, \mathcal{PT}] = 0, \quad \text{and} \quad \mathcal{PT}v_n = v_n, \quad (2.92)$$

with v_n denoting the eigenvectors of \mathcal{M} , the eigenvalues λ_n of \mathcal{M} are real. When in (2.92) only the first relation holds and $\mathcal{PT}v_n \neq v_n$, the \mathcal{PT} -symmetry is spontaneously broken and some of the eigenvalues emerge in complex conjugate pairs.

To check this statement for our concrete matrix and in particular to construct an explicit expression for the \mathcal{P} -operator we compute first the normalised left and right eigenvectors for this non-Hermitian matrix as defined in (2.85)

$$v_j = (-1)^{\delta_{-,j}} u_j^* = \frac{1}{N_j} \{-\lambda_j \Lambda_j - \kappa, -i\Lambda_j^3 c_\mu \mu^2, -c_\mu c_\nu \mu^2 \nu^2\}, \quad j = 0, \pm, \quad (2.93)$$

with normalisation constants

$$N_\pm^2 = (\kappa + \lambda_\pm \Lambda_\pm) \lambda_\pm (\lambda_+ - \lambda_-), \quad (2.94)$$

$$N_0^2 = \kappa \lambda_- \lambda_+, \quad (2.95)$$

where we abbreviated $\Lambda_j := \lambda_j + c_2 m_2^2 + c_3 m_3^2$ and $\Lambda_j^k := \lambda_j + c_k m_k^2$. We confirm that the set of vectors $\{v_j, u_j\}$ with $j = 0, \pm$ form indeed a biorthonormal basis by verifying (2.86).

Next we use relation (2.88) to compute the \mathcal{P} -operator

$$\mathcal{P} = \sum_{j=0,\pm} \frac{s_j}{N_j^2} \begin{pmatrix} (\Lambda_j^2 \Lambda_j^3 + \nu^4)^2 & i\mu^2 \Lambda_j^3 (\Lambda_j^2 \Lambda_j^3 + \nu^4) & \mu^2 \nu^2 (\Lambda_j^2 \Lambda_j^3 + \nu^4) \\ -i\mu^2 \Lambda_j^3 (\Lambda_j^2 \Lambda_j^3 + \nu^4) & \mu^4 (\Lambda_j^3)^2 & -i\nu^2 \mu^4 \Lambda_j^3 \\ \mu^2 \nu^2 (\Lambda_j^2 \Lambda_j^3 + \nu^4) & i\nu^2 \mu^4 \Lambda_j^3 & \mu^4 \nu^4 \end{pmatrix}. \quad (2.96)$$

Given all possibilities for the signatures s_n , we have found eight different \mathcal{CP} -operators. All of them satisfy the two relations in (2.84). However, two signatures

are very special as for them the expressions simplify considerably

$$\mathcal{P}(s_0 = \pm 1, s_- = \mp 1, s_+ = \pm 1) = \begin{pmatrix} \pm 1 & 0 & 0 \\ 0 & \mp 1 & 0 \\ 0 & 0 & \pm 1 \end{pmatrix}. \quad (2.97)$$

Moreover, in this case, the \mathcal{P} -operators are indeed the operators involved in the $\mathcal{CPT}_{1/2}$ -symmetry transformation, concretely showing a connection between the field theoretic modified \mathcal{CPT} operator with quantum mechanical \mathcal{PT} operator.

Notice that at the exceptional point, $\lambda_- = \lambda_+$, the normalisation factors N_{\pm} becomes zero so that the eigenvectors v_{\pm} and u_{\pm} are no longer defined. Passing this point corresponds to breaking the \mathcal{PT} -symmetry spontaneously, and the second relation in (2.92) no longer holds.

To complete the discussion, we end this subsection by calculating the quantum mechanical C operator as defined in equation (2.89) in two alternative ways to

$$C = \sum_{j=0,\pm} \frac{(-1)^{\delta_{-,j}} s_j}{N_j^2} \begin{pmatrix} (\Lambda_j^2 \Lambda_j^3 + \nu^4)^2 & i\mu^2 \Lambda_j^3 (\Lambda_j^2 \Lambda_j^3 + \nu^4) & \mu^2 \nu^2 (\Lambda_j^2 \Lambda_j^3 + \nu^4) \\ i\mu^2 \Lambda_j^3 (\Lambda_j^2 \Lambda_j^3 + \nu^4) & -\mu^4 (\Lambda_j^3)^2 & i\nu^2 \mu^4 \Lambda_j^3 \\ \mu^2 \nu^2 (\Lambda_j^2 \Lambda_j^3 + \nu^4) & i\nu^2 \mu^4 \Lambda_j^3 & \mu^4 \nu^4 \end{pmatrix}. \quad (2.98)$$

We verify that C does indeed satisfy all the relations in (2.90). The Dyson operator is identified as $\eta = U^{-1}$ with $T = (v_0, v_+, v_-)$ and the metric operator as $\rho = \eta^\dagger \eta$. Since $\det T = i\lambda_- \lambda_+ (\lambda_- - \lambda_+) \mu^4 \nu^2 / N_0 N_- N_+$ both operators exist in the \mathcal{PT} -symmetric regime. The fact that the C -operator is not unique [109] is a well known fact, similarly as for the metric operator.

2.3.4 Goldstone bosons in \mathcal{CPT} -symmetric and broken regimes

The Goldstone boson in the \mathcal{CPT} -symmetric regime

Let us now compute the explicit expression for the Goldstone boson. As we have seen in section 2.3.2, the Goldstone boson emerges from the lower right block

$$B_2^2 = \begin{pmatrix} \frac{c_3 m_3^2 \mu^4}{\kappa} & c_\mu \mu^2 & 0 \\ -c_\mu \mu^2 & -c_2 m_2^2 & -c_\nu \nu^2 \\ 0 & c_\nu \nu^2 & -c_3 m_3^2 \end{pmatrix}, \quad (2.99)$$

so that it suffices to consider that part of the squared mass matrix. Denoting the quantities related to the lower right block by a subscript r and the upper left block

by ℓ , we decompose the Lagrangian into $\mathcal{L}_3 = \mathcal{L}_{3,\ell} + \mathcal{L}_{3,r}$ and define the quantities

$$\begin{aligned}\hat{\Phi}_r &:= (\hat{\chi}_1, \hat{\varphi}_2, \hat{\chi}_3), & (B_2^2)_r v_i &= \lambda_i v_i, & (B_2^2)_r^\dagger u_i &= \lambda_i u_i, \\ U &:= (v_0, v_+, v_-), & U^{-1} &= (u_0, u_+, u_-) = U^T I, & i &= 0, \pm.\end{aligned}\quad (2.100)$$

Where $I = \text{diag}(1, -1, 1)$. Similarly for $\mathcal{L}_{3,\ell}$, which we, however, do not analyse here as it does not contain a Goldstone boson. Thus, as long as the spectrum of B_2^2 is not degenerate, and hence all the eigenvectors v_i are linearly independent, the matrix U diagonalizes the lower right block of the squared mass matrix $U^{-1}(B_2^2)_r U = D$ with $\text{diag} D = (\lambda_0, \lambda_+, \lambda_-) = (m_0^2, m_+^2, m_-^2)$. As argued in general in equation (2.72), we may therefore define the fields ψ_k , $k = 0, \pm$, with masses m_i by re-writing the mass term

$$\begin{aligned}\hat{\Phi}_r^T (B_2^2)_r \hat{\Phi}_r &= \sum_{k=0,\pm} m_k^2 \psi_k^2 = \sum_{k=0,\pm} m_k^2 (\hat{\Phi}_r^T I U)_k (U^{-1} \hat{\Phi}_r)_k \\ &= \sum_{k=0,\pm} m_k^2 (\hat{\Phi}_r^T I U)_k (U^T I \hat{\Phi}_r)_k.\end{aligned}\quad (2.101)$$

Hence, the Goldstone field corresponding to ψ_0 is expressible as

$$\psi_{\text{Gb}} := \left(U^T I \hat{\Phi}_r \right)_0. \quad (2.102)$$

The unnormalised right eigenvectors for B_2^2 are computed to

$$v_i = \{-\lambda_i \Lambda_i - \kappa, \Lambda_i^3 c_\mu \mu^2, c_\mu c_\nu \mu^2 \nu^2\}, \quad i = 0, \pm, \quad (2.103)$$

where Λ_i and Λ_i^3 are defined in the previous subsection. The explicit form of the Goldstone boson field in the original fields becomes

$$\psi_{\text{Gb}} := \frac{1}{\sqrt{N}} \left(-\kappa \hat{\chi}_1 - c_3 c_\mu m_3^2 \mu^2 \hat{\varphi}_2 + c_\mu c_\nu \mu^2 \nu^2 \hat{\chi}_3 \right), \quad (2.104)$$

with normalisation factor

$$N = m_3^4 (m_2^4 - \mu^4) + (2c_2 c_3 m_2^2 m_3^2 + \mu^4) \nu^4 + \nu^8 = \kappa^2 \left(1 - \frac{\mu^2}{\bar{\mu}_s^2} \right), \quad (2.105)$$

where $\bar{\mu}_s$ is found by solving $\det(B_2^2(\bar{\mu})) = 0$, for which $\lambda_- = 0$, that is the zero-exceptional point. Other fields in the Lagrangian can be defined in the same manner. Computing the determinant of U to $\det U = c_\nu \lambda_- \lambda_+ (\lambda_- - \lambda_+) \nu^2 \mu^4$, the origin of

this singularity is clear, as U is not invertible for vanishing for $\lambda_- = 0$ and at the standard exceptional points when $\lambda_- = \lambda_+$. The former scenario occurs for $\mu = \bar{\mu}_s$ and the latter for $\mu_e^\pm = [\kappa(\kappa - m_3^4 + \nu^4 \pm 2c_\nu \nu^2 \sqrt{\kappa})]^{1/4} / m_3$, where $\kappa = c_2 c_3 m_2^2 m_3^2 + \nu^4$. So that in these circumstances, the Goldstone boson of the form (2.104) does not exist. We discuss these two scenarios separately in the next two sections.

The Goldstone boson at the standard exceptional point

As pointed out in the previous section, at the exceptional point when $\lambda_- = \lambda_+ =: \lambda_e$ the matrix U is no longer invertible so that ψ_{Gb} in (2.102) becomes ill-defined. However, when $\mu = \mu_e^+ = \mu_e$ we may transform the lower right block of B_2^2 into Jordan normal form as

$$T^{-1} [B_2^2(\mu = \mu_e)]_r T = \begin{pmatrix} 0 & 0 & 0 \\ 0 & \lambda_e & a \\ 0 & 0 & \lambda_e \end{pmatrix} = J, \quad (2.106)$$

for some as yet unspecified constant $a \in \mathbb{R}$. For simplicity we select here the upper sign of the two possibilities μ_e^\pm . We can then express the transformed action expanded around the vacuum Φ_2^0 and formulate the Goldstone boson in terms of the original fields

$$\begin{aligned} \hat{\mathcal{I}}_3 &= -\frac{1}{2} \int d^4x \left[\hat{\Phi}^T I(\square + M_2^2) \hat{\Phi} + \mathcal{L}_{\text{int}}(\hat{\Phi}) + \mathcal{L}_{3,\ell} \right] \\ &= -\frac{1}{2} \int d^4x \left[\hat{\Phi}^T I T(\square + J) T^{-1} \hat{\Phi} + \mathcal{L}_{\text{int}}(\hat{\Phi}) + \mathcal{L}_{3,\ell} \right] \\ &= -\frac{1}{2} \int d^4x \left[\sum_{i=1}^3 \psi_i \square \psi_i + \lambda_e (\psi_2^2 + \psi_3^2) + a \psi_2^L \psi_3^R + \mathcal{L}_{\text{int}}(\psi_i) + \mathcal{L}_{3,\ell} \right]. \end{aligned} \quad (2.107)$$

We have introduced here the fields

$$\psi_i := \sqrt{\psi_i^L \psi_i^R}, \quad \psi_i^L := (\hat{\Phi}_r^T I T)_i, \quad \psi_i^R := (T^{-1} \hat{\Phi}_r)_i, \quad (2.108)$$

with the Goldstone boson at the exceptional point being identified as $\psi_{\text{Gb}}^e := \psi_1$. We will see below that the Goldstone boson defined with the above definition admits a linear form in terms of the old fields. Notice that when $T^T I T = \mathbb{I}$, the fields coincide, i.e. we have $\psi_i^L = \psi_i^R = \psi_i$. Let us now determine the matrix T and demonstrate that it is well-defined. We take $\mu = \mu_e$ so that the nonzero eigenvalue for $M_2^2(\mu_e)$

becomes

$$\lambda_e = \frac{\nu^4 - m_3^4 + c_\nu \nu^2 \sqrt{\kappa}}{c_3 m_3^2}. \quad (2.109)$$

Using the eigenvalues corresponding to the zero eigenvalues of $M_2^2(\mu_e)$ and the eigenvector corresponding to the eigenvalue λ_e in the first and second column of T , respectively, we solve equation (2.106) for T as

$$T = \begin{pmatrix} -\kappa c_3 m_3^2 & -c_3 m_3^2 \mu_e^2 & t \\ m_3^4 \mu_e^2 & \kappa + c_\nu \nu^2 \sqrt{\kappa} & s \\ c_3 c_\nu \nu^2 m_3^2 \mu_e^2 & c_3 m_3^2 \sqrt{\kappa} & \frac{s - \sqrt{\kappa}}{c_3 m_3^2 + \lambda_e} \nu^2 \end{pmatrix}, \quad (2.110)$$

with abbreviations $t := (1 - m_3^4 - \nu^4) \mu_e^2 / (\lambda_e \sqrt{\kappa})$, $s := t (\lambda_e / \mu_e^2 - c_3 m_3^2 \mu_e^2 / \kappa) - \nu^2$ and a as defined in (2.106) taken to $a = \nu^2 / m_3^6$. We compute $\det T = \kappa m_3^4 \lambda_e^2$. We have imposed here $\psi_1^L = \psi_1^R = \psi_1$. Using these expression, we obtain from (2.108) the Goldstone boson at the exceptional point as

$$\psi_{\text{Gb}}^e = \frac{1}{\kappa c_3 m_3^2 \lambda_e^2} (-\kappa \hat{\chi}_1 - m_3 \mu_e^2 \hat{\varphi}_2 + \nu^2 \mu_e^2 \hat{\chi}_3). \quad (2.111)$$

Thus at the exceptional point the Goldstone boson ψ_{Gb}^e is well-defined unless $\lambda_e = 0$, $\kappa = 0$ or $m_3 = 0$, as in these cases the matrix T is not invertible. Crucially, the above Goldstone boson can not be obtained continuously from equation (2.104), which means that the identification of the Goldstone boson in the \mathcal{PT} symmetric region and the standard exceptional points needs separate treatments.

The Goldstone boson at the zero-exceptional point

Another interesting point at which the general expression for the Goldstone boson in (2.102) is not valid occurs for $\mu = \bar{\mu}_s$, that is when $\lambda_- = 0$ and $\det(B_2^2(\bar{\mu}_s)) = 0$, i.e. at the zero-exceptional point. Since the lower right block B_2^2 can not be diagonalised, the best we can do is to transform into the variation of the Jordan normal form

$$S^{-1} [M_2^2(\mu = \bar{\mu}_s)]_r S = \begin{pmatrix} 0 & 0 & b \\ 0 & \lambda_s & 0 \\ 0 & 0 & 0 \end{pmatrix} = K, \quad (2.112)$$

for some as yet unspecified constant $b \in \mathbb{R}$. As before we can then express the transformed action expanded around the vacuum Φ_2^0 and formulate the Goldstone boson in terms of the original fields

$$\begin{aligned}\hat{\mathcal{I}}_3 &= -\frac{1}{2} \int d^4x \left[\hat{\Phi}^T I (\square + M_2^2) \hat{\Phi} + \mathcal{L}_{\text{int}}(\hat{\Phi}) + \mathcal{L}_{3,\ell} \right], \\ &= -\frac{1}{2} \int d^4x \left[\hat{\Phi}^T I S (\square + K) S^{-1} \hat{\Phi} + \mathcal{L}_{\text{int}}(\hat{\Phi}) + \mathcal{L}_{3,\ell} \right], \\ &= -\frac{1}{2} \int d^4x \left[\sum_{i=1}^3 \psi_i \square \psi_i + \lambda_s \psi_2^2 + b \psi_1^L \psi_3^R + \mathcal{L}_{\text{int}}(\psi_i) + \mathcal{L}_{3,\ell} \right],\end{aligned}\tag{2.113}$$

where we introduced

$$\psi_i := \sqrt{\psi_i^L \psi_i^R}, \quad \psi_i^L := (\hat{\Phi}_r^T I S)_i, \quad \psi_i^R := (S^{-1} \hat{\Phi}_r)_i.\tag{2.114}$$

Taking $\mu = \bar{\mu}_s$, the only nonzero eigenvalue for $M_2^2(\bar{\mu}_s)$ becomes

$$\lambda_z = \frac{(c_2 m_2^2 + 2c_3 m_3^2) \nu^4 - c_3 m_3^6}{m_3^4 - \nu^4}.\tag{2.115}$$

Using the null vector of $M_2^2(\bar{\mu}_s)$ and the eigenvector corresponding to the eigenvalue λ_e in the first and second column of S , respectively, we solve equation (2.112) for S to

$$S = \begin{pmatrix} -\sqrt{m_3^4 - \nu^4} & -\nu^2 \kappa & 0 \\ c_3 m_3^2 & (c_2 m_2^2 + c_3 m_3^2) \nu^2 \sqrt{m_3^4 - \nu^4} & \frac{b}{\kappa} (\nu^4 - m_3^4) \\ \nu^2 & (m_3^4 - \nu^4)^{3/2} & -\frac{b}{\kappa} (c_2 m_2^2 + c_3 m_3^2) \nu^2 \end{pmatrix}.\tag{2.116}$$

We compute $\det S = -b \lambda_z^2 (m_3^4 - \nu^4)^2 / \kappa$. The massive field ψ_2 can be identified easily for any value of b as

$$\psi_2 = \frac{1}{N_2} \psi_2^L\tag{2.117}$$

when noting that

$$\psi_2^L = N_2^2 \psi_2^R = -\kappa \nu^2 \hat{\chi}_1 - (c_2 m_2^2 + c_3 m_3^2) \nu^2 \sqrt{m_3^4 - \nu^4} \hat{\varphi}_2 + (m_3^4 - \nu^4)^{3/2} \hat{\chi}_3,$$

with $N_2 = (m_3^4 - \nu^4) \lambda_z$. However, we can not identify the Goldstone boson simply as ψ_1 , since we can no longer achieve $\psi_1^L \propto \psi_1^R \propto \psi_1$. Given the eigenvalue spectrum we

have now two massless particles that interact with each other and it is impossible to distinguish the Goldstone boson from the massless particle. The peculiar behaviour at the zero-exceptional point was also discussed by Philip Mannheim [79] in the context of the \mathcal{I}_2 -model.

2.3.5 Summary

We have considered the model (2.33) for $n = 3$ and analysed the classical masses of the fundamental particles at $U(1)$ invariant and broken vacua. In each case, we have observed non-trivial physical regions. However, most notably in the $U(1)$ broken vacuum, the physical regions were bounded by exceptional point, zero exceptional point and singularities. Moreover, the singularity is a novel feature of the $n = 3$ case as it was not observed in the $n = 2$ case [78]. We have also found a quantum mechanical \mathcal{P} operator by treating the mass matrix as a finite-dimensional 6-level Hamiltonian and observed that some of the \mathcal{P} operators are equivalent to the \mathcal{P} operators at the level of the field-theoretic action. Finally, we have derived the explicit forms of the Goldstone boson using the biorthonormal basis at \mathcal{CPT} symmetric regions and at the exceptional point where the basic form of the Goldstone boson changes (i.e. not only the overall factor but the linear combination changes). This change is also a novelty of the $n = 3$ case as we will not observe this in the $n = 2$ case. The Goldstone boson's explicit form could not be found due to the non-diagonalisability of the mass matrix at zero exceptional point.

2.4 Spontaneous symmetry breaking of global non-Abelian group

This section extends the Goldstone theorem on the non-Hermitian quantum field theories with Abelian group symmetry to global non-Abelian symmetry. Initially our model contains two complex two-component scalar fields possessing a $SU(2)$ -symmetry, but we will also indicate how our findings extend to the general case. Similar to the previous section, in the \mathcal{PT} -symmetric regime and at the standard exceptional point, the Goldstone theorem applies. However, different identification procedures need to be employed. At the zero exceptional points, the Goldstone boson can not be identified. Comparing our approach, based on the pseudo-Hermiticity of the model, to an alternative approach that utilises surface terms to achieve compati-

bility for the non-Hermitian system, we find that the explicit forms of the Goldstone boson fields are different.

2.4.1 A \mathcal{CPT} -symmetric non-Hermitian model with global $SU(2)$ -symmetry

Let us now verify the general statements in section 2.2 for a more concrete system. We consider the action

$$S_{su2} = \int d^4x \left[\sum_{i=1}^2 \left(|\partial_\mu \phi_i|^2 + m_i^2 |\phi_i|^2 \right) - \mu^2 \left(\phi_1^\dagger \phi_2 - \phi_2^\dagger \phi_1 \right) - \frac{g}{4} |\phi_1|^4 \right], \quad (2.118)$$

where the two complex scalar fields $\phi_i = (\phi_i^1, \phi_i^2)^T$, $i = 1, 2$, are taken to be in the fundamental or spin 1/2 representation of $SU(2)$ and $g, \mu \in \mathbb{R}$ are constants. We allow here for $m_i \in \mathbb{R}$ or $m_i \in i\mathbb{R}$, so that $m_i \rightarrow c_i m_i$ with $c_i = 1$ or $c_i = -1$, respectively, takes care of these two possibilities. For simplicity we suppress the parameters c_i until we analyse the physical parameter space in section 2.4.2. We observe that the action S_{su2} has the three properties i) - iii) mentioned in section 2.2. It is invariant under a global continuous symmetry $\phi_j^k \rightarrow \phi_j^k + \delta\phi_j^k$ where $\delta\phi_j^k = i\alpha_a T_a^{kl} \phi_j^l$ with $SU(2)$ -Lie algebraic generators T_a , is invariant under two discrete antilinear symmetries $\mathcal{CPT}_\pm : \phi(x_\mu) \rightarrow \pm\sigma_3 \phi^*(-x_\mu)$, with σ_3 denoting one of the Pauli spin matrices, and the potential $V(\phi)$ in (2.118) is evidently not Hermitian.

Equivalent Hermitian actions

More explicitly in components and transformed to the real fields $\varphi_j^k, \chi_j^k \in \mathbb{R}$, via $\phi_j^k = 1/\sqrt{2}(\varphi_j^k + i\chi_j^k)$, the action S_{su2} reads

$$S_{su2} = \int d^4x \left[\frac{1}{2} \sum_{j,k=1}^2 \left(\partial_\mu \varphi_j^k \right)^2 + \left(\partial_\mu \chi_j^k \right)^2 + m_j^2 \left(\varphi_j^k \right)^2 + m_j^2 \left(\chi_j^k \right)^2 \right. \\ \left. + i2\mu^2 \left(\chi_1^k \varphi_2^k - \varphi_1^k \chi_2^k \right) - \frac{g}{16} \left\{ \left(\varphi_1^1 \right)^2 + \left(\varphi_1^2 \right)^2 + \left(\chi_1^1 \right)^2 + \left(\chi_1^2 \right)^2 \right\}^2 \right]. \quad (2.119)$$

The direct functional variation of this action will lead to inconsistent equations of motion as extensively discussed in previous section. We therefore seek a suitable

similarity transformation to resolve this issue. Using the Dyson map

$$\begin{aligned} \eta = & \exp\left(\frac{\pi}{2} \int d^3x \left[\Pi_2^{\varphi,1}(\mathbf{x},t)\varphi_2^1(\mathbf{x},t)\right]\right) \exp\left(\frac{\pi}{2} \int d^3x \left[\Pi_2^{\varphi,2}(\mathbf{x},t)\varphi_2^2(\mathbf{x},t)\right]\right) \\ & \times \exp\left(\frac{\pi}{2} \int d^3x \left[\Pi_2^{\chi,1}(\mathbf{x},t)\chi_2^1(\mathbf{x},t)\right]\right) \exp\left(\frac{\pi}{2} \int d^3x \left[\Pi_2^{\chi,2}(\mathbf{x},t)\chi_2^2(\mathbf{x},t)\right]\right), \end{aligned} \quad (2.120)$$

with canonical momenta $\Pi_j^{\varphi,k} = \partial_t \varphi_j^k$, $\Pi_j^{\chi,k} = \partial_t \chi_j^k$ and $\Pi_j^{\phi,k} = \partial_t \phi_j^k$, $j, k = 1, 2$, the adjoint actions of η on the real and complex scalar fields and canonical momenta is computed to

$$\eta \varphi_j^k \eta^{-1} = (-i)^{\delta_{2j}} \varphi_j^k, \quad \eta \chi_j^k \eta^{-1} = (-i)^{\delta_{2j}} \chi_j^k, \quad \eta \phi_j^k \eta^{-1} = (-i)^{\delta_{2j}} \phi_j^k, \quad (2.121)$$

$$\eta \Pi_j^{\varphi,k} \eta^{-1} = i^{\delta_{2j}} \Pi_j^{\varphi,k}, \quad \eta \Pi_j^{\chi,k} \eta^{-1} = i^{\delta_{2j}} \Pi_j^{\chi,k}, \quad \eta \Pi_j^{\phi,k} \eta^{-1} = i^{\delta_{2j}} \Pi_j^{\phi,k}. \quad (2.122)$$

Thus we can utilize η to transform S_{su2} into a Hermitian action, i.e. remaining invariant under complex conjugation,

$$\begin{aligned} \hat{S}_{su2} = & \int d^4x \left[\sum_{j,k=1}^2 (-1)^{\delta_{2j}} \frac{1}{2} \left[\left(\partial_\mu \varphi_j^k\right)^2 + \left(\partial_\mu \chi_j^k\right)^2 + m_j^2 \left(\varphi_j^k\right)^2 + m_j^2 \left(\chi_j^k\right)^2 \right] \right. \\ & \left. + \mu^2 \left(\chi_1^k \varphi_2^k - \varphi_1^k \chi_2^k\right) - \frac{g}{16} \left[\left(\varphi_1^1\right)^2 + \left(\varphi_1^2\right)^2 + \left(\chi_1^1\right)^2 + \left(\chi_1^2\right)^2 \right]^2 \right]. \end{aligned} \quad (2.123)$$

It is useful to note here for our analysis, especially with regard to the generalisations to systems with symmetries of higher rank, that the action \hat{S}_{su2} can also be cast into a more compact form as

$$\begin{aligned} \hat{S}_{su2} = & \int d^4x \left[\sum_{i=1}^2 \partial_\mu \Phi_i I \partial^\mu \Phi_i + \partial_\mu \Psi_i I \partial^\mu \Psi_i + \frac{1}{2} \Phi_i^T H_+ \Phi_i + \frac{1}{2} \Psi_i^T H_- \Psi_i \right. \\ & \left. - \frac{g}{16} \left(\Phi_i^T E \Phi_i + \Psi_i^T E \Psi_i \right)^2 \right], \end{aligned} \quad (2.124)$$

$$= \int d^4x \left[\partial_\mu F \hat{I} \partial^\mu F + \frac{1}{2} F^T \hat{H} F - \frac{g}{16} \left(F^T \hat{E} F \right)^2 \right], \quad (2.125)$$

where we defined the matrices and vectors

$$\begin{aligned} H_\pm = & \begin{pmatrix} m_1^2 & \pm \mu^2 \\ \pm \mu^2 & -m_2^2 \end{pmatrix}, \quad I = \begin{pmatrix} 1 & 0 \\ 0 & -1 \end{pmatrix}, \quad E = \begin{pmatrix} 1 & 0 \\ 0 & 0 \end{pmatrix}, \\ \Phi_j = & \begin{pmatrix} \varphi_1^j \\ \chi_2^j \end{pmatrix}, \quad \Psi_j = \begin{pmatrix} \chi_1^j \\ \varphi_2^j \end{pmatrix}, \end{aligned} \quad (2.126)$$

$\Phi = (\Phi_1, \Phi_2)$, $\Psi = (\Psi_1, \Psi_2)$, $F = (\Phi, \Psi) = (\varphi_1^1, \chi_2^1, \varphi_1^2, \chi_2^2, \chi_1^1, \varphi_2^1, \chi_1^2, \varphi_2^2)$, $\text{diag}\hat{I} = \{I, I, I, I\}$, $\text{diag}\hat{H} = \{H_+, H_+, H_-, H_-\}$, $\text{diag}\hat{E} = \{E, E, E, E\}$.

$SU(2)$ and \mathcal{CPT}_\pm -symmetry

Let us now analyse the model \hat{S}_{su2} in more detail. First, we verify the $SU(2)$ -symmetry of the action and its effect on different fields. Noting that the change in the complex scalar fields is $\delta\phi_j^k = i\alpha_a T_a^{kl} \phi_j^l$, with the generators T_a of the symmetry transformation taken to be standard Pauli matrices σ_a , $a \in \{1, 2, 3\}$, we directly identify the infinitesimal changes for the real component fields as

$$\delta\varphi_j^1 = -\alpha_1\chi_j^2 + \alpha_2\varphi_j^2 - \alpha_3\chi_j^1, \quad \delta\chi_j^1 = \alpha_1\varphi_j^2 + \alpha_2\chi_j^2 + \alpha_3\varphi_j^1, \quad (2.127)$$

$$\delta\varphi_j^2 = -\alpha_1\chi_j^1 - \alpha_2\varphi_j^1 + \alpha_3\chi_j^2, \quad \delta\chi_j^2 = \alpha_1\varphi_j^1 - \alpha_2\chi_j^1 - \alpha_3\varphi_j^2. \quad (2.128)$$

It is easily verified that the Hermitian action \hat{S}_{su2} remains invariant under the transformations (2.127), (2.128). For the 4 and 8-component fields the symmetries (2.127), (2.128) then translate into

$$\delta\Phi = -\alpha_1(\sigma_1 \otimes \sigma_3)\Psi + i\alpha_2(\sigma_2 \otimes \mathbb{I})\Phi - \alpha_3(\sigma_3 \otimes \sigma_3)\Psi, \quad (2.129)$$

$$\delta\Psi = \alpha_1(\sigma_1 \otimes \sigma_3)\Phi + i\alpha_2(\sigma_2 \otimes \mathbb{I})\Psi + \alpha_3(\sigma_3 \otimes \sigma_3)\Phi, \quad (2.130)$$

$$\delta F = i[-\alpha_1(\sigma_2 \otimes \sigma_1 \otimes \sigma_3) + \alpha_2(\mathbb{I} \otimes \sigma_2 \otimes \mathbb{I}) - \alpha_3(\sigma_2 \otimes \sigma_3 \otimes \sigma_3)]F, \quad (2.131)$$

with \otimes denoting the standard tensor product of matrices (i.e. Kronecker product). These expressions may be applied to the action in the forms (2.124) and (2.125), respectively, to verify the $SU(2)$ -symmetry.

The antilinear \mathcal{CPT}_\pm -symmetries manifest themselves as

$$\mathcal{CPT}_\pm: \varphi_j^k(x_\mu) \rightarrow \mp(-1)^j \varphi_j^k(-x_\mu), \quad \chi_j^k(x_\mu) \rightarrow \pm(-1)^j \chi_j^k(-x_\mu), \quad (2.132)$$

$$\Phi(x_\mu) \rightarrow \pm\Phi(-x_\mu), \quad \Psi(x_\mu) \rightarrow \mp\Psi(-x_\mu), \quad (2.133)$$

$$F(x_\mu) \rightarrow \pm(\sigma_3 \otimes \mathbb{I} \otimes \mathbb{I})F(-x_\mu), \quad (2.134)$$

which can be verified in (2.123), (2.124) and (2.125), respectively.

$SU(2)$ -symmetry invariant and breaking vacua

Let us now compute the vacua from (2.9) with potential as specified in (2.123). We find there are only two types of vacua, that either break or respect the $SU(2)$ -symmetry,

$$F_0^b = (x, -ax, y, -ay, z, az, \pm\mathcal{R}, \pm a\mathcal{R}), \quad (2.135)$$

$$F_0^s = (0, 0, 0, 0, 0, 0, 0, 0), \quad (2.136)$$

respectively. We introduced the notation $x := \varphi_1^{0,1}$, $y := \varphi_1^{0,2}$, $z := \chi_1^{0,1}$, for the vacuum field components and $a := \mu^2/m_2^2$, $\mathcal{R} := \sqrt{R^2 - (x^2 + y^2 + z^2)}$, $R^2 := 4(\mu^2 + m_1^2 m_2^2)/gm_2^2$ for convenience. We note that the defining relation for \mathcal{R} can be interpreted as a three sphere in \mathbb{R}^4 with center $(\mathcal{R}, x, y, z) = (0, 0, 0, 0)$ and radius R , which is the geometrical configuration expected from its topological isomorphism with the $SU(2)$ -group manifold. We note that the points $\mu^2 = -m_1^2 m_2^2$ are special as there the three sphere collapses to a point and the symmetry of the vacuum is restored $F_0^b \rightarrow F_0^s$.

The symmetry properties of the vacua are easily established. Identifying the generators T_a of the symmetry transformation as Pauli matrices, where we drop the usual factor of 1/2, we compute the action on the vacuum states, say $\phi_j^0 = (\phi_j^{0,1}, \phi_j^{0,2})^T$ for $j = 1, 2$. We find

$$T_1 \phi_j^0 = (\phi_j^{0,2}, \phi_j^{0,1})^T, \quad T_2 \phi_j^0 = (-i\phi_j^{0,2}, i\phi_j^{0,1})^T, \quad T_3 \phi_j^0 = (\phi_j^{0,1}, -\phi_j^{0,2})^T, \quad (2.137)$$

so that for non-zero fields the vacuum will always break the symmetry with respect to the action of T_1 and T_2 . The action of T_3 seems to require only $\phi_j^{0,2} = 0$, in order to achieve invariance. However, apart from F_0^s there is no possible choice for the fields in F_0^b so that $\phi_j^{0,1} \neq 0$ in that case.

Let us now make use of the argument in (2.27) and employ the $SU(2)$ -symmetry to transform the vacuum F_0^b into a physically equivalent, but more manageable one. Choosing two simple target vacua $\check{\phi}_1^0$ and $\check{\phi}_2^0$, we attempt therefore to simultaneously

solve the two equations

$$e^{i\alpha_a T_a} \phi_1^0 = [\cos \rho \mathbb{I} + i \sin \rho (\mathbf{n} \cdot \boldsymbol{\sigma})] \phi_1^0 = \check{\phi}_1^0 = \begin{pmatrix} 0 \\ \pm ir \end{pmatrix}, \quad (2.138)$$

$$e^{i\alpha_a T_a} \phi_2^0 = [\cos \rho \mathbb{I} + i \sin \rho (\mathbf{n} \cdot \boldsymbol{\sigma})] \phi_2^0 = \check{\phi}_2^0 = \begin{pmatrix} 0 \\ \pm ar \end{pmatrix}, \quad (2.139)$$

by using the well known formula $e^{i\rho \mathbf{n} \cdot \boldsymbol{\sigma}} = \cos \rho \mathbb{I} + i \sin \rho (\mathbf{n} \cdot \boldsymbol{\sigma})$ with $\rho = \sqrt{\alpha_1^2 + \alpha_2^2 + \alpha_3^2}$, $\mathbf{n} = (\alpha_1, \alpha_2, \alpha_3)/\rho$ and $T_a = \sigma_a$. The vacuum fields are parametrised as

$$\begin{aligned} \phi_1^0 &= \begin{pmatrix} \varphi_1^{0,1} + i\chi_1^{0,1} \\ \varphi_1^{0,2} + i\chi_1^{0,2} \end{pmatrix} = \begin{pmatrix} x + iz \\ y + iR \end{pmatrix}, \\ \text{and } \phi_2^0 &= \begin{pmatrix} \varphi_2^{0,1} + i\chi_2^{0,1} \\ \varphi_2^{0,2} + i\chi_2^{0,2} \end{pmatrix} = \begin{pmatrix} -az + iax \\ -aR + iay \end{pmatrix}, \end{aligned} \quad (2.140)$$

so that the form of the target vacuum is motivated by setting $x = y = z = 0$. We only keep one of the sign in (2.135) and solve (2.138), (2.139) by

$$x = \frac{r}{\rho} \sin \rho \alpha_1, \quad y = -\frac{r}{\rho} \sin \rho \alpha_3, \quad z = -\frac{r}{\rho} \sin \rho \alpha_2, \quad (2.141)$$

so that $R = r \cos \rho$. For the vacuum F_0^b this translates with (2.131) into

$$\mathcal{T} F_0^b = \check{F}_0^b, \quad (2.142)$$

where

$$\begin{aligned} \mathcal{T} &= \cos(\rho) \mathbb{I}_8 - i \frac{\sin(\rho)}{\rho} [\alpha_1 (\sigma_2 \otimes \sigma_1 \otimes \sigma_3) - \alpha_2 (\mathbb{I} \otimes \sigma_2 \otimes \mathbb{I}) + \alpha_3 (\sigma_2 \otimes \sigma_3 \otimes \sigma_3)], \\ \check{F}_0^b &= (0, 0, 0, 0, 0, 0, \pm r, \pm ar). \end{aligned} \quad (2.143)$$

We note that $\det \mathcal{T} = 1$ and as required $\mathcal{T}^T = \mathcal{T}^{-1}$. Evidently \check{F}_0^b is of a more convenient form of the vacuum than F_0^b and we shall therefore use it from here on.

2.4.2 Physical regions

Mass squared matrices

Next, we use the different vacua and expand the potentials around them to determine the mass squared matrix. Applying the definition in (2.26) to our Lagrangian

(2.125), we find that the mass matrices are

$$\begin{aligned}
M_{ij}^2 &:= \left(\hat{I} \frac{\delta^2 V(F_0)}{\delta F^2} \right)_{ij} \tag{2.144} \\
\frac{\delta^2 V(F_0)}{\delta F^2} &= -\hat{H}_{ij} + \frac{g}{2} (\hat{E} F_0)_i (\hat{E} F_0)_j + \frac{g}{4} (F_0^T \hat{E} F_0) E_{ij}, \\
V &= -\frac{1}{2} F^T \hat{H} F + \frac{g}{16} (F^T \hat{E} F)^2.
\end{aligned}$$

Expanding first around the $SU(2)$ -symmetric vacuum F_0^s we find the mass squared matrix

$$M_s^2 = \begin{pmatrix} -m_1^2 & \mu^2 & 0 & 0 & 0 & 0 & 0 & 0 \\ -\mu^2 & -m_2^2 & 0 & 0 & 0 & 0 & 0 & 0 \\ 0 & 0 & -m_1^2 & \mu^2 & 0 & 0 & 0 & 0 \\ 0 & 0 & -\mu^2 & -m_2^2 & 0 & 0 & 0 & 0 \\ 0 & 0 & 0 & 0 & -m_1^2 & -\mu^2 & 0 & 0 \\ 0 & 0 & 0 & 0 & \mu^2 & -m_2^2 & 0 & 0 \\ 0 & 0 & 0 & 0 & 0 & 0 & -m_1^2 & -\mu^2 \\ 0 & 0 & 0 & 0 & 0 & 0 & \mu^2 & -m_2^2 \end{pmatrix}, \tag{2.145}$$

with two fourfold degenerate eigenvalues

$$\lambda_{\pm}^s = -\frac{1}{2} \left(m_1^2 + m_2^2 \pm \sqrt{(m_1^2 - m_2^2)^2 - 4\mu^4} \right). \tag{2.146}$$

As expected from (2.26) there are no Goldstone bosons emerging in this $SU(2)$ -invariant case.

Expanding instead around the $SU(2)$ -symmetry breaking vacuum F_0^b , we obtain the mass squared matrix

$$M_b^2 = \begin{pmatrix} \frac{g(\varphi_1^1)^2}{2} + \frac{\mu^4}{m_2^2} & \mu^2 & \frac{g\varphi_1^1\varphi_1^2}{2} & 0 & \frac{g\varphi_1^1\chi_1^1}{2} & 0 & -\frac{\varphi_1^1 g R}{2} & 0 \\ -\mu^2 & -m_2^2 & 0 & 0 & 0 & 0 & 0 & 0 \\ \frac{g\varphi_1^1\varphi_1^2}{2} & 0 & \frac{g(\varphi_1^2)^2}{2} + \frac{\mu^4}{m_2^2} & \mu^2 & \frac{g\varphi_1^2\chi_1^1}{2} & 0 & -\frac{\varphi_1^2 g R}{2} & 0 \\ 0 & 0 & -\mu^2 & -m_2^2 & 0 & 0 & 0 & 0 \\ \frac{g\varphi_1^1\chi_1^1}{2} & 0 & \frac{g\varphi_1^2\chi_1^1}{2} & 0 & \frac{g(\varphi_1^2)^2}{2} + \frac{\mu^4}{m_2^2} & -\mu^2 & -\frac{\chi_1^1 g R}{2} & 0 \\ 0 & 0 & 0 & 0 & \mu^2 & -m_2^2 & 0 & 0 \\ -\frac{\varphi_1^1 g R}{2} & 0 & -\frac{\varphi_1^2 g R}{2} & 0 & -\frac{\chi_1^1 g R}{2} & 0 & \frac{gR^2}{2} + \frac{\mu^4}{m_2^2} & -\mu^2 \\ 0 & 0 & 0 & 0 & 0 & 0 & \mu^2 & -m_2^2 \end{pmatrix}.$$

The expansion around \tilde{F}_0^b yields the same matrix with $\varphi_1^1 = \chi_1^1 = \varphi_1^2 = 0$.

$$M_b^2 = \begin{pmatrix} \frac{\mu^4}{m_2^2} & \mu^2 & 0 & 0 & 0 & 0 & 0 & 0 \\ -\mu^2 & -m_2^2 & 0 & 0 & 0 & 0 & 0 & 0 \\ 0 & 0 & \frac{\mu^4}{m_2^2} & \mu^2 & 0 & 0 & 0 & 0 \\ 0 & 0 & -\mu^2 & -m_2^2 & 0 & 0 & 0 & 0 \\ 0 & 0 & 0 & 0 & \frac{\mu^4}{m_2^2} & -\mu^2 & 0 & 0 \\ 0 & 0 & 0 & 0 & \mu^2 & -m_2^2 & 0 & 0 \\ 0 & 0 & 0 & 0 & 0 & 0 & \frac{gR^2}{2} + \frac{\mu^4}{m_2^2} & -\mu^2 \\ 0 & 0 & 0 & 0 & 0 & 0 & \mu^2 & -m_2^2 \end{pmatrix}. \quad (2.147)$$

As expected from (2.27) and (2.142), both matrices share the same field independent eigenvalues, that is two different ones each with a threefold degeneracy and two eigenvalues that may give rise to an exceptional point

$$\lambda_{1,2,3}^b = 0, \quad \lambda_{4,5,6}^b = \frac{\mu^4}{m_2^2} - m_2^2, \quad \lambda_{\pm}^b = K \pm \sqrt{K^2 + 2L}. \quad (2.148)$$

For convenience we defined here $K := 3\mu^4/2m_2^2 + m_1^2 - m_2^2/2$ and $L := \mu^4 + m_1^2 m_2^2$. We confirm the expectation from Goldstone's theorem to find three massless Goldstone bosons in the symmetry breaking sector, since none of the three $SU(2)$ -generators leaves the vacuum F_0^b invariant.

According to the relation (2.26) we may compute the corresponding eigenvectors with zero eigenvalue directly from the $SU(2)$ -symmetry transformation. When applying the infinitesimal changes for the component fields (2.127) and (2.128) to the vacuum F_0^b , we obtain the vectors

$$\nu_1^0 = \frac{1}{\sqrt{N}} \left\{ R, -aR, -\chi_1^1, \frac{\mu^2 \chi_1^1}{m_2^2}, \varphi_1^2, \frac{\mu^2 \varphi_1^2}{m_2^2}, \varphi_1^1, \frac{\mu^2 \varphi_1^1}{m_2^2} \right\}, \quad (2.149)$$

$$\nu_2^0 = \frac{1}{\sqrt{N}} \left\{ \varphi_1^2, -\frac{\mu^2 \varphi_1^2}{m_2^2}, -\varphi_1^1, \frac{\mu^2 \varphi_1^1}{m_2^2}, -R, -aR, -\chi_1^1, -\frac{\mu^2 \chi_1^1}{m_2^2} \right\}, \quad (2.150)$$

$$\nu_3^0 = \frac{1}{\sqrt{N}} \left\{ -\chi_1^1, \frac{\mu^2 \chi_1^1}{m_2^2}, -R, aR, \varphi_1^1, \frac{\mu^2 \varphi_1^1}{m_2^2}, -\varphi_1^2, -\frac{\mu^2 \varphi_1^2}{m_2^2} \right\}, \quad (2.151)$$

with $N := -4L\lambda_{4,5,6}^b/gm_2^4$. These vectors have been normalised to respect the biorthonormality where the left vector u is related to the right vector via $u = \hat{I}\nu$. We verify that the ν_i^0 , $i = 1, 2, 3$, are indeed eigenvectors of M_b^2 with zero eigenvalues. Furthermore, we observe from the normalization constant that at the

zero exceptional points, i.e. for $\mu^4 = m_2^4$ when $\lambda_{4,5,6}^b = 0$ and $\mu^4 = -m_1^2 m_2^2$ when $\lambda_-^b = 0$, these vectors are not defined. We may ignore the case $\lambda_-^b = 0$ in what follows as in this case the $SU(2)$ -symmetry is restored with $\check{F}_0^b \rightarrow F_0^s$.

Physical regions

We will now analyse the system's parameter space and identify the physical regions based on a meaningful mass squared matrix. To cover all possible cases we are setting therefore in all expressions $m_i^2 \rightarrow c_i m_i^2$. For the model expanded around the broken vacuum, the physical regions are then determined by $\lambda_{\pm}^b \geq 0$, $\lambda_{4,5,6}^b \geq 0$ corresponding to the four inequalities

$$K \geq 0, \quad L \leq 0, \quad K^2 + 2L \geq 0, \quad c_2 \mu^4 \geq c_2 m_2^4, \quad (2.152)$$

for the four cases $c_1 = \pm 1$, $c_2 = \pm 1$. All constraints can be expressed as functions of the two ratios $(\mu^4/m_1^4, m_2^2/m_1^2)$. We find that no solutions exist for $c_1 = c_2$, apart from setting $\mu = m_2 = 0$, so that in these two case the model is unphysical. The physical regions for the remaining two cases $c_1 = -c_2 = \pm 1$ are depicted in figure 2.4.

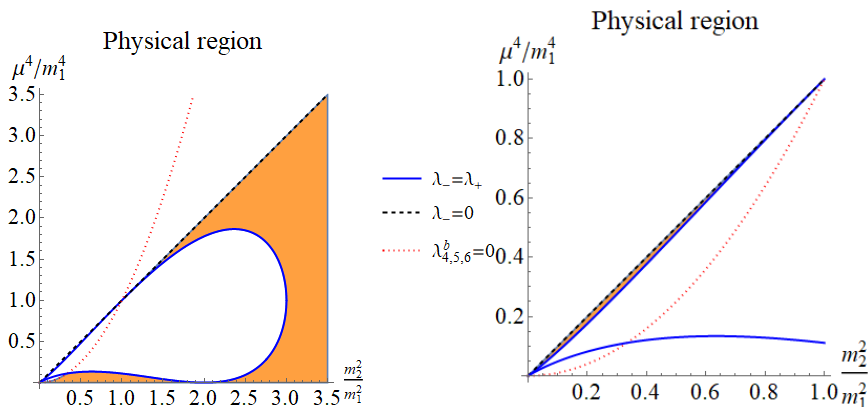


Figure 2.4: Physical regions (in orange) in parameter space bounded by exceptional and zero exceptional points as function of $(\mu^4/m_1^4, m_2^2/m_1^2)$ for the theory expanded around the $SU(2)$ -symmetry breaking vacuum. Left panel for $c_1 = -c_2 = 1$ and right panel for $c_1 = -c_2 = -1$.

The two different cases depicted in figure 2.4 do not have any physical regions that intersect. The case $c_1 = -c_2 = 1$ was also analysed within the *surface term approach* in [81] and our results appear to match exactly. The case $c_1 = -c_2 = -1$ was not dealt with in [81], but as seen in figure 2.4, it also contains a well defined small physical region. We note that for our model with two complex scalar fields,

the physical regions have no boundary corresponding to singularities, which appears to be a feature only occurring for the theories with more than two complex scalar fields, as we observed in the previous section.

Finally in figure 2.5 we also depict the physical regions for the model expanded around the $SU(2)$ -symmetric vacuum. Similar to the symmetric vacuum case considered in the previous section see figure 2.1, the physical region is non-trivial.

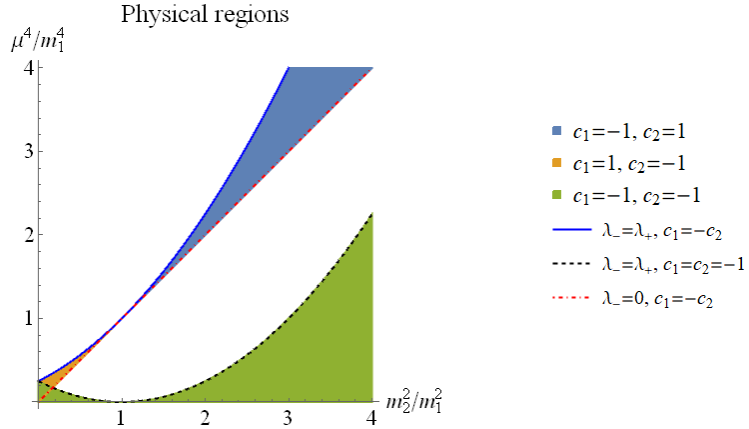


Figure 2.5: Physical regions (in orange, blue and green) in parameter space bounded by exceptional and zero exceptional points as function of $(\mu^4/m_1^4, m_2^2/m_1^2)$ for the theory expanded around the $SU(2)$ -symmetry invariant vacuum.

Here only the case $c_1 = c_2 = 1$ does not contain a physical region apart from $\mu = m_2 = 0$. The three different cases depicted in figure 2.5 do not have any physical regions that intersect, apart from the small region near the origin.

The figure 2.5 can also be seen as a physical region of the model (2.123) before the symmetry breaking. This is because the squared mass matrix obtained by expanding around the trivial vacuum is equivalent to the squared mass matrix before expanding the model. From this observation, the physical theory such as $c_1 = c_2 = -1$ become unphysical after $SU(2)$ symmetry breaking.

2.4.3 Goldstone bosons in \mathcal{CPT} symmetric and \mathcal{CPT} broken regimes

The Goldstone bosons in the \mathcal{CPT} -symmetric regime

We may now compute the Goldstone bosons in terms of the original fields similarly as discussed in the previous section. Defining for this purpose the remaining right eigenvectors $v_i, i = 4, \dots, 8$, and a matrix U containing all of them as column vectors as

$$M_b^2 v_i = \lambda_i^b v_i, \quad U := (v_1, v_4, v_2, v_5, v_3, v_6, v_-, v_+), \quad i = 1, \dots, 6, \pm, \quad (2.153)$$

we diagonalize the mass squared matrix by means of the similarity transformation $U^{-1}M_b^2U = D$ with $\text{diag}D = (\lambda_1^b, \lambda_4^b, \lambda_2^b, \lambda_5^b, \lambda_3^b, \lambda_6^b, \lambda_-^b, \lambda_+^b) = (m_1^2, \dots, m_8^2)$. For $\mu^4 \neq m_2^4$ and $K^2 \neq -2L$, that are the zero and standard exceptional points, we define the fields ψ_i with masses m_i by re-writing the squared mass term as

$$\begin{aligned} F^T M_b^2 F &= \sum_{k=1}^8 m_k^2 \psi_k^2 = \sum_{k=1}^8 m_k^2 (F^T I U)_k (U^{-1} F)_k \\ &= \sum_{k=1}^8 m_k^2 (F^T I U)_k (U^T I F)_k. \end{aligned} \quad (2.154)$$

Hence, the three Goldstone fields are identified as

$$\psi_\ell^{\text{Gb}} := (U^T I F)_\ell, \quad \ell = 1, 3, 5. \quad (2.155)$$

Setting in M_b^2 the fields $\chi_1^{0,1}$, $\varphi_1^{0,1}$, $\varphi_1^{0,2}$ to zero we compute

$$U = \begin{pmatrix} H_- & 0 & 0 & 0 & 0 \\ 0 & H_- & 0 & 0 & 0 \\ 0 & 0 & H_+ & 0 & 0 \\ 0 & 0 & 0 & \lambda_-^b + m_2^2 & \lambda_+^b + m_2^2 \\ 0 & 0 & 0 & \mu^2 & \mu^2 \end{pmatrix}, \quad (2.156)$$

with $\det U = 2\mu^2(\mu^4 - m_2^4)^3 \sqrt{K^2 + 2L}$, so that the explicit form of the Goldstone boson fields in the original fields result to

$$\psi_1^{\text{Gb}} = \frac{\mu^2 \varphi_2^1 - m_2^2 \chi_1^1}{\sqrt{m_2^4 - \mu^4}}, \quad \psi_3^{\text{Gb}} = \frac{m_2^2 \varphi_1^2 + \mu^2 \chi_2^2}{\sqrt{m_2^4 - \mu^4}}, \quad \psi_5^{\text{Gb}} = \frac{m_2^2 \varphi_1^1 + \mu^2 \chi_2^1}{\sqrt{m_2^4 - \mu^4}}. \quad (2.157)$$

As U is not invertible at the exceptional points for $\mu^4 = m_2^4$ and $K^2 = -2L$ or $\mu = 0$, we need to treat these cases separately. We note that these expressions differ from those obtained in [81].

The Goldstone bosons at the exceptional point

At the standard exceptional point, i.e. when $K^2 = -2L$ and hence $\lambda_+^b = \lambda_-^b$, the two eigenvectors v_- and v_+ coalesce so that the matrix U is no longer invertible.

The Goldstone boson fields may take on a different form, as found in the previous section. Analogues to the previous section, instead of diagonalising the mass squared matrix, we can convert it into Jordan normal form using a similarity transformation. Making m_1 the dependent variable, the exceptional point occurs when $m_1^2 = \pm\mu^2 - m_2^2/2 - 3\mu^4/2m_2^2$ so that the Jordan normal form becomes

$$\text{diag}D_e = (0, \lambda_e^b, 0, \lambda_e^b, 0, \lambda_e^b, \Lambda), \quad \lambda_e^b = \frac{\mu^4}{m_2^2} - m_2^2, \quad (2.158)$$

$$\Lambda = \begin{pmatrix} \pm\mu^2 - m_2^2 & \pm(\alpha - \beta)\mu^2 \\ 0 & \pm\mu^2 - m_2^2 \end{pmatrix},$$

which can be obtained from the similarity transformation $U_e^{-1}M_e^2U_e = D_e$ with U_e equalling U with the lower right block replaced by

$$\begin{pmatrix} 1 & \alpha \\ 1 & \beta \end{pmatrix}. \quad (2.159)$$

We compute now $\det U = (\alpha - \beta)(\mu^4 - m_2^4)^3$. Instead of the definition of the Goldstone boson given in equation (2.155), we will resort to the alternative definition used in equation (2.114). Surprisingly the form of the Goldstone boson at the exceptional point coincides with the expressions in (2.155). This differs from the previous section where the Goldstone at the exceptional point was analytically different from the one defined in the \mathcal{PT} -symmetric region. The reason for this is clear if one looks at the squared mass matrix (2.147). The Goldstone boson is defined using the eigenvectors of the bottom right 2×2 block matrix. The only standard exceptional point in the block diagonal matrix (2.147) comes from the remaining three identical 2×2 block matrices. Since the bottom block matrix is perfectly diagonalisable using the biorthonormal basis, one obtains the same form as in the \mathcal{PT} -symmetric region even at the exceptional point.

The behaviour at the zero exceptional points is similar, as discussed in more detail in the previous section. For $\mu^4 = m_2^4$ (i.e. when $\lambda_{4,5,6}^b = 0$), the matrix U that diagonalises M^2 does not exist. Therefore, the Goldstone bosons are not expressible in terms of the original fields in the action. The zero exceptional point for $\mu^4 = -m_1^2m_2^2$ when $\lambda_-^b = 0$ needs no discussion as at this point the original $SU(2)$ -symmetry is restored.

2.4.4 Summary

We have performed the same analysis as in the previous section, where we have promoted the symmetry group of the model considered before from $U(1)$ to $SU(2)$ but reduced the number of fields from $n = 3$ to $n = 2$ to simplify the analysis. We have observed two distinct physical regions of the model, related by swapping the signs of the mass parameters. The explicit forms of the Goldstone bosons are also found except at the exceptional point.

Two models considered in this section (Let us denote by $n = 2, SU(2)$ model) and previous (Let us denote by $n = 3, U(1)$ model) share same results, such as

- The Goldstone bosons can be identified in the \mathcal{PT} -symmetric region and at the exceptional point. However the definition changes at the exceptional point.
- The Goldstone bosons can not be identified at the zero exceptional point.
- Physical region are bounded by exceptional point and zero exceptional points.

However, two models also admit novel features, only present in one of the model.

- The Goldstone boson defined at exceptional point and in the \mathcal{PT} symmetric regions can not be continuously deformed by varying the parameter values in $n = 3, U(1)$ model, but this is possible in $n = 2, SU(2)$ model.
- Physical regions are also bounded by the singularity in $n = 3, U(1)$. However, such singularities do not exist in the $n = 2, SU(2)$ model.

2.5 Spontaneous symmetry breaking of local non-Abelian group

In this section, we extend the previous section's model to be invariant under local non-Abelian gauge symmetry. This will introduce a new massless real vector field called the gauge field. We demonstrate that the two aspects of the mechanism, that is, giving mass to gauge vector fields and at the same time preventing the existence of massless Goldstone fields, remain to be synchronised in all regimes characterised by a modified \mathcal{CPT} symmetry. In the domain of parameter space where the “would-be Goldstone bosons” can be identified, the gauge vector bosons become massive, and the Goldstone bosons cease to exist. The mechanism is also

intact at the standard exceptional points. However, at the zero exceptional points, when the eigenvalues of the mass squared matrix vanish irrespective of the symmetry breaking, the mechanism breaks down as the Goldstone bosons can not be identified and the gauge vector fields remain massless.

We will also consider a different model where the fields are taken to be in the adjoint representation of $SU(2)$ instead of fundamental representation. We verify that the phenomena mentioned above can also be observed in this case. In addition, this model is known to possess a non-trivial solution to the equations of motion called the t'Hooft-Polyakov monopole, which will be the main focus of the next chapter.

2.5.1 A $SU(2)$ -model in the fundamental representation

We start by applying the pseudo-Hermitian approach to a model with local $SU(2) \times U(1)$ -symmetry previously studied using the surface term approach in [81].

$$\mathcal{L}_2 = \sum_{i=1}^2 |D_\mu \phi_i|^2 + m_i^2 |\phi_i|^2 - \mu^2 (\phi_1^\dagger \phi_2 - \phi_2^\dagger \phi_1) - \frac{g}{4} (|\phi_1|^2)^2 - \frac{1}{4} \text{Tr} (F_{\mu\nu} F^{\mu\nu}). \quad (2.160)$$

Here $g, \mu \in \mathbb{R}$, $m_i \in \mathbb{R}$ or $m_i \in i\mathbb{R}$ are constants. When compared to [8] we have replaced here as usual the standard derivatives ∂_μ by covariant derivatives $D_\mu := \partial_\mu - ieA_\mu$, involving a charge $e \in \mathbb{R}$ and the Lie algebra valued gauge fields $A_\mu := \tau^a A_\mu^a$. Here the τ^a , $a = 1, 2, 3$, are taken to be Pauli matrices, which when re-defined as $i(-1)^{a+1}\tau^a$ are the generators of $SU(2)$. We have also added the standard Yang-Mills term comprised of the Lie algebra valued field strength $F_{\mu\nu} := \partial_\mu A_\nu - \partial_\nu A_\mu - ie[A_\mu, A_\nu]$. The two complex scalar fields ϕ_i are taken to be in the representation space of fundamental representation of $SU(2)$. The model described by \mathcal{L}_2 admits a global continuous $U(1)$ -symmetry, a local continuous $SU(2)$ -symmetry and two discrete antilinear \mathcal{CPT} -symmetries given in Eq. (2.35). Crucially the corresponding Hamiltonian of \mathcal{L}_2 is not Hermitian, which at this point is simply to be understood as the Lagrangian \mathcal{L}_2 not being invariant under complex conjugation. The Abelian version of \mathcal{L}_2 was discussed in [79, 7].

As argued in [8], it is useful to decompose the complex fields into their real components $\phi_j^k = 1/\sqrt{2}(\varphi_j^k + i\chi_j^k)$ with $\varphi_j^k, \chi_j^k \in \mathbb{R}$. Thus simply rewriting the complex scalar fields in equation (2.1) in terms of their real and imaginary components we

obtain the following Lagrangian

$$\begin{aligned}
\mathcal{L}_2 = & \frac{1}{2} \sum_{k=1}^2 \sum_{j=1}^2 \left\{ \left[\partial_\mu \varphi_j^k + e(A_\mu \chi_j)^k \right] \left[\partial^\mu \varphi_j^k + e(A^\mu \chi_j)^k \right]^* \right. & (2.161) \\
& + \left[\partial_\mu \chi_j^k - e(A_\mu \varphi_j)^k \right] \left[\partial^\mu \chi_j^k - e(A^\mu \varphi_j)^k \right]^* \\
& - 2\text{Im} \left[\left[\partial_\mu \varphi_j^k + e(A_\mu \chi_j)^k \right]^* \left[\partial^\mu \chi_j^k - e(A^\mu \varphi_j)^k \right] \right] \\
& + m_j^2 \left[(\varphi_j^k)^2 + (\chi_j^k)^2 \right] - 2i\mu^2 (\varphi_1^k \chi_2^k - \chi_1^k \varphi_2^k) \\
& \left. - \frac{1}{4} F_{\mu\nu}^k (F^k)^{\mu\nu} \right\} - \frac{g}{16} \left[\sum_{k=1}^2 (\varphi_1^k)^2 + (\chi_1^k)^2 \right]^2.
\end{aligned}$$

We use here the standard notation $*$ for complex conjugation and \dagger for the simultaneous conjugation with transposition.

The $SU(2)$ -symmetry manifests itself as follows: A change in the complex scalar fields due to this symmetry is $\delta\phi_j^k = i\alpha_a T_a^{kl} \phi_j^l$, where the generators T_a of the symmetry transformation are the standard Pauli matrices σ_a , $a = 1, 2, 3$. The infinitesimal changes for the real component fields are then identified as

$$\delta\varphi_j^1 = -\alpha_1 \chi_j^2 + \alpha_2 \varphi_j^2 - \alpha_3 \chi_j^1, \quad \delta\chi_j^1 = \alpha_1 \varphi_j^2 + \alpha_2 \chi_j^2 + \alpha_3 \varphi_j^1, \quad (2.162)$$

$$\delta\varphi_j^2 = -\alpha_1 \chi_j^1 - \alpha_2 \varphi_j^1 + \alpha_3 \chi_j^2, \quad \delta\chi_j^2 = \alpha_1 \varphi_j^1 - \alpha_2 \chi_j^1 - \alpha_3 \varphi_j^2, \quad (2.163)$$

which leave the above Lagrangian invariant. The discrete antilinear \mathcal{CPT}_\pm -symmetries manifest themselves as

$$\mathcal{CPT}_\pm : \varphi_j^k(x_\mu) \rightarrow \mp(-1)^j \varphi_j^k(-x_\mu), \quad \chi_j^k(x_\mu) \rightarrow \pm(-1)^j \chi_j^k(-x_\mu). \quad (2.164)$$

A noteworthy remark is that it is straightforward to generalise the model from a locally $SU(2)$ -invariant one to a locally $SU(N)$ -invariant one by extending the sum over k from 2 to N , while keeping the $U(1)$ -symmetry global. In what follows, we will focus on $N = 2$.

A crucial feature of \mathcal{L}_2 is that its \mathcal{CPT} -invariance translates into pseudo Hermiticity [110, 111], meaning that it can be mapped to a real Lagrangian \mathfrak{l}_2 by means of the adjoint action of a Dyson map η as $\mathfrak{l}_2 = \eta \mathcal{L}_2 \eta^{-1}$. This may be achieved by

the slightly modified version of the Dyson map used in [79, 8]

$$\eta_2^\pm = \exp \left(\pm \sum_{i=1}^2 \int d^3x \left[\Pi^{\varphi_2^i}(t', \vec{x}) \varphi_2^i(t', \vec{x}) + \Pi^{\chi_2^i}(t', \vec{x}) \chi_2^i(t', \vec{x}) \right] \right). \quad (2.165)$$

We denote here the time-dependence by t' to indicate that commutators are understood as equal time commutators for the canonical momenta $\Pi^{\varphi_2^i} = \partial_t \varphi_2^i$ and $\Pi^{\chi_2^i} = \partial_t \chi_2^i$, $i = 1, 2$. satisfying $[\psi_j^k(\mathbf{x}, t), \Pi^{\psi_l^m}(\mathbf{y}, t)] = i\delta_{jl}\delta_{km}\delta(\mathbf{x} - \mathbf{y})$, $j, k, l, m = 1, 2$, for $\psi = \varphi, \chi$.

Hence η_2^\pm is not to be viewed as explicitly time-dependent as discussed in much detail for instance in [112]. The adjoint action of η_2^\pm on the individual fields maps as

$$\varphi_1^k \rightarrow \varphi_1^k, \quad \varphi_2^k \rightarrow -i\varphi_2^k, \quad \chi_1^k \rightarrow \chi_1^k, \quad \chi_2^k \rightarrow -i\chi_2^k, \quad A_\mu \rightarrow A_\mu. \quad (2.166)$$

Where $k \in \{1, 2\}$. Thus, we convert the complex Lagrangian into the real Lagrangian

$$\begin{aligned} \mathfrak{l}_2 = & \frac{1}{2} \sum_{j=1}^2 (-1)^{j+1} \left\{ |\partial_\mu \varphi_j + e(A_\mu \chi_j)|^2 + |\partial_\mu \chi_j - e(A_\mu \varphi_j)|^2 + m_j^2 [\varphi_j \cdot \varphi_j + \chi_j \cdot \chi_j] \right. \\ & \left. - 2\text{Im} \left[[\partial_\mu \varphi_j + e(A_\mu \chi_j)]^* \cdot [\partial^\mu \chi_j - e(A^\mu \varphi_j)] \right] + (-1)^j 2\mu^2 (\varphi_1 \cdot \chi_2 - \chi_1 \cdot \varphi_2) \right\} \\ & - \frac{g}{16} [\varphi_1 \cdot \varphi_1 + \chi_1 \cdot \chi_1]^2 - \frac{1}{4} \text{Tr} (F_{\mu\nu} F^{\mu\nu}). \end{aligned} \quad (2.167)$$

Here we have applied the pseudo-Hermitian approach by performing a BRST quantisation before proceeding with the method explained in equation (2.20). The detail of this can be found in appendix D. Introducing the 2 two-component fields of the form

$$\Phi^k := \begin{pmatrix} \varphi_1^k \\ \chi_2^k \end{pmatrix}, \quad \Psi^k := \begin{pmatrix} \chi_1^k \\ \varphi_2^k \end{pmatrix}, \quad k = 1, 2, \quad (2.168)$$

we can re-write the Lagrangians \mathcal{L}_2 and \mathfrak{l}_2 more compactly. Defining the 2×2 matrices

$$H_\pm := \begin{pmatrix} m_1^2 & \pm\mu^2 \\ \pm\mu^2 & -m_2^2 \end{pmatrix}, \quad \mathcal{I} := \begin{pmatrix} 1 & 0 \\ 0 & -1 \end{pmatrix}, \quad E := \begin{pmatrix} 1 & 0 \\ 0 & 0 \end{pmatrix}, \quad (2.169)$$

Recall that these block matrices are equal to the ones defined in section 2.4.1, equation (2.126), therefore in this model, we should expect exactly the same eigenvalues

of the mass matrix found in equation (2.148). The real Lagrangian \mathfrak{l}_2 acquires the form

$$\begin{aligned} \mathfrak{l}_2 &= \frac{1}{2} \{ [\partial_\mu \Phi + e \mathcal{I} A_\mu \Psi]^* \mathcal{I} [\partial^\mu \Phi + e \mathcal{I} A^\mu \Psi] + [\partial_\mu \Psi - e \mathcal{I} A_\mu \Phi]^* \mathcal{I} [\partial^\mu \Psi - e \mathcal{I} A^\mu \Phi] \\ &\quad - 2 \text{Im} [(\partial_\mu \Phi + e \mathcal{I} A_\mu \Psi)^* (\partial^\mu \Psi - e \mathcal{I} A^\mu \Phi)] + \Phi^T H_+ \Phi + \Psi^T H_- \Psi \} \\ &\quad - \frac{g}{16} (\Phi^T E \Phi + \Psi^T E \Psi)^2 - \frac{1}{4} \text{Tr} (F_{\mu\nu} F^{\mu\nu}). \end{aligned} \quad (2.170)$$

We have simplified here the index notation by implicitly contracting, keeping in mind that we are summing over two separate index sets $k \in \{1, 2\}$ and $j \in \{1, 2\}$. For instance, we set

$$(IA_\mu \Phi)_\alpha^k \rightarrow \mathcal{I}_{\alpha\beta} A_\mu^{kj} \Phi_\beta^j, \quad \Phi^{kT} H_+ \Phi^k \rightarrow \Phi^T H_+ \Phi \quad (2.171)$$

$$[\partial_\mu \Phi_j^k + e (\mathcal{I} A_\mu \Psi)_j^k]^* \mathcal{I}_{j\ell} [\partial^\mu \Phi_\ell^k + e (\mathcal{I} A^\mu \Psi)_\ell^k] \rightarrow [\partial_\mu \Phi + e \mathcal{I} A_\mu \Psi]^* \mathcal{I} [\partial^\mu \Phi + e \mathcal{I} A^\mu \Psi] \quad (2.172)$$

In this formulation we may think of the real and complex Lagrangians, \mathfrak{l}_2 and \mathcal{L}_2 , as being simply related by a kind of Wick rotation in the field-configuration space

$$\Phi^k \rightarrow T \Phi^k, \quad \Psi^k \rightarrow T \Psi^k, \quad \text{with } T := \begin{pmatrix} 1 & 0 \\ 0 & -i \end{pmatrix}. \quad (2.173)$$

The symmetry breaking vacuum

The vacuum solutions Φ_0^k, Ψ_0^k by solving $\delta V = 0$, which amounts to solving the two equations

$$\left(-H_- + \frac{g}{4} R^2 E\right) \Psi_0^k = 0, \quad \left(-H_+ + \frac{g}{4} R^2 E\right) \Phi_0^k = 0, \quad k = 1, 2, \quad (2.174)$$

with $R^2 := |(\phi_1^0)^1|^2 + |(\phi_1^0)^2|^2 = \frac{1}{2} \sum_{k=1}^2 \Phi_0^{kT} E \Phi_0^k + \Psi_0^{kT} E \Psi_0^k = \text{const}$. Hence in the real component field configuration space the vacuum manifold is a S^3 -sphere with radius R . Consequently, we may consider the equations (2.174) as two eigenvalue equations. Thus, besides the trivial $SU(2)$ -invariant vacuum $\Phi_0^k = \Psi_0^k = 0$, $k = 1, 2$, we must have zero eigenvalues in both equations, which is equivalent to requiring

$$R^2 = \frac{4}{gm_2^2} (\mu^4 + m_1^2 m_2^2). \quad (2.175)$$

Since R^2 is positive, this equality imposes restrictions on the parameters g, μ and the possible choices for $m_1 \in \mathbb{R}$, $m_2 \in i\mathbb{R}$ or $m_1 \in i\mathbb{R}$, $m_2 \in \mathbb{R}$. The corresponding vectors that satisfy equation (2.174), suitably normalized with regard to the standard

inner product, are

$$\Psi_0^2 = N_\Psi \begin{pmatrix} m_2^2 \\ \mu^2 \end{pmatrix}, \quad \Phi_0^2 = N_\Phi \begin{pmatrix} -m_2^2 \\ \mu^2 \end{pmatrix}. \quad (2.176)$$

Note that we do not consider the biorthonormal basis here because the matrices appearing in the equation (2.174) are real symmetric matrices. The biorthonormal basis are required once these real symmetric matrices are multiplied by I , which corresponds to the squared mass matrices defined in equation (2.26). Imposing now the constraint on R^2 as stated after equation (2.174), a possible solution is $\Phi_0^1 = \Psi_0^1 = \Phi_0^2 = 0$ and Ψ_0^2 as defined in (2.176) with normalization constant $N_\Psi = \pm\sqrt{2}R/m_2^2$. Hence we recover the symmetry breaking vacuum used in [7].

The Higgs mechanism

Let us now demonstrate how the gauge vector boson acquires a finite mass and how at the same time, the emergence of a Goldstone boson is prevented by the Higgs mechanism [3, 4, 5, 6]. We will investigate this in the \mathcal{CPT} -symmetric regime, at the exceptional points and even in the spontaneously broken \mathcal{CPT} -symmetric regime. The mechanism breaks down at the zero exceptional points.

Expanding the potential

$$V = -\Phi^\top H_+ \Phi - \Psi^\top H_- \Psi + \frac{g}{16} \left(\Phi^\top E \Phi + \Psi^\top E \Psi \right)^2 \quad (2.177)$$

around the vacuum specified at the end of the previous subsection leads to

$$\begin{aligned} V(\Phi_0 + \Phi, \Psi_0 + \Psi) &= V(\Phi_0, \Psi_0) + \frac{1}{2} \Phi^i \frac{\partial^2 V(\Phi_0, \Psi_0)}{\partial \Phi^i \partial \Phi^j} \Big|_{\Phi_0} \Phi^j \\ &\quad + \frac{1}{2} \Psi^i \frac{\partial^2 V(\Phi_0, \Psi_0)}{\partial \Psi^i \partial \Psi^j} \Big|_{\Psi_0} \Psi^j + \Phi^i \frac{\partial^2 V(\Phi_0, \Psi_0)}{\partial \Phi^i \partial \Psi^j} \Big|_{\Phi_0, \Psi_0} \Psi^j + \dots \\ &= \frac{1}{2} \sum_{i=1}^2 -\Phi^{i\top} \left(H_+ - \frac{g}{4} R^2 E \right) \Phi^i - \Psi^{1\top} \left(H_- - \frac{g}{4} R^2 E \right) \Psi^1 \\ &\quad - \Psi^{2\top} \left[H_- - \frac{g}{4} R^2 E - \frac{g}{2} (E \Psi_0^2)(E \Psi_0^2) \right] \Psi^2 + \dots \end{aligned} \quad (2.179)$$

As expected, multiplying the Hessians in (2.179) by \mathcal{I} gives back the squared mass matrix (2.147). The kinetic term is almost unchanged except for the term involving

Ψ^2

$$\begin{aligned}
T &= \frac{1}{2} [\partial_\mu \Phi + e\mathcal{I}A_\mu \Psi]^\dagger \mathcal{I} [\partial^\mu \Phi + e\mathcal{I}A^\mu \Psi] + \text{Re} \left\{ (\partial_\mu \Phi + e\mathcal{I}A_\mu \Psi)^\dagger \mathcal{I} (e\mathcal{I}A^\mu \Psi_0) \right\} \\
&\quad - \text{Im} \left\{ (\partial_\mu \Phi + e\mathcal{I}A_\mu \Psi + e\mathcal{I}A_\mu \Psi_0)^\dagger (\partial^\mu \Psi - e\mathcal{I}A^\mu \Phi) \right\} \\
&\quad + \frac{1}{2} e^2 (A_\mu \Psi_0)^\dagger \mathcal{I} (A^\mu \Psi_0). \tag{2.180}
\end{aligned}$$

The last term corresponds to the mass term of the gauge vector boson that we evaluate to

$$\begin{aligned}
\frac{1}{2} e^2 (A_\mu \Psi_0)^* \mathcal{I} (A^\mu \Psi_0) &= \frac{1}{2} e^2 (A_\mu \Psi_0)^{*k} \mathcal{I}_{\alpha\beta} (A^\mu \Psi_0)_\beta^k \tag{2.181} \\
&= \frac{1}{2} e^2 \left(A_\mu^\dagger A^\mu \right)^{kj} (\Psi_0)_\alpha^k \mathcal{I}_{\alpha\beta} (\Psi_0)_\beta^j \\
&= \frac{1}{2} e^2 \left(A_\mu^\dagger A^\mu \right)^{22} (\Psi_0)_\alpha^2 \mathcal{I}_{\alpha\beta} (\Psi_0)_\beta^2 \\
&= \frac{1}{2} e^2 A_\mu^a A^{b\mu} (\tau^{a\dagger} \tau^b)^{22} \frac{2R^2}{m_2^4} (m_2^4 - \mu^4) \\
&= \frac{1}{2} m_g^2 A_\mu^a A^{a\mu},
\end{aligned}$$

where we used the standard relation $\tau^{a\dagger} \tau^b = \tau^a \tau^b = \delta_{ab} \mathbb{1} + i\varepsilon_{abc} \tau^c$. Therefore we read off the mass of each of the three components of the gauge vector boson as

$$m_g := \frac{\sqrt{2}eR}{m_2^2} \sqrt{m_2^4 - \mu^4}. \tag{2.182}$$

In the previous section, we identified the physical regions in the parameter space in which the squared mass matrix has non-negative eigenvalues and in which the Goldstone bosons can be identified. Let us now compare those regions with the values for which the gauge vector boson becomes massive. We immediately see from the expression in (2.182) that the gauge vector boson remains massless when $\mu^4 = m_2^4$ or when $R = 0$, i.e. $\mu^4 = -m_1^2 m_2^2$. The first value corresponds to the zero exceptional points where the mass matrix (bottom right block of the matrix (2.147)) is non-diagonalisable. The second value is when the vacuum solution becomes zero, meaning the spontaneous symmetry breaking can not occur. Therefore the Higgs mechanism can not be observed in this case. The zero exceptional point is distinct from standard exceptional points where two eigenvalues coalesce and become complex thereafter, here at $\lambda = \frac{\mu^4}{m_2^2} - m_2^2$. See the appendix B for a more detailed explanation about the distinction between these types of exceptional points.

Thus the two aspects of the Higgs-mechanism, i.e. giving mass to the gauge vector boson and at the same time preventing the existence of the Goldstone bosons, remain to go hand in hand. In the \mathcal{CPT} -symmetric regime the mechanism applies, but at the zero exceptional points the Higgs-mechanism breaks down as the Goldstone bosons are not identifiable and at the same time the gauge vector boson remains massless. In contrast, at the exceptional point the Goldstone bosons are identifiable, (although in a different manner with different forms for the case of three complex scalar, see section 2.3.4), and the gauge vector bosons become massive.

Let us see this in detail and replace $m_i^2 \rightarrow c_i m_i^2$, with $c_i = \pm 1$ to account for all possibilities in signs. We found in previous section that physical regions only exist for the two cases $c_1 = -c_2 = 1$ and $c_1 = -c_2 = -1$, therefore, $c_1 c_2 = -1$. For the two cases we may then write

$$\frac{m_g^2}{m_1^2} = c_2 \frac{8e^2}{g} \frac{m_1^2}{m_2^2} \left(\frac{m_2^4}{m_1^4} - \frac{\mu^4}{m_1^4} \right) \left(\frac{\mu^4}{m_1^4} - \frac{m_2^2}{m_1^2} \right), \quad (2.183)$$

noting that m_g^2/m_1^2 only depends on the two parameters m_2^2/m_1^2 and m_2^4/m_1^4 similarly as the eigenspectrum of the squared mass matrix [81, 7]. We require the right hand side of equation (2.183) to be positive as depicted in figure 2.6.

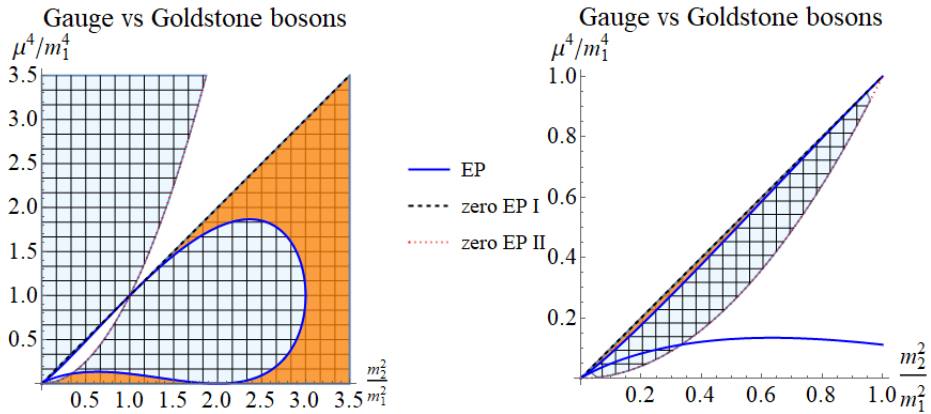


Figure 2.6: Regions, for which the gauge vector boson is massive (blue with mesh) versus physical regions (orange) in which the would be Goldstone boson can be identified, bounded by exceptional and zero exceptional points as texttion of $(\mu^4/m_1^4, m_2^2/m_1^2)$ for the theory expanded around the SU(2)-symmetry breaking vacuum. Left panel for $c_1 = -c_2 = 1$ and right panel for $c_1 = -c_2 = -1$. The coupling constant g must be positive.

We observe in figure 2.6 that while the region in which the Goldstone boson can be identified is bounded by exceptional as well as zero exceptional points, the exceptional points lie well inside the region for which the gauge vector boson is massive, i.e. they acquire a mass in the \mathcal{CPT} -symmetric regime as well as in the

spontaneously broken \mathcal{CPT} -symmetric regime. In the \mathcal{CPT} -symmetric regime this agrees well with the findings that at these points the “would-be Goldstone boson” is prevented from existing as a massless particle. We may think of the sign change in front of the mass terms, $c_i \rightarrow -c_i$, that relates the left to the right panel as a phase transition [113].

Let us now demonstrate this behaviour in detail and expand for this purpose the Lagrangian around the symmetry broken vacuum up to second order in the fields

$$\begin{aligned} \mathfrak{l}_2 = & \sum_{k=1}^2 \frac{1}{2} \partial_\mu \Phi^{kT} \mathcal{I} \partial^\mu \Phi^k + \frac{1}{2} \partial_\mu \Psi^{kT} \mathcal{I} \partial^\mu \Psi^k - \frac{1}{2} \Phi^{kT} \left(H_+ + \frac{g}{4} R^2 E \right) \Phi^k \quad (2.184) \\ & - \frac{1}{2} \Psi^{1T} \left(H_- - \frac{g}{4} R^2 E \right) \Psi^1 - \frac{1}{2} \Psi^{2T} \left(H_+ - \frac{g}{4} R^2 E - \frac{g}{2} (E \Psi_{(0)}^2) (E \Psi_{(0)}^2) \right) \Psi^2 \\ & + e \text{Re} \left[\partial_\mu \Phi^\dagger (A^\mu \Psi_0) \right] + e \text{Im} \left[(\mathcal{I} A_\mu \Psi_0)^\dagger \partial^\mu \Psi \right] + \frac{1}{2} m_g^2 A_\mu^a A^{a\mu} + \dots \end{aligned}$$

We recall now from the previous section as well as the general argument presented in section 2.2 that the first two lines of the Lagrangian \mathfrak{l}_2 can be diagonalized and the Goldstone bosons can be identified in terms of the field content of the model. Furthermore, the Goldstone modes are eigenvectors with zero eigenvalues of squared mass matrices

$$M_\pm^2 := \mathcal{I} \left(-H_\pm + \frac{g}{4} R^2 E \right), \quad (2.185)$$

computed above as Ψ_0^2 and $\mathcal{I} \Psi_0^2$, so that the Goldstone modes are proportional to these two vectors. The explicit forms of the Goldstone fields were found in equation (2.157), denoted as ψ_5^{Gb} , ψ_3^{Gb} and ψ_1^{Gb} , therein. We express them here as

$$G^1 := \frac{e}{m_g} (\Psi_0^2)^T \Phi^1, \quad G^3 := \frac{e}{m_g} (\Psi_0^2)^T \Phi^2, \quad G^2 := -\frac{e}{m_g} (\Psi_0^2)^T \mathcal{I} \Psi^1, \quad (2.186)$$

respectively. As expected for the Higgs mechanism the number of “would be Goldstone bosons” equals the amount of massive vector gauge bosons. The fact that the Goldstone modes are inverse proportional to the mass of the gauge bosons explains that they can not be identified for massless gauge bosons. Keeping now only the Goldstone kinetic term from the first two lines of the Lagrangian \mathfrak{l}_2 and the one

involving the gauge fields in equation (2.184), we obtain

$$\begin{aligned} \mathfrak{l}_2 &= \sum_{a=1}^3 \frac{1}{2} \partial_\mu G^a \partial^\mu G^a + e \operatorname{Re} \left[\partial_\mu \Phi^\dagger (A^\mu \Psi_0) \right] \\ &\quad + e \operatorname{Im} \left[(\mathcal{I} A_\mu \Psi_0)^\dagger \partial^\mu \Psi \right] + \frac{1}{2} m_g^2 A_\mu^a A^{a\mu} + \dots \end{aligned} \quad (2.187)$$

Using the explicit representations of the Pauli matrices, the real and imaginary parts are determined as

$$\begin{aligned} \operatorname{Re} \left[\partial_\mu \Phi^T A^\mu \Psi_0 \right] &= A_\mu^a \operatorname{Re} \left[\partial_\mu \Phi^T \tau^a \Psi_0 \right] \\ &= A_\mu^1 \partial_\mu \Phi^T \tau^1 \Psi_0 + A_\mu^3 \partial_\mu \Phi^T \tau^3 \Psi_0 \\ &= A_\mu^1 \partial_\mu (\Phi^1)^T \Psi_0^2 - A_\mu^3 \partial_\mu (\Phi^2)^T \Psi_0^2 \\ &= A_\mu^1 \frac{m_g}{e} \partial^\mu G^1 - \frac{m_g}{e} A_\mu^3 \partial^\mu G^3 \\ \operatorname{Im} \left[(\mathcal{I} A_\mu \Psi_0)^\dagger \partial^\mu \Psi \right] &= A_\mu^a \operatorname{Im} \left[\Psi_0^T \tau^a \mathcal{I} \partial^\mu \Psi \right] = -i (A_\mu^2 \Psi_0^T \tau^2 \mathcal{I} \partial^\mu \Psi) \\ &= A_\mu^2 (\Psi_0^2)^T \mathcal{I} \partial^\mu \Psi^1 = -A_\mu^2 \frac{m_g}{e} \partial^\mu G^2. \end{aligned} \quad (2.188)$$

Finally the Lagrangian in (2.187) can be simplified to

$$\begin{aligned} \mathfrak{l}_2 &= \sum_{a=1}^3 \frac{1}{2} \partial_\mu G^a \partial^\mu G^a - m_g A_\mu^1 \partial^\mu G^1 + m_g A_\mu^2 \partial^\mu G^2 - m_g A_\mu^3 \partial^\mu G^3 \\ &\quad + \frac{1}{2} m_g^2 A_\mu^a A^{a\mu} + \dots \\ &= \frac{1}{2} m_g^2 \left(A_\mu^1 - \frac{1}{m_g} \partial_\mu G^1 \right)^2 + \frac{1}{2} m_g^2 \left(A_\mu^2 + \frac{1}{m_g} \partial_\mu G^2 \right)^2 \\ &\quad + \frac{1}{2} m_g^2 \left(A_\mu^3 + \frac{1}{m_g} \partial_\mu G^3 \right)^2 + \dots \\ &= \frac{1}{2} \sum_{a=1}^3 m_g^2 B_\mu^a B^{a\mu} + \dots, \end{aligned} \quad (2.190)$$

where we defined the new vector gauge particle with component fields $B_\mu^a := A_\mu^a - \frac{1}{m_g} \partial_\mu G^a$. We may also replace A_μ^a by B_μ^a in the field strength $F_{\mu\nu}$ so that A_μ can be eliminated entirely from the Lagrangian. We see that the Higgs-mechanism applies as long as $m_g \neq 0$. However, at the zero exceptional points, not only the gauge boson mass vanishes, but the Higgs mechanism no longer applies, in the sense that we can not remove the degrees of freedom of Goldstone bosons.

Notice that the above calculation does not refer to whether the theory is in the \mathcal{CPT} -symmetric or broken regions. In fact, the Higgs mechanism also works in the

\mathcal{CPT} broken region because the only requirements for the mechanism to hold are

1. Gauge masses are non-zero $m_g \neq 0$.
2. The block diagonal part of the mass matrix with zero eigenvalue is biorthonormalisable.

The above two conditions are satisfied in three disconnected regions, i) \mathcal{CPT} -symmetric region, ii) \mathcal{CPT} -broken regions, iii) standard exceptional points. Of course, the \mathcal{CPT} -broken region is disregarded as we consider the application of our theory to particle physics, where the rest masses of the particle can not be negative or complex.

From $SU(2)$ to $SU(N)$

We end this subsection by discussing the generalisation from $SU(2)$ to $SU(N)$. For this purpose, we simply replace the Pauli matrices in all our expressions by the traceless and Hermitian $N \times N$ -matrices $\{\tau^a\}_{a=1,\dots,N^2-1}$. Multiplying these matrices with i corresponds to the $SU(N)$ -generators T^a with $a = 1, \dots, (N^2 - 1)$. The vacua are still determined by the solutions of the eigenvalue problem (2.174) with zero eigenvalue condition

$$R^2 = \frac{1}{2} \sum_{i=1}^N \Phi_0^{iT} E \Phi_0^i + \Psi_0^{iT} E \Psi_0^i = \text{constant} = \frac{4}{gm_2^2} (\mu^4 + m_1^2 m_2^2). \quad (2.191)$$

The zero eigenvalue condition implies that the vacuum manifold is a S^{2N-1} -sphere with radius R . This follows from the fact that $SU(N)$ acts on the $2N$ dimensional space spanned by $(\varphi_1^0)^i, (\chi_1^0)^i, i = 1, \dots, N$, with norm equal to R^2 . On this space $SU(N - 1)$ simply permutes the fields amongst themselves, hence acting as a stabilizer or isotropy subgroup. Thus the vacuum manifold corresponds to the coset $SU(N)/SU(N - 1) \cong S^{2N-1}$.

As we discussed in section 2.2, we may utilise the symmetry of the Lagrangian to transform the vacua into convenient forms without changing the eigenvalue spectrum of the mass matrix. Thus using the elements $\tau \in SU(N)/SU(N - 1) \subset SU(N)$ we may transform the vacuum into the form

$$\Phi_0^i = 0, \quad \Psi_0^i = \frac{\sqrt{2}R}{\sqrt{N}m_2^2} \begin{pmatrix} m_2^2 \\ \mu^2 \end{pmatrix}, \quad \text{for } i = 1, \dots, N, \quad (2.192)$$

satisfying the constraint (2.191). Let us now use this $SU(N)$ -symmetry breaking vacuum to calculate the mass of the gauge vector boson. Dropping here the kinetic term reported in (2.180) and considering only the relevant term in the Lagrangian we obtain

$$\begin{aligned} \mathfrak{L}_A & : = \frac{1}{2} e^2 A_\mu^a A^{b\mu} \left(\tau^{a\dagger} \tau^b \right)_{ij} (\Psi_0)_\alpha^i \mathcal{I}_{\alpha\beta} (\Psi_0)_\beta^j \\ & = \frac{1}{N} e^2 A_\mu^a A^{b\mu} R^2 \left(1 - \frac{\mu^4}{m_2^4} \right) \sum_{i,j=1}^N \left(\tau^a \tau^b \right)_{ij}. \end{aligned} \quad (2.193)$$

The last factor uses $\tau^a \tau^b = \frac{1}{2N} \delta_{ab} \mathbb{I}_N + \frac{1}{2} \sum_{c=1}^{N^2-1} (i f_{abc} + g_{abc}) \tau^c$, where the g_{abc} and f_{abc} are completely symmetric and anti-symmetric tensors, respectively. We note that $\sum_{i,j=1}^N (\tau^c)_{ij} = \text{Tr}(\tau^c) = 0$ by definition of τ^c and $\sum_{i,j=1}^N (\mathbb{I}_N)_{ij} = \text{Tr} \mathbb{I}_N = N$. Thus we can diagonalise \mathfrak{L}_A , computing

$$\mathfrak{L}_A = \frac{R^2}{2N} e^2 \left(1 - \frac{\mu^4}{m_2^4} \right) A_\mu^a A^{a\mu} = \frac{1}{2} m_g^2 A_\mu^a A^{a\mu}, \quad (2.194)$$

from which we read off the masses $m_g^{(a)}$ of the $N^2 - 1$ gauge vector bosons. We note that once again they vanish at the zero exceptional points, but now for all $SU(N)$ -models.

2.5.2 A $SU(2)$ -symmetric model in the adjoint representation

We end the chapter by discussing spontaneous symmetry breaking in the $SU(2)$ gauge theory, where fields are now in the adjoint representation. This model is attractive because it possesses a non-trivial solution to the equations of motion called the t'Hooft-Polyakov monopole. We will study the monopole solution in detail in the next chapter. This final subsection will verify that the phenomena we observed in the previous subsection also apply to this model.

We consider here a non-Hermitian $SU(2)$ -invariant Lagrangian

$$\begin{aligned} \mathcal{L}_2^{\text{ad}} & = \frac{1}{4} \text{Tr} (D\phi_1)^2 + \frac{1}{4} \text{Tr} (D\phi_2)^2 + \frac{m_1^2}{4} \text{Tr}(\phi_1^2) + \frac{m_2^2}{4} \text{Tr}(\phi_2^2) \\ & \quad - i \frac{\mu^2}{2} \text{Tr}(\phi_1 \phi_2) - \frac{g}{64} [\text{Tr}(\phi_1^2)]^2 - \frac{1}{8} \text{Tr} (F^2), \end{aligned} \quad (2.195)$$

where as in equation (2.161) we take $g, \mu \in \mathbb{R}$, $m_i \in \mathbb{R}$ or $m_i \in i\mathbb{R}$, to be constants. The two complex scalar fields are expressed as $\phi_i = \phi_i^a T^a$, $i = 1, 2$ and $a = 1, 2, 3$, where the T^a are the three $SU(2)$ -generators in the adjoint representation that,

up to a factor of 2, satisfy the same algebra as the Pauli spin matrices, that is $[T^a, T^b] = i\varepsilon_{abc}T^c$. Hence, the adjoint representation is $(T^a)_{bc} = -i\varepsilon_{abc}$, i.e. to be explicit

$$T^1 = \begin{pmatrix} 0 & 0 & 0 \\ 0 & 0 & -i \\ 0 & i & 0 \end{pmatrix}, \quad T^2 = \begin{pmatrix} 0 & 0 & i \\ 0 & 0 & 0 \\ -i & 0 & 0 \end{pmatrix}, \quad T^3 = \begin{pmatrix} 0 & -i & 0 \\ i & 0 & 0 \\ 0 & 0 & 0 \end{pmatrix}, \quad (2.196)$$

such that $\text{Tr}(T^a T^b) = 2\delta^{ab}$ and therefore $\text{Tr}(\phi^2) = 2\sum_{a=1}^3 \phi^a \phi^a$. The $SU(2)$ -symmetry in the adjoint representation for each generator T^a is therefore

$$\phi_j \rightarrow e^{i\alpha T^a} \phi_j e^{-i\alpha T^a} \approx \phi_j - \alpha \varepsilon_{abc} \phi_j^b T^c, \quad (2.197)$$

so that the infinitesimal changes to the fields ϕ_i^a result to

$$\delta\phi_i^a = -\alpha \varepsilon_{abc} \phi_i^b. \quad (2.198)$$

The vector field A_μ now transforms as

$$A_\mu \rightarrow e^{i\alpha^a(x)T^a} A_\mu e^{-i\alpha^a(x)T^a} + \frac{1}{e} \partial_\mu \alpha^a(x) T^a, \quad (2.199)$$

with the field strength tensor $F_\mu^a = \partial_\mu A_\nu^a - \partial_\nu A_\mu^a + ie\epsilon^{abc} A_\mu^b A_\nu^c$, respecting the above symmetry.

In more a compact form the Lagrangian in (2.195) can be expressed equivalently as

$$\mathcal{L}_2^{\text{ad}} = \frac{1}{2} D_\mu \phi_i^a D^\mu \phi_i^a - \frac{1}{2} \phi_i^a M_{ij}^2 \phi_j^a - \frac{g}{16} (\phi_i^a E_{ij} \phi_j^a)^2 - \frac{1}{4} F_{\mu\nu}^a (F^{\mu\nu})^a, \quad (2.200)$$

where repeated indices are summed over the appropriate index sets $i, j, \mu, \nu \in \{1, 2\}$ and $a, b \in \{1, 2, 3\}$. The matrix M^2 is defined as

$$M^2 = \begin{pmatrix} -m_1^2 & i\mu^2 \\ i\mu^2 & -m_2^2 \end{pmatrix}, \quad (2.201)$$

and E as in (2.169). The covariant derivative in the adjoint representation acting

on a real components field takes on the form

$$(D_\mu \phi_i)^a := \partial_\mu \phi_i^a + e \varepsilon_{abc} A_\mu^b \phi_i^c. \quad (2.202)$$

Pursuing here a pseudo-Hermitian approach we perform a similarity transformation by the Dyson map

$$\eta = \prod_{a=1}^3 e^{\frac{\pi}{2} \int d^3x [\Pi_2^a \phi_2^a]}. \quad (2.203)$$

From appendix D, this transformation maps the complex Lagrangian $\mathcal{L}_2^{\text{ad}}$ to a real Lagrangian

$$\mathfrak{L}_2^{\text{ad}} = \frac{1}{2} (D_\mu \phi_i)^a \mathcal{I}_{ij} (D^\mu \phi_j)^a + \frac{1}{2} \phi_i^a H_{ij} \phi_j^a - \frac{g}{16} (\phi_i^a E_{ij} \phi_j^a)^2 - \frac{1}{4} F_{\mu\nu}^a F^{a\mu\nu}, \quad (2.204)$$

where repeated indices are summed over and the matrix H is defined as

$$H := \begin{pmatrix} m_1^2 & -\mu^2 \\ -\mu^2 & -m_2^2 \end{pmatrix}, \quad \mathcal{I} := \begin{pmatrix} 1 & 0 \\ 0 & -1 \end{pmatrix}, \quad E := \begin{pmatrix} 1 & 0 \\ 0 & 0 \end{pmatrix}. \quad (2.205)$$

We note here that the potential term is similar to one of the diagonal block of the model (2.170) in previous subsection and model (2.125) in section 2.4.1 but with $g/16$ replaced with g and no $1/2$ in front of the Hessian matrix. Although the dimensionality of the mass matrix will be different, we will see that eigenvalues of the mass matrix will coincide with the eigenvalues in equation (2.148).

The $SU(2)$ -symmetry preserving and breaking vacua

To find the different types of vacua ϕ^0 , we need to solve again $\delta V = 0$. The corresponding functional variation of the Lagrangian in (2.204) leads to the three sets of equations

$$\left(H - \frac{g}{4} R^2 E \right) (\phi^0)^a = 0, \quad a = 1, 2, 3, \quad (2.206)$$

with $R^2 := (\phi_i^0)^a E_{ij} (\phi_j^0)^a$ (equivalent to the R defined in section 2.4.1). Next to the trivial $SU(2)$ -symmetry preserving solution $(\phi^0)^a = 0$, a $SU(2)$ -symmetry breaking solution is obtained by requiring $(\phi^0)^a$ to become an eigenvector with zero

eigenvalue of the matrix $H - gR^2E/4$, which is the case when

$$(\phi^0)^a = \frac{N_a}{m_2^2} \begin{pmatrix} m_2^2 \\ -\mu^2 \end{pmatrix}, \quad \text{and} \quad R^2 = 4 \frac{\mu^4 + m_1^2 m_2^2}{g m_2^2}, \quad (2.207)$$

where the N_a are arbitrary constants satisfying $R^2 = N_1^2 + N_2^2 + N_3^2$. Expressing the Lie algebra valued vacuum field $\phi_i^0 = (\phi_i^0)^a T^a$ in the matrix form of the adjoint representation (2.196) we obtain

$$\phi_1^0 = i \begin{pmatrix} 0 & -N_3 & N_2 \\ N_3 & 0 & -N_1 \\ -N_2 & N_1 & 0 \end{pmatrix}, \quad \text{and} \quad \phi_2^0 = -\frac{\mu^2}{m_2^2} \phi_1^0. \quad (2.208)$$

We can now apply the $SU(2)$ -symmetry to the vacuum state in the form

$$\phi^{\text{vac}} = [(\phi_1^0)^1, (\phi_2^0)^1, (\phi_1^0)^2, (\phi_2^0)^2, (\phi_1^0)^3, (\phi_2^0)^3], \quad (2.209)$$

so that the infinitesimal changes $\delta\phi_i(\phi^{\text{vac}})$ with (2.198) and (2.207) yield the following states for each generator

$$v_1^0 = \frac{\alpha_1}{m_2^2} (0, 0, N_3 m_2^2, -N_3 \mu^2, -N_2 m_2^2, N_2 \mu^2), \quad (2.210)$$

$$v_2^0 = \frac{\alpha_2}{m_2^2} (-N_3 m_2^2, N_3 \mu^2, 0, 0, N_1 m_2^2, -N_1 \mu^2), \quad (2.211)$$

$$v_3^0 = \frac{\alpha_3}{m_2^2} (N_2 m_2^2, -N_2 \mu^2, -N_1 m_2^2, N_1 \mu^2, 0, 0), \quad (2.212)$$

as solutions for ϕ^{vac} . Evidently, these states are linearly dependent as

$$\sum_{i=1}^3 \frac{N_i v_i^0}{\alpha_i} = 0. \quad (2.213)$$

According to Goldstone's theorem the states v_i^0 should be eigenvectors of the squared mass matrix with eigenvalue zero. As only two of them are linearly independent we expect to find two massless Goldstone bosons, which in our gauged model correspond to "would-be Goldstone bosons". Hence the $SU(2)$ -symmetry has been broken down to a $U(1)$ -symmetry, so that the group theoretical argument predicts two Goldstone bosons equal to the dimension of the coset $SU(2)/U(1)$.

The squared mass matrix

Expanding the Lagrangian in equation (2.204) about the vacuum solution gives

$$\begin{aligned} \mathfrak{V}_2^{\text{ad}} &= (D_\mu \phi_i)^a \mathcal{I}_{ij} (D_\mu \phi_j)^a - \frac{1}{2} \phi_i^a H_{ij}^{ab} \phi_j^b \\ &\quad + 2(D_\mu \phi_i^0)^a \mathcal{I}_{ij} (D^\mu \phi_j)^a + (D_\mu \phi_i^0)^a \mathcal{I}_{ij} (D_\mu \phi_j^0)^a + \mathcal{O}(\phi^3), \end{aligned} \quad (2.214)$$

where the last two terms originate from expanding the covariant kinetic term. The Hessian matrix is obtained by differentiating the potential term twice and inserting the vacuum solution

$$\hat{H}_{ij}^{ab} := \frac{\partial^2 \mathcal{V}}{\partial \phi_i^a \partial \phi_j^b} = -H_{ij} \delta^{ab} + \frac{g}{4} R^2 E_{ij} \delta^{ab} + \frac{g}{2} (E\phi^a)_i (E\phi^b)_j, \quad (2.215)$$

This is almost diagonal with the group indices but with non-zero off diagonal terms $(E\phi^a)_i (E\phi^b)_j$. However, this term can be simplified by insetting the explicit forms of the vacuum solutions

$$\begin{aligned} (E\phi_0^a)_i &= \begin{pmatrix} 1 & 0 \\ 0 & 0 \end{pmatrix} \begin{pmatrix} N_a \\ -\mu^2/m_2^2 \end{pmatrix} = N^a \begin{pmatrix} 1 \\ 0 \end{pmatrix} \\ &\implies (E\phi^a)_i (E\phi^b)_j = N^a N^b E_{ij}. \end{aligned} \quad (2.216)$$

Let us organise the Lagrangian in terms of the 6-component field defined as $\Psi := (\phi_1^1, \phi_2^1, \phi_1^2, \phi_2^2, \phi_1^3, \phi_2^3)$. Then the mass tensor $M_{ij}^{ab} := (IH)_{ij}^{ab}$ can be written as a 6×6 matrix

$$\begin{pmatrix} -m_1^2 + \frac{g}{4} R^2 + \frac{g}{2} N_1^2 & \mu^2 & \frac{g}{2} N_1 N_2 & 0 & \frac{g}{2} N_1 N_3 & 0 \\ -\mu^2 & -m_2^2 & 0 & 0 & 0 & 0 \\ \frac{g}{2} N_1 N_2 & 0 & -m_1^2 + \frac{g}{4} R^2 + \frac{g}{2} N_2^2 & \mu^2 & \frac{g}{2} N_2 N_3 & 0 \\ 0 & 0 & -\mu^2 & m_2^2 & 0 & 0 \\ \frac{g}{2} N_1 N_3 & 0 & \frac{g}{2} N_2 N_3 & 0 & -m_1^2 + \frac{g}{4} R^2 + \frac{g}{2} N_3^2 & \mu^2 \\ 0 & 0 & 0 & 0 & -\mu^2 & -m_2^2 \end{pmatrix}. \quad (2.217)$$

Notice that if one takes $N_1 = N_2 = 0$ and $N_3 = R$, then we obtain same mass matrix as equation (2.147) but with one different block structure. The six eigenvalues λ of M^2 are then computed to

$$\lambda_{1,2} = 0; \quad \lambda_{3,4} = \frac{\mu^4 - m_2^4}{m_2^2}, \quad \lambda_{\pm} = K \pm \sqrt{K^2 + 2L}, \quad (2.218)$$

with $\kappa := 3\mu^4/2m_2^2 - m_2^2/2 + m_1^2$ and $L = \mu^4 + m_1^2 m_2^2$. Notice that these eigenvalues are equivalent to the one found in equation (2.148) as one expect. We can now verify that the three vectors v_i^0 in (2.210)-(2.212), corresponding to the infinitesimal changes of the vacuum (2.207) under the action of the $SU(2)$ -symmetry, are indeed eigenvectors of M^2 with zero eigenvalues. Due to their linear dependence we may choose two of them to be associated with the two massless “would-be Goldstone bosons”.

We note that there are zero exceptional points at $\mu^4 = m_2^4$ when $\lambda_{3,4} = 0$, and at $\mu^4 = -m_1^2 m_2^2$ when either $\lambda_- = 0$ or $\lambda_+ = 0$. The standard exceptional point for which the two eigenvalues λ_- and λ_+ coalesce occurs when $-m_1^2 = 3\mu^4/2m_2^2 + m_2^2/2 \pm \mu^2$. The Jordan normal form become for the mass squared matrix becomes

$$\text{diag}D_e = (0, \lambda_e^b, 0, \lambda_e^b, 0, \lambda_e^b, \Lambda), \quad \lambda_e^b = \frac{\mu^4}{m_2^2} - m_2^2, \quad (2.219)$$

$$\Lambda = \begin{pmatrix} \pm\mu^2 - m_2^2 & \pm(\alpha - \beta)\mu^2 \\ 0 & \pm\mu^2 - m_2^2 \end{pmatrix},$$

for some arbitrary constants α and β .

We notice that the eigenvalues in (2.218) do not depend on the choice of the the normalisation constants N_a , since all of these vacua are equivalent as they are related by $SU(2)$ -symmetry transformations. The physical regions of the model are determined by the requirement that the eigenvalues are real and positive. Taking now account of the possibility that $m_i \in \mathbb{R}$ or $m_i \in i\mathbb{R}$, by allowing for different signs in front of the m_i^2 terms in setting $m_i^2 \rightarrow c_i m_i^2$, we find that the model does not possess any physical region when $c_1 = c_2 = \pm 1$ and physical regions when $c_1 = -c_2 = \pm 1$ as argued also in the section 2.4.2.

The would-be Goldstone bosons

Let us now identify the two massless Goldstone bosons $\psi_{1,2}^{\text{Gb}}$ in the different \mathcal{PT} -regimes by the same procedure as previously explained in [8, 7], with the difference that they will be made to vanish due to the presence of the gauge bosons. In terms of the original scalar fields in the model we identify the Goldstone bosons by evaluating

$$\psi_{1,2}^{\text{Gb}} := (U^T I\Psi)_{1,2}, \quad (2.220)$$

where the matrix U diagonalises the squared mass matrix by $U^{-1}M^2U = D$ with $\text{diag}D = (\lambda_1, \lambda_2, \lambda_3, \lambda_4, \lambda_-, \lambda_+)$ and $\text{diag}\hat{I} = \{\mathcal{I}, \mathcal{I}, \mathcal{I}\}$. In the \mathcal{PT} -symmetric regime the similarity transformation U is well defined by

$$U := (v_1, v_2, v_3, v_4, v_-, v_+), \quad (2.221)$$

where the v_i are the right eigenvectors of M^2 normalised with respect to the left eigenvectors. Up to normalisations constants for each eigenvector, we obtain in our example the concrete expressions

$$v_i = [(m_2^2 + \lambda_i) \tau_{i1}, -\mu^2 \tau_{i1}, (m_2^2 + \lambda_i) \tau_{i2}, -\mu^2 \tau_{i2}, (m_2^2 + \lambda_i) \tau_{i3}, -\mu^2 \tau_{i3}], \quad (2.222)$$

with $\tau_{12} = \tau_{23} = \tau_{32} = \tau_{43} = 0$, $\tau_{33} = \tau_{42} = \tau_{\pm 1} = -\tau_{13} = -\tau_{22} = N_1$, $\tau_{21} = \tau_{41} = \tau_{\pm 2} = N_2$ and $\tau_{11} = \tau_{31} = \tau_{\pm 3} = N_3$.

For convenience we take now $N_1 = N_2 = 0$, $N_3 = R$ and compute

$$\psi_1^{\text{Gb}} := \frac{m_2^2 \phi_1^3 + \mu^2 \phi_2^3}{\sqrt{m_2^4 - \mu^4}}, \quad \text{and} \quad \psi_2^{\text{Gb}} := \frac{m_2^2 \phi_1^2 + \mu^2 \phi_2^2}{\sqrt{m_2^4 - \mu^4}}. \quad (2.223)$$

We note that $\det U = \lambda_3 \lambda_4 (\lambda_- - \lambda_+) \mu^6 R^4$, indicating the breakdown of these expressions at the exceptional points when $\lambda_- = \lambda_+$, the zero exceptional point when $\lambda_3 = \lambda_4 = 0$ and at the trivial vacuum when $R = 0$, as previously observed in [8, 7]. However, at the exceptional point we may still calculate the expressions for the Goldstone boson when taking into account that in this case the two eigenvectors v_- and v_+ become identical. In order to obtain two linearly independent eigenvectors when the squared mass matrix is converted into its Jordan normal form we multiply two entries of the vector v_+ by some arbitrary constants $\alpha \neq \beta$ as $(v_+)_1 \rightarrow \alpha(v_+)_1$ and $(v_+)_2 \rightarrow \beta(v_+)_2$. With this change the matrix U becomes invertible as $\det U = \lambda_3 \lambda_4 (\beta - \alpha) (m_2^2 + \kappa) N_1^2 \mu^6 R^2$. We may now evaluate the expression in (2.220) obtaining the same formulae for the Goldstone bosons as in (2.223). At the zero exceptional point it is not possible to identify the Goldstone in terms of the original fields in the model.

The mass of the vector gauge boson

Finally we calculate the mass of the gauge vector bosons by expanding the minimal coupling term in equation (2.204) around the symmetry breaking vacuum (2.209)

$$\begin{aligned}
[D_\mu(\phi + \phi^0)]^T \mathcal{I} [D^\mu(\phi + \phi^0)] &= (D_\mu \phi^0)^T \mathcal{I} (D^\mu \phi^0) + \dots \\
&= e^2 \left[\varepsilon_{abc} A_\mu^b (\phi_i^0)^c \right] \mathcal{I}_{ij} \left(\varepsilon_{ade} A^{d\mu} (\phi_j^0)^e \right) + \dots \\
&= e^2 \left(A_\mu^a A^{a\mu} (\phi_i^0)^b \mathcal{I}_{ij} (\phi_j^0)^b - A_\mu^a A^{b\mu} (\phi_i^0)^b \mathcal{I}_{ij} (\phi_j^0)^a \right) + \dots,
\end{aligned} \tag{2.224}$$

where we used the standard identity $\varepsilon_{abc}\varepsilon_{ade} = \delta_{bd}\delta_{ce} - \delta_{be}\delta_{cd}$. A convenient choice for the normalization constants N_i that is compatible with (2.207) and diagonalizes (2.224) is to set two constants to zero and the remaining one to R . For instance, taking $N_1 = N_2 = 0$, $N_3 = R$ the only non-vanishing terms in (2.224) are

$$\begin{aligned}
[D_\mu(\phi + \phi^0)]^T \mathcal{I} [D^\mu(\phi + \phi^0)] &= e^2 (A_\mu^1 A^{1\mu} + A_\mu^2 A^{2\mu}) (\phi_i^0)^3 \mathcal{I}_{ij} (\phi_j^0)^3 + \dots \\
&= e^2 R^2 \left(1 - \frac{\mu^4}{m_2^4} \right) (A_\mu^1 A^{1\mu} + A_\mu^2 A^{2\mu}) + \dots
\end{aligned} \tag{2.225}$$

Thus for $\mu^4 \neq m_2^4$ and $R \neq 0$ we obtain two massive vector gauge bosons $m_g^{(1)}$ and $m_g^{(2)}$, that is one for each “would-be Goldstone boson”. When $\mu^4 = m_2^4$, that is then model is at the zero exceptional point, the gauge mass vector bosons remain massless. This feature is compatible with our previous observations in [8, 7] and above, that at these points the Goldstone bosons can not be identified.

We notice here that the two massive vector gauge bosons are proportional to the inner product of left and right eigenvectors

$$m_{\text{gauge}}^2 \propto \phi^{\text{vac}} \hat{I} \phi^{\text{vac}} \propto R^2 \left(1 - \frac{\mu^4}{m_2^4} \right). \tag{2.226}$$

Hence, the vanishing of the mass for the vector gauge bosons at the zero exceptional points can be associated with the inner product’s vanishing between left and right eigenvectors. This is reminiscent of the vanishing of the inner product at the standard exceptional points in different areas of non-Hermitian physics, which is responsible for interesting phenomena such as the stopping of light at these locations in the parameter space [114, 115].

2.5.3 Summary

We have considered two theories that differ by the representation of the fields in the fundamental (2.195) and the adjoint (2.160) representation. In both cases, we observed that the Higgs mechanism works in the \mathcal{PT} -symmetric region and the exceptional points. However, we observed that the Higgs mechanism does not occur at the zero exceptional points, because there is no explicit form of the Goldstone boson at the zero exceptional points. We have also observed that the physical region of the massive gauge particle included the physical region of the Higgs particles as a subset (see figure 2.6). The second model (2.160) showed the same phenomena as the first. However, the novelty of this model is that it contains the non-trivial solution to the equations of motion called the t'Hooft-Polyakov monopole. Therefore, the results found for the model (2.160) will be useful in the next chapter.

Chapter 3

Complex topological soliton solutions with real energies in non-Hermitian quantum field theories

3.1 Reality of the complex soliton solutions

The current chapter will focus on the different types of solution in the quantum field theory called the soliton solution, which are a non-trivial solution to the equations of motion of the quantum field theory. The classical mass of the soliton solution is found by inserting the solution into the Hamiltonian $M = H[\phi] = \int d^3x \mathcal{H}(\phi)$. Therefore, the techniques from \mathcal{PT} symmetric quantum mechanics can not be applied, where the reality of the non-Hermitian mass matrix was guaranteed by the corresponding \mathcal{PT} symmetry of the matrix.

In this chapter, we will study several different types of soliton solutions in various dimensions and models. Through studying different models, we have identified a common anti-linear symmetry between the solutions which guarantees the reality of the complex soliton solutions. To facilitate the legibility of the chapter, we will first state the reality condition of the complex soliton solutions in a general form and verify that indeed each soliton in different models respects this. We will show below that the energy of the soliton solutions are real when three conditions stated below holds. Therefore it is *sufficient* conditions to guarantee the reality of the model.

However, we do not claim that this is a *necessary* condition for a real classical mass.

Let $\{\phi_1, \phi_2\}$ be a set of distinct (or identical) solutions to the equations of motion $\delta\mathcal{L}/\delta\phi - \partial_\mu(\delta\mathcal{L}/\delta\partial_\mu\phi) = 0$. The classical masses of the solution is given by inserting the solution into the Hamiltonian, $M_i = H[\phi_i] = \int d^3x \mathcal{H}(\phi_i)$, for $i \in \{1, 2\}$. The classical mass of the solution ϕ_1 and ϕ_2 are real if there exist some anti-linear symmetry \mathcal{CPT} (note that is it not the standard \mathcal{CPT} symmetry in quantum field theory) such that three conditions are satisfied:

1. $\mathcal{CPT} : \mathcal{H}[\phi(x)] \rightarrow \mathcal{H}[\mathcal{CPT}\phi(x)] = \mathcal{H}^\dagger[\phi(-x)]$.
2. $\mathcal{CPT} : \phi_1(x) \rightarrow \phi_2(-x)$.
3. $H[\phi_1] = H[\phi_2]$.

If two solutions are identical $\phi_1 = \phi_2$, then the above condition reduces to the reality condition of the soliton solution already derived in [116]. Using the above three conditions, the reality of the classical mass can easily be shown by the following argument

$$\begin{aligned}
 M_1 &= \int d^3x \mathcal{H}[\phi(x)] \xrightarrow{\mathcal{CPT}} \int d^3x \mathcal{H}[\mathcal{CPT}\phi(x)] \stackrel{(1)}{=} \int d^3x \mathcal{H}^\dagger[\phi(-x)] = M_1^\dagger, \\
 &\stackrel{(2)}{=} \int d^3x \mathcal{H}[\phi_2(-x)] = M_2. \\
 &\implies M_1^\dagger = M_2 \stackrel{(3)}{\implies} M_1^\dagger = M_1.
 \end{aligned}$$

Where numbers above the equal signs indicate the condition number.

3.2 Topological Solitons in particle physics

In this section, we find 't Hooft-Polyakov monopole solutions in a non-Hermitian field theory, having local $SU(2)$ symmetry and anti-linear \mathcal{CPT} symmetry. Two of the main finding of this section are

1. Different similarity transformations result in different monopole solutions with same energy.
2. \mathcal{CPT} symmetry of the monopole solutions changes in different parameter regimes.

The first point will be the main discussion in section 3.2.4, where it follows from the novel feature of the non-Hermitian theory, where the similarity transformation is, in

general, non-unique. The second point will be the main discussion in section 3.2.5 where we will observe three separate regions of qualitatively different behaviours in parameter space bounded by different types of exceptional points with different \mathcal{CPT} symmetries in each region.

3.2.1 Soliton solution in a Hermitian model with $SU(2)$ gauge symmetry

This subsection briefly reviews the t'Hooft-Polyakov monopole in Hermitian quantum field theory with local $SO(3)$ symmetry. The rest of the section extends the idea discussed in this subsection to non-Hermitian theory and utilises the methods and results already obtained in the first chapter.

Let us begin with a local $SO(3)$ symmetric gauge field theory.

$$\mathcal{L} = \frac{1}{2} D_\mu \phi^a D^\mu \phi^a - V(\phi) - \frac{1}{4} F_\mu^a F^{a\mu\nu}. \quad (3.1)$$

The Lagrangian consist of a three component real scalar fields $\{\phi^a\}_{a=1,2,3}$ and the three gauge fields $\{A_\mu^a\}_{a=1,2,3}$ with the covariant derivative defined as $D_\mu \phi^a := \partial_\mu \phi^a + e(A_\mu \times \phi)^a$, where e is a charge of the gauge field A_μ . The kinetic term of the gauge fields is defined with the field strength tensor $F_{\mu\nu}^a = \partial_\mu A_\nu^a - \partial_\nu A_\mu^a + e(A_\mu \times A_\nu)^a$. The potential is

$$V = -\frac{\mu}{2} \phi^a \phi^a + \frac{\lambda}{4} (\phi^a \phi^a)^2, \quad (3.2)$$

with vacuum solutions $\sum_a \phi_0^a \phi_0^a = \mu/\lambda$ found by solving $\delta V = 0$, as explained in the previous chapter. By redefining the potential as $V \rightarrow V - \delta V(\phi_0) \equiv \tilde{V}$, one can show that the potential vanishes at the vacuum solution, $\tilde{V}(\phi_0) = 0$. We will use V and \tilde{V} interchangeably as it is simply a shift by a constant. The equations of motion of ϕ^a and A_μ for this model are

$$D_\nu F_a^{\nu\mu} - e(\phi \times D^\mu \phi)_a = 0, \quad D_\mu D^\mu \phi^a + \frac{\delta V}{\delta \phi^a} = 0 \quad (3.3)$$

The t'Hooft-Polyakov monopole is a non-trivial solution to the above differential equation. From appendix A.1 we know that the non-trivial solution to the above equation needs to converge to the constant solution which minimise the entire action $S[\phi_0] = 0$, called the vacuum solution. If the action has no gauge fields, then such

constant can be found by solving $\delta V(\phi) = 0$. However, since the kinetic term is modified to accommodate for the local symmetry, the vacuum solution also needs to satisfy extra condition $D_\mu \phi_0 = e(A_\mu^0 \times \phi_0) = 0$. To distinguish this vacuum solution from the non-gauged vacuum solution, it is often referred to as *Higgs vacuum* [117].

The resulting Higgs vacuum solution for this model is

$$\phi_0^a = \sqrt{\frac{\mu}{\lambda}} \hat{r}_n^a \quad (3.4)$$

$$(A_i^0)^a = -\frac{1}{er} \epsilon^{iaj} \hat{r}_n^j + \hat{r}_n^a A_i, \quad (A_0^0)^a = 0. \quad (3.5)$$

The Ansatz for the gauge field $(A_i^0)^a$ is taken from [118] where A_μ is some space-time vector field. The radial unit vector $\hat{r}_n, n \in \mathbb{Z}$ is defined by

$$\hat{r}_n^a = \begin{pmatrix} \sin(\theta) \cos(n\varphi) \\ \sin(\theta) \sin(n\varphi) \\ \cos(\theta) \end{pmatrix}. \quad (3.6)$$

Notice that the solution ϕ_0^a is a mapping from the 2 sphere in space-time to the 2-sphere in field configuration space. Therefore the solution belongs to the 2nd homotopy group $\pi^2(S^2) = \mathbb{Z}$, meaning there are $n \in \mathbb{Z}$ many topologically inequivalent solutions labelled by n . This is precisely the reason why the above Higgs vacua are defined for every $n \in \mathbb{Z}$. In appendix A.2, it is explicitly shown that the integer n corresponds to the winding number of the mapping $\phi_0^a : S^2 \rightarrow S^2$.

Keeping in mind that the solutions need to converge to the above Higgs vacuum solutions in an asymptotic limit, let us choose a set of static spherical Ansatz

$$\phi^a = \hat{r}^a h(r), \quad A_i^a = \epsilon^{aib} \hat{r}^b \left(\frac{1-u(r)}{er} \right), \quad A_0^a = 0. \quad (3.7)$$

Here $\hat{r}^a = (x, y, z)/\sqrt{x^2 + y^2 + z^2}$ is a normalised vector $\sum_a r^a r^a = 1$ and the radius r from the origin $(x, y, z) = (0, 0, 0)$. Inserting this parametrisation into the equations of motion, one obtains

$$h'' + \frac{2}{r} h' - \frac{2u^2 h}{r^2} + \lambda(v^2 - h^2)h = 0, \quad (3.8)$$

$$u'' - \frac{u(u^2 - 1)}{r^2} - e^2 u h^2 = 0, \quad (3.9)$$

where $h' = \partial_r h$ represents the radial derivative. The approximate solution to this

differential equation was found by Prasad and Sommerfield [119] by taking a twofold scaling limit $\mu \rightarrow 0, \lambda \rightarrow 0$ but keeping the vacuum solution $v = \sqrt{\mu/\lambda}$ invariant. This limit is often called the Bogoliubov Prasad Sommerfield (BPS) limit. The solutions were found by solving the simplified differential equations with the extra assumption that the solutions asymptote to the vacuum solution in the spatial infinity. This constraint follows from Derrick's scaling argument (see appendix A), which ensures that the energy of the solution is finite. The solutions are

$$h = v \coth(evr) - \frac{1}{er}, \quad u = \frac{evr}{\sinh(evr)}. \quad (3.10)$$

One can check that this solution satisfies the differential equations (3.8) and (3.9) given that the fourth term of the equation (3.8) vanishes by the BPS limit. The classical mass of this monopole solution can be found by directly inserting it into the Hamiltonian. However, there is a more elegant way to obtain the mass using the method which we refer to as the BPS method. The Hamiltonian of the model (3.1) in the BPS limit is

$$H = \frac{1}{2} \int d^3x \left[(\mathcal{E}_i^a)^2 + (\mathcal{B}_i^a)^2 + (\Pi^a)^2 + ((D_i\phi)^a)^2 \right]. \quad (3.11)$$

Where $\mathcal{E}_i^a \equiv -\mathcal{F}_{0i}^a$, $\mathcal{B}_i^a \equiv -\frac{1}{2}\epsilon_i{}^{jk}\mathcal{F}_{jk}^a$. Since we are only considering the static solution, the electric field \mathcal{E} vanishes. Then notice that

$$\mathcal{B}_i^a \mathcal{B}_i^a + (D_i\phi)^a (D_i\phi)^a = (\mathcal{B}_i^a \mp (D_i\phi)^a) (\mathcal{B}_i^a \mp (D_i\phi)^a) \pm 2\mathcal{B}_i^a (D_i\phi)^a.$$

Using this, the Hamiltonian can be rewritten as

$$\begin{aligned} H &= \frac{1}{2} \int d^3x \left[2\mathcal{B}_i^a (D_i\phi)^a + (\mathcal{B}_i^a - (D_i\phi)^a)^2 + (\Pi^a)^2 + V \right] \quad (3.12) \\ &\geq \frac{1}{2} \int d^3x [2\mathcal{B}_i^a (D_i\phi)^a] = \int d^3x [\mathcal{B}_i \cdot \partial_i\phi + e\mathcal{B}_i \cdot (\mathcal{A}_i \times \phi)] \\ &= \int d^3x [\mathcal{B}_i \cdot \partial_i\phi - e\phi \cdot (\mathcal{A}_i \times \mathcal{B}_i)] \\ &= \int d^3x [\mathcal{B}_i \cdot \partial_i\phi + \phi \cdot \partial_i\mathcal{B}_i] \\ &= \int d^3x [\partial_i\mathcal{B}_i \cdot \phi] = \lim_{r \rightarrow \infty} \int_{S_r} dS_i [\mathcal{B}_i \cdot \phi] \\ &= \phi_0^a \lim_{r \rightarrow \infty} \int_{S_r} dS_i [\mathcal{B}_{0i}^a]. \end{aligned}$$

The dot product represent the contraction of group indices $\sum_a \phi^a \phi^a \equiv \phi \cdot \phi$ and S_r is a 2-sphere with radius r . Going from the third line to fourth line, we used $D_i B_i^a = \partial_i \mathcal{B}_i^a + e(\mathcal{A}_a \times \mathcal{B}_i) = 0$ which can be shown from the Bianchi identity $D_\mu \epsilon^{\mu\nu\rho\sigma} F_{\rho\sigma}^a = 0$. The fifth line is obtained by using the Gauss theorem at some fixed value of the radius r . Since we are integrating over the 2 sphere with large radius, the integrand $\mathcal{B}_i \cdot \phi$ is defined far from the origin. This means we can replace the integrand with the Higgs vacuum solution $\{\phi_0^a, \mathcal{B}_{0i}^a\}$, required by the Derrick's theorem. This is how the last line is obtained.

Surprisingly, this inequality (3.12) becomes an equality for the solutions (3.10) because the quantity appearing in the bracket $\mathcal{B}_i^a - (D_i \phi)^a$ vanishes with the solution (3.10), resulting in a much simpler form of the energy. The explicit value of \mathcal{B}_{0i}^a can be obtained by inserting the expressions from (3.5) into

$$\mathcal{B}_{0i}^a = -\frac{1}{2} \epsilon_i^{jk} (\partial_j \mathcal{A}_k^0 - \partial_k \mathcal{A}_j^0 + e \mathcal{A}_j^0 \times \mathcal{A}_k^0)^a. \quad (3.13)$$

After a lengthy calculation presented in appendix A.2.1 this expression can be simplified to $\mathcal{B}_{0i}^a = \hat{\phi}^{0a} B_i = \hat{r}_n^a B_i$, where $\hat{\phi}^{0a}$ is a normalised solution $\sum_a \hat{\phi}^{0a} \hat{\phi}^{0a} = 1$. The B_i is defined as

$$B_i \equiv -\frac{1}{2} \epsilon_{ijk} \left\{ \partial^j A^k - \partial^k A^j + \frac{1}{e} \hat{r}_n \cdot (\partial^j \hat{r}_n \times \partial^k \hat{r}_n) \right\}. \quad (3.14)$$

Notice that integrating the first term over the 2-sphere gives zero by Stoke's theorem $\int_S \partial \times A = \int_{\partial S} A = 0$ where one can show that Stoke's theorem on closed surface gives zero by dividing the sphere into two open surfaces. The second term is a topological term which can be evaluated as

$$\int dS_i B_i = -\frac{4\pi n}{e}. \quad (3.15)$$

The explicit calculation is in appendix A.2.1 and also [120]. This is the magnetic charge of the monopole solutions. Finally we obtain the energy of the t'Hooft-Polyakov monopole

$$E = \frac{1}{2} \int d^3x [2\mathcal{B}_i^a (D_i \phi)^a] = \frac{4|n|\mu\pi}{ev}. \quad (3.16)$$

The first-order differential equation $\mathcal{B}_i^a - (D_i \phi)^a$ which saturate the inequality in

equation 3.12 is called the BPS equation. More example of models which possess the solutions to the BPS equation are explored in section 3.3.

3.2.2 Soliton solution in a non-Hermitian model with $SU(2)$ gauge symmetry

Here we begin with the non-Hermitian $SU(2)$ gauge theory with matter fields in the adjoint representation given in equation (2.195). This action is invariant under the local $SU(2)$ transformation of the matter fields (2.197) and gauge fields (2.199) given in section 2.5.2. The action (2.195) is also symmetric under modified \mathcal{CPT} symmetry which transform two fields ϕ_1 and ϕ_2 as

$$\mathcal{CPT} : \phi_1(t, \vec{x}) \rightarrow \phi_1(-t, -\vec{x}) , \quad \phi_2(t, \vec{x}) \rightarrow -\phi_2(-t, -\vec{x}) , \quad i \rightarrow -i. \quad (3.17)$$

The equations of motion for the fields ϕ_i and A_μ of the Lagrangian (2.195) are

$$(D_\mu D^\mu \phi_i)^a + \frac{\delta V}{\delta \phi_i^a} = 0 , \quad D_\nu F_a^{\nu\mu} - e\epsilon_{abc}\phi_1^b (D^\mu \phi)^c + e\epsilon_{abc}\phi_2^b (D^\mu \phi)^c = 0. \quad (3.18)$$

We have already introduced the similarity transformation in section 2.5. However, there are further possibilities for the similarity transformation such as

$$\eta_\pm = \prod_{a=1}^3 \exp \left(\pm \frac{\pi}{2} \int d^3x \Pi_2^a \phi_2^a \right). \quad (3.19)$$

We did not consider different possibilities of the similarity transformation in the last chapter because they do not affect the eigenvalues of the transformed mass matrix. However, we will see in this section that different transformations can lead to different soliton solutions with the same energy. This non-uniqueness of the metric is analogues to the non-uniqueness of the metric and its connection to the observables in the quantum mechanical setting discussed in [20, 29].

The adjoint action of η_\pm maps the complex action in equation (2.195) into the

following real action

$$\begin{aligned}
\mathfrak{s} &= \int d^4x \left[\frac{1}{4} \text{Tr} (D\phi_1)^2 - \frac{1}{4} \text{Tr} (D\phi_2)^2 + c_1 \frac{m_1^2}{4} \text{Tr}(\phi_1^2) - c_2 \frac{m_2^2}{4} \text{Tr}(\phi_2^2) \right. \\
&\quad \left. - c_3 \frac{\mu^2}{2} \text{Tr}(\phi_1\phi_2) - \frac{g}{64} (\text{Tr}(\phi_1^2))^2 - \frac{1}{8} \text{Tr}(F^2) \right] \\
&\equiv \int d^4x \left[\frac{1}{4} \text{Tr} (D\phi_1)^2 - \frac{1}{4} \text{Tr} (D\phi_2)^2 - V - \frac{1}{8} \text{Tr}(F^2) \right].
\end{aligned} \tag{3.20}$$

Notice that this action is equivalent to the action (2.204) if $c_3 = 1$. The parameter c_3 indicates the different similarity transformations by taking the values ± 1 for η_{\pm} , respectively.

As discussed in the previous chapter, the action (3.20) is real, but the mass matrix of the fields ϕ_1 and ϕ_2 are still non-Hermitian. Therefore one needs to diagonalise the Lagrangian by employing a biorthonormal basis. However, we will still directly analyse the above action as we will observe at the end of this section an interesting exchange of the \mathcal{CPT} -symmetry between the monopole solutions of ϕ_1 and ϕ_2 in different physical regions, which is invisible if one directly analyses the fully diagonalised Lagrangian.

As explained in appendix A.1 and also in previous section, the monopole solution is required to asymptotically converges to the Higgs vacuum, which is found by solving $\delta V = 0$ and $D_\mu \phi_\alpha = 0$. The first equation can be simplified by choosing an Ansatz $(\phi_i^0)^a(t, \vec{x}) = h_i^0 \hat{r}^a(\vec{x})$ where $\hat{r} = (x, y, z)/\sqrt{x^2 + y^2 + z^2}$ and $\{h_i^0\}$ are some constants to be determined. Inserting this Ansatz to equation (2.204), we find

$$V = -\frac{1}{2} h_i H_{ij} h_j + \frac{g}{16} h_1^4. \tag{3.21}$$

Then the vacuum equation $\delta V = 0$ is reduced to simple coupled third order algebraic equations

$$\begin{aligned}
\frac{g}{4} (h_1^0)^3 - c_1 m_1^2 h_1^0 + c_3 \mu^2 h_2^0 &= 0, \\
c_2 m_2^2 h_2^0 + c_3 \mu^2 h_1^0 &= 0,
\end{aligned} \tag{3.22}$$

$$D_\mu \phi_\alpha = 0. \tag{3.23}$$

The resulting vacuum solutions are

$$h_2^0 = -\frac{c_2 c_3 \mu^2}{m_2^2} h_1^0, \quad (h_1^0)^2 = 4 \frac{c_2 \mu^4 + c_1 m_1^2 m_2^2}{g m_2^2} := R^2, \quad (3.24)$$

$$(A_i^0)^a = -\frac{1}{e} \epsilon^{abc} \hat{r}^b \partial_i \hat{r}^c + \hat{r}^a A_i = -\frac{1}{e r} \epsilon^{iaj} \hat{r}^j + \hat{r}^a A_i, \quad (A_0^0)^a = 0,$$

The A_i are arbitrary functions of space-time. The asymptotic condition can be written more explicitly if we consider the spherical Ansatz

$$(\phi_\alpha^{cl})^a(\vec{x}) = h_\alpha(r) \hat{r}^a, \quad (A_i^{cl})^a = \epsilon^{iaj} \hat{r}^j A(r), \quad (A_0^{cl})^a = 0, \quad (3.25)$$

where the subscript cl denotes the classical solutions to the equations of motion equation (3.18). The difference between this Ansatz (3.25) and the Higgs vacuum (3.24) is that the quantity h_i now depends on the spatial radius $h_i = h_i(r)$. Here we are only considering the static Ansatz to simplify our calculation, but one may of course also consider the time-dependent solution. For the monopole solution to have finite energy, we require the two matter fields of equation (3.25) to approach the vacuum solutions in equation (3.24) at spatial infinity

$$\lim_{r \rightarrow \infty} h_1(r) = h_1^{0\pm} = \pm R, \quad \lim_{r \rightarrow \infty} h_2(r) = h_2^{0\pm} = \mp \frac{c_2 c_3 \mu^2}{m_2^2} R. \quad (3.26)$$

Also notice that at some fixed value of the radius r , the vacuum solutions ϕ_α^0 and monopole solutions ϕ_α^{cl} both belongs to the 2-sphere in the field configuration space. For example, ϕ_1^0 belong to the 2-sphere with radius R because $(\phi_1^0)^2 = R^2$. Therefore we can apply the analysis from the previous section and notice that the radius r can be redefined to equation (3.6) where the integer n represent the winding number as shown in appendix A.2.1.

Since we require the monopole and vacuum solutions to smoothly deform into each other at spacial infinity, both solutions need to share the winding number. It is important to note that winding numbers of ϕ_1 and ϕ_2 need to be equal to satisfy $D\phi_1 = D\phi_2 = 0$ and therefore we will denote the winding numbers of ϕ_1 and ϕ_2 as n collectively. If they are not equal we would have $D\phi_1 = 0$ but $D\phi_2 \neq 0$. Next, let us insert our Ansatz equation (3.25) into the equations of motion equation (3.18). We will also take the Ansatz (3.7) for the gauge field A_μ . These Ansatz are more in line with the original Ansatz given in [119, 121] and also discussed in the previous section, compare to equation (3.25). Inserting these expressions into the equations

of motion equation (3.18) we find

$$u''(r) + \frac{u(r)[1-u^2(r)]}{r^2} + \frac{e^2 u(r)}{2} \{h_2^2(r) - h_1^2(r)\} = 0, \quad (3.27)$$

$$h_1''(r) + \frac{2h_1'(r)}{r} - \frac{2h_1(r)u^2(r)}{r^2} + g \left\{ -c_1 \frac{m_1^2}{g} h_1(r) + c_3 \frac{\mu^2}{g} h_2(r) + \frac{1}{4} h_1^3(r) \right\} = 0, \quad (3.28)$$

$$h_2''(r) + \frac{2h_2'(r)}{r} - \frac{2h_2(r)u^2(r)}{r^2} + c_2 m_2^2 \left\{ h_2(r) + c_3 \frac{\mu^2}{m_2^2} h_1(r) \right\} = 0. \quad (3.29)$$

Notice that these differential equations are similar to the ones discussed in [119, 121] and also discussed in the previous section, but with the extra field h_2 and extra differential equation equation (3.29). In the Hermitian model, the exact solutions to the differential equations were found by taking the parameter limit called the BPS limit [119, 121] where parameters in the theory are taken to zero while keeping the vacuum solution finite. Here we will follow the same procedure and take the parameter limit where quantities in the curly brackets of equation (3.28) and (3.29) vanish but keeping the vacuum solutions equation (3.24) finite. We will see in section 3.2.4 that we also find the approximate solutions in this limit. However, before we solve the differential equations, let us discuss the energy bound of the monopole.

3.2.3 The energy bound

The energy of the monopole can be found by inserting the monopole solution into the corresponding Hamiltonian of equation (3.20).

$$\begin{aligned} \mathfrak{h} = \int d^3x & \left[Tr(E^2) + Tr(B^2) + Tr\{(D_0\phi_1)^2\} + Tr\{(D_i\phi_1)^2\} \right. \\ & \left. - Tr\{(D_0\phi_2)^2\} - Tr\{(D_i\phi_2)^2\} + V \right], \end{aligned} \quad (3.30)$$

where E, B are $E_a^i = F_a^{0i}$, $B_a^i = -\frac{1}{2}\epsilon^{ijk}F_a^{jk}$, $i, j, k \in \{1, 2, 3\}$. The gauge is fixed to be the radiation gauge (i.e $A_a^0 = 0, \partial_i A_a^i = 0$). Notice that our monopole Ansatz equation (3.22) is static with no electric charge $E_i^a = 0$ and therefore the above Hamiltonian reduces to

$$\begin{aligned} E &= \int d^3x \left[Tr(B^2) + Tr\{(D_i\phi_1)^2\} - Tr\{(D_i\phi_2)^2\} + V \right] \\ &= 2 \int d^3x \left[B_i^a B_i^a + (D_i\phi_1)^a (D_i\phi_1)^a - (D_i\phi_2)^a (D_i\phi_2)^a + \frac{1}{2}V \right]. \end{aligned} \quad (3.31)$$

Here, we simplified our expression by dropping the superscripts $A_i^{cl} \rightarrow A_i$, $\phi_\alpha^{cl} \rightarrow \phi_\alpha$. We also keep in mind that these fields depend on the winding numbers $n \in \mathbb{Z}$. Recalling from section 3.2.1 that in the Hermitian model (i.e, when $\phi_2 = 0$) one can rewrite the kinetic term as $B^2 + D\phi^2 = (B - D\phi)^2 + 2BD\phi$ and find the lower bound to be $\int 2BD\phi$. Here we will follow the similar procedure but introducing some arbitrary constant $\alpha, \beta \in \mathbb{R}$ such that $B^2 = \alpha^2 B - \beta^2 B$ where $\alpha^2 - \beta^2 = 1$. This will allow us to rewrite the above energy as

$$E = 2 \int d^3x \left[\alpha^2 \left\{ B_i^a + \frac{1}{\alpha} (D_i \phi_1)^a \right\}^2 - \beta^2 \left\{ B_i^a + \frac{1}{\beta} (D_i \phi_2)^a \right\}^2 \right. \\ \left. + 2 \{ -\alpha B_i^a (D_i \phi_1)^a + \beta B_i^a (D_i \phi_2)^a \} + \frac{1}{2} V \right]. \quad (3.32)$$

To proceed from here, we need to assume extra constraints on α and β such that the following inequalities are true

$$\int d^3x \left[\alpha^2 \left\{ B_i^a + \frac{1}{\alpha} (D_i \phi_1)^a \right\}^2 - \beta^2 \left\{ B_i^a + \frac{1}{\beta} (D_i \phi_2)^a \right\}^2 \right] \geq 0, \quad (3.33)$$

$$\int d^3x V \geq 0. \quad (3.34)$$

Following the same procedure discussed in equation (3.12), the lower bound of the energy is written as

$$E \geq 2 \int d^3x [-\alpha B_i^a (D_i \phi_1)^a + \beta B_i^a (D_i \phi_2)^a] \quad (3.35) \\ = 2 \int d^3x \left[-\alpha \left\{ B_i^a \partial_i \phi_1^a + e B_i^a \epsilon^{abc} A_i^b \phi_1^c \right\} + \beta \left\{ B_i^a \partial_i \phi_2^a + e B_i^a \epsilon^{abc} A_i^b \phi_2^c \right\} \right] \\ = 2 \int d^3x \left[-\alpha \left\{ B_i^a \partial_i \phi_1^a + \left(-e \epsilon^{abc} A_i^b B_i^c \right) \phi_1^a \right\} \right. \\ \left. + \beta \left\{ B_i^a \partial_i \phi_2^a + \left(-e \epsilon^{abc} A_i^b B_i^c \right) \phi_1^a \phi_2^c \right\} \right] \\ = 2 \int d^3x [-\alpha \{ B_i^a \partial_i \phi_1^a + \partial_i B_i^a \phi_1^a \} + \beta \{ B_i^a \partial_i \phi_2^a + \partial_i B_i^a \phi_1^a \}] \\ = 2 \int d^3x [-\alpha \partial_i (B_i^a \phi_1^a) + \beta \partial_i (B_i^a \phi_2^a)] \\ = \lim_{r \rightarrow \infty} \left(-2\alpha \int_{S_r} dS_i [B_i^a \phi_1^a] + 2\beta \int_{S_r} dS_i [B_i^a \phi_2^a] \right),$$

where in the fourth line we used $D_i B_i^a = 0$ which can be shown from the Bianchi identity $D_\mu \epsilon^{\mu\nu\rho\sigma} F_{\rho\sigma}^a = 0$. The last line is obtained by using the Gauss theorem at some fixed value of the radius r . Since the ϕ_i^a in the integrand are only defined over

the 2-sphere with large radius, we can use the asymptotic conditions Eq. (3.26) and replace the monopole solutions $\{\phi_\alpha^a, B_i^a\}$ with the Higgs vacuum $\{(\phi_\alpha^0)^a, (B_i^0)^a\}$

$$\begin{aligned} E &\geq (-2\alpha\phi_1^{0a} + 2\beta\phi_2^{0a}) \lim_{r \rightarrow \infty} \int_{S_r} dS_i (B_i^0)^a \\ &= \left(\mp 2\alpha R \hat{r}_n^a \mp 2\beta \frac{c_2 c_3 \mu^2}{m_2^2} R \hat{r}_n^a \right) \lim_{r \rightarrow \infty} \int_{S_r} dS_i (B_i^0)^a, \end{aligned} \quad (3.36)$$

where the upper and lower signs of the above energy correspond to the upper and lower signs of the vacuum solutions in equation (3.24). The explicit value and calculation of the integration $\int_{S_r} dS_i (B_i^0)^a$ is given in previous section and discussed in appendix A.2.1. We recall that the integer n , which corresponds to the winding number of the solution comes from the Ansatz $B_i^a = \hat{\phi}^{0a} B_i$, where B_i is defined in equation (3.14). In our case there is an ambiguity of whether to choose $B_i^a = \hat{\phi}_1^{0a} B_i$ or $B_i^a = \hat{\phi}_2^{0a} B_i$. Now we see explicitly the reason why we choose to keep the same integer values for solutions ϕ_1^0 and ϕ_2^0 as discussed in the paragraph before equation (3.27). If the integer values of \hat{r}_n^a in solutions ϕ_1^0, ϕ_2^0 are different, then the integration $\int_{S_r} dS_i (B_i^0)^a$ will be different, leading to an inconsistent energy.

Finally we find our lower bound of the monopole energy

$$E \geq \mp 2R \left(\alpha + \beta \frac{c_2 c_3 \mu^2}{m_2^2} \right) \hat{r}_n^a \hat{r}_n^a \left(\frac{-4\pi n}{e} \right) = \frac{\pm 8\pi n R}{e} \left(\alpha + \beta \frac{c_2 c_3 \mu^2}{m_2^2} \right). \quad (3.37)$$

Notice that we have some freedom to choose $\alpha, \beta \in \mathbb{R}$ as long as our initial assumptions (3.33) are satisfied. We will see in the next section that we can take a parameter limit of our model which saturates the above inequality and gives exact values to α and β .

3.2.4 The fourfold BPS scaling limit

Our main goal is now to solve the coupled differential equations equation (3.27)-(3.29). Prasad, Sommerfield, and Bogomolny [119, 121] managed to find the exact solution by taking the parameter limit, which simplifies the differential equations. The multiple scaling limit is taken so that all the parameters of the model tend to zero with some combinations of the parameter remaining finite. The combinations are taken so that the vacuum solutions stay finite in this limit. Inspired by this, we

will take here a fourfold scaling limit

$$g, m_1, m_2, \mu \rightarrow 0, \quad \frac{m_1^2}{g} < \infty, \quad \frac{\mu^2}{g} < \infty, \quad \frac{\mu^2}{m_2^2} < \infty. \quad (3.38)$$

This will ensure that the vacuum solutions equation (3.24) stays finite, but crucially the curly bracket parts in equation (3.28), (3.29) vanish. There is a physical motivation for this limit in which the mass ratio of the Higgs and gauge mass are taken to be zero (i.e $m_{\text{Higgs}} \ll m_g$) as described in [122]. We will see in the next section that the same type of behaviour is present in our model, hence justifying equation (3.38). The resulting set of differential equations, after taking the BPS limit is similar to the ones considered in [119, 121] with the slightly different quadratic term in equation (3.27). It is natural to consider a similar Ansatz as given in [119, 121]

$$u(r) = \frac{evr}{\sinh(evr)}, \quad (3.39)$$

$$h_1(r) = -\alpha \left(v \coth(evr) - \frac{1}{er} \right) \equiv -\alpha f(r), \quad (3.40)$$

$$h_2(r) = -\beta \left(v \coth(evr) - \frac{1}{er} \right) \equiv -\beta f(r), \quad (3.41)$$

where $\alpha, \beta \in \mathbb{R}$ were introduced in section 3.2.3 and $f(r) \equiv \{v \coth(evr) - \frac{1}{er}\}$. One can check that this Ansatz indeed satisfies differential equations equation (3.27)-(3.29) in the BPS limit. We have decided to put a prefactor α and β in front of equation (3.40),(3.41) to satisfy the differential equation equation (3.27). Note that if we take $\alpha = 1$ we get exactly the same as given in [119, 121], which is known to satisfy the first order differential equation called Bogomolny equation $B_i - D_i\phi = 0$. The Ansatz (3.39)-(3.41) only differs from the ones given in [119, 121] by the prefactors α and β , and therefore our Ansatz should satisfy Bogomolny equation with the appropriate scaling to cancel the prefactor in equation (3.40),(3.41)

$$B_i^b + \frac{1}{\alpha} (D_i\phi_1)^b = 0, \quad (3.42)$$

$$B_i^b + \frac{1}{\beta} (D_i\phi_2)^b = 0, \quad (3.43)$$

where $\phi_\alpha \equiv h_\alpha(r)\hat{r}_n$. If we compare these equations to the terms appearing in the energy of the monopole equation (3.32), then we can saturate the inequality in

equation (3.37) by

$$E[\phi_1, \phi_2] = \frac{\pm 8\pi n R}{e} \left(\alpha + \beta \frac{c_2 c_3 \mu^2}{m_2^2} \right), \quad (3.44)$$

where upper and lower signs correspond to the vacuum solutions equation (3.24), when taking the square root. We can calculate the explicit forms of α and β by comparing the asymptotic conditions in equation (3.26)

$$\lim_{r \rightarrow \infty} h_1^\pm = h_1^{0\pm} = \pm R, \quad \lim_{r \rightarrow \infty} h_2^\pm = h_2^{0\pm} = \mp \frac{c_2 c_3 \mu^2}{m_2^2} R, \quad (3.45)$$

with the asymptotic values of equation (3.39)-(3.41)

$$\lim_{r \rightarrow \infty} u(r) = 0, \quad \lim_{r \rightarrow \infty} h_1^\pm(r) = -\alpha v, \quad \lim_{r \rightarrow \infty} h_2^\pm(r) = -\beta v. \quad (3.46)$$

By Derrick's scaling argument, the two asymptotic values (3.45) and (3.46) should match, resulting in algebraic equations for α and β . Using $\alpha^2 - \beta^2 = 1$ and assuming $m_2^4 \geq \mu^4$, we find the four set of real solutions

$$\alpha = \mp(\pm) \frac{m_2^2}{l}, \quad v = (\pm) \frac{Rl}{m_2^2}, \quad \beta = \pm(\pm) \frac{c_2 c_3 \mu^2}{l}, \quad (3.47)$$

where $l = \sqrt{m_2^4 - \mu^4}$. The plus-minus signs in the brackets correspond to the two possible solutions to the algebraic equation $\alpha^2 - \beta^2 = 1$. These need to be distinguished from the upper and lower signs of α and β which correspond to the vacuums solutions (3.24). Inserting the explicit values of α and β to the energy equation (3.44) we find

$$E[\phi_1, \phi_2] \equiv (\pm) \frac{8\pi n R}{em_2^2} \left(\frac{-m_2^4 + \mu^4}{l} \right) = (\pm) \frac{-8\pi n R}{em_2^2} l, \quad (3.48)$$

with corresponding solutions

$$\begin{aligned} h_1^\pm(r) &= \pm(\pm) \frac{m_2^2}{l} \left[\frac{Rl}{m_2^2} \coth \left(\frac{eRl}{m_2^2} r \right) - \frac{1}{er} \right], \\ h_2^\pm(r) &= \mp(\pm) \frac{c_2 c_3 \mu^2}{l} \left[\frac{Rl}{m_2^2} \coth \left(\frac{eRl}{m_2^2} r \right) - \frac{1}{er} \right]. \end{aligned} \quad (3.49)$$

It is crucial to note that although it seems like there are two monopole solutions $\{h_1^\pm, h_2^\pm\}$, the two solution are related non-trivially in its asymptotic limit by the

constraint $\lim h_2^\pm = (-c_2 c_3 \mu^2 / m_2^2) \lim h_1^\pm$ given in equation (3.22). For example, one can not choose $\{h_1^+, h_2^-\}$ as a solution as this will break the asymptotic constraint.

The solution (3.49) can be constrained further by imposing that the energy (3.48) is real and positive.

$$E[\phi_1, \phi_2] > 0 \implies -(\pm) \frac{8\pi n R}{em_2^2} l \implies -(\pm)n > 0. \quad (3.50)$$

Therefore we can ensure positive energy if $(\pm) = \text{sign}(n)$. The final form of the monopole solution with positive energy are

$$\begin{aligned} h_1^\pm(r) &= \pm \text{sign}(n) \frac{m_2^2}{l} \left[\frac{Rl}{m_2^2} \coth\left(\frac{eRl}{m_2^2} r\right) - \frac{1}{er} \right], \\ h_2^\pm(r) &= \mp \text{sign}(n) \frac{c_2 c_3 \mu^2}{l} \left[\frac{Rl}{m_2^2} \coth\left(\frac{eRl}{m_2^2} r\right) - \frac{1}{er} \right]. \end{aligned} \quad (3.51)$$

with energy $E = 8|n|\pi l R / em_2^2$. We conclude this subsection by observing that the above solution depends on the parameter c_3 , which takes value $\{-1, 1\}$ depending on the choice of the similarity transformation. Choosing different values of c_3 also result in a different asymptotic values (3.45), meaning solutions for $c_3 = 1$ and $c_3 = -1$ are topologically different. Since the energy is independent of c_3 , two distinct solutions share the same energy. Respecting one of the main features of similarity transformation, which is to preserve the energy of the transformed Hamiltonian.

In the next section, we will investigate in detail how the solution changes and new \mathcal{CPT} symmetry emerges by changing the parameter values.

3.2.5 Real and complex monopole solutions with real energies

This section will investigate the behaviour of the solution (3.51) in different regimes of the parameter spaces. We will compare the physical regions of monopoles and gauge particles found in the previous chapter. We will see that the two regions coincide, but the solutions in different regions possess different \mathcal{CPT} symmetries. Different symmetries of solutions in different regions are not the coincident but the consequence of the three realty conditions stated in section 3.1. In fact, it is deeply related to the reality of energy, which will be explored at the end of this section.

Higgs mass and exceptional points

Let us recall the masses of the particles (2.218) (which are also equivalent to (2.148)) and the gauge mass (2.225). Reintroducing the parameters c_1, c_2 in (2.217) and (2.225), we find

$$m_0^2 = c_2 \frac{\mu^4 - m_2^4}{m_2^2}, \quad m_{\pm}^2 = K \pm \sqrt{K^2 + 2L}, \quad m_g = e \frac{Rl}{m_2^2}, \quad (3.52)$$

where $K = c_1 m_1^2 - c_2 \frac{m_2^2}{2} + \frac{3\mu^4}{2c_2 m_2^2}$ and $L = \mu^4 + c_1 c_2 m_1^2 m_2^2$. Notice that the masses do not depend on c_3 , meaning they do not depend on the similarity transformation as expected. We also comment that in the BPS limit we have $m_0 = m_{\pm} = 0$, but m_g and M_{\pm} stays finite, such that the ratios m_{Higgs}/m_g vanish in the BPS limit. This is in line with the Hermitian case [122], providing the physical interpretation $m_{\text{Higgs}} \ll m_g$ for the BPS limit.

In section 2.4.2, the physical region, where all values of equation (3.52) stay real and positive, were investigated with the figure 2.4 showing two disconnected regions for $c_1 = -c_2 = 1$ and $c_1 = -c_2 = -1$. Since the monopole energy is proportional to the gauge mass in terms of R and l , the physical region coincides with the one shown in figure 2.4.

One may notice that when $c_2 = 1$, requiring positive mass $m_0^2 > 0$ implies that $\mu^4 - m_2^4 > 0$. This means the quantity $l = \sqrt{m_2^4 - \mu^4}$ is purely imaginary. One may then discard this region as unphysical. However, we will see in next section that there is a disconnected region beyond $\mu^4 - m_2^4 > 0$, which admit real energy because R also becomes purely complex. This is not a coincidence and in fact we will see an emerging new \mathcal{CPT} symmetry for the monopoles.

In the rest of the section, we will exclusively focus on the monopole and gauge masses. The main message of this subsection is the emerging symmetry responsible for the reality of the monopole masses. The requirement to make the whole theory physical demands also to consider the intersecting of the physical regions between monopole masses and Higgs masses. As an example, we plot all the masses of the theory in figure 3.1. As one can see, the intersecting points of the physical regions of Higgs masses and monopole/gauge masses are non-trivial. However, we do not need to know the exact intersecting point. There are two reasons for this:

- i) From section 2.5, we already know that the physical regions of Higgs masses

and gauge mass always intersect.

- ii) The analysis done in the rest of the section applies to any point in the physical regions of monopole/gauge masses, so we can assume that the full theory is in the physical regions.

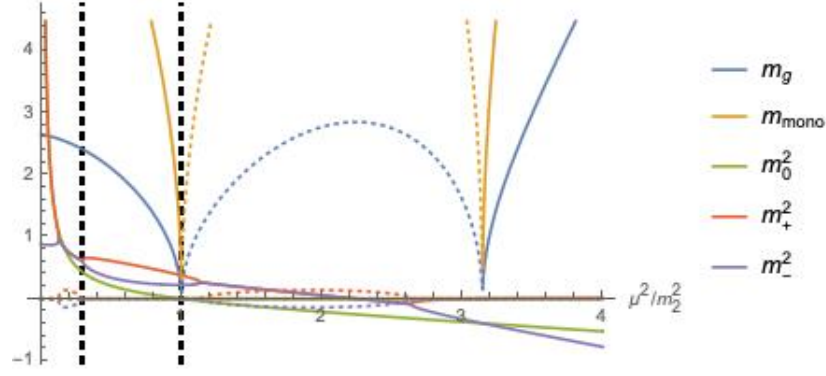


Figure 3.1: Monopole, gauge and Higgs masses plotted for $m_1^2/g = -0.44$, $\mu/g = -0.14$, $e = 2$, $c_1 = -c_2 = -1$. The solid line represent the real part and dotted line represent the imaginary part of the masses. The dotted vertical lines indicate the boundaries of the physical regions where all the masses acquire real positive values.

Change in \mathcal{CPT} symmetry and complex monopole solution

We begin by introducing the useful quantities $m_1^2/g \equiv X$, $\mu^2/g \equiv Y$, $\mu^2/m_2^2 \equiv Z$. The gauge mass, monopole mass and monopole solutions can be rewritten in terms of these quantities

$$m_g = eR\sqrt{1-Z^2}, \quad m_{\text{mono}} = \frac{8|n|\pi R}{e}\sqrt{1-Z^2}, \quad (3.53)$$

$$h_1^\pm(r) = \pm \frac{\text{sign}(n)}{\sqrt{1-Z^2}} \left[R\sqrt{1-Z^2} \cosh\left(eR\sqrt{1-Z^2}r\right) - \frac{1}{er} \right], \quad (3.54)$$

$$h_2^\pm(r) = \mp \frac{\text{sign}(n)c_2c_3Z}{\sqrt{1-Z^2}} \left[R\sqrt{1-Z^2} \cosh\left(eR\sqrt{1-Z^2}r\right) - \frac{1}{er} \right]. \quad (3.55)$$

Where $R^2 = 4(c_2ZY + c_1X)$. The monopole masses are plotted against the gauge mass for fixed parameters with $n \in \{1, 2, 3, 4\}$ in figure 3.2 with weak and strong couplings $e = 2, e = 10$. Notice that the gauge mass is smaller than any of the monopole masses for weak coupling, but when e is large enough, some of the monopole masses can become smaller than the gauge mass. This is clear by inspecting the monopole and gauge mass in equation (3.53) and two masses coincide when $e = \sqrt{8|n|\pi}$. Note that $n = 0$ is not a monopole mass as it corresponds to the solution with zero winding number, which is topologically equivalent to the trivial solution.

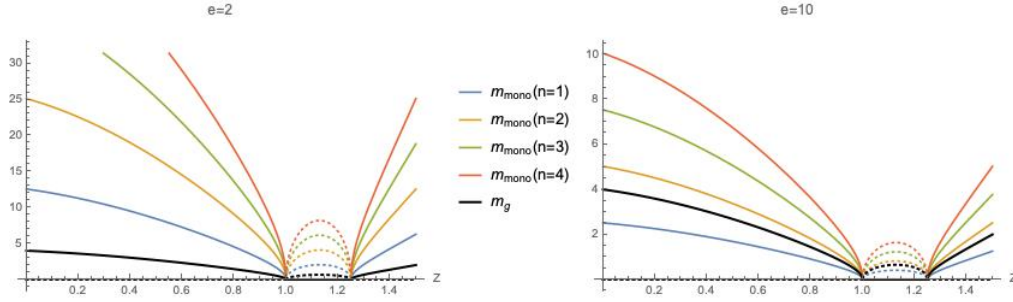


Figure 3.2: Monopole and gauge masses plotted for $X = 1, Y = 0.8, e = 2, c_1 = -c_2 = 1$. The solid line represent the real part and dotted line represent the imaginary part of the masses.

From figure 3.2, we also observe disconnected regions where both monopole and gauge masses become real to purely complex. A more detailed plot of this is shown in figure 3.3. Region 2 is bounded by two points with lower bound $\mu^2/m_2^2 = 1$ corresponds to the zero exceptional point where the vacuum manifolds stay finite (i.e. spontaneous symmetry breaking occur). However, the Higgs mechanism fails, as discussed in the previous section. The upper bounds correspond to the point where the vacuum manifold vanishes. Therefore, the spontaneous symmetry breaking does not occur, implying that the gauge field do not acquire mass though Higgs mechanism, resulting in a massless gauge fields. Most crucially, an interesting region (denoted by region 3 in figure 3.4) reappear as one increases the value of Z . The profile function in region 3 is purely complex, which signals that this may lead to complex energies. However, as one can see from figure 3.3, the energy is real. The reason for the real energy is that the conditions stated in the previous section hold. We will show below the \mathcal{CPT} symmetry responsible for the reality of the energy. Note that the profile function h_2 only differ from h_1 by some factor in front. Therefore we omitted it from the plot.

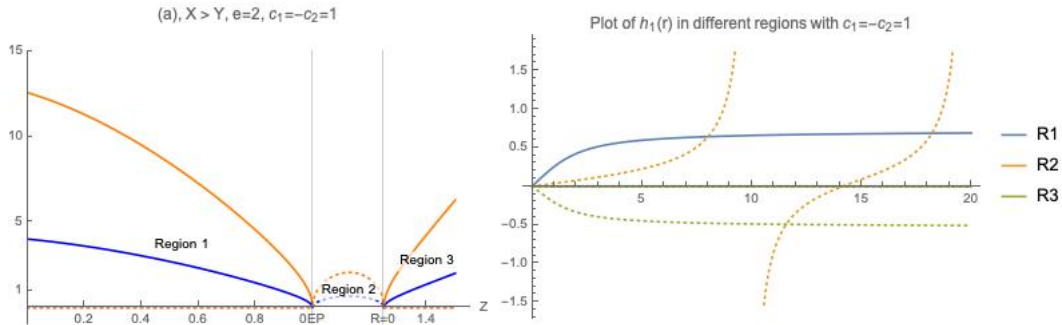


Figure 3.3: Both panels are plotted for $X = 1, Y = 0.8, n = 1, e = 2$. The solid line represent the real part and dotted line represent the imaginary part of the masses. Panel (a) shows the monopole and gauge masses against $Z \geq 0$, with vertical lines indicating the location of the boundaries of three regions. The panel (b) shows three profile function $h_1(r)$ defined on each regions indicated in panel (a).

Another physical region is when $c_1 = -c_2 = -1$. The monopole and gauge masses for this case is plotted in figure 3.4. We observe almost an identical plot from the figure 3.3 but with real and imaginary parts swapped. The profile functions also respect these changes as regions 1, and 3 no longer have a definite asymptotic value. The boundaries are unchanged, as one can see from the figure 3.4.

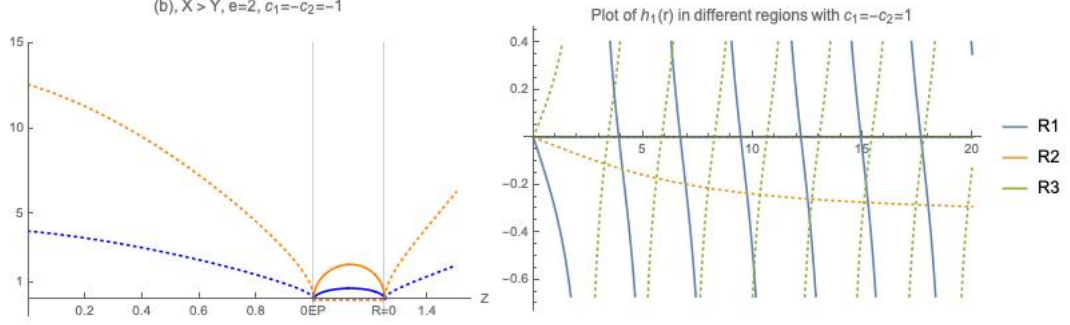


Figure 3.4: Both panels are plotted for $X = 1, Y = 1, n = 1, e = 2$. The solid line represent the real part and dotted line represent the imaginary part of the masses.

Finally, there is an interesting parameter point $X = Y$ where the region 2 vanishes (see figure 3.5). The two boundaries $Z^2 = 1$ and $c_2ZY + c_1X = 0$ coincide when $X = Y$ and the zero exceptional point no longer exists because the spontaneous symmetry breaking does not occur in this case.

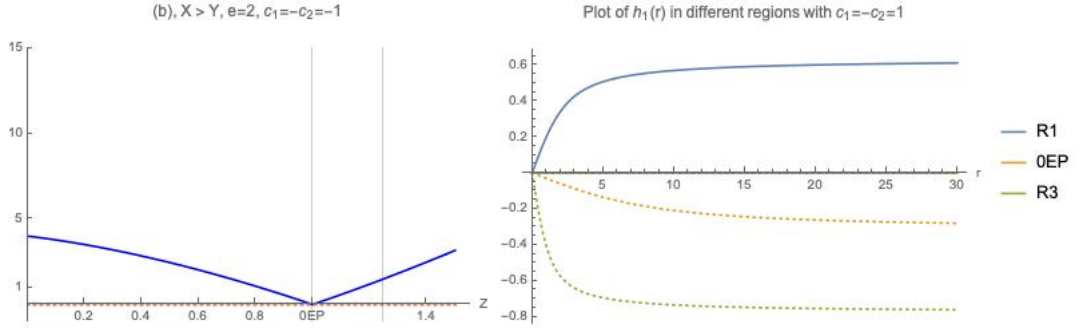


Figure 3.5: Both panels are plotted for $X = 1, Y = 1, n = 1, e = 2$. The solid line represent the real part and dotted line represent the imaginary part of the masses.

Next let us explain the reality of the energies in different regions. First, to realise the conditions (1)-(3), stated in section 3.1, we require following transformations

$$CPT : \begin{cases} h_2^\pm(r) \rightarrow -h_2^\pm(r), & h_1^\pm(r) \rightarrow h_1^\pm(r) & \text{in region 1} \\ \text{No symmetry} & & \text{in region 2} \\ h_2^\pm(r) \rightarrow -(h_2^\pm(r))^*, & h_1^\pm(r) \rightarrow (h_1^\pm(r))^* & \text{in region 3} \end{cases} \quad (3.56)$$

By using the explicit forms of the solutions (3.54, 3.55). We can show that the above

transformations satisfies condition (2) in regions (1) and (3).

$$\mathcal{CPT} : \begin{cases} h_2^\pm(r) \rightarrow -h_2^\pm(r) = h_2^\mp(r), & h_1^\pm(r) \rightarrow h_1^\pm(r) & \text{in region 1} \\ h_2^\pm(r) \rightarrow -(h_2^\pm(r))^* = h_2^\pm, & h_1^\pm(r) \rightarrow (h_1^\pm(r))^* = h_1^\mp & \text{in region 3} \end{cases} \quad (3.57)$$

Notice that in regions (1) and (3) the \mathcal{CPT} relates two distinct solutions in two different ways. For example, h_2^\pm is mapped to h_2^\mp in region (1) but it is mapped to itself in region (3).

Finally the condition (3) is satisfied because the energy does not depend on the \pm signs of the solutions. This explains the real energies of complex monopoles in region 3 and complex energy in region 2. Indeed we observe the predicted behaviour in figure 3.3. The region 2 is a hard barrier between two \mathcal{CPT} symmetric regions where solutions are either real or purely imaginary. The same analysis can be done in the other physical region $c_1 = -c_2 = -1$ where the symmetry is now

$$\mathcal{CPT} : \begin{cases} \text{No symmetry} & \text{in region 1} \\ h_2^\pm(r) \rightarrow -(h_2^\pm(r))^*, & h_1^\pm(r) \rightarrow (h_1^\pm(r))^* & \text{in region 2} \\ \text{No symmetry} & \text{in region 3} \end{cases} \quad (3.58)$$

We have observed that one can find a well-defined monopole solution in two disconnected regions. However, in the full theory, it is only one of the regions which are considered physical. This is because the Higgs mass m_0^2 is either positive or negative depending on which side of $Z^2 = 1$ it is defined. Because two disconnected regions are defined on either side of the zero exceptional point $Z^2 = 1$, the full physical region restricts one from moving region (1) to region (3) by changing Z . This is most clearly seen in the figure 3.1 where the plot of m_0^2 (green line) becomes negative beyond the zero exceptional point. Therefore the region (3) does not coincide with the physical region shown in figure 2.6. This may imply that the purely complex monopole solution we observed is not a possible solution of the theory. However, the purely complex solution can exist in the full physical region. An example of this is shown in the figure 3.6 where we observe that the profile function h_1 (therefore h_2) is purely complex, and the Higgs masses, gauge mass are all real and positive

Finally we comment on the diagonalisation of the Lagrangian. As stated at the beginning of this section, the changing of the \mathcal{CPT} -symmetry in going from region 1 to 3 is only visible because we have worked with the action (3.20) instead of fully

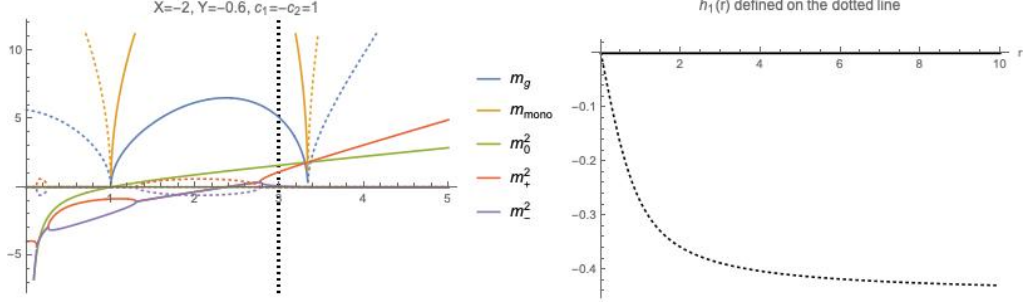


Figure 3.6: Both panels are plotted for $X = 1, Y = 1, n = 1, e = 2$. The solid line represent the real part and dotted line represent the imaginary part of the masses.

diagonalised Lagrangian. If we now assume that we diagonalised and repeated the analysis of this section, we would have found the monopole solutions (3.54) and (3.55) but with a linear combination of the fields ϕ_1 and ϕ_2 defined in equation (2.26) (note that the equation (2.26) is only used for would-be Goldstone but same definition can be used for other fields)

$$\psi^a = \frac{m_2^2 \phi_1^a + \mu^2 \phi_2^a}{\sqrt{m_2^4 - \mu^4}}, \quad a \in \{1, 2\}. \quad (3.59)$$

Recalling that $\phi_i^a = h_i \hat{r}^a$, one of the fields becomes

$$\psi^1 = \frac{m_2^2 h_1 + \mu^2 h_2}{\sqrt{m_2^4 - \mu^4}} \hat{r}^a. \quad (3.60)$$

Then notice that in the region 3, the field ψ^1 is real because the overall quantity $\sqrt{m_2^4 - \mu^4}$ is purely complex in region 3. Therefore we would not have observed the changing of the \mathcal{CPT} -symmetry. We can conclude that *different \mathcal{CPT} -symmetries of the complex solutions combine to one \mathcal{CPT} -symmetry in the diagonalised theory.*

In next two section, we will consider models where there is no known Dyson map. Therefore it is important to identify the appropriate \mathcal{CPT} -symmetry of the solutions to guarantee the real energy.

3.2.6 Summary

We have found the t'Hooft-Polyakov monopole solution (3.51) in the non-Hermitian theory by drawing an analogue from the standard procedure in the Hermitian theory. The monopole masses were plotted with the massive gauge and Higgs masses where the physical region of the monopole masses coincides with that of the gauge mass. It was also observed that there are two distinct physical regions bounded by the

zero exceptional point and the parameter limit where the vacuum manifold becomes trivial. The profile function (radial part of the monopole solution) is plotted in figures 3.3, 3.4, 3.5, where it is real and purely complex in the regions 1 and 3 respectively. Incidentally, the CPT -symmetries of the solution are different in the regions 1 and 3.

3.3 Topological solitons in 1 + 1 dimensions

This section will extend the study of the BPS soliton solution observed in the last section by taking the special limit in the equations of motion. The focus will be on the 1 + 1 dimensional non-Hermitian field theories to simplify the analysis. We investigate three different types of non-Hermitian field theories.

1. A complex version of a logarithmic potential that possess BPS super-exponential kink and antikink solutions.
2. Two copies of Hermitian sine-Gordon theories, coupled with non-Hermitian metric term.
3. A Complex extended sine-Gordon theory with known similarity transformation.

Despite the fact that all soliton solutions obtained in this manner are complex in the non-Hermitian theories, we show that they possess real energies. For the complex extended sine-Gordon model, we establish explicitly that the energies are the same as those in an equivalent pair of a non-Hermitian and Hermitian theory obtained from a pseudo-Hermitian approach by means of a Dyson map, which also maps a complex solution to a real solution. We argue that the reality of the energy is due to the topological properties of the complex BPS solutions. These properties generally result from modified versions of antilinear CPT symmetries that relate self-dual and an anti-self-dual theories.

3.3.1 BPS solitons from self-duality and anti-self-duality

The authors in [123] take an energy functional E and a topological charge Q of the form

$$E = \frac{1}{2} \int d^2x \left[A_\alpha^2 + \tilde{A}_\alpha^2 \right], \quad \text{and} \quad Q = \int d^2x \left[A_\alpha \tilde{A}_\alpha \right], \quad (3.61)$$

as a starting point for the setup of a BPS theory, where the quantities $A_\alpha(\phi, \partial_\mu\phi)$, $\tilde{A}_\alpha(\phi, \partial_\mu\phi)$ are functions of the fields ϕ appearing in the Lagrangian \mathcal{L} of the field theory under consideration and at most of first order derivatives thereof. It is clear that the relations in (3.61) ensure that the topological charge is always a lower bound for the energy $E \geq |Q|$. Following [123], one may then use these definitions to derive two equations, one being the Euler-Lagrange equation resulting from varying E and the other from considering infinitesimal changes $\delta\phi$ in Q and demanding $\delta Q = 0$. The latter requirement incorporates that Q is interpreted as a topological charge, which should be a homotopy invariant, i.e. invariant under smooth variations in the fields. The compatibility between these two equations then implies (anti)-self-duality of the quantities A_α , \tilde{A}_α and moreover that Q saturates the Bogomolny bound for the energy E

$$A_\alpha = \pm \tilde{A}_\alpha, \quad \text{and} \quad E = |Q|. \quad (3.62)$$

Evidently the energies of the self-dual and anti-self-dual fields are the same. Assuming next the existence of a pre-potential $U(\phi)$ defined as $\eta_{ab}^{-1}(\frac{\partial U}{\partial\phi_a})(\frac{\partial U}{\partial\phi_b}) = \mathcal{V}(\phi)$ where \mathcal{V} is a potential of the model, one may write the energy functional and the topological charge for the static solutions as

$$\begin{aligned} E &= \int_{-\infty}^{\infty} dx \left[\frac{1}{2} \eta_{ab} \partial_\mu \phi_a \partial^\mu \phi_b + \mathcal{V}(\phi) \right] \\ &= \frac{1}{2} \int_{-\infty}^{\infty} dx \left[\eta_{ab} \partial_\mu \phi_a \partial^\mu \phi_b + \eta_{ab}^{-1} \frac{\partial U}{\partial\phi_a} \frac{\partial U}{\partial\phi_b} \right], \end{aligned} \quad (3.63)$$

$$Q = \int_{-\infty}^{\infty} dx \frac{\partial U}{\partial x} = \int_{-\infty}^{\infty} dx \frac{\partial U}{\partial\phi_a} \partial_x \phi_a = \lim_{x \rightarrow \infty} U[\phi(x)] - \lim_{x \rightarrow -\infty} U[\phi(x)]. \quad (3.64)$$

Comparing the general expressions for A_α and \tilde{A}_α in (3.61) with those for $U(\phi)$ in (3.63), (3.64) implies the identifications

$$A_a = \rho_{ab} \partial_x \phi_b, \quad \text{and} \quad \tilde{A}_a = \frac{\partial U}{\partial\phi_b} \rho_{ba}^{-1}, \quad (3.65)$$

where ρ factorizes the target space metric as $\rho^T \rho = \eta$. The (anti)-self-duality relations in (3.62), then become equivalent to the pair of BPS equations in the form

$$\partial_x \phi_b = \pm \eta_{ab}^{-1} \frac{\partial U}{\partial\phi_b}. \quad (3.66)$$

Allowing the scalar fields to be complex and the potential to be non-Hermitian, the reality of the energy could be guaranteed when the Hamiltonian is \mathcal{CPT} -symmetric satisfying $\mathcal{H}[\phi(x)] = \mathcal{H}^\dagger[\phi(-x)]$ by employing the same argument as in [116]

$$E = \int_{-\infty}^{\infty} dx \mathcal{H}[\phi(x)] = - \int_{\infty}^{-\infty} dx \mathcal{H}[\phi(-x)] = \int_{-\infty}^{\infty} dx \mathcal{H}^\dagger[\phi(x)] = E^*. \quad (3.67)$$

Since in the scenario considered here the self-duality imposes the kinetic energy to equal the potential energy, it would suffice therefore to establish that

$$\mathcal{V}[\phi_\pm(x)] = \mathcal{V}^\dagger[\phi_\pm(-x)], \quad \text{or} \quad \mathcal{V}[\phi_\pm(x)] = \mathcal{V}^\dagger[\phi_\mp(-x)] \quad (3.68)$$

in order to ensure the reality of the energy by means of (3.67). Note that the second condition in equation (3.68) is precisely the condition (1) presented in section 3.1. In fact, we shall demonstrate that the first condition is broken in all of our examples, highlighting the three conditions as an extension of the one proposed in [116]. We have denoted here by ϕ_\pm the solutions of (3.66) corresponding to the two options for the sign in (3.62). Evidently it follows from (3.61) that the energy is the same for either choice. The second option in (3.68) is novel due to the set up involving anti-self-duality and not available in the standard setting in many other integrable systems [116, 124, 125, 126]. Alternatively, by analysing directly the model, the energy is real if

$$\lim_{x \rightarrow \infty} \text{Im} \{U[\phi(x)]\} = \lim_{x \rightarrow -\infty} \text{Im} \{U[\phi(x)]\}. \quad (3.69)$$

Finally let us comment on the stability of the solutions. The topological charge given in equation (3.61) can be seen as a lower bound of the energy functional

$$\frac{1}{2} \int d^2x \left[A^2 + \tilde{A}^2 \right] = \frac{1}{2} \int d^2x \left[\left(A \pm \tilde{A} \right)^2 \mp 2A\tilde{A} \right] \geq \mp \int d^2x A\tilde{A}. \quad (3.70)$$

This was also discussed briefly in the previous section. However, since A and \tilde{A} can be complex, the inequality above might be violated. This problem is resolved once the similarity transformation of the theory is identified. Unfortunately finding the similarity transformation is in general very difficult as discussed in the introduction. Therefore, for some of the examples in this section and next, we directly analyse the complex theory with complex solutions. Crucially for any similarity transforma-

tions the energy of the solution is unchanged, meaning the topological charge of the solution is a well-defined lower bound of the energy. Therefore, the only quantity we will analyse in the complex theory is the energy of the solutions. We will see in section 3.4.2 that some of the complex solution stay complex even after similarity transformation. In such case, the complex solution is non physical in a particular Hermitian theory obtained by a particular similarity transformation. However, as explained above, it may have a different similarity transformation where the solution becomes physical in different theory.

We shall now analyse several different theories with concrete choices for pre-potential that lead to non-Hermitian scalar field theory with an antilinear symmetry.

3.3.2 A non-Hermitian BPS theory with super-exponential kink solutions

We start by generalising a Hermitian field theory that was recently studied by Kumar, Khare and Saxena [127] to one with two-component complex fields in a non-Hermitian setting. The original model was motivated in parts by its proximity to a ϕ^6 -type potential and its feature of minimal nonlinearity. Interestingly, this model possesses kink and antikink solutions with a super-exponential profile rather than the more standard arctan type solutions, seen in sine-Gordon theory. This feature survives our generalisation, and the complex BPS solutions interpolating between five out of nine vacua of our model have real energies.

To set up the field theory we choose the target space metric and the pre-potential as

$$\eta = \begin{pmatrix} 1 & -i\lambda \\ -i\lambda & 1 \end{pmatrix}, \quad \text{and} \quad U(\phi_1, \phi_2) = \frac{\mu_1}{2} \phi_1^2 \ln(\phi_1^2) + \frac{\mu_2}{2} \phi_2^2 \ln(\phi_2^2), \quad (3.71)$$

with $\lambda, \mu_1, \mu_2 \in \mathbb{R}$, respectively. Using the relation between the potential and the pre-potential (3.63) we obtain from the Ansatz (3.71) the non-Hermitian potential

$$\mathcal{V}(\phi_1, \phi_2) = \frac{1}{1 + \lambda^2} \sum_{i=1}^2 \frac{\mu_i^2}{2} [\phi_i + \phi_i \ln(\phi_i^2)]^2 + i \frac{\lambda}{1 + \lambda^2} \prod_{i=1}^2 \mu_i [\phi_i + \phi_i \ln(\phi_i^2)]. \quad (3.72)$$

According to the standard pseudo-Hermitian approach to non-Hermitian field theories, one may seek a similarity transformation using a well defined Dyson map, e.g. [75, 79, 7, 8, 9], to map the theory to a Hermitian theory or introduce non-vanishing

surface terms [77, 88, 82, 81, 83] and analyse these systems. However, as we shall demonstrate below, just as in a standard quantum mechanical setting [104, 111], the energy is preserved in this process so that one may also analyse the solutions of the non-Hermitian theory directly.

Note that the complex theory and solutions can only be viewed as a physical theory if an appropriate metric is chosen (see section 2.3.3). Therefore, directly analysing the quantities other than energy such as position, momentum of the soliton in the complex theory is not physical unless the metric is fixed. Our approach is further justified in section 3.3.4, where we shall present an explicit system for which a non-Hermitian Hamiltonian is related to a Hermitian Hamiltonian by means of an explicit nontrivial Dyson map.

Using the BPS equations (3.66), the static solutions associated with the potential (3.72) are the two pairs of coupled first-order differential equations

$$BPS_1^\pm : \partial_x \phi_1 = \pm \frac{\mu_1 [\phi_1 + \phi_1 \ln(\phi_1^2)]}{\lambda^2 + 1} \pm i\lambda \frac{\mu_2 [\phi_2 + \phi_2 \ln(\phi_2^2)]}{\lambda^2 + 1} =: F_1^\pm, \quad (3.73)$$

$$BPS_2^\pm : \partial_x \phi_2 = \pm i\lambda \frac{\mu_1 [\phi_1 + \phi_1 \ln(\phi_1^2)]}{\lambda^2 + 1} \pm \frac{\mu_2 [\phi_2 + \phi_2 \ln(\phi_2^2)]}{\lambda^2 + 1} =: F_2^\pm. \quad (3.74)$$

We will need both versions in (3.73) and (3.74) to verify the general argument that guarantees the reality of the energy. We observe that these equations are compatible under two types of modified \mathcal{CPT} -transformations

$$\mathcal{CPT}_\pm : \begin{cases} \phi_1(x) & \rightarrow \pm [\phi_1(-x)]^\dagger \\ \phi_2(x) & \rightarrow \mp [\phi_2(-x)]^\dagger \end{cases}, \Leftrightarrow BPS_i^\pm \rightarrow (BPS_i^\mp)^*. \quad (3.75)$$

Using these symmetries we can derive the second relation in (3.68). We notice that a modified \mathcal{CT} -transformation $\phi_1(x) \rightarrow -[\phi_1(x)]^\dagger$, $\phi_2(x) \rightarrow -[\phi_2(x)]^\dagger$ is achieving the compatibility $BPS_i^\pm \rightarrow (BPS_i^\pm)^*$. However, this symmetry can not be employed in the argument in (3.67) that guarantees the reality of the energy. The introduction of time by means of a standard Lorentz transformation, $x \rightarrow (x - vt)/\sqrt{1 - v^2}$, will not change this feature, so that the reality of the energy is not a consequence of this particular antilinear symmetry. Moreover, we do not find solutions below that posses this kind of \mathcal{CT} -symmetry.

Let us now solve the pair of the two BPS equations (3.73) and (3.74). In the Hermitian limit, when $\lambda = 0$, the equations decouple, and the solutions can be

obtained in an explicit analytical form as double exponentials

$$\phi_i(x) = \exp\left(-\frac{1}{2} + \frac{1}{2}e^{2(\mu_i x + \kappa_i)}\right), \quad (3.76)$$

with integration constants $\kappa_i \in \mathbb{C}$ and $i = 1, 2$. We fix our constants in such a way that we obtain proper kink and antikink solutions with well-defined asymptotic behaviour. We select our solutions as

$$\phi_i^{a+}(x) = \exp\left(-\frac{1}{2} - \frac{1}{2}e^{2\mu_i x}\right), \quad \phi_i^{k+}(x) = -\exp\left(-\frac{1}{2} - \frac{1}{2}e^{2\mu_i x}\right), \quad \mu_i \geq 0, \quad (3.77)$$

$$\phi_i^{k-}(x) = \exp\left(-\frac{1}{2} - \frac{1}{2}e^{2\mu_i x}\right), \quad \phi_i^{a-}(x) = -\exp\left(-\frac{1}{2} - \frac{1}{2}e^{2\mu_i x}\right), \quad \mu_i < 0, \quad (3.78)$$

so that $\phi_i^{a+}(0) = \phi_i^{k-}(0) = 1/e$, $\phi_i^{k+}(0) = \phi_i^{a-}(0) = -1/e$ and $\phi_i^{a+}(x) = \phi_i^{k-}(-x) = -\phi_i^{k+}(x) = -\phi_i^{a-}(-x)$. The asymptotic limits are therefore

$$\begin{aligned} \lim_{x \rightarrow -\infty} \phi_i^{a+}(x) &= \lim_{x \rightarrow \infty} \phi_i^{k-}(x) = \frac{1}{\sqrt{e}}, \\ \lim_{x \rightarrow -\infty} \phi_i^{k+}(x) &= \lim_{x \rightarrow \infty} \phi_i^{a-}(x) = -\frac{1}{\sqrt{e}}, \\ \lim_{x \rightarrow \infty} \phi_i^{a+}(x) &= \lim_{x \rightarrow \infty} \phi_i^{k+}(x) = \lim_{x \rightarrow -\infty} \phi_i^{a-}(x) = \lim_{x \rightarrow -\infty} \phi_i^{k-}(x) = 0. \end{aligned} \quad (3.79)$$

Hence, using the expression for the pre-potential (3.64) we obtain for all combinations the same real energy as function of μ_1, μ_2

$$E^{\phi_1^{pn}, \phi_2^{qm}}(\mu_1, \mu_2) = \frac{|\mu_1| + |\mu_2|}{2e}, \quad p, q = k, a; \quad n, m = \pm; \quad \mu_1, \mu_2 \in \mathbb{R}. \quad (3.80)$$

In the non-Hermitian scenario, when $\lambda \neq 0$, we solve the two sets of coupled BPS equations (3.73) and (3.74) numerically. Some sample computations are presented in figure 3.7.

We observe that for increasing values of the coupling constants μ_i the real parts of ϕ_i approach $H(-x)/\sqrt{e}$ with $H(x)$ denoting the Heaviside step function. The imaginary parts keep oscillating with larger amplitudes with increasing μ and crucially vanish at $x \rightarrow \pm\infty$, which means that the energy is also given by the expression in (3.80) for all values of λ . The analytical solution for $\lambda = 0$ are smooth kinks and antikinks who also approach a Heaviside step function for increasing values of μ_i .

We also observe from our numerical solutions in figure 3.7 that the solutions

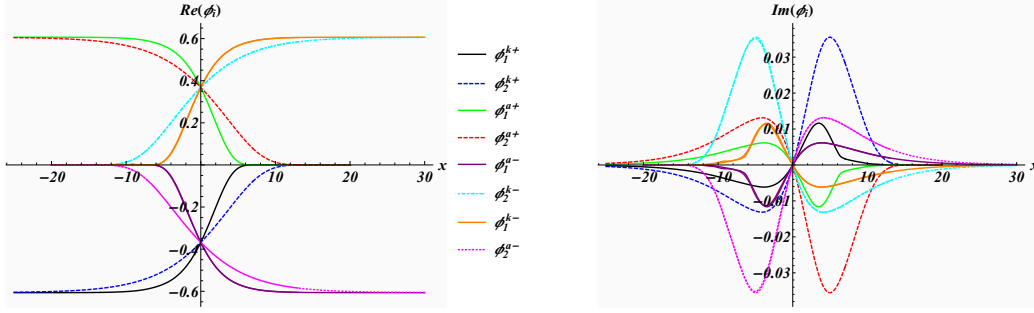


Figure 3.7: Complex BPS kink and antikink solutions of the two pairs of coupled BPS equations (3.73) and (3.74) associated to the potential (3.72) with initial values $\phi_1^{k+}(0) = \phi_2^{k+}(0) = \phi_1^{a-}(0) = \phi_2^{a-}(0) = -1/e$ and $\phi_1^{a+}(0) = \phi_2^{a+}(0) = \phi_1^{k-}(0) = \phi_2^{k-}(0) = 1/e$ for $\mu_1 = 0.2$, $\mu_2 = 0.1$, $\lambda = 0.1$.

realise the \mathcal{CPT}_- -symmetry as

$$\phi_1^{k+}(x) = -[\phi_1^{k-}(-x)]^\dagger, \quad \phi_1^{a+}(x) = -[\phi_1^{a-}(-x)]^\dagger, \quad \phi_2^{k\pm}(x) = [\phi_2^{a\mp}(-x)]^\dagger. \quad (3.81)$$

Using now the properties of the kink and antikink solutions (3.81) we derive for the potential

$$\begin{aligned} \mathcal{V}_\lambda [\phi_1^{k+}(x), \phi_2^{k+}(x)] &= \mathcal{V}_\lambda \left\{ -[\phi_1^{k-}(-x)]^\dagger, [\phi_2^{a-}(-x)]^\dagger \right\} \\ &= \mathcal{V}_\lambda^\dagger \left\{ [\phi_1^{k-}(-x)], [\phi_2^{a-}(-x)] \right\}, \end{aligned} \quad (3.82)$$

and similarly for the other pairs of solutions. Changing the initial conditions, we may also construct solutions that manifest the \mathcal{CPT}_+ -symmetry. The relation in (3.82) is precisely the second option in (3.68) that relates solutions of the self-dual system to solutions of the anti-self-dual system. As the energies in both systems must be the same, it is guaranteed to be real.

Next, we will identify which vacua are interpolated by which kind of BPS solution. It is easy to check that the real part of the potential has nine minima at

$$\begin{aligned} v^{\pm\pm} &= (\pm e^{-1/2}, \pm e^{-1/2}), \quad v^{0\pm} = (0, \pm e^{-1/2}), \\ v^{\pm 0} &= (\pm e^{-1/2}, 0), \quad v^{00} = (0, 0), \end{aligned} \quad (3.83)$$

corresponding to the fixed points of the dynamical system (3.73) and (3.74) as solutions of $F_1^\pm(\phi_1, \phi_2) = F_2^\pm(\phi_1, \phi_2) = 0$. Next we compute the eigenvalues of the

Jacobian matrix at these fixed points

$$J = \left(\begin{array}{cc} \partial_{\phi_1} F_1^\pm & \partial_{\phi_2} F_1^\pm \\ \partial_{\phi_1} F_2^\pm & \partial_{\phi_2} F_2^\pm \end{array} \right) \Big|_{v^{i,j}}, \quad i, j = 0, +, -, \quad (3.84)$$

in order to determine their stability. For the F^+ -system with $\mu_i > 0$ we find that $J(v^{\pm\pm})$ has two positive eigenvalues, $J(v^{00})$ has two negative eigenvalues and $J(v^{0\pm})$, $J(v^{\pm 0})$ have a positive and a negative eigenvalue. For $\phi_i \rightarrow 0$ we have to evaluate the values in an ε -neighbourhood. This means, see e.g. [128], that $v^{\pm\pm}$ are unstable fixed points, $v^{0\pm}$ and $v^{\pm 0}$ are saddle points and v^{00} is the only stable fixed point. For the F^- -system still with $\mu_i > 0$ all signs of the eigenvalues are reversed. Changing the sign of μ_i will also reverse the sign of one eigenvalue. Using the solutions from above as represented in figure 3.7, we have the following interpolations between the different vacua

$$\begin{array}{c|c} \begin{array}{c} F_+ \text{ system} \\ \hline v^{--} \quad \underbrace{\phi_1^{k+} \phi_2^{k+}}_{\rightarrow} \quad v^{00} \quad \big| \quad v^{++} \quad \underbrace{\phi_1^{a+} \phi_2^{a+}}_{\rightarrow} \quad v^{00} \end{array} & \begin{array}{c} F_- \text{ system} \\ \hline v^{00} \quad \underbrace{\phi_1^{a-} \phi_2^{k-}}_{\rightarrow} \quad v^{-+} \quad \big| \quad v^{00} \quad \underbrace{\phi_1^{k-} \phi_2^{a-}}_{\rightarrow} \quad v^{+-} \end{array} \end{array} \quad (3.85)$$

This behaviour is also confirmed by the gradient flow for F^+ that is indicated in figure 3.8 superimposed onto the potential. We obtain similar relations for the F^- -system.

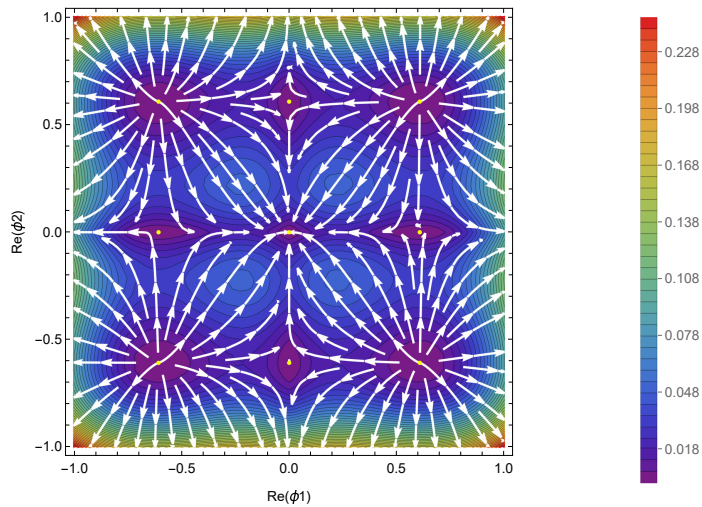


Figure 3.8: Real part of the potential $\mathcal{V}(\phi_1, \phi_2)$ in (3.72) as a function of $\text{Re}\phi_1$ and $\text{Re}\phi_2$ with the gradient flow of the real parts of F^+ superimposed in white. The kink-kink, kink-antikink, antikink-kink and antikink-antikink interpolate between the different types of stable and unstable vacua as specified in (3.85)

When passing from the \mathcal{V}_+ -theory to the \mathcal{V}_- -theory, we pass through the special point $\mu_1 = \mu_2 = 0$. The energy (3.80) is defined for all values and does not become complex. To investigate this point further, the next model is designed in such a way that it appears to have an exceptional point, which, however, turns out to be not genuine.

3.3.3 A non-Hermitian coupled sine-Gordon model

Next, we consider a modified version of a model whose real variant has been investigated recently in [129]. We generalise that model to one involving a complex non-Hermitian potential with a complex two-component scalar field and add an additional term designed in such a way that we obtain an exceptional point [130]. We shall demonstrate that the system possesses complex solutions to its BPS equations with real energies in a certain region in the parameter space where the topological charge of the system is well-defined and real. There is also a region in which the energy is not well defined and not finite on the entire real x -axis.

Choosing the target space metric and the pre-potential as

$$\eta = \begin{pmatrix} 1 & -i\lambda \\ -i\lambda & 1 \end{pmatrix}, \quad \text{and} \quad U(\phi_1, \phi_2) = -(\cos \phi_1 + \mu \phi_1 + \cos \phi_2), \quad (3.86)$$

$\lambda, \mu \in \mathbb{R}$, respectively. The potential resulting from the expression in (3.63) is derived as

$$\mathcal{V}(\phi_1, \phi_2) = \frac{1}{2(1 + \lambda^2)} \left[(\sin \phi_1 - \mu)^2 + 2i\lambda (\sin \phi_1 - \mu) \sin \phi_2 + \sin^2 \phi_2 \right]. \quad (3.87)$$

We note that the singularity at $\lambda = 1$ present in the real version of this model discussed in [129] has been removed as the quantity $1/(1 - \lambda^2)$ becomes $1/(1 + \lambda^2)$. The static versions of the BPS equations (3.66) obtained from (3.87) are the pairs of complex coupled first-order equations

$$BPS_1^\pm : \quad \partial_x \phi_1 = \pm \frac{1}{1 + \lambda^2} (\sin \phi_1 - \mu + i\lambda \sin \phi_2) =: G_1^\pm, \quad (3.88)$$

$$BPS_2^\pm : \quad \partial_x \phi_2 = \pm \frac{1}{1 + \lambda^2} [i\lambda (\sin \phi_1 - \mu) + \sin \phi_2] =: G_2^\pm. \quad (3.89)$$

These equations are compatible under the modified \mathcal{CPT} -transformation

$$\mathcal{CPT} : \begin{cases} \phi_1(x) & \rightarrow & [\phi_1(-x)]^\dagger \\ \phi_2(x) & \rightarrow & -[\phi_2(-x)]^\dagger \end{cases}, \quad \Leftrightarrow BPS_i^\pm \rightarrow (BPS_i^\mp)^*. \quad (3.90)$$

Notice that we require again both signs to achieve consistency under the \mathcal{CPT} -conjugation. It is precisely this symmetry that is needed to derive the second relation in (3.68) and the condition (1) from section 3.1. Trying instead to realise the compatibility of BPS_i^+ or BPS_i^- with itself requires just a modified \mathcal{CT} -transformation $\phi_1(x) \rightarrow [\phi_1(x)]^\dagger$, $\phi_2(x) \rightarrow -[\phi_2(x)]^\dagger$, which as for the previous model is, however, not sufficient to be used in the argument in (3.67) that ensures the reality of the energy.

In the Hermitian limit, when $\lambda = 0$, the two pairs of BPS equations decouple and are easily solved analytically by the kink and antikink solutions for the upper and lower sign, respectively,

$$\phi_1^{\pm(n)}(x) = 2 \arctan \left\{ \frac{1}{\mu} \left[1 + \sqrt{1 - \mu^2} \tanh \left(\frac{1}{2} \sqrt{1 - \mu^2} (\pm x + \kappa_1) \right) \right] \right\} + 2\pi n, \quad (3.91)$$

$$\phi_2^{\pm(n)}(x) = 2 \arctan (e^{\pm x + \kappa_2}) + 2\pi n, \quad (3.92)$$

where $n \in \mathbb{Z}$ and integration constants $\kappa_1, \kappa_2 \in \mathbb{R}$. From the asymptotic limits

$$\lim_{x \rightarrow \infty} \phi_1^{+(n)}(x) = \lim_{x \rightarrow -\infty} \phi_1^{-(n)}(x) = 2n\pi + \text{sign}(\mu)\pi - \arcsin(\mu), \quad (3.93)$$

$$\lim_{x \rightarrow -\infty} \phi_1^{+(n)}(x) = \lim_{x \rightarrow \infty} \phi_1^{-(n)}(x) = 2n\pi + \text{sign}(\mu) \arcsin(\mu), \quad (3.94)$$

$$\lim_{x \rightarrow \pm\infty} \phi_2^{+(n)}(x) = \lim_{x \rightarrow \mp\infty} \phi_2^{-(n)}(x) = 2n\pi + \frac{\pi \pm \pi}{2}, \quad (3.95)$$

for $|\mu| \leq 1$, we obtain from (3.64) for both signs the same expression for the energy as a function of μ

$$E^\pm(\mu) = 2 \left[1 + \sqrt{1 - \mu^2} - \mu \arctan \left(\frac{\sqrt{1 - \mu^2}}{\mu} \right) \right]. \quad (3.96)$$

For $|\mu| > 1$ the limits $\lim_{x \rightarrow \pm\infty} \phi_i(x)$ are not well defined as the solutions become periodic in this case. Limiting this case to a theory on a finite interval will, however, still gives real energies. For instance, for an interval $[a, b]$ with $\kappa_1 = \kappa_2 = n = 0$ we

compute the energy

$$E^\pm(\mu) = \pm\mu z(x) - \cos[z(x)] \pm \tanh x|_{x=b}^a. \quad (3.97)$$

with $z(x) = 2 \arctan \left\{ [\mp 1 + \sqrt{\mu^2 - 1} \tan(x/2\sqrt{\mu^2 - 1})]/\mu \right\}$. This is real and well defined as long as one avoids $a, b = (2n\pi + \pi)/\sqrt{\mu^2 - 1}$, $n \in \mathbb{Z}$. In the non-Hermitian scenario, when $\lambda \neq 0$, we solve the coupled equations (3.88) and (3.89) numerically, see figure 3.9 for some sample behaviours.

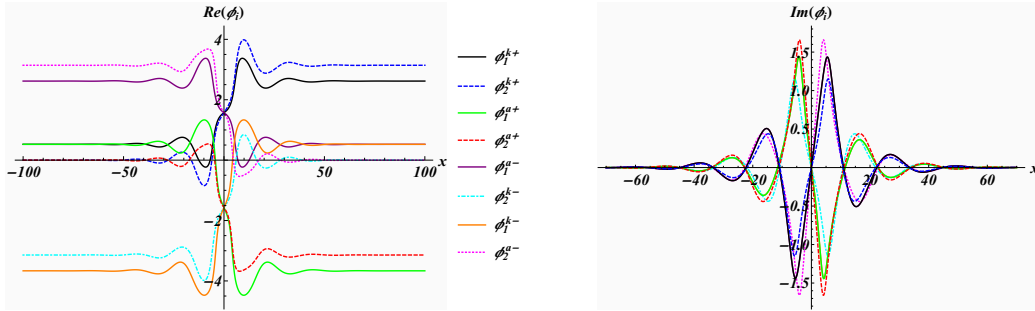


Figure 3.9: Complex BPS kink and antikink solutions of the pair of BPS equations (3.88) and (3.89) with initial values $\phi_1^{k+}(0) = \phi_2^{k+}(0) = \phi_2^{k-}(0) = \phi_1^{a-}(0) = \pi/2$ and $\phi_1^{a+}(0) = \phi_2^{a+}(0) = \phi_1^{k-}(0) = \phi_2^{a-}(0) = -\pi/2$ for $\lambda = 3$, $\mu = 0.5$.

We observe that the real parts are perturbed versions of the smooth kink and antikink solution of the Hermitian case, which exhibit more and more oscillations near the origin as λ increases. Asymptotically the solutions of the Hermitian and non-Hermitian cases tend to the same value. Crucially, we read off the CPT -symmetry (3.90) for the solutions

$$\phi_1^{k\pm}(x) = [\phi_1^{a\mp}(-x)]^\dagger, \quad \phi_2^{k+}(x) = -[\phi_2^{k-}(-x)]^\dagger, \quad \phi_2^{a+}(x) = -[\phi_2^{a-}(-x)]^\dagger, \quad (3.98)$$

from which we derive for the potential

$$\begin{aligned} \mathcal{V}_\lambda [\phi_1^{k+}(x), \phi_2^{k+}(x)] &= \mathcal{V}_\lambda \left\{ [\phi_1^{a-}(-x)]^\dagger, -[\phi_2^{k-}(-x)]^\dagger \right\} \\ &= \mathcal{V}_\lambda^\dagger \left\{ \phi_1^{a-}(-x), \phi_2^{k-}(-x) \right\}. \end{aligned} \quad (3.99)$$

This is once more the second option in (3.68). Thus assuming the energies of kinks and antikinks in the $+$ system are the same as the antikinks and kinks in the $-$ system, respectively, this energy is guaranteed to be real.

Since the limits $x \rightarrow \pm\infty$ for these solutions are the same as for $\lambda = 0$, the expression for the energy $E(\mu)$ in (3.96) holds for all values of λ . Considering the

expression in (3.96), it appears that $\mu = 1$ is an exceptional point of the system and that for $|\mu| > 1$, one might obtain complex conjugate pairs of eigenvalues. However, just as in the previous model, when the threshold is passed into that region, the asymptotic limits of the kink solutions are no longer defined, meaning the expression for the energy becomes meaningless. Moreover, when defining the theory on a finite interval in space, the energy is still real and does not occur in complex conjugate pairs. In order to qualify $\mu = 1$ as a genuine exceptional point of the complex solution, we expect to also find a BPS solution with finite complex energy beyond the exceptional point. However, in this example the solutions and energy becomes divergent. Hence we conclude that $\mu = 1$ is not an exceptional point. Note that the zero exceptional point of the monopole solution, we considered in section 3.2 was the zero exceptional point of the mass matrix of the theory. Therefore, it was a zero exceptional point of the Higgs and Goldstone fields, but not the monopole.

Next we identify the precise relation on which vacua are connected by which of the various BPS solutions. The infinite amount of vacua of the potential (3.87) are easily found to be

$$v_1^{(n,m)} = (\arcsin \mu + 2\pi n, m\pi), \quad \text{and} \quad v_2^{(n,m)} = (\pi - \arcsin \mu + 2n\pi, m\pi), \quad (3.100)$$

corresponding to the fixed points of the dynamical system (3.88) and (3.89), that are the solutions of $G_1^\pm(\phi_1, \phi_2) = G_2^\pm(\phi_1, \phi_2) = 0$. Computing once more the eigenvalues of the Jacobian matrix at these fixed points

$$J = \left(\begin{array}{cc} \partial_{\phi_1} G_1^\pm & \partial_{\phi_2} G_1^\pm \\ \partial_{\phi_1} G_2^\pm & \partial_{\phi_2} G_2^\pm \end{array} \right) \Big|_{v_j^{(n,m)}}, \quad (3.101)$$

with $j = 1, 2$, we find for the $+$ system that $J(v_1^{(n,2m)})$ has two positive eigenvalues, $J(v_2^{(n,2m+1)})$ has two negative eigenvalues and $J(v_1^{(n,2m+1)})$, $J(v_2^{(n,2m)})$ have a positive and a negative eigenvalue. For the $-$ system the signs are reversed. Thus the vacua $v_1^{(n,2m+1)}$, $v_2^{(n,2m)}$ are always saddle points, $v_1^{(n,2m)}$ are unstable/stable nodes (G^+/G^-) and $v_2^{(n,2m+1)}$ are stable/unstable nodes (G^-/G^+). Hence the kink and antikink solutions only interpolate between the vacua $v_1^{(n,2m)}$ and $v_2^{(n,2m+1)}$ as indicated for an example in figure 3.10 with the accompanying gradient flow. The

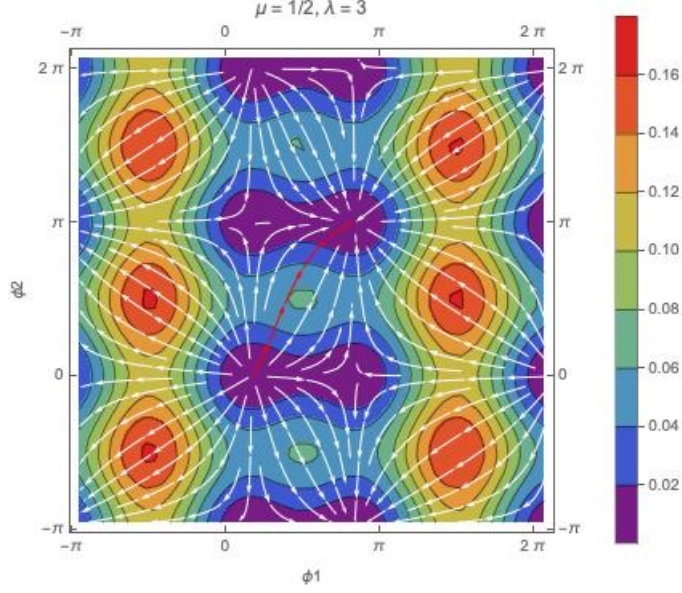


Figure 3.10: Real part of the potential $\mathcal{V}(\phi_1, \phi_2)$ as a function of $\text{Re}\phi_1$ and $\text{Re}\phi_2$ with the gradient flow of the real parts of G^+ superimposed in white. The kink solutions $\phi_1^{k+}(x)$, $\phi_2^{k+}(x)$ interpolate between the vacua $v_1^{(0,0)}$ and $v_2^{(0,1)}$ (red dots) as indicated by the red solid trajectory.

solutions of G_+ system are depicted in figure 3.10 interpolate the vacua $v_i^{(n,m)}$ as

$$v_1^{(0,0)} \xrightarrow{\phi_1^{k+} \phi_2^{k+}} v_2^{(0,1)}, \quad v_1^{(0,0)} \xrightarrow{\phi_1^{a+} \phi_2^{a+}} v_2^{(-1,1)}. \quad (3.102)$$

The G_- system admit same flow map as figure 3.10 but with every flow in the opposite direction. The solutions interpolating vacua are

$$v_2^{(0,-1)} \xrightarrow{\phi_1^{a-} \phi_2^{k-}} v_1^{(0,0)}, \quad v_2^{(-1,1)} \xrightarrow{\phi_1^{k-} \phi_2^{a-}} v_1^{(0,0)}. \quad (3.103)$$

hence confirming the consistency of the above. The other vacua $v_i^{(n,m)}$ for different choices of n and m are obtained by including the n -dependence into the solutions.

In both of our previous examples, we have directly analyzed the complex non-Hermitian systems. In analogy to the treatment of many quantum systems, such an approach is especially meaningful under the assumption that there exists an equivalent Hermitian system with the same energy. In the next section, we present such a system and thus further justify our approach.

3.3.4 Complex extended sine-Gordon model and its Hermitian partner

In this section we investigate a model with two complex fields consisting of two copies of sine-Gordon models of which one is complex \mathcal{PT} -symmetrically extended

$$\mathcal{V}(\phi_1, \phi_2) = \frac{m^2}{2\mu^2} \left[\sqrt{1 - \varepsilon^2} - \cos(\mu\phi_1) - i\varepsilon \sin(\mu\phi_1) \right] + \frac{m^2}{\mu^2} \sin^2\left(\frac{\mu}{2}\phi_2\right), \quad (3.104)$$

with constants $m, \mu \in \mathbb{R}$ and $|\varepsilon| \leq 1$. For simplicity, we have not introduced an interaction term between ϕ_1 and ϕ_2 as the feature we are trying to illustrate can even be shown for a theory with one field only. We keep a second field to maintain similarity with the previously discussed systems and directly compare the BPS solutions for the two fields. The constant term proportional to $\sqrt{1 - \varepsilon^2}$ is introduced for convenience. In order to find a Hermitian partner potential \mathfrak{v} to the non-Hermitian potential \mathcal{V} we employ now a Dyson map originally found in [75]

$$\tilde{\eta} = \exp \left[\frac{\text{arctanh}\varepsilon}{\mu} \int dx \pi_1(x, t) \right]. \quad (3.105)$$

Here the momentum operator $\pi_1(x, t) := \partial_t \phi_1(x, t)$ satisfies the canonical equal time commutation relation $[\phi_1(x, t), \pi_1(y, t)] = i\delta(x - y)$. The inverse adjoint action of $\tilde{\eta}$ on \mathcal{V} then leads to

$$\mathfrak{v}(\phi_1, \phi_2) = \tilde{\eta}^{-1} \mathcal{V} \tilde{\eta} = \frac{m^2}{\mu^2} \left[\sqrt{1 - \varepsilon^2} \sin^2\left(\frac{\mu}{2}\phi_1\right) + \sin^2\left(\frac{\mu}{2}\phi_2\right) \right], \quad (3.106)$$

whereas the kinetic term remains unchanged as $\tilde{\eta}$ commutes with it. Even though we are here mainly interested in the properties of classical solutions, we briefly drew on the quantum field theory version of the model in order to carry out the similarity transformation. The effect of the adjoint action of $\tilde{\eta}$ on any smooth function of the fields (ϕ_1, ϕ_2) is $(\phi_1, \phi_2) \rightarrow (\phi_1 + i/\mu \text{arctanh}\varepsilon, \phi_2)$.

We shall now demonstrate that the energies of the BPS solutions for the system involving the non-Hermitian potential \mathcal{V} and the Hermitian potential \mathfrak{v} are identical and real. Following the procedure of the previous sections, we first note that the

potential \mathcal{V} can be derived from the pre-potential

$$U(\phi_1, \phi_2) = -\frac{2^{3/2}m}{\mu^2} \left[(1 - \varepsilon^2)^{1/4} \cos\left(\frac{\mu}{2}\phi_1 - \frac{i}{2}\operatorname{arctanh}\varepsilon\right) + \cos\left(\frac{\mu}{2}\phi_2\right) \right], \quad (3.107)$$

when taking the metric of the target space simply to be diagonal $\operatorname{diag}\eta = (1, 1)$.

According to (3.66) the two pairs of coupled BPS equations are therefore

$$BPS_1^\pm : \quad \partial_x \phi_1 = \pm \frac{m\sqrt{2}(1 - \varepsilon^2)^{1/4}}{\mu} \sin\left(\frac{\mu}{2}\phi_1 - \frac{i}{2}\operatorname{arctanh}\varepsilon\right), \quad (3.108)$$

$$BPS_2^\pm : \quad \partial_x \phi_2 = \pm \frac{m\sqrt{2}}{\mu} \sin\left(\frac{\mu}{2}\phi_2\right). \quad (3.109)$$

Once again we can identify a pair of modified \mathcal{CPT} -transformations under which these equations are compatible

$$\mathcal{CPT}_\pm : \quad \begin{cases} \phi_1(x) & \rightarrow -[\phi_1(-x)]^\dagger \\ \phi_2(x) & \rightarrow \pm[\phi_2(-x)]^\dagger \end{cases}, \quad \Leftrightarrow BPS_i^\pm \rightarrow (BPS_i^\mp)^*. \quad (3.110)$$

We solve the equations (3.108) and (3.109) by

$$\phi_1^{k/a^+}(x) = -\left[\phi_1^{k/a^-}(-x)\right]^* = \pm \frac{4}{\mu} \arctan\left[e^{mx(1-\varepsilon^2)^{1/4}/\sqrt{2}+\mu\kappa_1/2}\right] + \frac{i}{\mu} \operatorname{arctanh}\varepsilon, \quad (3.111)$$

$$\phi_2^{k/a^+}(x) = -\left[\phi_2^{k/a^-}(-x)\right]^* = \pm \frac{4}{\mu} \arctan\left[e^{mx/\sqrt{2}+\mu\kappa_2/2}\right], \quad (3.112)$$

with integration constants $\kappa_1, \kappa_2 \in \mathbb{C}$. The solution respect the \mathcal{CPT}_- -symmetry as indicated, which leads to the relation

$$\mathcal{V}\left[\phi_1^{k/a^+}(x), \phi_2^{k/a^+}(x)\right] = \mathcal{V}^*\left[\phi_1^{k/a^-}(-x), \phi_2^{k/a^-}(-x)\right], \quad (3.113)$$

for the potential that guarantees the reality of the energy when arguing along the same lines as above.

We may of course also compute the energies directly from the asymptotic limits of the solutions. For $|\varepsilon| \leq 1$ we find

$$\lim_{x \rightarrow \pm\infty} \phi_j^{k/a^+}(x) = \lim_{x \rightarrow \mp\infty} \phi_j^{a^-}(x) = \frac{\pi}{\mu} \pm \frac{\pi}{\mu} + \delta_{1j} \frac{i}{\mu} \operatorname{arctanh}\varepsilon, \quad (3.114)$$

$$\lim_{x \rightarrow \pm\infty} \phi_j^{a^+}(x) = \lim_{x \rightarrow \mp\infty} \phi_j^{k/a^-}(x) = -\frac{\pi}{\mu} \mp \frac{\pi}{\mu} + \delta_{1j} \frac{i}{\mu} \operatorname{arctanh}\varepsilon, \quad (3.115)$$

which by (3.64) gives the real energies

$$E^{\phi_1^{pn}, \phi_2^{qn}}(m, \mu, \varepsilon) = \frac{4\sqrt{2}m}{\mu^2} \left[1 + (1 - \varepsilon^2)^{1/4} \right], \quad p, q = k, a; \quad n = \pm; \quad m, \mu \in \mathbb{R}. \quad (3.116)$$

The special point $\varepsilon = 1$ is not an exceptional point as the BPS solutions for ϕ_1 and ϕ_2 have no definite asymptotic values. For $|\varepsilon| > 1$ the energies become complex, albeit not complex conjugate. The reason for the latter is that the \mathcal{CPT} -symmetry is not just broken for the solutions, but also at the level of the Hamiltonian. It is now easy to verify that the pre-potential $\mathbf{u}(\phi_1, \phi_2)$ leading to the real potential $\mathbf{v}(\phi_1, \phi_2)$ is simply obtained as $\mathbf{u} = \tilde{\eta}^{-1}U\tilde{\eta}$. The solutions to the real BPS equations are then given by (3.111) and (3.112) with $(\phi_1, \phi_2) \rightarrow (\phi_1 - i\text{arctanh}(\varepsilon)/\mu, \phi_2)$. The expression for the energy $E = \lim_{x \rightarrow \infty} \mathbf{u}(\phi_1, \phi_2) - \lim_{x \rightarrow -\infty} \mathbf{u}(\phi_1, \phi_2)$ is then the same as the one in (3.116).

3.3.5 Summary

We defined the BPS solution and studied three models containing BPS solutions: super-exponential, non-Hermitian coupled sine-Gordon, and complex sine-Gordon models. In all three models, we have found the complex solution with real and finite energies and identified the \mathcal{CPT} -symmetry responsible for the reality. We plotted the gradient flow for the first two models to show how the solution flows from one vacuum to the other. In the last model, we have identified the similarity transformation and compared the energy of the solutions in non-Hermitian and Hermitian counterparts and observed that they are indeed equal.

3.4 Topological solitons in nuclear physics

We conclude the chapter by investigating several complex versions of extensions and restrictions of the Skyrme model with a well-defined BPS limit. The models studied possess complex kink, anti-kink, semi-kink, massless and purely imaginary compacton BPS solutions that all have real energies. The reality of the energies for a particular solution is guaranteed when a modified antilinear \mathcal{CPT} -symmetry maps the Hamiltonian functional to its parity time-reversed complex conjugate and the solution field to itself or a new field with degenerate energy. In addition to the known BPS Skyrmion configurations we find new types that we refer to as step,

cusps, shells, and purely imaginary compacton solutions.

3.4.1 The Skyrme model - extensions and restrictions

To establish our notations and conventions, we briefly recall some key aspects and definitions of the Skyrme model. Largely following [131, 132], we consider an extended version of the standard Skyrme model described by variants of a Lagrangian density of the general form

$$\mathcal{L} = \tilde{\mathcal{L}}_0 + \mathcal{L}_2 + \mathcal{L}_4 + \mathcal{L}_6 + \mathcal{L}_0, \quad (3.117)$$

where the different terms are defined as

$$\begin{aligned} \mathcal{L}_2 &:= -\frac{f_\pi^2}{2} \text{Tr}(L_\mu L^\mu), & \mathcal{L}_4 &:= \frac{1}{16e^2} \text{Tr}([L_\mu, L_\nu]^2), \\ \mathcal{L}_6 &:= -\lambda^2 N_0^2 B_\mu B^\mu, & \mathcal{L}_0 &:= -\mu^2 V, \end{aligned} \quad (3.118)$$

with Lie algebraic currents in form of right Maurer Cartan forms, topological current and $SU(2)$ -group valued Skyrme fields

$$L_\mu := U^\dagger \partial_\mu U, \quad B^\mu := \frac{1}{N_0} \varepsilon^{\mu\nu\rho\tau} \text{Tr}(L_\nu L_\rho L_\tau), \quad U := e^{i\zeta(\sigma \cdot \vec{n})}, \quad (3.119)$$

respectively. Here f_π can be interpreted as the pion decay constant, and the dimensionless constant e is referred to as the Skyrme parameter. As is well known, these parameters can be scaled away to set them both to 1 in what follows. Moreover, we denote by σ the standard Pauli matrices and take the three-component unit vector to be of the form $\vec{n} = (\sin \Theta \cos \Phi, \sin \Theta \sin \Phi, \cos \Theta)$ rather than the rational map or stereographic projection often used instead in this context, see, e.g. [133]. Our space-time metric g is taken to be $\text{diag} g = (1, -1, -1, -1)$. The normalization constant N_0 is chosen in such a way that the Baryon number $B = \int B_0 d^3x \in \mathbb{Z}$ becomes an integer as it should be for a two flavour theory to guarantee that Baryons with an even and odd number of quarks are Bosons and Fermions, respectively. See for instance [134] for a more detailed reasoning on this issue. For a standard static compacton solution the normalization constant is usually taken to be $N_0 = 24\pi^2$.

Dropping and decomposing terms or further specifying the potential in the general Lagrangian \mathcal{L} gives rise to different versions of the model. The original Skyrme model [135] is comprised of the sum of the sigma model term \mathcal{L}_2 and the Skyrme

term \mathcal{L}_4 with occasionally the potential term $\tilde{\mathcal{L}}_0$ added which is of the same functional form as \mathcal{L}_0 . The BPS version of the model introduced in [131] consists of the sum of \mathcal{L}_6 , that mimics the interactions generated by the vector mesons, and the potential term \mathcal{L}_0 .

Consistent submodels may be obtained by further decomposing terms in \mathcal{L} . With our choice of the parameterization for the $SU(2)$ -group valued element U the various parts of the Lagrangian take on the following forms: For reasons that will become clear below, we decompose the sigma model and the Skyrme term as

$$\mathcal{L}_2 = \mathcal{L}_2^{(1)} + \mathcal{L}_2^{(2)}, \quad \text{and} \quad \mathcal{L}_4 = \mathcal{L}_4^{(1)} + \mathcal{L}_4^{(2)}, \quad (3.120)$$

with

$$\mathcal{L}_2^{(1)} = \sin^2 \zeta (\Theta_\mu \Theta^\mu + \Phi_\mu \Phi^\mu \sin^2 \Theta), \quad (3.121)$$

$$\mathcal{L}_2^{(2)} = \zeta_\mu \zeta^\mu, \quad (3.122)$$

$$\mathcal{L}_4^{(1)} = \sin^2 \zeta [\Theta_\mu \zeta^\mu \Theta_\nu \zeta^\nu - \Theta_\mu \Theta^\mu \zeta_\nu \zeta^\nu + \sin^2 \Theta (\Phi_\mu \zeta^\mu \Phi_\nu \zeta^\nu - \Phi_\mu \Phi^\mu \zeta_\nu \zeta^\nu)], \quad (3.123)$$

$$\mathcal{L}_4^{(2)} = \sin^4 \zeta \sin^2 \Theta (\Theta_\mu \Phi^\mu \Theta_\nu \Phi^\nu - \Theta_\mu \Theta^\mu \Phi_\nu \Phi^\nu) \quad (3.124)$$

where Θ, Φ are defined above as angles of the unit vector \vec{n} and the Lorentz index indicate the derivative $\Theta_\mu := \partial_\mu \Theta$, $\Phi_\mu := \partial_\mu \Phi$. The extended part computes with

$$B^\mu = \frac{1}{2N_0} \sin^2 \zeta \sin \Theta \mathcal{B}^\mu, \quad \mathcal{B}^\mu := \varepsilon^{\mu\nu\rho\tau} \zeta_\nu \Theta_\rho \Phi_\tau \quad (3.125)$$

to

$$\mathcal{L}_6 = -\frac{\lambda^2}{4} \sin^4 \zeta \sin^2 \Theta \mathcal{B}_\mu \mathcal{B}^\mu = \frac{\lambda^2}{4} \sin^4 \zeta \sin^2 \Theta \left[\varphi_0^a Q_a^i \varphi_0^b Q_b^i - \mathcal{B}_0 \mathcal{B}_0 \right], \quad (3.126)$$

where $Q_a^i := \frac{1}{2} \varepsilon_{abc} \varepsilon^{ijk} \varphi_j^b \varphi_k^c$, $\varphi := (\zeta, \Theta, \Phi)$ and $a, b, c, i, j, k \in \{1, 2, 3\}$.

Finally, the pion mass term in the standard BPS version of the model (BPSS) $\mathcal{L}_0^{BPSS} = -\mu^2 V$ is taken to involve the potential $V = \frac{1}{2} \text{Tr}(\mathbb{I} - U) = 1 - \cos \zeta$, but we will allow here other forms of the potential as well. Further extensions, including for instance, a sextic derivative term [136] or multiplying the terms with field-dependent coupling constants [137] have also been studied.

In what follows, we shall investigate different combinations of various complex extended or deformed versions of different parts of this model related to the form of \mathcal{L} in (3.117).

3.4.2 Pseudo Hermitian variants of Skyrme models

In this section, our first guiding principle is to identify a \mathcal{CPT} -symmetry in a Hermitian Hamiltonian and extend the model by deforming or adding complex terms to convert it into a non-Hermitian Hamiltonian that still respects this symmetry. Subsequently, we try to identify a pseudo-Hermitian counterpart in a similar fashion as what is by now standard for non-Hermitian quantum mechanical systems [104, 111].

Complex boosted BPS Skyrme models

We start with the standard BPS Skyrme model consisting of $\mathcal{L}_6 + \mathcal{L}_0^{BPSS}$ by noting that it remains invariant under the antilinear \mathcal{CPT} -transformation: $\zeta \rightarrow -\zeta$, $\imath \rightarrow -\imath$. Thus we may introduce a complex shift in $\zeta \rightarrow \zeta + \imath\kappa$ with $\kappa \in \mathbb{R}$ without breaking that symmetry. We will later see that this anti-linear symmetry is not the appropriate symmetry to satisfy the three conditions stated in section 3.1 but there is a non-trivial anti-linear symmetry of the solution which satisfies the three conditions.

We denote here and in what follows the imaginary unit as $\imath := \sqrt{-1}$ to distinguish it from indices i . Choosing $\kappa = -\arctan\epsilon$ with $\epsilon \in \mathbb{R}$ and using the identities $\sqrt{1-\epsilon^2} \sin(\zeta - \imath\arctan\epsilon) = \sin\zeta - \imath\epsilon \cos\zeta$, $\sqrt{1-\epsilon^2} \cos(\zeta - \imath\arctan\epsilon) = \cos\zeta + \imath\epsilon \sin\zeta$, we obtain a \mathcal{CPT} -symmetrically extended BPS Skyrme model of the form

$$\mathcal{L}_b = -\frac{\lambda^2}{4} (\sin\zeta - \imath\epsilon \cos\zeta)^4 \sin^2\Theta \mathcal{B}_\mu \mathcal{B}^\mu - \mu^2 \left(\sqrt{1-\epsilon^2} - \cos\zeta - \imath\epsilon \sin\zeta \right), \quad (3.127)$$

after re-scaling the coupling constants as $\lambda \rightarrow \lambda(1-\epsilon^2)$, $\mu \rightarrow \mu(1-\epsilon^2)^{1/4}$. By design, for vanishing ϵ the model reduces to the standard BPS Skyrme model $\lim_{\epsilon \rightarrow 0} \mathcal{L}_b = \mathcal{L}_6 + \mathcal{L}_0^{BPSS}$ as introduced and discussed in [131]. We shall now demonstrate that the energies for the topological solutions to the equations of motion resulting from \mathcal{L}_b and its corresponding Hermitian counterpart are identical and real.

Topological energies for the real solutions of the Hermitian counterpart

At first we derive the Hamiltonian corresponding to \mathcal{L}_b in the standard fashion by computing the conjugate canonical momenta

$$\Pi^a = \frac{\delta \mathcal{L}_b}{\delta \varphi_0^a} = G_{ac} \varphi_0^c, \quad \text{with } G_{ac} = \frac{\lambda^2}{2} (\sin \zeta - \nu \epsilon \cos \zeta)^4 \sin^2 \Theta \mathcal{Q}_a^i \mathcal{Q}_c^i, \quad (3.128)$$

so that

$$\mathcal{H}_b = \frac{1}{2} \Pi^a G_{ac}^{-1} \Pi^c - \mathcal{L}_b, \quad \text{with } G_{ac}^{-1} = \frac{2 \varphi_i^a \varphi_i^c}{J^2 \lambda^2 (\sin \zeta - \nu \epsilon \cos \zeta)^4 \sin^2 \Theta}, \quad (3.129)$$

where $J := \frac{1}{2} \varepsilon_{abc} \varepsilon^{ijk} \varphi_i^a \varphi_j^b \varphi_k^c$.

While overall our considerations are mainly classical as before, we now briefly appeal to the quantum field theoretic version of the model, by assuming the standard canonical equal time commutation relation $[\varphi^a(r, t), \Pi^b(r', t)] = i \delta^{ab} \delta(r - r')$ between the fields $\varphi^a(r, t)$ and their conjugate momentum operators $\Pi^a(r, t)$. We then use a slightly modified version of the Dyson operator as employed in [75, 11] and in the previous section

$$\eta = \exp \left[-\text{arctanh} \epsilon \sum_a \int dx \Pi^a(r, t) \right], \quad (3.130)$$

to map the non-Hermitian Hamiltonian functional \mathcal{H}_b to a Hermitian counterpart \mathfrak{h}_b by means of the adjoint action of η

$$\mathfrak{h}_b = \eta \mathcal{H}_b \eta^{-1} = \frac{1}{2} \Pi^a G_{ac}^{-1} \Pi^c + \frac{\tilde{\lambda}^2}{4} \sin^4 \zeta \sin^2 \Theta \mathcal{B}_\mu \mathcal{B}^\mu + \tilde{\mu}^2 (1 - \cos \zeta). \quad (3.131)$$

We notice that \mathfrak{h}_b is in fact the standard BPS Skyrme model with reversing the previous re-scaling of the coupling constants as $\lambda \rightarrow \tilde{\lambda} = \lambda(1 - \epsilon^2)$, $\mu \rightarrow \tilde{\mu} = \mu(1 - \epsilon^2)^{1/4}$.

In this case the static BPS solution that saturates the Bogomolny bound is known to be computable exactly [131] when using spherical space-time coordinates $(x, y, z) \rightarrow (r, \theta, \phi)$ with $r \in [0, \infty)$, $\theta \in [0, \pi)$, $\phi \in [0, 2\pi)$ and the identifications $\Theta = \theta$, $\Phi = n\phi$ with $n \in \mathbb{Z}$ together with the assumption that ζ is a function of r only. In this case one obtains a well-defined real compacton solution, see e.g. [138]

for what that entails in general,

$$\zeta_r(r) = \begin{cases} 2 \arccos \left(\frac{1}{\sqrt{2}} \left| \frac{\tilde{\mu}}{n\lambda} \right|^{1/3} r \right) & \text{for } r \in \left[0, r_c = \sqrt{2} \left| \frac{n\tilde{\lambda}}{\tilde{\mu}} \right|^{1/3} \right] \\ 0 & \text{otherwise} \end{cases}, \quad (3.132)$$

with real energy

$$E = 8\pi\tilde{\mu}^2 \int_0^{r_c} r^2 V[\zeta_r(r)] dr = \frac{64}{15} \sqrt{2} |n| \tilde{\mu} \tilde{\lambda} \pi (1 - \epsilon^2)^{5/4}. \quad (3.133)$$

Next we show that there are in fact more solutions in this case and how the same energy results from a direct computation for the complex solution of the non-Hermitian system (3.127).

Energies for the complex solutions of the non-Hermitian system

We adopt here and below the approach proposed in [123] as outlined in section 3.3.1, which slightly reformulates the BPS theory and exploits the self-duality and anti-self-duality between certain fields. For this purpose, we first note that the Hamiltonian density for static solutions may be expressed as

$$\mathcal{H}_b = A^2 + \tilde{A}^2, \quad (3.134)$$

with

$$\begin{aligned} A &:= \frac{\lambda}{2} (\sin \zeta - \imath \epsilon \cos \zeta)^2 \sin \Theta \mathcal{B}_0, \\ \tilde{A} &= \mu V = \mu \left(\sqrt{1 - \epsilon^2} - \cos \zeta - \imath \epsilon \sin \zeta \right)^{1/2}. \end{aligned} \quad (3.135)$$

Once more, the self-duality and anti-self-duality between the fields A and \tilde{A}

$$A = \pm \tilde{A}, \quad (3.136)$$

is then interpreted as being identical to the BPS equations [121, 119]. The energy functional for the solutions of (3.136) therefore acquires the form

$$E_b = \int d^3x \left[A^2 + \tilde{A}^2 \right] = \pm 2 \int d^3x A \tilde{A}. \quad (3.137)$$

Explicitly the BPS equations (3.136) may be written as

$$\frac{\lambda (\sin \zeta - \imath \epsilon \cos \zeta)^2}{2 \mu \sqrt{V}} \sin \Theta \varepsilon^{ijk} \partial_i \zeta \partial_j \Theta \partial_k \Phi = \pm 1. \quad (3.138)$$

Since $\varepsilon_{ijk} \zeta_i \Theta_j \Phi_k$ is simply the Jacobian for the variable transformation $(x, y, z) \rightarrow (\Theta, \Phi, \zeta)$ the multiplication of (3.138) by the volume element d^3x leads to

$$\frac{\lambda (\sin \zeta - \imath \epsilon \cos \zeta)^2}{2 \mu \sqrt{V}} \sin \Theta d\zeta d\Theta d\Phi = \pm r^2 \sin \theta dr d\theta d\phi, \quad (3.139)$$

where we used spherical coordinates on the right hand side. With the same identifications between (r, θ, ϕ) and (ζ, Θ, Φ) as chosen in the previous section and together with the aforementioned trigonometric identities the relation (3.139) converts into

$$\frac{n\tilde{\lambda}}{2r^2} \sin^2(\zeta - \imath \arctan \epsilon) \frac{d\zeta}{dr} = \pm \tilde{\mu} \sqrt{1 - \cos(\zeta - \imath \arctan \epsilon)}. \quad (3.140)$$

These equations are easily integrated out by separating variables. Corresponding to the different branches we obtain different types of solutions

$$\begin{aligned} \zeta_{i,m}^\pm(r) &= \tilde{\zeta}_{i,m}^\pm(r) + \imath \arctan \epsilon \\ &= 2 \arccos \left[\omega^i \frac{(n\tilde{\lambda}c \mp \tilde{\mu}r^3)^{1/3}}{\sqrt{2}n^{1/3}\tilde{\lambda}^{1/3}} \right] + 2\pi m + \imath \arctan \epsilon, \end{aligned} \quad (3.141)$$

for $i = 0, 1, 2$, $m \in \mathbb{Z}$ and $\omega = e^{2\pi i/3}$ denoting the third root of unity. We analytically continue here the arccos-function to the entire complex plane by the well-known formula $\arccos z = -i \ln(z \pm \sqrt{z^2 - 1})$. Note that for the Hermitian case, i.e. $\epsilon = 0$, all these solutions also arise, but in that case one simply discards the complex solutions or the parts of the solutions that become complex after a certain value of r , by requiring solutions to be real. In order to identify possible compacton solutions in the real part we need to specify the critical values r_0 for which the solution vanish, $\tilde{\zeta}_i^\pm(r_0) = 0$, and also those values r_π for which $\tilde{\zeta}_i^\pm(r_\pi) = \pi$. We obtain

$$r_{0,i}^\pm := \omega^i \left[\frac{\pm n\tilde{\lambda}(c - 2^{3/2})}{\tilde{\mu}} \right]^{1/3}, \quad \text{and} \quad r_{\pi,i}^\pm := \omega^i \left(\frac{\pm n\tilde{\lambda}c}{\tilde{\mu}} \right)^{1/3}. \quad (3.142)$$

These values are irrelevant when complex, whereas when real they may produce different types of scenarios depending on their ordering and signs of the constants. In figure 3.11 we depict some interesting possibilities.

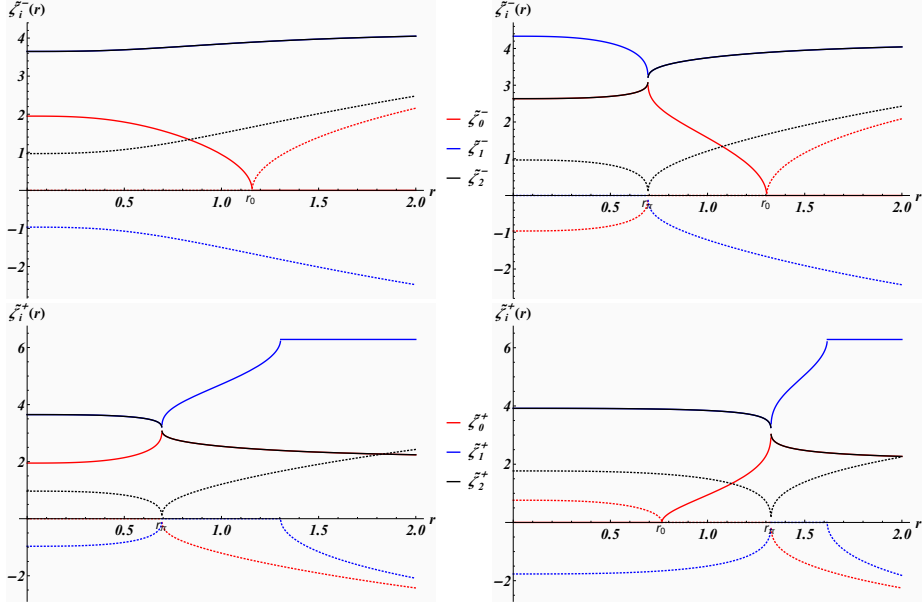


Figure 3.11: The $\tilde{\zeta}$ -part of the solutions of the BPS equation (3.140) for different scenarios with $n = \bar{\lambda} = 1$, $\mu = 3/2$ and different choices for c . The different relative orderings are: panel (a) $r_\pi \leq 0 \leq r_0$ with $c = 1/2$, panel (b) $0 \leq r_\pi \leq r_0$ with $c = -1/2$, panel (c) $r_0 \leq 0 \leq r_\pi$ with $c = 1/2$ and panel (d) $0 \leq r_0 \leq r_\pi$ with $c = 7/2$. Real parts correspond to solid lines and imaginary parts to dotted ones.

It is clear from figure 3.11 that we may construct compacton type solutions in various ways. Obvious choices are

$$\begin{aligned} \tilde{\zeta}_{\text{BPS}}(r) &:= \begin{cases} \tilde{\zeta}_{0,0}^- & \text{for } 0 \leq r \leq r_0^- \\ 0 & \text{for } r_0^- < r \end{cases}, \\ \tilde{\zeta}_{\text{St}}(r) &:= \begin{cases} \tilde{\zeta}_{1,0}^- & \text{for } 0 \leq r \leq r_\pi^- \\ \tilde{\zeta}_{0,0}^- & \text{for } r_\pi^- \leq r \leq r_0^- \\ 0 & \text{for } r_0^- < r \end{cases}. \end{aligned} \quad (3.143)$$

Noting that $r_{\pi,i}^+(c) = r_{\pi,i}^-(-c)$, we may also glue together solution that are self-dual with those that are anti-self-dual as

$$\begin{aligned} \tilde{\zeta}_{\text{Cusp}}(r) &:= \begin{cases} \tilde{\zeta}_{0,0}^+(c > 0) & \text{for } 0 \leq r \leq r_\pi^+ = r_\pi^- \\ \tilde{\zeta}_{0,0}^-(c < 0) & \text{for } r_\pi^- \leq r \leq r_0^- \\ 0 & \text{for } r_0^- < r \end{cases}, \\ \tilde{\zeta}_{\text{Shell}}(r) &:= \begin{cases} 0 & \text{for } r < r_0^+ \\ \tilde{\zeta}_{0,0}^+(c > 0) & \text{for } r_0^+ \leq r \leq r_\pi^+ = r_\pi^- \\ \tilde{\zeta}_{0,0}^-(c < 0) & \text{for } r_\pi^- \leq r \leq r_0^- \\ 0 & \text{for } r_0^- < r \end{cases}. \end{aligned} \quad (3.144)$$

A purely imaginary compacton solution is obtained as $\tilde{\zeta}_{\text{iBPS}}(r) := \tilde{\zeta}_{0,0}^+$ for $r < r_0^+$ and 0 otherwise. Here and below, our terminology is inspired by the radial profile of our solutions. We have dropped the second subscript on $r_{0,i}^\pm$ and $r_{\pi,i}^\pm$ as the branch that produces a real values depends on the values of $\tilde{\lambda}$, $\tilde{\mu}$ and c . It appears that in this way, one is combining solutions from different equations. However, noting that the equation of motion resulting from (3.127) is simply the square of the BPS equations (3.140), see, e.g. [131] for a derivation when $\epsilon = 0$, we adopt here the view that the latter is more fundamental. Hence, we are combining solutions for one single equation with different choices of integration constants in different domains. Whilst the first-order derivative are discontinuous at the ‘gluing points’ r_0^\pm and r_π^\pm in the solutions in (3.143) and (3.144), we may argue here in a similar way as in [131] to establish that the solutions are in fact well defined solutions. The derivative $d\tilde{\zeta}/dr$ always occurs multiplied with a $\sin^2 \tilde{\zeta}$ in the BPS equations, so that the left and right limits of this combination is always finite at the glueing points, but might differ by a sign. Since this sign is irrelevant in the equations of motion, the solutions are well defined and lead to meaningful values for the energy density and the Baryon number density. We depict the configurations (3.144) - (3.143) in figure 3.12.

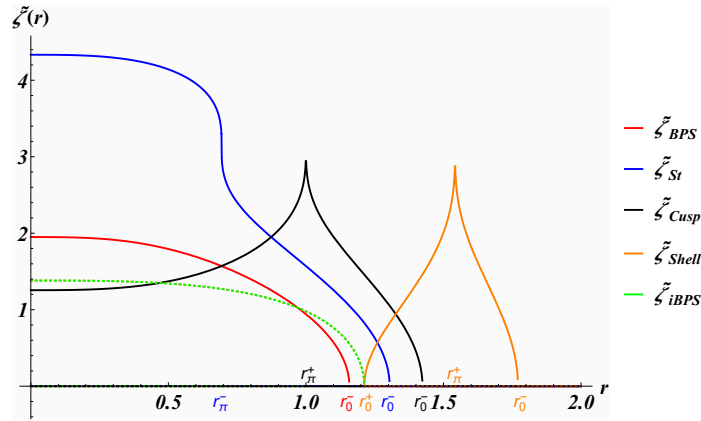


Figure 3.12: The BPS solution $\tilde{\zeta}_{\text{BPS}}$ with $n = 1$, $c = 1/2$, $\tilde{\mu} = 3/2$, $\tilde{\lambda} = 1$, the step solution $\tilde{\zeta}_{\text{St}}$ with $n = 1$, $-c = 1/2$, $\tilde{\mu} = 3/2$, $\tilde{\lambda} = 1$, the cusp solution $\tilde{\zeta}_{\text{Cusp}}$ with $n = 1$, $c = 3/2$, $\tilde{\mu} = 3/2$, $\tilde{\lambda} = 1$, the shell solution $\tilde{\zeta}_{\text{Shell}}$ with $n = 1$, $c = 11/2$, $\tilde{\mu} = 3/2$, $\tilde{\lambda} = 1$ and the purely imaginary solution $\tilde{\zeta}_{\text{iBPS}}$ with $n = 1$, $c = 11/2$, $\tilde{\mu} = 3/2$, $\tilde{\lambda} = 1$.

In figure 3.13 we present the Skyrmion solutions of compacton type (3.144) - (3.143) as slices in form of level curves. We may compare with figure 3.12. In panel (a) we have a standard real (fractional) Skyrmion $\tilde{\zeta}_{\text{BPS}}$ starting at a finite value at $r = 0$ and then decaying to zero at some critical value r_0^- . In panel (b) we depict the solution $\tilde{\zeta}_{\text{St}}$ taking on the form of a step like function with an inflection

point at r_π^- . The solution $\tilde{\zeta}_{\text{Cusp}}$ shown in panel (c) has a discontinuous first order derivative at $r = r_\pi^+ = r_\pi^-$, which is usually referred to as peakons in the context of 1+1 dimensional integrable systems. The most interesting structure $\tilde{\zeta}_{\text{Shell}}$ is seen in panel (d), which corresponds to a real shell with a peakon structure. We may even change this solution in the region $r < r_0^+$, by defining it as $\tilde{\zeta}_{\text{Core}}(r) = \tilde{\zeta}_{0,0}^+$ for $r < r_0^+$, hence adding a purely imaginary core to it. It turns out that this is consistent as the core has also real energies despite the fact that it is complex.

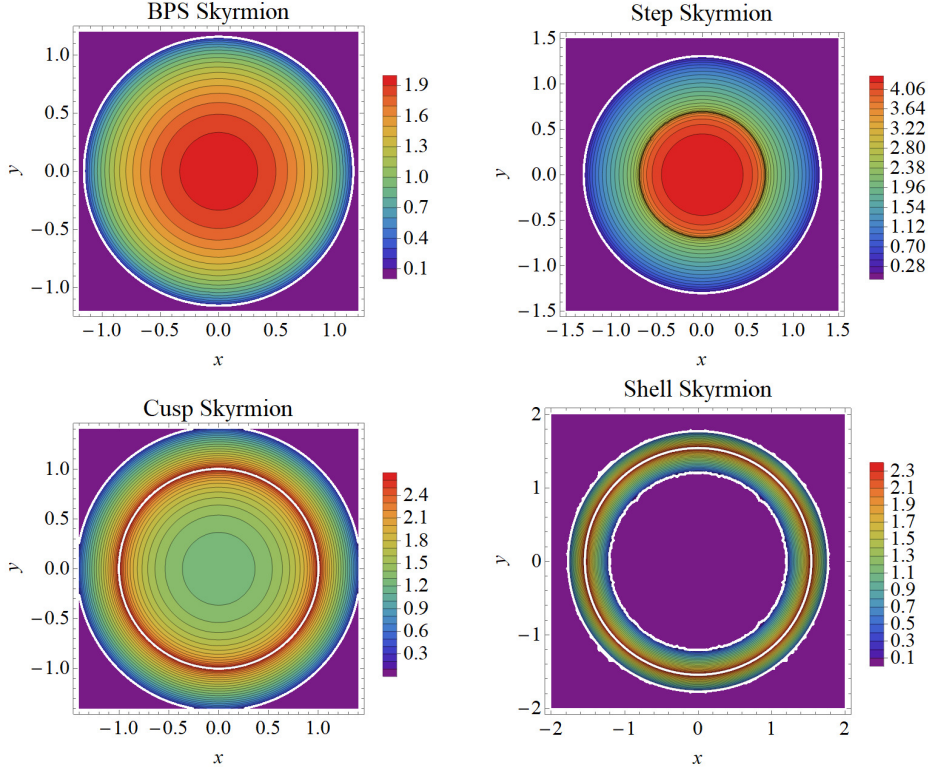


Figure 3.13: Different types of solutions to the equations of motion as defined in (3.144) - (3.143) with parameters $n = \tilde{\lambda} = 1$, $\tilde{\mu} = 3/2$ and $c = 1/2$ in panel (a), $c = -1/2$ in panel (b), $c = 3/2$ in panel (c), $c = 11/2$ in panel (d).

Next we demonstrate that all types of solutions depicted in figures 3.12 and 3.13 possess real energies. We compute these energies on some domain $r \in [\tilde{r}_c, r_c]$ by using the general expression (3.137)

$$E = \pm \tilde{\lambda} \tilde{\mu} \int d^3x \left[(\sin \zeta - \nu \epsilon \cos \zeta)^2 \sin \Theta \mathcal{B}_0 \left(\sqrt{1 - \epsilon^2} - \cos \zeta - \nu \epsilon \sin \zeta \right)^{1/2} \right] \quad (3.145)$$

$$\begin{aligned} &= \pm 4\pi \tilde{\lambda} \tilde{\mu} n \int_{\tilde{r}_c}^{r_c} dr \left[\sin^2(\zeta(r) - \nu \arctan \epsilon) \sqrt{1 - \cos(\zeta(r) - \nu \arctan \epsilon)} \frac{d\zeta}{dr} \right] \\ &= 8\pi \tilde{\mu}^2 \int_{\tilde{r}_c}^{r_c} dr \left[r^2 V(\zeta(r)) \right]. \end{aligned} \quad (3.146)$$

In the last step we used once more equation (3.140). For the solutions $\tilde{\zeta}_{\text{BPS}}$, $\tilde{\zeta}_{\text{St}}$ and

$\tilde{\zeta}_{\text{Cusp}}$ we calculate

$$E_{\text{BPS/St,Cusp}} = \frac{8}{15} n \tilde{\mu} \tilde{\lambda} \pi \left(8\sqrt{2} \mp 10c \pm 3c^{5/3} \right), \quad (3.147)$$

for $c \geq 0$ on the domains as indicated in figure 3.11. One may question if the energy of the cusp and shell solutions should be evaluated with the formula (3.146) as they do not fully satisfies the BPS equations, but only partially, depending on the region of the domain for the values of $r \in \mathbb{R}$. Although cumbersome, the energy of the cusp and shell solutions has been calculated using the full expression of the energy and it is found that surprisingly it coincide with the energy found by above expression.

The upper signs in equation (3.147) stand here for BPS and the lower signs for the step and cusp solutions, with the same energies. As expected, the expressions (3.147) reduce to the energy of the standard real case (3.133) in the limit $c \rightarrow 0$, since in that case the fractional BPS Skyrmons become full BPS Skyrmons with $\zeta(r=0) = \pi$. For the shell solution $\tilde{\zeta}_{\text{Shell}}$ and the purely imaginary core solution $\tilde{\zeta}_{\text{iBPS}}$ we obtain the real energies

$$E_{\text{Shell}} = \frac{128}{15} \sqrt{2} n \tilde{\mu} \tilde{\lambda} \pi, \quad \text{and} \quad E_{\text{iBPS}} = -E_{\text{BPS}}, \quad (3.148)$$

respectively. The reality of the solutions is ensured by verifying that the respective solutions satisfy all three conditions (1)-(3) from section 3.1 for a particular \mathcal{CPT}' -symmetry. With condition (1) we identify here the symmetry to

$$\mathcal{CPT}' : \zeta(x_\mu) \rightarrow \zeta^*(-x_\mu) + 2i \arctan \epsilon = \zeta(-x_\mu). \quad (3.149)$$

We are considering static solutions in which the angle dependence has already been eliminated, so that our solutions only depend on r . Hence the change in the arguments of the fields $x_\mu \rightarrow -x_\mu$ is automatically satisfied. The \mathcal{CPT}' -symmetry condition (3.149) is then easily verified for our solutions $\zeta_{i,m}^\pm(r)$ in (3.141): $\zeta_{i,m}^\pm(r) \rightarrow \left[\zeta_{i,m}^\pm(r) \right]^* + 2i \arctan \epsilon = \zeta_{i,m}^\pm(r)$. Since the solutions are mapped to themselves, the condition (iii) is automatically satisfied and energies for these solutions must be real. Notice that the symmetry \mathcal{CPT}' differs from the symmetry \mathcal{CPT} we used for the construction of the model.

Apart from ζ_{iBPS} all the solutions are mapped to real solutions via similarity transformation. Therefore, their corresponding energies saturate the lower Bogo-

molny bound. However, we note that ζ_{iBPS} is nonphysical since its corresponding energy is not bounded from below. This is either seen from (3.148) or more generally from (3.137), which implies that for purely imaginary A and \tilde{A} the right-hand side constitutes an upper bound for the energy.

We conclude this section with a brief comment on the values for the Baryon number. The Baryon number is given by

$$B = \int d^3x B_0. \quad (3.150)$$

Where B_0 is the 0th component of the $SU(2)$ valued objects defined in equation (3.119).

$$B_\mu = \frac{1}{24\pi} \epsilon^{\mu\nu\rho\sigma} \text{Tr}(L_\nu L_\rho L_\sigma), \quad L_\mu = U^\dagger \partial_\mu U. \quad (3.151)$$

Using Maurer-Cartan form $U^\dagger \delta U / \delta \phi^a = M_{ab} \sigma^b$ we have

$$L_\mu = U^\dagger \partial_\mu U = \partial_\mu \phi^a U^\dagger \frac{\delta U}{\delta \phi^a} = \partial_\mu \phi^a M_{ab} \sigma^b. \quad (3.152)$$

The explicit form of the matrix M_{ab} found by using the Ansatz given in section 3.4.1

$$B_0 = \frac{12}{N_0} \sin^2(\phi^1) \sin(\phi^2) \epsilon^{ijk} \nabla_i \phi^1 \nabla_j \phi^2 \nabla_k \phi^3, \quad (3.153)$$

where $\{\phi^1, \phi^2, \phi^3\} = \{\zeta, \Theta, \Phi\}$ to match the notation in section 3.4.1. Insert this to the definition of the Baryon number we find

$$B = \frac{12}{N_0} \int d^3x \left[\sin^2(\phi^1) \sin(\phi^2) \left(\epsilon^{ijk} \nabla_i \phi^1 \nabla_j \phi^2 \nabla_k \phi^3 \right) \right] \quad (3.154)$$

Notice that the expression in the square bracket is the volume form so we can perform coordinate transformation to the field space (ϕ^1, ϕ^2, ϕ^3)

$$B = \frac{12}{N_0} \int d\phi^1 d\phi^2 d\phi^3 \left[\sin^2(\phi^1) \sin(\phi^2) \right]. \quad (3.155)$$

For usual Ansatz $\phi^1 = \phi^1(r)$, $\phi^2 = \theta$ and $\phi^3 = n\phi$ we find

$$B = \frac{48n\pi}{N_0} \int_{\phi^1(r_-)}^{\phi^1(r_+)} d\phi^1 \left[\sin^2 \phi^1 \right] = \frac{48n\pi}{N_0} \left[\frac{\phi^1}{2} - \frac{1}{4} \sin(2\phi^1) \right]_{\phi^1=\phi^1(r_-)}^{\phi^1(r_+)}, \quad (3.156)$$

where $\{r_-, r_+\}$ represents the generic end points of the profile compacton solution

$\phi^1 = \zeta$. For the above quantity to equal n , one must choose an appropriate normalisation N_0 and ensure that the endpoints of the compacton solutions do not depend on n . For example, solutions listed in figure 3.12 all have zero for the upper bound of the profile function $\zeta(r_+) = 0$. Except for the shell and cusp solutions, whether the Baryon number is an integer or not depends on their initial values at $r = 0$. The value of the profile function defined in equation (3.141) at $r = 0$ is independent of the integer n for all values of c . Therefore BPS, *i*BPS, and step functions all have integer Baryon numbers.

At first sight, the cusp and shell solutions seem to have zero Baryon numbers because their endpoints are zero. However, if one evaluates the Baryon number numerically by inserting the solution (3.144) in to the definition of the Baryon number (3.150), then the result is non-zero. The reason for this is most easily understood if we observe that the integration in equation (3.156) is a contour integration with the profile function as a path of the contour evolving by increasing $r \in [r_-, r_+]$. To evaluate the contour integration, one needs to specify the direction of the path. Since two solutions that compose cusp and shell solutions are solutions of self-dual and anti-self-dual BPS equations, they are equivalent by transforming $r \rightarrow -r$. This means the flow of the two contours is opposite. Therefore the Baryon number of the cusp and shell solutions should be given by evaluating the integration separately for two contours (or two sections separated by r_π^+ in figure 3.12) with opposite direction and subtract the two results, compensating for the fact that the two contours have opposite flow. Therefore the key quantity to investigate is the value of profile function (3.141) at $r = r_\pi^+$. By inspection, one may notice that the n appearing in r_π^+ cancels with the n in the profile function, meaning the shell and cusp solutions also have non-zero Baryon numbers. By appropriate normalisation N_0 , one can obtain an integer value for the Baryon number.

An interesting question is to determine whether the normalisation constant N_0 is universal among all five solutions. This can be answered without explicitly evaluating the Baryon number. The key values of each solutions which determines whether

the Baryon number is an integer are

$$\begin{aligned}\tilde{\zeta}_{\text{BPS}}(r=0) &= 2 \arccos\left(\frac{c^{1/3}}{\sqrt{2}}\right), \\ \tilde{\zeta}_{\text{St}}(r=0) &= 2 \arccos\left(e^{i2\pi/3} \frac{(-c)^{1/3}}{\sqrt{2}}\right), \\ \tilde{\zeta}_{\text{Cusp}}(r=r_\pi^+) &= \tilde{\zeta}_{\text{Shell}}(r=r_\pi^+) = \pi.\end{aligned}$$

If we want all solutions to have an integer value as a Baryon number, we require all quantities above to coincide. This is only possible when $c = 0$. In which case, the key quantity $r_\pi^\pm(c=0) = 0$, becomes zero and cusp, shell and step solutions all reduce to BPS solution. We can conclude that these distinct four solutions only appear when some of the Skyrmions are fractional, in their Baryon number.

It is worth pointing out that we may reach similar conclusions as in the boosted model discussed in this section for a model with complex rotated fields. With a slight modification of the Dyson map used in equation (2.51), having the effect on the fields is that they transform as $\varphi^a \rightarrow e^{-i\theta_a} \varphi^a$ and $\Pi^a \rightarrow e^{i\theta_a} \Pi^a$, we may construct a new complex models. The model obtained in this manner also possesses complex BPS solutions with real energies.

3.4.3 Skyrme model with semi-kink and massless solutions

While most Skyrme solutions are of compacton type, there exist also interesting variants of the model $\mathcal{L}_0 + \mathcal{L}_6$ with potentials that lead to solutions which are partly of kink type with real energies. We consider here the potential

$$V_{SK}(\zeta) = \sin^2 \zeta (1 + \cos \zeta)^2. \quad (3.157)$$

The corresponding BPS equations

$$\tan\left(\frac{\zeta}{2}\right) \frac{d\zeta}{dr} = \pm \frac{2\mu}{n\lambda} r^2, \quad (3.158)$$

are easily solved to

$$\zeta_s^\pm(r) = 2s \arccos\left(e^{\mp \frac{\mu r^3}{3n\lambda} - c}\right), \quad (3.159)$$

with $s = \pm 1$ and c denoting an integration constant. A similar solutions to $s = 1$ was found in [139]. Evidently we have $\zeta_s^\pm(r_0^\pm) = 0$ for $r_{0,i}^\pm = \omega^i(\mp 3n\lambda c/\mu)^{1/3}$ and asymptotically ζ_s^\pm acquires a finite value $\lim_{r \rightarrow \infty} \zeta_s^\pm(r) = s\pi$ for $\pm\mu/n\lambda > 0$. We depict some sample solutions in figure 3.14 panel (a). For $r < r_0$ we notice the previously observed standard real or purely imaginary compacton solutions, but for $r > r_0$ the solutions ζ_\pm^\pm exhibit the interesting feature of being of compacton type at $r = r_0$ and of kink type when $r \rightarrow \infty$.

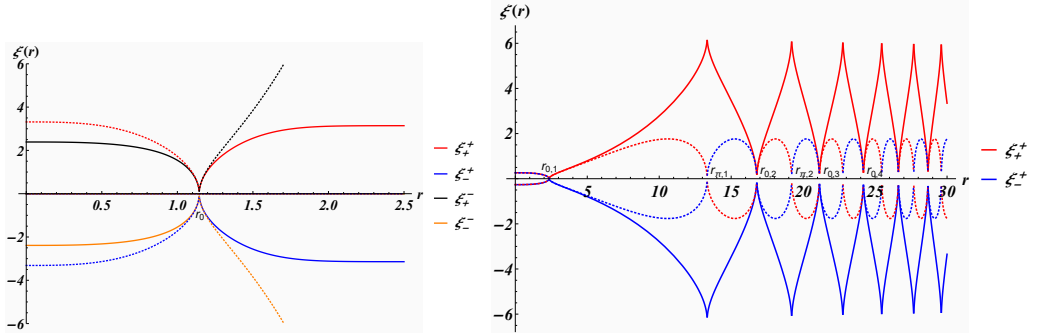


Figure 3.14: Panel (a): Purely imaginary and real compacton and semi-kink solutions (3.159) resulting from the potential $V_{SK}(\zeta)$ with parameter choices $n = \lambda = 1$, $\mu = 2$ and $c = \pm 1$ for $\gamma = \mp 1$. Panel (b): Complex solutions with zero energy resulting from the potential $V_{m0}(\zeta)$ with parameter choices $n = \lambda = 10$, $\mu = 2$ and $c = \pm 25.15$ for $\gamma = \mp 1$. Real parts correspond to solid lines and imaginary parts to dotted ones.

Crucially, it turns out that the energies of these solutions are all real and finite.

From the general expression (3.146) we compute

$$E_{\text{semi-kink}}(\zeta_s^-) = \frac{16n\lambda\mu\pi}{3}, \quad (3.160)$$

$$E_{\text{real compacton}}(\zeta_s^-) = -(4e^{-6c} - 3e^{-8c} - 1) E_{\text{semi-kink}}, \quad (3.161)$$

$$E_{\text{purely imaginary compacton}}(\zeta_s^+) = (4e^{6c} - 3e^{8c} - 1) E_{\text{semi-kink}}, \quad (3.162)$$

for $c > 0$ and $n\lambda\mu > 0$.

Another interesting variant emerges when considering the potential $V_{m0}(\zeta) = -V_{SK}(\zeta)$. In this case the solutions become $\check{\zeta}_s^\pm(r) = 2s \arccos(e^{\mp i \frac{\mu r^3}{3n\lambda} - ic})$, which vanish for $r_{0,i}^\pm = \omega^i(\mp 3n\lambda(c + 2\pi m)/\mu)^{1/3}$ with $m \in \mathbb{Z}$ and $\check{\zeta}_s^\pm(r_{\pi,i}^\pm) = 2\pi s$ for $r_{\pi,i}^\pm = \omega^i[\mp 3n\lambda(c + 2\pi(m + 1/2))/\mu]^{1/3}$. A sample solution is depicted in figure 3.14 panel (b). We observe a re-occurring complex periodic shell solution that becomes squeezed for increasing r . Interestingly the energies for these type of shell solutions

is vanishing

$$8\pi\mu^2 \int_{r_0^+}^{r_0^-} dr [r^2 V_{m0}(\check{\zeta}_s^\pm(r))] = 0. \quad (3.163)$$

Therefore the energy of the shell solution is zero. Let us also analyse the Baryon number in this case. From the previous section, one might suspect that the Baryon number of this solution is non-zero, as was the case for the shell solution in the previous case. However, this solution differs from the previous shell solution at a crucial point. The shell solution from the previous section was composed of two solutions of the self-dual and anti-self-dual BPS equations. The current shell solution is a solution of one of the BPS equation. Therefore the contour of the integration is a closed contour with the consistent flow in the correction direction. Since the integrand of the Baryon number in equation (3.156) is analytic everywhere in the complex plane, the contour integration of the closed path is zero by Cauchy's theorem. We can conclude that the Baryon number for this particular shell solution is zero.

We observe from (3) that the energies of the solutions are ensured to be real by the \mathcal{CPT}_\pm -symmetries: $\zeta(r) \rightarrow \pm\zeta^*(r)$. For the same reasons as in the previous subsection there is no effect on the arguments of the fields. For the complex solution $\check{\zeta}_s^\pm$ this reads $\mathcal{CPT}_\pm: \check{\zeta}_s^\pm(c) \rightarrow [\check{\zeta}_{\pm s}^\pm(c)]^* = \check{\zeta}_{\pm s}^\mp(-c)$. Thus in this case this \mathcal{CPT}_\pm -symmetries map solutions to different solutions. However, invoking condition (3) and noting that the energies for $\check{\zeta}_s^\pm(r)$ are the same for both BPS equations and independent of s, c , they must be real.

3.4.4 Skyrme model with a Bender-Boettcher type potential

We will now investigate further variants of the model $\mathcal{L}_0 + \mathcal{L}_6$ by allowing for a wider range of potentials in \mathcal{L}_0 , including the possibilities of functions of just ζ . This will break the symmetry of the original Lagrangian, but here we are only interested in the solutions to the BPS equations and their energy. Since the anti-linear symmetry guarantees the reality of the energies, we will still expect to find real energies. As a first example we consider the potential

$$V_{BB}(\zeta) = (i\zeta)^\varepsilon \sin^4 \zeta, \quad \varepsilon \in \mathbb{R}. \quad (3.164)$$

This potential closely resembles the classical prototype potential studied in \mathcal{PT} -symmetric quantum mechanics [1], remaining invariant under the \mathcal{CPT} -transformation: $\zeta \rightarrow -\zeta, \iota \rightarrow -\iota$. Using the same parameterization and reasonings as in the previous sections, the BPS equations derived in analogy to (3.140) read

$$\frac{n\lambda \sin^2(\zeta)}{2\mu \sqrt{V_{BB}}} d\zeta = \pm r^2 dr \quad \Rightarrow \quad \frac{d\zeta}{dr} = \pm \frac{2\mu}{n\lambda} (\iota\zeta)^{\varepsilon/2} r^2. \quad (3.165)$$

These equations are easily integrated, acquiring the following Gaussian form

$$\zeta_m^\pm(r) = \left[\left| \frac{n\lambda}{\mu(\varepsilon-2)} \right| \frac{1}{(c+r^3/3)} \right]^{\frac{2}{\varepsilon-2}} e^{\iota\pi(\frac{3s}{2-\varepsilon}-\frac{1}{2})} e^{2\pi\iota\frac{2m}{\varepsilon-2}}, \quad (3.166)$$

where $s = \pm 1, c \in \mathbb{R}, m \in \mathbb{Z}$. In principle the integration constant c could be complex, but we only obtain real energies for $c \in \mathbb{R}$ so we ignore that possibility in what follows. We have defined the constant $s := \text{sign}[\pm n\lambda/\mu(\varepsilon-2)]$ where as above sign denotes the signum function. The last factor accounts for all the branches of ζ , as can either be seen by inserting $1 = e^{2\pi\iota m}$ into the square bracket or by noting that $\zeta \rightarrow \zeta e^{2\pi\iota\frac{2m}{\varepsilon-2}}$ is a symmetry of equation (3.165). The BPS solutions $\zeta_m^\pm(r)$ exhibit two different types of qualitative behaviour. When $c \in \mathbb{R}^-, \varepsilon < 2$ we obtain compacton solutions with finite values at $r = 0$ and $\zeta_m^\pm[(3|c|)^{1/3}] = 0$. For $c \in \mathbb{R}^+, \varepsilon > 2$ the solutions are finite at $r = 0$ and tend to zero only for $r \rightarrow \infty$. We illustrate these types of behaviour in figure 3.15.

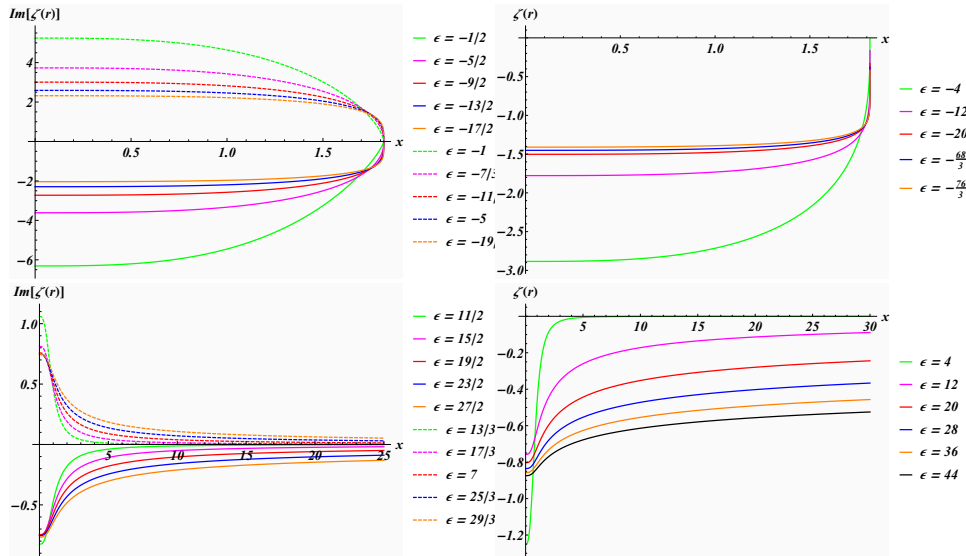


Figure 3.15: BPS solutions $\zeta_m^\pm(r)$ for a Skyrme model with a Bender-Boettcher type potential for the parameter choices $\lambda = 1, \mu = 2, n = 1$. In panels (a), (b) we have taken $c = -2$ and in panels (c), (d) we have $c = 0.2$.

By the same reasoning as in the previous subsections the energies for these solutions are computed to

$$E_{\text{BB}}^{\pm} = 8\pi\mu^2 \int_0^{r_c} dr [r^2 V(\zeta_m^{\pm}(r))], \quad (3.167)$$

where $r_c = (3|c|)^{1/3}$ for the compacton solutions and $r_c \rightarrow \infty$ for the unbounded ones. As is evident from (3.164) these energies can be real when ζ is either purely imaginary or real. Together with (3.166) real energies are found when

$$\zeta \in -i\mathbb{R}^+: \quad \varepsilon = \frac{4m + 4\ell - 3s}{2\ell}, \quad \ell, m \in \mathbb{N}, \quad (3.168)$$

$$\zeta \in i\mathbb{R}^+: \quad \varepsilon = \frac{2 + 4m + 4\ell - 3s}{1 + 2\ell}, \quad m, \varepsilon \in \mathbb{N}, \ell \in \mathbb{N}_0, \quad (3.169)$$

$$\zeta \in \mathbb{R}: \quad \varepsilon = \frac{2(1 + 4m + 2\ell - 3s)}{1 + 2\ell}, \quad \ell, m \in \mathbb{N}_0, \ell, \varepsilon \in 4\mathbb{N}. \quad (3.170)$$

Examples for these solutions are depicted in figure 3.15. In panel (b) of that figure we also displayed a two solution real solutions with $\varepsilon \notin 4\mathbb{N}$. Next we plot the corresponding energies for these cases as functions of ε in figure 3.16.

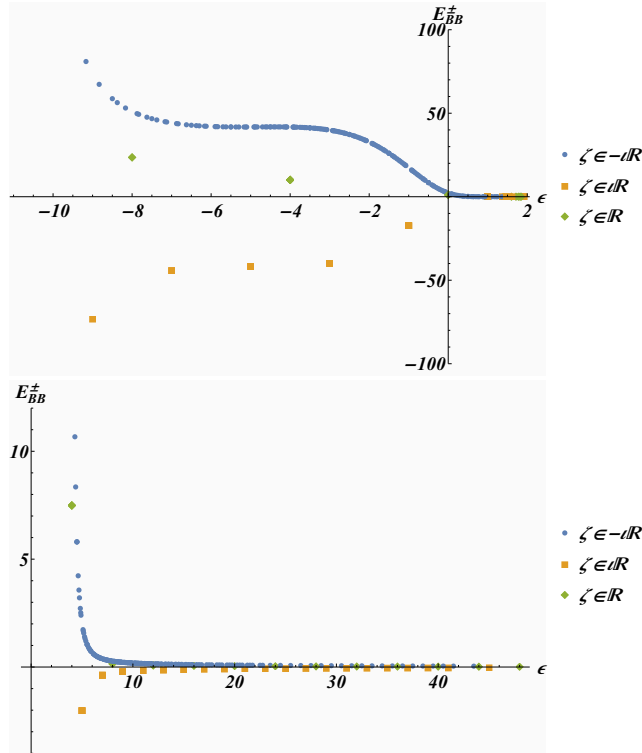


Figure 3.16: Real energies E_{BB}^{\pm} of the compacton (panel a) and unbounded (panel b) BPS solutions for the cases (3.168) - (3.170) with $\lambda = 1$, $\mu = 2$, $n = 1$ and $c = 0.2$ for several values of ℓ, m .

We observe from figure 3.16 that the energies are finite and follow distinct curves

for the different cases. Moreover, for the case $\zeta \in -i\mathbb{R}^+$ the curve is fairly dense and becomes more connected when including more values for ℓ and m , hence ε . In the other cases this can not be achieved due to the additional restriction on ε so that the distribution is more sparse. The transition at $\varepsilon = 2$ is not smooth.

For these models the \mathcal{CPT}' -symmetry identified from (3) must act as $\zeta \rightarrow -\zeta^*$. For our solutions in (3.166) this becomes $\zeta_m^\pm \rightarrow -(\zeta_m^\pm)^* = \zeta_{-m}^\mp$. Noting now that $\varepsilon(m, \ell, s) = \varepsilon(-m, -\ell, -s)$ in (3.168) and $\varepsilon(m, \ell, s) = \varepsilon(-m, -\ell - 1, -s)$ in (3.169), (3.170), we simply have to choose a new $\ell' = -\ell$, $\ell' = -\ell - 1$, respectively, to obtain the same value for ε . This establishes that $E[\zeta_m^\pm] = E[\zeta_{-m}^\mp]$ so that condition (iii) in (3) also holds and the energy must therefore be real. Notice once more that the \mathcal{CPT}' -symmetry that ensures the reality of the energies is different from \mathcal{CPT} , that was observed initially for $V_{BB}(\zeta)$.

3.4.5 Skyrme model with complex trigonometric potentials

Next we study a model for which the Hamiltonian respects again the \mathcal{CPT} -symmetry: $\zeta \rightarrow -\zeta$, $i \rightarrow -i$, but which has solutions transforming under a \mathcal{CPT}' -symmetry to satisfy (1) with conditions (2) and/or (3) violated. Thus we are in the broken \mathcal{CPT}' -regime. For this purpose we consider the variant of the model $\mathcal{L}_0 + \mathcal{L}_6$ involving the trigonometric potential

$$V_T(\zeta) = \sin^4 \zeta \cos^4(\zeta + i\varepsilon), \quad \varepsilon \in \mathbb{R}. \quad (3.171)$$

We notice that unlike as in the pseudo Hermitian model discussed in section 3 only one of the factors in the potential is shifted so that the potential is not simply boosted and most likely not pseudo Hermitian. The BPS equations take the form

$$\frac{n\lambda \sin^2 \zeta}{2\mu \sqrt{V_T}} d\zeta = \pm r^2 dr \quad \Rightarrow \quad \frac{d\zeta}{dr} = \pm 3\alpha \cos^2(\zeta + i\varepsilon)r^2, \quad (3.172)$$

where we abbreviated $\alpha := \frac{2\mu}{3n\lambda}$. Integrating this equation we find the solutions

$$\zeta_{\alpha, \gamma}^\pm(r) = -i\varepsilon \pm \arctan \alpha(r^3 + \gamma). \quad (3.173)$$

with integration constant $\gamma \in \mathbb{C}$. The symmetry identified from condition (i) in (1) acts as \mathcal{CPT}' : $\zeta_{\alpha, \gamma}^\pm \rightarrow -(\zeta_{\alpha, \gamma}^\pm)^* = \zeta_{\alpha, \gamma}^\mp$. Thus the second condition (2) still holds. However, the energies of the two solutions related in this manner are in general

not degenerate, i.e. $E[\zeta_{\alpha,\gamma}^+] \neq E[\zeta_{\alpha,\gamma}^-]$. Depending on the nature of the integration constant γ we find two different types of behaviour and we can still find discrete values for the two \mathcal{CPT}' related solutions that have degenerate energies.

Real integration constants $\gamma \in \mathbb{R}$

Computing the energy $E_{\alpha,\gamma}^{\pm}$ as in the previous sections, the real and imaginary part acquire the form

$$\text{Re } E_{\alpha,\gamma}^{\pm} = \frac{1}{32} \left(\frac{\pi}{\alpha} - \frac{2\gamma}{\alpha^2\gamma^2+1} \right) + \frac{1}{48} \left(\frac{2\gamma(\alpha^2\gamma^2+3)}{(\alpha^2\gamma^2+1)^2} - \frac{\pi}{\alpha} \right) \cosh 2\epsilon \quad (3.174)$$

$$+ \frac{\gamma(\alpha^2\gamma^2-3) \cosh 4\epsilon}{72(\alpha^2\gamma^2+1)^3} + \frac{\gamma(2 \cosh 2\epsilon - 3)}{48\alpha} \arctan \alpha\gamma, \\ \text{Im } E_{\alpha,\gamma}^{\pm} = \mp \frac{\sinh 2\epsilon ([3\alpha^2\gamma^2-1] \cosh(2\epsilon) + 3 + 3\alpha^2\gamma^2)}{36\alpha(\alpha^2\gamma^2+1)^3}. \quad (3.175)$$

This in general the energy is complex and we have $E_{\alpha,\gamma}^+ = (E_{\alpha,\gamma}^-)^*$ and the model is in the broken \mathcal{CPT}' -phase. However, we note that the imaginary part vanishes when parameterizing the integration constant as

$$\gamma_{\ell}(\alpha, \epsilon) = \ell \text{sech } \epsilon \frac{\sqrt{\cosh 2\epsilon - 3}}{\sqrt{6\alpha}}, \quad \ell = \pm. \quad (3.176)$$

In this case we have also satisfied condition (iii) in (3) with $E[\zeta_{\alpha,\gamma}^+] = E[\zeta_{\alpha,\gamma}^-]$ and the \mathcal{CPT}' -symmetry is restored. In order to keep the condition $\gamma \in \mathbb{R}$, we must restrict $|\epsilon| \in [\frac{1}{2} \text{arccosh } 3, \infty)$.

Purely imaginary integration constants $\gamma \in i\mathbb{R}$

Taking now γ to be purely imaginary the \mathcal{CPT}' -symmetry acts as \mathcal{CPT}' : $\zeta_{\alpha,\gamma}^{\pm} \rightarrow -(\zeta_{\alpha,\gamma}^{\pm})^* = \zeta_{\alpha,-\gamma}^{\mp}$. The real and imaginary parts of the energies become now

$$\text{Re } E_{\alpha,\gamma}^{\pm} = \frac{\pi}{32\alpha} \left(1 - \frac{2}{3} \cosh 2\epsilon \right), \quad (3.177)$$

$$\text{Im } E_{\alpha,\gamma}^{\pm} = \pm \frac{\sinh 2\epsilon ([1+3\alpha^2\gamma^2] \cosh 2\epsilon - 3 + 3\alpha^2\gamma^2)}{36\alpha(1-\alpha^2\gamma^2)^3} + \gamma \frac{(2 \cosh 2\epsilon - 3)}{48\alpha} \arctan \alpha\gamma \\ - \frac{\gamma(\alpha^2\gamma^2+3) \cosh 4\epsilon + (1-\alpha^2\gamma^2)(3-\alpha^2\gamma^2) \cosh 2\epsilon}{72(1-\alpha^2\gamma^2)^3}. \quad (3.178)$$

Interestingly the real part becomes very simple and does not depend on the integration constant γ . We may, however, still find values for γ as function of α and ϵ for

which the imaginary part (3.178) vanishes, but not in a closed form as in (3.176). In this case condition (iii) in (3) becomes $E[\zeta_{\alpha,\gamma}^+] = E[\zeta_{\alpha,-\gamma}^-]$ and the \mathcal{CPT}' -symmetry is also restored.

3.4.6 A new Skyrme submodel with complex BPS solutions and real energy

By decomposing the sigma model and the Skyrme term, Adam, Sanchez-Guillen and Wereszczynski noticed in [140] that one may define further consistent and solvable submodels by combining terms from either decomposition as

$$\mathcal{L}_+^{(1)} := \mathcal{L}_2^{(1)} + \mathcal{L}_4^{(1)}, \quad \text{and} \quad \mathcal{L}_+^{(2)} := \mathcal{L}_2^{(2)} + \mathcal{L}_4^{(2)}.$$

Choosing the coupling constant in front of \mathcal{L}_4 to be negative relative to \mathcal{L}_2 , we consider now a slight modification of the second submodel defined by the Lagrangian densities

$$\mathcal{L}_-^{(2)} := \lambda \left(\mathcal{L}_2^{(2)} - \mathcal{L}_4^{(2)} \right), \quad \lambda \in \mathbb{C}. \quad (3.179)$$

The corresponding Hamiltonian density for static solutions may then be written as

$$\mathcal{H}_-^{(2)} = \lambda(\nabla\zeta)^2 - \lambda \sin^4 \zeta \sin^2 \Theta (\nabla\Theta \times \nabla\Phi)^2 = A^2 + \tilde{A}^2, \quad (3.180)$$

where the dual fields are defined as

$$A_i = \sqrt{\lambda}\zeta_i, \quad \text{and} \quad \tilde{A}_i = \iota\sqrt{\lambda}\sin^2 \zeta \sin \Theta \varepsilon_{ijk} \Theta_j \Phi_k. \quad (3.181)$$

Thus, the Hamiltonian density is of the same generic form as for the class of general BPS models discussed in [123]. Hence, following the same reasoning, the imposition of a self-duality and anti-self-duality between A_i and \tilde{A}_i ,

$$A_i = \pm \tilde{A}_i \quad (3.182)$$

selects out the BPS equations [121, 119] as explained above. Thus the energy functional $E_-^{(2)}$ for the solutions of (3.182) therefore acquires the form as in equation (3.137).

We now solve the BPS equations (3.182) and subsequently compute the energies

$E_-^{(2)}$ for the solutions obtained. Multiplying (3.182) by $\Theta_i, \Phi_i, \zeta_i$ and summing over i we obtain the respective equations

$$\zeta_i \Theta_i = 0, \quad \zeta_i \Phi_i = 0, \quad \text{and} \quad \zeta_i \zeta_i = \pm \iota \sin^2 \zeta \sin \Theta \varepsilon_{ijk} \zeta_i \Theta_j \Phi_k. \quad (3.183)$$

The first two constraints are satisfied by a suitable choice of the space-time dependence of Θ, Φ, ζ . Since $\varepsilon_{ijk} \zeta_i \Theta_j \Phi_k$ is simply the Jacobian for the variable transformation $(x, y, z) \rightarrow (\Theta, \Phi, \zeta)$, the multiplication of the last equation by the volume element d^3x in (3.183) leads to

$$(\nabla \zeta)^2 d^3x = \pm \iota \sin^2 \zeta \sin \Theta d\Theta d\Phi d\zeta. \quad (3.184)$$

Similarly as above, we choose spherical space-time coordinates $(x, y, z) \rightarrow (r, \theta, \phi)$ with $r \in [0, \infty), \theta \in [0, \pi), \phi \in [0, 2\pi)$, identify $\Theta = \theta, \Phi = n\phi$ with $n \in \mathbb{Z}$ and assume $\zeta(r) \in \mathbb{C}$. These choices will automatically solve the first two equations in (3.183), whereas the last one reduces to

$$\frac{d\zeta}{dr} = \pm \iota \frac{n}{r^2} \sin^2 \zeta. \quad (3.185)$$

Apart from the ι , this equation coincides with equation (3.6) in [140] derived for $\mathcal{L}_+^{(2)}$ by expressing the unit vector \vec{n} by means of a stereographic projection. We solve equation (3.185) to

$$\zeta_{\pm}^{(m)}(r) = \iota \operatorname{arccoth} \left(c \mp \frac{n}{r} \right) + m\pi, \quad c \in \mathbb{C}, m \in \mathbb{Z}. \quad (3.186)$$

As seen in figure 3.17 the imaginary parts of these solutions tend to zero for $r \rightarrow \infty$, whereas the real parts approach asymptotically the constant value $m\pi + \tilde{c}/2$ when taking $c = \iota \cot(\tilde{c}/2), \tilde{c} \in \mathbb{R} \setminus \{2n\pi\}$ with $n \in \mathbb{Z}$. Moreover $\lim_{r \rightarrow 0} \zeta_{\pm}^{(m)}(r) = m\pi$.

At first sight the solution (3.186) may seem to be unattractive due to its complex nature. However, first of all it is continuous throughout the entire range of r and thus overcomes an issue of the real solutions $\zeta_r^{(m)} = \operatorname{arccot} \left(c - \frac{n}{r} \right) + m\pi$ found for $\mathcal{L}_+^{(2)}$ in [140], which are discontinuous at $r = n/c$. Moreover the energies for these

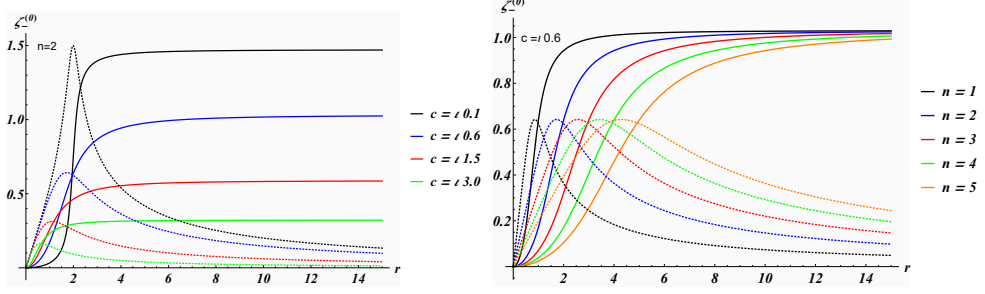


Figure 3.17: Complex BPS solutions $\zeta_-^{(0)}$ for different values of n and the initial condition c for $\mathcal{L}_-^{(2)}$. Real parts as solid and imaginary parts as dotted lines.

solutions are real. We compute

$$\begin{aligned}
E_-^{(2)}(\zeta) &= \pm 2i\lambda \int d^3x [\sin^2 \zeta \sin \Theta \varepsilon_{ijk} \zeta_i \Theta_j \Phi_k] \quad (3.187) \\
&= \pm 2in\lambda \int d\theta d\phi d\zeta [\sin^2 \zeta \sin \theta] \\
&= \pm 8\pi in\lambda \int_0^\infty dr \left[\sin^2 \zeta \frac{d\zeta}{dr} \right] \\
&= \pm 8\pi in\lambda \int_{\zeta(0)}^{\zeta(\infty)} d\zeta [\sin^2 \zeta] = \pm 2\pi in\lambda [2\zeta - \sin(2\zeta)]|_{\zeta(0)}^{\zeta(\infty)}. \quad (3.188)
\end{aligned}$$

Thus taking now the complex coupling constant to be of the form $\lambda = i\tilde{\lambda}$, $\tilde{\lambda} \in \mathbb{R}$, we obtain for solutions $\zeta_\pm^{(m)}$ the real energies

$$E_-^{(2)}(\zeta_\pm^{(m)}) = \pm 2\pi n \tilde{\lambda} [\sin(\tilde{c}) - \tilde{c}]. \quad (3.189)$$

We identify the \mathcal{CPT} -symmetry from (3.180) as $\mathcal{CPT} : \zeta \rightarrow \zeta^*$, which for our solution (3.186) becomes $\zeta_\pm^{(m)}(\tilde{c}) \rightarrow [\zeta_\pm^{(m)}(\tilde{c})]^* = \zeta_\mp^{(-m)}(-\tilde{c})$. Since $E_-^{(2)}[\zeta_\pm^{(m)}(\tilde{c})] = E_-^{(2)}[\zeta_\mp^{(-m)}(-\tilde{c})]$, the energies are guaranteed to be real by the antilinear symmetry \mathcal{CPT} .

3.4.7 Summary

We have begun by reviewing the Hermitian Skyrme model, then extended to the non-Hermitian case with the complex potential term. We have considered four different models with complex potentials presented in sections 3.4.2-3.4.5 and one model presented in section 3.4.6, where the non-Hermiticity comes from the previously unexplored combination of the sub-Lagrangian shown in equation (3.179). In the first model shown in section 3.4.2, we have also developed a new way to construct a solution by pasting two solutions at the point of discontinuity, shown in figure 3.12.

In all models, the \mathcal{CPT} -symmetries were identified. Notably, some of the symmetries were non-trivial such as in equation (3.149), where it is difficult to pre-determine it unless the solution is known. The model considered in section 3.4.5 satisfied the \mathcal{CPT} -symmetry, but the condition (3) presented in section 3.1 was violated, resulting in a complex solution except at specific fixed point in the parameter space. In other words, the physical region is very restrictive (in fact, it is a point).

Chapter 4

Conclusion

Many aspects of non-Hermitian quantum field theories were analysed in this thesis. Concise summaries of the main features were presented at the end of each sections. Here we conclude with a list of some notable results we have obtained. In this thesis, we have

- observed the breakdown of Higgs mechanism at the zero exceptional point.
- confirmed the Higgs mechanism at exceptional points.
- observed the vanishing gauge mass at the zero exceptional point.
- confirmed the existence of complex t'Hooft-Polyakov monopole in non-Hermitian theory with real energy.
- observed the vanishing monopole mass at the zero exceptional point.
- discovered the reality condition for the complex solutions of the equations of motion.
- identified non-trivial CPT -symmetries, responsible for the reality of the energy.
- confirmed the existence of complex BPS Skyrmons in non-Hermitian theory with real energy.
- confirmed the existence of complex BPS Skyrmons in Hermitian theory with real energy.

As discussed in the introduction, the non-Hermitian quantum mechanics in a closed system is well-establish on the basis of many applications in other fields of physics.

However, the non-Hermitian quantum field theory development is still in its infancy, and there are many open questions to be answered.

From chapter 2, we have left questions such as the derivation of the metric operator, which respect the (zero) exceptional point, and the consequence of the ambiguous metric operator to Goldstone and Higgs mechanism. The quantisation is still an open issue to be addressed, and in particular, the connection between the metric operator and the path-integral has not been explored in-depth (except for [76, 141]). Another attractive avenue for further investigations is the Goldstone theorem in 1+1 dimensional non-Hermitian theory. This is because, in the Hermitian theory, the theorem does not apply when the spacial dimension is $d \leq 2$ [142].

In chapter 3, we have explored the soliton solutions in non-Hermitian theory. We have employed the pseudo-Hermitian approach to finding the monopole solution; it would be interesting to find the monopole solution using the alternative method first proposed in [77]. One of the novel features of the non-Hermitian theory is the existence of the exceptional point. Therefore the natural question is to find out if one could find a soliton solution with a more structured exceptional point. This question can have a physical significance. For example, the exceptional point is significant in optics as a point where the gain and loss of the waveguide becomes unbalanced. The Skyrme model considered is also used as an approximate model of the nuclei. It was known to give a good approximation for large Baryon number [143], and recently, the approximation was improved to include the smaller Baryon number [144]. Therefore, calculating the binding energy and consequence of exceptional points in non-Hermitian theory are exciting challenges.

In conclusion, we have demonstrated the potential significance of non-Hermitian extended quantum field theory. A wide range of applications of quantum field theory in many areas of physics means the non-Hermitian extension and its novel features may lead to many discoveries of new phenomena. We are confident that our investigation has contributed to further understanding the non-Hermitian quantum field theory and opened up a new avenue such as non-Hermitian BPS solitons solutions to investigate.

Appendix A

The topology of the monopole solutions and Derrick's scaling argument

A.1 Derrick's scaling argument

We wish to find a time-independent solution to the equations of motion (3.3) with finite energy (i.e. $\int d^3x \mathcal{L} < \infty$). According to G.H. Derrick [145], such solutions do not exist in a non-gauge field theory with spatial dimension larger than 3. To see this, let us consider a multi-component real scalar field Lagrangian

$$\mathcal{L} = \frac{1}{2} \partial_\mu \phi_a G^{ab}(\phi) \partial^\mu \phi_b - V(\phi). \quad (\text{A.1})$$

Given a static solution (i.e. $\partial_0 \phi_{cl} = 0$ and $\delta S[\phi_{cl}] = 0$) with finite energy $E = \int d^D x \mathcal{H} > 0$ where \mathcal{H} is a corresponding Hamiltonian and D is the spatial dimension. The kinetic part and potential part of the Hamiltonian can be written by confining the system in a square box Λ^D

$$I_K^\Lambda[\phi] \equiv \int_0^\Lambda d^D x \left[\frac{1}{2} \partial_i \phi_{cla} G^{ab}(\phi) \partial_i \phi_{clb} \right], \quad I_V^\Lambda[\phi] \equiv \int_0^\Lambda d^D x [V(\phi_{cl})]. \quad (\text{A.2})$$

Where $\int_0^\Lambda d^D x \equiv \int_0^\Lambda dx_1 \int_0^\Lambda dx_2 \cdots \int_0^\Lambda dx_D$. The energy of the classical solution ϕ_{cl} is

$$E^\Lambda[\phi_{cl}] \equiv I_K^\Lambda[\phi_{cl}] + I_V^\Lambda[\phi_{cl}]. \quad (\text{A.3})$$

Let us re-scale the radial spatial length by $\phi(t, \vec{x}) \rightarrow \phi(t, r\vec{x}) \equiv \phi^r(t, \vec{x})$. Then the kinetic and potential term can be written as

$$I_V^\Lambda[\phi^r] = \int_0^\Lambda d^D x [V(\phi^r(x))] = \int_0^{r\Lambda} d^D x \left[\frac{1}{r^D} V(\phi(x)) \right] = \frac{1}{r^D} I_V^\Lambda[\phi], \quad (\text{A.4})$$

$$I_K^\Lambda[\phi^r] = \frac{1}{r^{D-2}} I_K^\Lambda[\phi]. \quad (\text{A.5})$$

Note that in quantum field theory, the space-time volume is assumed to be infinite. Therefore the square box needs to expand to infinity $\Lambda \rightarrow \infty$. The static solution ϕ_{cl} also satisfies the following two conditions

$$\lim_{\Lambda \rightarrow \infty} E^\Lambda[\phi_{cl}] = \text{constant}, \quad \left. \frac{\delta E[\phi]}{\delta \phi} \right|_{\phi=\phi_{cl}} = 0. \quad (\text{A.6})$$

Let us define the energy of the re-scaled solution by $E(r) := \lim_{\Lambda \rightarrow \infty} E^\Lambda[\phi_{cl}^r]$. Then the equation (A.6) implies that $E(1) = \text{constant}$ and $\left. \frac{d}{dr} E(r) \right|_{r=1} = 0$. Combining this with equation (A.5) and (A.4) we find

$$(D-2)I_K[\phi_{cl}] + DI_V[\phi_{cl}] = 0 \quad (\text{A.7})$$

Since we assume $I_K \geq 0, I_V \geq 0$, for each spatial dimensions, we find the relation between the kinetic and potential energies.

$$\begin{aligned} D=0 & \quad 2I_K[\phi_{cl}] = I_V[\phi_{cl}], \\ D=1 & \quad I_K[\phi_{cl}] = I_V[\phi_{cl}], \\ D=2 & \quad I_V[\phi_{cl}] = 0, \\ D \geq 3 & \quad I_K[\phi_{cl}] = I_V[\phi_{cl}] = 0. \end{aligned} \quad (\text{A.8})$$

This concludes Derrick's argument that for spatial dimension larger than 3 (i.e. $D \geq 3$), the only finite energy solution is a constant vacuum solution. This is a problem if one wants to find a finite energy non-trivial solution in the physical space-time where the spatial dimension is 3. Fortunately the above relations (A.8) take on a different form when the theory is modified to accommodate for a gauge symmetry. Let us consider a gauge field theory with local $SO(3)$ symmetry. The corresponding Lagrangian is

$$\mathcal{L} = -\frac{1}{2} \text{Tr}(\mathcal{F}_{\mu\nu} \mathcal{F}^{\mu\nu}) + \frac{1}{2} \text{Tr}(D_\mu \phi D^\mu \phi) - V \quad (\text{A.9})$$

where the trace is over the group index and the covariant derivative is defined as $D_\mu\phi^a := \partial_\mu\phi^a + e\epsilon^{abc}A_\mu^b\phi^c$. For simplicity, let us assume the vanishing of the electric field $\mathcal{E}_i = \mathcal{F}_{0i} = 0$ and denote the kinetic and potential parts of the action as

$$I_F[A] = \int d^D x \frac{1}{2} \text{Tr}(F^2), \quad I_K[\phi, A] = \int d^D x \text{Tr}(D_i\phi D_i\phi), \quad I_V[\phi] = \int d^D x V. \quad (\text{A.10})$$

Letting $\phi_{cl}, A_{cl\mu}$ be classical solutions of our gauged theory. We re-scale once more the length

$$\phi_{cl}(x) \rightarrow \phi_{cl}(rx) \equiv \phi_r, \quad (\text{A.11})$$

$$A_{cl\mu}(x) \rightarrow A_{cl\mu}(rx) \equiv A_{r\mu}. \quad (\text{A.12})$$

If we define the re-scaled energy as $E(\lambda) \equiv E[\phi_r, A_r] = I_F[A_r] + I_K[\phi_r, A_r] + I_V[\phi_r]$ then

$$E(r) = r^{4-D} I_F[A_{cl}] + r^{2-D} I_K[\phi_{cl}, A_{cl}] + r^{-D} I_V[\phi_{cl}]. \quad (\text{A.13})$$

Now recall that $\frac{d}{dr}E(1) = 0$ we have

$$(D-4)I_F[A_{cl}] + (D-2)I_K[\phi_{cl}, A_{cl}] + DI_V[\phi_{cl}] = 0. \quad (\text{A.14})$$

This shows that we could have non-constant solution for $D \geq 3$. Furthermore, by inspecting the vacuum solutions of the theory, one can impose extra constraint on the asymptotic behaviour of the non-trivial solutions. Let us denote the non-trivial solutions, which is inequivalent to the vacuum solution as ϕ_{cl} . By definition, the non-trivial soliton satisfies

$$\delta S|_{\phi_{cl}} = 0. \quad (\text{A.15})$$

Next, let us define a collection of vacuum field configurations \mathcal{M}_0 defined by

$$\mathcal{M}_0 = \{\phi \mid I_V[\phi] = 0, \quad I_K[\phi] = 0\}. \quad (\text{A.16})$$

If the theory is symmetric under global symmetry (i.e. ungauged), then the solutions belongs to \mathcal{M}_0 are called vacuum solutions. On the other hand, for the local symmetric theory (i.e. gauge theory) the solutions are called the *Higgs vacuum*.

Since the non-trivial solution $\phi_{cl}(t, \vec{x})$ gives a finite energy (i.e. $I_V[\phi_{cl}] \leq \infty$). Inserting the non-trivial solution ϕ_{cl} into the equation (A.4) implies that the non-trivial solution must asymptote to the Higgs vacuum solution

$$I_V[\phi_{clr}] = \frac{1}{r^D} I_V[\phi_{cl}] \text{ and } I_V[\phi_{cl}] \leq \infty \quad (\text{A.17})$$

$$\implies \lim_{r \rightarrow \infty} I_V[\phi_{clr}] = 0 \iff \lim_{r \rightarrow \infty} \phi_{cl}(t, r\vec{x}) \in \mathcal{M}_0.$$

We conclude that the non-trivial solution to the equations of motion of a theory with local symmetry have finite energy if and only if it asymptotes to the Higgs vacuum solution in the spatial infinity.

A.2 The topology of the monopole solutions

A.2.1 Deriving equation (3.15)

The main aim of this appendix is to explicitly derive equation (3.14) and (3.15). Let us start with the definition of the homotopy class, adapted from [146]. Consider a map/loop $f : S^1 \rightarrow \mathcal{M}$ from a circle S^1 to a topological space \mathcal{M} . The *homotopy class of f at $x_0 \in \mathcal{M}$* is an equivalence class $[f]$ where two loops are said to be equivalent if they can be continuously deformed into each other. A set of homotopy classes at $x_0 \in \mathcal{M}$ forms a group with group action

$$f \star g(x) = \begin{cases} f(2x) & x \in [0, \frac{1}{2}] \\ g(2x - 1) & x \in [\frac{1}{2}, 1] \end{cases}. \quad (\text{A.18})$$

This group is called the *first homotopy group* or *fundamental group* and denoted as $\pi_1(\mathcal{M}, x_0)$. The *n -th homotopy group* is simply replacing S^1 with S^n and denoted as $\pi_n(\mathcal{M}, x_0)$. Let us consider a simple example $\mathcal{M} = S^1$ where the mapping is now between two circles

$$\alpha : S^1 \rightarrow S^1_{\text{target}},$$

$$\theta \mapsto \alpha(\theta), \quad (\text{A.19})$$

where θ is an angle of your rotation in S^1 and $\alpha(\theta)$ is an angle of rotation in S^1_{target} . Let us consider a specific form of the mapping $\alpha_n(\theta) \equiv n\theta$ where the domain of the mapping is $\theta \in (0, 2\pi]$ and the range is $\alpha(\theta) \in (0, 2n\pi]$. Therefore, the integer n

counts the number of times the function α goes around the circle. This quantity is called the *winding number* and in this example it is defined as

$$n \equiv \frac{1}{2\pi} \int_0^{2\pi} d\alpha = \frac{1}{2\pi} \int_0^{2\pi} d\theta \frac{d\alpha(\theta)}{d\theta}, \quad (\text{A.20})$$

where normalisation 2π is found by $\int_0^{2\pi} d\theta = 2\pi$. Next we see that two mappings α_n and α_m with different integers $n \neq m$ are topologically inequivalent as they can not continuously deformed into each other. One can also check that the group multiplication is satisfied $\alpha_n \star \alpha_m(\theta) = (n + m)\theta$. Therefore, the set of equivalence classes $[\alpha]$ form a group \mathbb{Z} . This means that the first homotopy group is the set of integer numbers $\pi_1(S^1) = \mathbb{Z}$.

We can repeat this for S^2 with loops defined by

$$\begin{aligned} (\alpha, \beta) : S^2 &\rightarrow S^2_{\text{target}} \\ (\theta, \varphi) &\mapsto (\alpha(\theta, \varphi), \beta(\theta, \varphi)) \end{aligned} \quad (\text{A.21})$$

Where explicit form of α and β are chosen to be $\alpha(\theta, \varphi) = \theta$, $\beta(\theta, \varphi) = n\varphi$. Analogous to the equation (A.20), the winding number is given by

$$\begin{aligned} n &= \frac{1}{4\pi} \int d\alpha d\beta \sin(\alpha) = \frac{1}{4\pi} \int d\theta d\phi [\sin(\alpha) \det(J)] \\ &= \frac{1}{4\pi} \int d\theta d\phi \left[\sin(\alpha) \left(\frac{\partial\alpha}{\partial\theta} \frac{\partial\beta}{\partial\phi} - \frac{\partial\alpha}{\partial\phi} \frac{\partial\beta}{\partial\theta} \right) \right], \end{aligned} \quad (\text{A.22})$$

where $d\alpha d\beta \sin(\alpha)$ is a solid angle. Let us define a unit vector on sphere

$$\hat{x}(\alpha, \beta) = (\sin(\alpha) \cos(\beta), \sin(\alpha) \sin(\beta), \cos(\alpha))^T \equiv (x^1, x^2, x^3). \quad (\text{A.23})$$

This can be seen as a smooth mapping from a two sphere to a two sphere

$$\hat{x} : S^2 \rightarrow S^2. \quad (\text{A.24})$$

Using this, we can rewrite our winding number in terms of this unit vector as

$$n = \frac{1}{4\pi} \int d\alpha d\beta \sin(\alpha) = \frac{1}{4\pi} \int dS x^a x^a = \frac{1}{4\pi} \int dS^a x^a, \quad (\text{A.25})$$

where we used the definition of a solid angle $dS x^a \equiv dS^a$ and $dS \equiv d\alpha d\beta \sin(\alpha)$.

Next we recall the Gauss's theorem $\int dS^a f^a = \int d^3x \frac{\partial}{\partial x^a} f^a$. Using this, the above surface integral can be rewritten in terms of the volume integral

$$n = \frac{1}{4\pi} \int dS^a x^a = \frac{1}{4\pi} \int d^3x \frac{\partial}{\partial x^a} x^a = \frac{3}{4\pi} \frac{1}{6} \int d^3x 6 = \frac{1}{8\pi} \int d^3x \epsilon_{abc} \epsilon^{abc}, \quad (\text{A.26})$$

where we have used $\partial x^a / \partial x^a = 3$ and $6 = \epsilon^{abc} \epsilon_{abc}$. Next let us perform a coordinate transformation in the 3 dimensional space. The coordinate transformation is implemented though the following identity

$$\int d^3x \epsilon_{abc} = \int d^3y \left[\epsilon_{ijk} J_a^i J_b^j J_c^k \right], \quad (\text{A.27})$$

where $J_a^i \equiv \frac{\partial x^i}{\partial y^a}$ are Jacobians. Inserting this expression into equation (A.26), we find

$$\begin{aligned} n &= \frac{1}{8\pi} \int d^3x \left[\epsilon_{abc} \epsilon^{abc} \right] = \frac{1}{8\pi} \int d^3y \left[\epsilon^{abc} \epsilon_{ijk} \frac{\partial x^i}{\partial y^a} \frac{\partial x^j}{\partial y^b} \frac{\partial x^k}{\partial y^c} \right] \\ &= \frac{1}{8\pi} \int d^3y \left[\frac{\partial}{\partial y^a} \left(\epsilon^{abc} \epsilon_{ijk} x^i \frac{\partial x^j}{\partial y^b} \frac{\partial x^k}{\partial y^c} \right) \right], \end{aligned} \quad (\text{A.28})$$

where in the last line we used the fact that terms like $\epsilon^{abc} \partial_a \partial_b x^j$ will be zero because of the anti-symmetric tensor ϵ^{abc} . Finally we use the stokes theorem again and find

$$\begin{aligned} n &= \frac{1}{8\pi} \int d^3y \left[\frac{\partial}{\partial y^a} \left(\epsilon^{abc} \epsilon_{ijk} x^i \frac{\partial x^j}{\partial y^b} \frac{\partial x^k}{\partial y^c} \right) \right] = \frac{1}{8\pi} \int dS^a \left[\epsilon^{abc} \epsilon_{ijk} x^i \frac{\partial x^j}{\partial y^b} \frac{\partial x^k}{\partial y^c} \right] \\ &= \frac{1}{8\pi} \int dS_a \epsilon^{abc} x \cdot (\partial_b x \times \partial_c x) \end{aligned} \quad (\text{A.29})$$

Where $\partial_a \equiv \frac{\partial}{\partial y^a}$. One may notice that this is equivalent to the third term in equation (3.14) if one identifies x with the radial unit vector \hat{r} defined in equation (3.6). This implies that the equation (3.15) follows immediately from the above equation (A.29). In order to complete the argument in section 3.2.1, we are left with the derivation of equation (3.14) from (3.13).

A.2.2 Deriving equation (3.14) from (3.13)

Let us begin with the general Ansatz (3.5) given in section 3.2.1.

$$\sum_{a=1}^3 (\phi^a(t, \vec{x}))^2 = v^2 \quad \text{and} \quad (D_\mu \phi_0)^a = \partial_\mu \phi_0^a - e \epsilon^{abc} \mathcal{A}_\mu^b \phi_0^c = 0, \quad (\text{A.30})$$

where $v^2 = \mu/\lambda$ to coincide with the result in section 3.2.1. However, we will keep the quantities generic in this section. Therefore, the the general solution \mathcal{A}_μ^a is taken to be

$$\mathcal{A}_{0\mu}^a = \frac{1}{v^2 e} \epsilon^{abc} \phi_0^b \partial_\mu \phi_0^c + \frac{1}{v} \phi_0^a A_\mu \equiv \frac{1}{e} \epsilon^{abc} \hat{\phi}_0^b \partial_\mu \hat{\phi}_0^c + \hat{\phi}_0^a A_\mu. \quad (\text{A.31})$$

Where A_μ is some space-time vector field and $\hat{\phi}_0^a \equiv \frac{1}{v} \phi_0^a$. To verify equation (3.14), let us insert the equation (A.31) in to the field strength tensor

$$\mathcal{F}_{\mu\nu}^a = 2\partial_{[\mu} \mathcal{A}_{\nu]}^a - e \epsilon^{abc} \mathcal{A}_\mu^b \mathcal{A}_\nu^c. \quad (\text{A.32})$$

Where the square bracket in the subscript is an anti-symmetrizer $f_{[\mu} g_{\nu]} \equiv \frac{1}{2}(f_\mu g_\nu - f_\nu g_\mu)$. For simplicity let us write $\hat{\phi}_0^a = \hat{\phi}^a$ and $\mathcal{A}_0 = \mathcal{A}$. To begin with, we focus on the first term of equation (A.32).

$$\begin{aligned} \partial_{[\mu} \mathcal{A}_{\nu]}^a &= \partial_{[\mu} \left(\frac{1}{e} \epsilon^{abc} \hat{\phi}^b \partial_{\nu]} \hat{\phi}^c + \hat{\phi}^a A_{\nu]} \right) \\ &= \frac{1}{e} \epsilon^{abc} \left(\partial_\mu \hat{\phi}^b \partial_\nu \hat{\phi}^c + \hat{\phi}^b \partial_{[\mu} \partial_{\nu]} \hat{\phi}^c \right) + A_{[\nu} \partial_{\mu]} \hat{\phi}^a + \hat{\phi}^a \partial_{[\mu} A_{\nu]} \\ &= A_{[\nu} \partial_{\mu]} \hat{\phi}^a + \hat{\phi}^a \partial_{[\mu} A_{\nu]} + \frac{1}{e} \epsilon^{abc} \partial_\mu \hat{\phi}^b \partial_\nu \hat{\phi}^c. \end{aligned} \quad (\text{A.33})$$

In the second line, we used the commutativity of the derivatives $\partial_{[\mu} \partial_{\nu]} = 0$. The second term of equation (A.32) is

$$\begin{aligned} \epsilon^{abc} \mathcal{A}_\mu^b \mathcal{A}_\nu^c &= \epsilon^{abc} \left(\frac{1}{e} \epsilon^{bde} \hat{\phi}^d \partial_\mu \hat{\phi}^e + \hat{\phi}^b A_\mu \right) \left(\frac{1}{e} \epsilon^{cfg} \hat{\phi}^f \partial_\nu \hat{\phi}^g + \hat{\phi}^c A_\nu \right) \\ &= \left(\frac{2}{e} \phi^{[c} \partial_\mu \phi^{a]} + \epsilon^{abc} \hat{\phi}^b A_\mu \right) \left(\frac{1}{e} \epsilon^{cfg} \hat{\phi}^f \partial_\nu \hat{\phi}^g + \hat{\phi}^c A_\nu \right), \end{aligned} \quad (\text{A.34})$$

where we have used $\epsilon^{abc} \epsilon^{aed} = (\delta^{be} \delta^{cd} - \delta^{bd} \delta^{ce})$. Expanding the above bracket, we can rewrite equation (A.34) in terms of A_μ and ϕ

$$\begin{aligned} \epsilon^{abc} \mathcal{A}_\mu^b \mathcal{A}_\nu^c &= \frac{2}{e^2} \epsilon^{cfg} \phi^{[c} \partial_\mu \phi^{a]} \hat{\phi}^f \partial_\nu \hat{\phi}^g + \frac{2}{e} \phi^{[c} \partial_\mu \phi^{a]} \hat{\phi}^c A_\nu \\ &\quad + \frac{1}{e} \epsilon^{abc} \epsilon^{fgc} \hat{\phi}^b A_\mu \hat{\phi}^f \partial_\nu \hat{\phi}^g + \epsilon^{abc} \hat{\phi}^b A_\mu \hat{\phi}^c A_\nu \\ &= -\frac{1}{e^2} \epsilon^{cfg} \phi^a \partial_\mu \phi^c \hat{\phi}^f \partial_\nu \hat{\phi}^g + \frac{2}{e} \phi^{[c} \partial_\mu \phi^{a]} \hat{\phi}^c A_\nu + \frac{2}{e} \hat{\phi}^b A_\mu \hat{\phi}^{[a} \partial_\nu \hat{\phi}^{b]} \\ &= -\frac{1}{e^2} \epsilon^{cfg} \phi^a \partial_\mu \phi^c \hat{\phi}^f \partial_\nu \hat{\phi}^g + \frac{1}{e} \phi^c \partial_\mu \phi^a \hat{\phi}^c A_\nu - \frac{1}{e} \hat{\phi}^b A_\mu \hat{\phi}^b \partial_\nu \hat{\phi}^a \end{aligned} \quad (\text{A.35})$$

$$\begin{aligned}
&= -\frac{1}{e^2}\epsilon^{cfg}\phi^a\partial_\mu\phi^c\hat{\phi}^f\partial_\nu\hat{\phi}^g + \frac{1}{e}\partial_\mu\phi^a A_\nu - \frac{1}{e}A_\mu\partial_\nu\hat{\phi}^a \\
&= \frac{2}{e}A_{[\nu}\partial_{\mu]}\phi^a - \frac{1}{e^2}\phi^a\left(\epsilon^{bcd}\phi^c\partial_\mu\phi^b\partial_\nu\phi^d\right),
\end{aligned}$$

where several identities $\epsilon^{abc}\hat{\phi}^b\hat{\phi}^c = 0$, $\epsilon^{abc}\epsilon^{aed} = (\delta^{be}\delta^{cd} - \delta^{bd}\delta^{ce})$, $\hat{\phi}^a\hat{\phi}^a = 1$ and $0 = \frac{1}{2}\partial(\hat{\phi}^a\hat{\phi}^a) = \hat{\phi}^a\partial\hat{\phi}^a$ are used to simplify the expression. The second term of the last line can be simplified further by noticing that for any tensor V , we have $V^{[abcd]} = 0$ because the group index only takes values between 1 and 3. Utilising this property, we have

$$\begin{aligned}
0 &= \phi^{[a}\epsilon^{bcd]}\phi^c\partial_\mu\phi^b\partial_\nu\phi^d = \left(\phi^a\epsilon^{bcd} + \phi^d\epsilon^{abc} + \phi^c\epsilon^{dab} + \phi^b\epsilon^{cda}\right)\phi^c\partial_\mu\phi^b\partial_\nu\phi^d \quad (\text{A.36}) \\
&= \phi^a\epsilon^{bcd}\phi^c\partial_\mu\phi^b\partial_\nu\phi^d + \epsilon^{dab}\partial_\mu\phi^b\partial_\nu\phi^d \\
\implies \phi^a\left(\epsilon^{bcd}\phi^c\partial_\mu\phi^b\partial_\nu\phi^d\right) &= -\epsilon^{abc}\partial_\mu\phi^b\partial_\nu\phi^c,
\end{aligned}$$

where in the second line we used $0 = \frac{1}{2}\partial(\hat{\phi}^a\hat{\phi}^a) = \hat{\phi}^a\partial\hat{\phi}^a$. Finally the field strength tensor can be rewritten in terms of A_μ and ϕ as

$$\begin{aligned}
\mathcal{F}_{\mu\nu}^a &= 2\left(A_{[\nu}\partial_{\mu]}\hat{\phi}^a + \hat{\phi}^a\partial_{[\mu}A_{\nu]} + \frac{1}{e}\epsilon^{abc}\partial_\mu\hat{\phi}^b\partial_\nu\hat{\phi}^c\right) - e\left(\frac{2}{e}A_{[\nu}\partial_{\mu]}\phi^a + \frac{1}{e^2}\epsilon^{abc}\partial_\mu\phi^b\partial_\nu\phi^c\right) \\
&= \phi^a(2\partial_{[\mu}A_{\nu]}) + \frac{1}{e}\epsilon^{abc}\partial_\mu\phi^b\partial_\nu\phi^c \\
&= \hat{\phi}^a\left(2\partial_{[\mu}A_{\nu]} - \frac{1}{e}\left(\epsilon^{bcd}\phi^c\partial_\mu\phi^b\partial_\nu\phi^d\right)\right) \\
&= \hat{\phi}^a\left(2\partial_{[\mu}A_{\nu]} - \frac{1}{e}\hat{\phi}\cdot\left(\partial_\mu\hat{\phi}\times\partial_\nu\hat{\phi}\right)\right), \quad (\text{A.37})
\end{aligned}$$

Notice that the quantity appearing in the bracket, which we denote by $F_{\mu\nu}$, is equivalent to the $U(1)$ field strength tensor. Now we find the important result

$$\mathcal{F}_{\mu\nu}^a|_{\mathcal{A}=\mathcal{A}_0} \equiv \mathcal{F}_{0\mu\nu}^a = \hat{\phi}_0^a F_{\mu\nu}. \quad (\text{A.38})$$

Recall from section A.1 that the finite energy solution will approach Higgs vacuum ϕ_0^a . So the field strength tensor of finite energy solution will approach electromagnetic field strength tensor (i.e $U(1)$ strength tensor). By using the definition of the magnetic field, we find

$$B_i = -\frac{1}{2}\epsilon_{ijk}F^{jk} = -\frac{1}{2}\epsilon_{ijk}\left(2\partial^{[j}A^{k]} - \frac{1}{e}\hat{\phi}\cdot\left(\partial^j\hat{\phi}\times\partial^k\hat{\phi}\right)\right). \quad (\text{A.39})$$

This is precisely what we claimed in equation (3.14).

Finally let us comment on the physical implication of the winding number. From electromagnetism, the magnetic charge is given by

$$g \equiv \int d\vec{S} \cdot \vec{B} \quad (\text{A.40})$$

Inserting the magnetic field (A.39) into the definition of the magnetic charge, we find

$$g = - \int dS^i \epsilon_{ijk} 2\partial^{[j} A^{k]} + \frac{2}{e} \int dS^i \epsilon_{ijk} \hat{\phi} \cdot \left(\partial^j \hat{\phi} \times \partial^k \hat{\phi} \right) \quad (\text{A.41})$$

$$= \frac{2}{e} \int dS^i \epsilon_{ijk} \hat{\phi}_{Higg} \cdot \left(\partial^j \hat{\phi}_{Higg} \times \partial^k \hat{\phi}_{Higg} \right) \quad (\text{A.42})$$

where first term in the first line vanishes due to Stokes' theorem. Now recall that we found a similar mapping $\hat{x} : S^2 \rightarrow S^2$ equation (A.24) which can be categorised by integers given by the winding number equation (A.29). If we redo the calculation of section A.2 but with $\hat{\phi}_{Higg}$ instead of \hat{x} , we find the integer

$$n = \frac{1}{8\pi} \int dS_i \epsilon^{ijk} \hat{\phi}_{Higg} \cdot (\partial_j \hat{\phi}_{Higg} \times \partial_k \hat{\phi}_{Higg}) = \frac{1}{8\pi} \left(\frac{eg}{2} \right). \quad (\text{A.43})$$

So the magnetic charge of $\hat{\phi}_{Higg}^n$ is

$$g = \frac{16\pi n}{e}. \quad (\text{A.44})$$

Appendix B

Type I (standard) versus type II (zero) exceptional points

This appendix presents a discussion illustrating the two types of exceptional points for a finite-dimensional matrix with one free parameter. Many types of exceptional points exist, often referred to as a higher-order exceptional point or *EPN* where the integer N indicates the number of coalescing eigenvalues. However, we will focus on two types: the type I (standard) exceptional point and the type II (zero) exceptional point. The main distinction is their behaviour beyond the exceptional point where the coalesced eigenvalues become real for type II and complex for type I. The zero exceptional points occur when two eigenvalues coalesce at zero, hence the name.

As an example, we consider here a (3×3) -matrix of a very generic form that occurs for instance as a building block of the squared mass matrix in the model discussed in section 2.3, see equation (2.75) therein,

$$H = \begin{pmatrix} A & W & 0 \\ -W & B & -V \\ 0 & V & -C \end{pmatrix}. \quad (\text{B.1})$$

Here we carry out the discussion for a Hamiltonian H , having in mind the analogy to the squared mass matrix. The determinant is easily computed to $\det H = A\kappa - CW^2$, $\kappa := V^2 - BC$. In order to obtain a zero eigenvalue, $\lambda_0 = 0$, we enforce now the determinant to vanish by setting $A = W^2C/\kappa$. The other two eigenvalues then

become

$$\begin{aligned}\lambda_{\pm} &= \frac{\kappa(B-C) + CW^2 \pm \tau}{2\kappa}, \\ \tau &= \sqrt{\kappa^2((B+C)^2 - 4V^2) + 2\kappa W^2(C(B+C) - 2V^2) + C^2W^4}.\end{aligned}\tag{B.2}$$

According to [36], the exceptional points are identified by simultaneously solving the two equations

$$\det(H - \lambda\mathbb{I}) = 0, \quad \text{and} \quad \frac{d}{d\lambda} \det(H - \lambda\mathbb{I}) = 0,\tag{B.3}$$

for W and λ , obtaining the two sets of eigenvalues

$$\left\{ \lambda_{\pm}^e = \frac{\hat{\kappa}^2 - \sqrt{\kappa}V}{C}, \lambda_0 = 0 \right\} \text{ and } \left\{ \lambda_{-}^0 = \lambda_0 = 0, \lambda_{+}^0 = \frac{C^3 + BV^2 - 2CV^2}{\hat{\kappa}^2} \right\}\tag{B.4}$$

for the critical parameters

$$W^e = \frac{\tilde{\kappa}}{C}, \quad \text{and} \quad W^0 = i\frac{\kappa}{\hat{\kappa}},\tag{B.5}$$

respectively. We abbreviated $\tilde{\kappa} := \pm\sqrt{\kappa(\kappa + V^2 - C^2) \pm 2\kappa^{3/2}V}$ and $\hat{\kappa} := \sqrt{V^2 - C^2}$. The first set of eigenvalues in (B.4) correspond to the standard exceptional point and the second set to the zero exceptional point.

Next we calculate the bi-orthonormal basis from the normalised left and right eigenvectors $u_i, v_i, i = 0, \pm$, respectively, for H

$$\begin{aligned}v_0 &= \frac{1}{\sqrt{N_0}}(-\kappa, CW, VW), \\ v_{\pm} &= \frac{1}{\sqrt{N_{\pm}}}(W(\hat{\kappa}^2 - C\lambda_{\pm}), \kappa(C + \lambda_{\pm}), V\kappa), \quad u_i = Uv_i.\end{aligned}\tag{B.6}$$

with $U = \text{diag}(1, -1, 1)$ and normalisation constants $N_0 = \kappa^2 + W^2\hat{\kappa}^2$, $N_{\pm} = V^2\kappa^2 + W^2[V^2 - C(C + \lambda_{\pm})]^2 - (C + \lambda_{\pm})^2\kappa^2$. By construction these vectors satisfy the orthonormality relation $u_i \cdot v_j = \delta_{ij}$.

We observe now that at the standard exceptional point the two eigenvectors for the non-normalised (N_{\pm} become zero at the exceptional points) eigenvalues λ_{\pm}^e coalesce, which distinguishes exceptional points from standard degeneracy. The left

and right eigenvectors become in this case

$$v_{\pm}^{e,r} = (\tilde{\kappa}, V\sqrt{\kappa} - \kappa, C\sqrt{\kappa}), \quad v_0^{e,r} = (-C\kappa, C\tilde{\kappa}, V\tilde{\kappa}), \quad (\text{B.7})$$

$$v_{\pm}^{e,l} = (\tilde{\kappa}, \kappa - V\sqrt{\kappa}, C\sqrt{\kappa}), \quad v_0^{e,l} = (-C\kappa, -C\tilde{\kappa}, V\tilde{\kappa}), \quad (\text{B.8})$$

with

$$v_{\pm}^{e,l} \cdot v_{\pm}^{e,r} = 0, \quad \text{and} \quad v_0^{e,l} \cdot v_0^{e,r} = C^2 (\kappa^2 - \tilde{\kappa}^2) + V^2 \tilde{\kappa}^2. \quad (\text{B.9})$$

Similarly, at the zero exceptional point the eigenvectors for the eigenvalues λ_0 and λ_-^0 coalesce, which qualifies this point also to be called “exceptional” in the standard terminology. In this case the left and right eigenvectors become

$$v_+^{0,r} = (V\kappa, iV\hat{\kappa}(C - B), i\hat{\kappa}^3), \quad v_-^{0,r} = v_+^{0,r} = (i\hat{\kappa}, C, V), \quad (\text{B.10})$$

$$v_+^{0,l} = (V\kappa, iV\hat{\kappa}(B - C), i\hat{\kappa}^3), \quad v_-^{0,l} = v_+^{0,l} = (i\hat{\kappa}, -C, V), \quad (\text{B.11})$$

with

$$v_+^{e,l} \cdot v_+^{e,r} = (C^3 + BV^2 - 2CV^2)^2, \quad \text{and} \quad v_+^{0,l} \cdot v_+^{0,r} = 0. \quad (\text{B.12})$$

In order to understand the key difference between these two types of exceptional points we consider at first the eigenvalues (B.2) near the critical values in (B.5). Concerning the standard exceptional points we note that the two eigenvalues become identical when $\tau \rightarrow 0$. Thus writing $\tau/C^2 = [W^2 - (W^e)^2](W^2 - \tilde{W})$, with \tilde{W} being the second root of the polynomial in W^2 under the square root, it is now clear that if we consider the eigenvalues as functions of W^2 the argument of the square root has different signs for $W^2 = (W^e)^2 + \epsilon$ and $W^2 = (W^e)^2 - \epsilon$. Hence the eigenvalues are real on one side of the exceptional point in the W^2 -parameter space and complex on the other. In contrast none of the eigenvalues becomes complex in the neighbourhood of the critical value W^0 .

For completion we also report the Dyson map and hence the metric operator for which the same behaviour may be observed. Using the operator that diagonalises the non-Hermitian Hamiltonian H

$$\eta = (v_0, v_+, v_-), \quad \rho = \eta\eta^\dagger, \quad (\text{B.13})$$

with determinant

$$\det \eta = \frac{V\kappa}{\sqrt{N_0 N_+ N_-}} (\lambda_- - \lambda_+) (\kappa^2 + W^2 \hat{\kappa}^2), \quad (\text{B.14})$$

we verify the pseudo and quasi Hermiticity relations

$$\eta^{-1} H \eta = h = h^\dagger, \quad \rho H = H^\dagger \rho. \quad (\text{B.15})$$

We observe that the map breaks down at both exceptional points, i.e. $\det \eta = 0$ for the critical values W^e and W^0 , and on one side of the standard exceptional point. In all other regions of the parameter space it holds. Thus we find the same behaviour as already observed for the analysis of the eigenvalues.

Appendix C

General interaction term

In the Lagrangian density functional considered in section 2.3, we chose a particularly simple interaction term and carried out our analysis for an even simpler version. In this section, we explore the possibilities of allowing for more general interaction terms so that the action still respects the discrete \mathcal{CPT} -symmetries (2.35) and the continuous global $U(1)$ -symmetry (2.36), while keeping the kinetic and mass term as previously. We present here explicitly the case for \mathcal{I}_3 , after which it becomes evident how to generalise to all \mathcal{I}_n . We carry out our analysis for the equivalent action $\hat{\mathcal{I}}_3$ defined in equation (2.62) but with arbitrary interaction term. The specific form of such action is

$$\hat{\mathcal{I}}_3[\Phi] = \frac{1}{2} \int d^4x \left[\partial_\mu \Phi^T I \partial^\mu \Phi - \Phi^T H \Phi - \frac{g}{8} (\Phi^T E \Phi)^2 - \frac{g}{8} (\Phi^T F \Phi)^2 \right], \quad (\text{C.1})$$

which is invariant under the $\widehat{\mathcal{CPT}}$ transformation defined in equation (2.54) and $U(1)$ transformation. The field vector is given by $\Phi := (\varphi_1, \chi_2, \varphi_3, \chi_1, \varphi_2, \chi_3)^T$. Each matrices in equation (C.1) are defined as

$$H = \begin{pmatrix} -c_1 m_1^2 & c_\mu \mu^2 & 0 & 0 & 0 & 0 \\ c_\mu \mu^2 & c_2 m_2^2 & c_\nu \nu^2 & 0 & 0 & 0 \\ 0 & c_\nu \nu^2 & -c_3 m_3^2 & 0 & 0 & 0 \\ 0 & 0 & 0 & -c_1 m_1^2 & -c_\mu \mu^2 & 0 \\ 0 & 0 & 0 & -c_\mu \mu^2 & c_2 m_2^2 & -c_\nu \nu^2 \\ 0 & 0 & 0 & 0 & -c_\nu \nu^2 & -c_3 m_3^2 \end{pmatrix}, \quad (\text{C.2})$$

$$E = \begin{pmatrix} A & 0 \\ 0 & \Omega A \Omega \end{pmatrix}, F = \begin{pmatrix} 0 & B \\ \Omega B \Omega & 0 \end{pmatrix}.$$

Here A and B can be arbitrary 3×3 -matrices and $\text{diag } \Omega = (-1, 1, -1)$.

We briefly show how the form of this action is obtained. The respective symmetries (2.54) and (2.36) are realised as follows

$$\widehat{\mathcal{CP}\mathcal{T}}_{1,2} : \hat{\mathcal{I}}_3[\Phi] = \hat{\mathcal{I}}_3[C_{1,2}\Phi] \quad (\text{C.3})$$

$$U(1) : \hat{\mathcal{I}}_3[\Phi] = \hat{\mathcal{I}}_3[U\Phi] \quad (\text{C.4})$$

with

$$C_{1,2} = \pm \begin{pmatrix} \mathbb{I}_3 & 0 \\ 0 & -\mathbb{I}_3 \end{pmatrix}, \quad U = \mathbb{I}_6 + \alpha\hat{\Omega} = \mathbb{I}_6 + \alpha \begin{pmatrix} 0 & \Omega \\ -\Omega & 0 \end{pmatrix}, \quad (\text{C.5})$$

when α is taken to be small. Next we compute how these symmetries are implemented when taking the interaction term to be of the general form

$$\frac{g}{16} (\Phi^T \hat{E} \Phi)^2, \quad \hat{E} = \begin{pmatrix} A & B \\ C & D \end{pmatrix}, \quad (\text{C.6})$$

with as yet unknown 3×3 -matrices A , B , C and D . The transformed Noether current (2.38) resulting from the $U(1)$ -symmetry (C.5)

$$j_\mu = \frac{\alpha}{2} (\partial_\mu \Phi^T \hat{\Omega} \Phi - \Phi^T \hat{\Omega} \partial_\mu \Phi) \quad (\text{C.7})$$

is vanishing upon using the equation of motion for the action $\hat{\mathcal{I}}_3[\Phi]$ with interaction term (3.165)

$$-\square\Phi - H\Phi - \frac{g}{4} (\Phi^T \hat{E} \Phi) \hat{E} \Phi = 0, \quad (\text{C.8})$$

if

$$\partial_\mu j^\mu = \frac{\alpha}{2} (\square\Phi^T \hat{\Omega} \Phi - \Phi^T \hat{\Omega} \square\Phi) = \frac{\alpha}{2} \Phi^T \left([\hat{\Omega}, H] - \frac{g}{4} \Phi^T \hat{E} \Phi [\hat{\Omega}, \hat{E}] \right) \Phi = 0. \quad (\text{C.9})$$

Combining the constraints for the $\widehat{\mathcal{CP}\mathcal{T}}$ and $U(1)$ -symmetry we require therefore

$$[\hat{\Omega}, H] = 0, \quad [\hat{\Omega}, \hat{E}] = 0, \quad [C_{1,2}, H] = 0, \quad [C_{1,2}, \hat{E}] = 0, \quad (\text{C.10})$$

or

$$\left[\hat{\Omega}, H\right] = 0, \quad \left[\hat{\Omega}, \hat{E}\right] = 0, \quad [C_{1,2}, H] = 0, \quad \left\{C_{1,2}, \hat{E}\right\} = 0, \quad (\text{C.11})$$

with $\{\cdot, \cdot\}$ denoting the anti-commutator. The solutions to (C.10) for $\widehat{\mathcal{CPT}}_1$ and $\widehat{\mathcal{CPT}}_2$ are E and F , respectively, whereas the solutions to (C.11) for $\widehat{\mathcal{CPT}}_1$ and $\widehat{\mathcal{CPT}}_2$ are F and E , respectively. This means the action (C.1) contains the most general $\widehat{\mathcal{CPT}}_{1,2}$ and $U(1)$ invariant interaction terms of the form (3.165). There is no distinction between a $\widehat{\mathcal{CPT}}_1$ or $\widehat{\mathcal{CPT}}_2$ -invariant action as the solutions of (C.10) and (C.11) always combine to allow for both $\widehat{\mathcal{CPT}}$ -symmetries to be implemented.

We carried out our analysis for the Goldstone boson for $\text{diag } A = (1, 0, 0)$ and $B = 0$, but from the above it is now evident how this structure of more complicated interaction terms generalises to $\hat{\mathcal{I}}_n$, and therefore \mathcal{I}_n , for $n > 3$. Similar computations can also be carried out for the symmetries $\mathcal{CPT}_{3/4}$ and $\mathcal{CP}'\mathcal{T}$, where \mathcal{P}' is any of the six remaining operators constructed in section 2.3.3. We note here that while it is a uniquely well defined process to identify the $\widehat{\mathcal{CPT}}$ -symmetries when given the \mathcal{CPT} -symmetries, that is going from \mathcal{I}_n to $\hat{\mathcal{I}}_n$, care needs to be taken in the inverse procedure.

Appendix D

Similarity transformation of gauge field theories

In section 2.4 and (2.5), we were required to perform the similarity transformation of the Lagrangian density of the general form

$$\mathcal{L} = \frac{1}{2}(D_\mu\phi)^2 - V(\phi) - \frac{1}{4}F_{\mu\nu}F^{\mu\nu}. \quad (\text{D.1})$$

Where the covariant derivative took the forms $D_\mu\phi = \partial_\mu - ieA_\mu\phi$ for the fundamental representation and $D_\mu\phi^a = \partial_\mu\phi^a + e\epsilon^{abc}A_\mu^b\phi^c$ for adjoint representation. In order to perform the transformation, one needs to Legendre transform the above Lagrangian, which is generally difficult for gauge theories as one needs to employ sophisticated quantisation procedures such as BRST quantisation. However, we will see that our particular similarity transformation will not affect the quantisation procedure.

Let us begin with the fundamental representation. The BRST Lagrangian of (2.160) is

$$\mathcal{L}_{\text{BRST}} = \mathcal{L}[\phi] + F[A_\mu]B - \partial_\mu\bar{c}\partial^\mu c \equiv |D_\mu\phi|^2 - V(\phi) + U(A_\mu, B, \partial_\mu c, \partial_\mu\bar{c}), \quad (\text{D.2})$$

where the gauge fixing is implemented through the equation $F[A_\mu] = 0$ and one auxiliary scalar field B and two auxiliary fermionic ghost fields c, \bar{c} are introduced to compensate for the extra degree of freedom due to the gauge freedom. For example, the Lorentz gauge is $F[A_\mu] = \partial_\mu A^\mu$. The potential $V(\phi)$ is the same non-Hermitian potential considered in equation (2.160) and (2.195). The auxiliary term U contains all the terms involving the auxiliary fields. By performing a Legendre transformation

and imposing equal-time commutation relations, one obtains the quantised field-theoretic Hamiltonian. For example, in the Lorentz gauge case $\partial_\mu A^\mu$, the equal-time commutation relations are

$$\begin{aligned} [\phi(t, \vec{x}), \Pi_\phi(t, \vec{y})] &= i\delta(\vec{x} - \vec{y}), \quad [A_i(t, \vec{x}), \Pi_{A_j}(t, \vec{y})] = i\delta_{ij}\delta(\vec{x} - \vec{y}) \quad (\text{D.3}) \\ [B(t, \vec{x}), \Pi_B(t, \vec{y})] &= i\delta(\vec{x} - \vec{y}), \quad \{c, \Pi_c\} = i\delta(\vec{x} - \vec{y}), \quad \{\bar{c}, \Pi_{\bar{c}}\} = i\delta(\vec{x} - \vec{y}), \end{aligned}$$

where $[\cdot, \cdot]$ and $\{\cdot, \cdot\}$ are commutator and anti-commutator respectively.

Next, we perform the similarity transformation. We will not explicitly write the Legendre transformed auxiliary terms as we will see that the only terms affected by the similarity transformation are the terms involving scalar fields.

$$\mathcal{H} = \sum_{\alpha=1,2} \dot{\phi}_\alpha \Pi_{\phi_\alpha} + \dot{\phi}_\alpha^\dagger \Pi_{\phi_\alpha^\dagger} + \dot{A}_i \Pi_{A_i} + \dot{B} \Pi_B + \dot{c} \Pi_c + \dot{\bar{c}} \Pi_{\bar{c}} - \mathcal{L}_{\text{BRST}}. \quad (\text{D.4})$$

Where $\Pi_\phi = \delta\mathcal{L}_{\text{BRST}}/\delta\dot{\phi} = (D_0\phi)^\dagger = \partial_0\phi^\dagger + ie(A_0\phi)^\dagger$ and $\Pi_{\phi^\dagger} = \delta\mathcal{L}_{\text{BRST}}/\delta\dot{\phi}^\dagger = (D_0\phi) = \partial_0\phi - ie(A_0\phi)$. Rewriting the Lagrangian in term of the canonical momenta, we have

$$\begin{aligned} \mathcal{H} &= \sum_{\alpha=1,2} \left(\Pi_{\phi_\alpha^\dagger} + ieA_0\phi_\alpha \right) \Pi_{\phi_\alpha} + \left(\Pi_{\phi_\alpha} - ie(A_0\phi_\alpha)^\dagger \right) \Pi_{\phi_\alpha^\dagger} \quad (\text{D.5}) \\ &\quad - \left[\Pi_{\phi_\alpha^\dagger} \Pi_{\phi_\alpha} - V(\phi, \mathcal{F}) \right] \\ &= \sum_{\alpha=1,2} \Pi_{\phi_\alpha^\dagger} \Pi_{\phi_\alpha} + ie \left[(A_0\phi_\alpha) \Pi_{\phi_\alpha} - (A_0\phi_\alpha)^\dagger \Pi_{\phi_\alpha^\dagger} \right] + V(\phi) + U(\mathcal{F}), \end{aligned}$$

where \mathcal{F} represent the rest of the quantities such as A_i, B, Π_{A_i}, \dots . Recall from section 2.5 that the real compounds to the complex fields $\phi_i^k = (\varphi_i^k + i\chi_i^k)/\sqrt{2}$ and its corresponding conjugate momenta transforms under the similarity transformation by the Dyson map (2.165)

$$\varphi_1^k \rightarrow \varphi_1^k, \quad \varphi_2^k \rightarrow -i\varphi_2^k, \quad \chi_1^k \rightarrow \chi_1^k, \quad \chi_2^k \rightarrow -i\chi_2^k, \quad A_\mu \rightarrow A_\mu, \quad (\text{D.6})$$

$$\Pi_{\varphi_1^k} \rightarrow \Pi_{\varphi_1^k}, \quad \Pi_{\varphi_2^k} \rightarrow i\Pi_{\varphi_2^k}, \quad \Pi_{\chi_1^k} \rightarrow \Pi_{\chi_1^k}, \quad \Pi_{\chi_2^k} \rightarrow i\Pi_{\chi_2^k}. \quad (\text{D.7})$$

The above Hamiltonian (D.5) can be transformed with the Dyson map (2.165) by either defining a new Dyson map or by rewriting the conjugate momenta $\{\Pi_\phi, \Pi_{\phi^\dagger}\}$ in terms of the conjugate momenta of real components. The relation between two

sets of conjugate momenta can be found by using the identities

$$\frac{\delta(D_0\phi_i)^k}{\delta\varphi_j^l} = \frac{\delta(D_0\phi_i)^{*k}}{\delta\varphi_j^l} = \delta_{ij}\delta^{kl}, \quad \frac{\delta(D_0\phi_i)^k}{\delta\chi_j^l} = -\frac{\delta(D_0\phi_i)^{*k}}{\delta\chi_j^l} = i\delta_{ij}\delta^{kl}. \quad (\text{D.8})$$

Using these relations one can find

$$\Pi_\varphi = \frac{\delta\mathcal{L}}{\delta\dot{\varphi}_i^k} = \text{Re}(D_0\phi_i)^k, \quad \Pi_\chi = \frac{\delta\mathcal{L}}{\delta\dot{\chi}_i^k} = \text{Im}(D_0\phi_i)^k. \quad (\text{D.9})$$

Finally the conjugate momenta of complex field can be written as

$$\Pi_\phi = (D_0\phi)^\dagger = \text{Re}(D_0\phi) - i\text{Im}(D_0\phi) = \Pi_\varphi - i\Pi_\chi \quad (\text{D.10})$$

$$\Pi_{\phi^\dagger} = (D_0\phi) = \text{Re}(D_0\phi) + i\text{Im}(D_0\phi) = \Pi_\varphi + i\Pi_\chi \quad (\text{D.11})$$

The similarity transformation of the complex fields and its corresponding canonical momenta are

$$\phi_1 \rightarrow \phi_1, \quad \phi_2 \rightarrow -i\phi_2, \quad \phi_1^\dagger \rightarrow \phi_1^\dagger, \quad \phi_2^\dagger \rightarrow -i\phi_2^\dagger \quad (\text{D.12})$$

$$\Pi_{\phi_1} \rightarrow \Pi_{\phi_1}, \quad \Pi_{\phi_2} \rightarrow i\Pi_{\phi_2}, \quad \Pi_{\phi_1^\dagger} \rightarrow \Pi_{\phi_1^\dagger}, \quad \Pi_{\phi_2^\dagger} \rightarrow i\Pi_{\phi_2^\dagger} \quad (\text{D.13})$$

Performing these transformation to the Hamiltonian (D.5), we find

$$\mathcal{H} = \sum_{\alpha=1,2} (-1)^{\alpha+1} \Pi_{\phi_\alpha^\dagger} \Pi_{\phi_\alpha} + ie \left[(A_0\phi_\alpha) \Pi_{\phi_\alpha} - (A_0\phi_\alpha)^\dagger \Pi_{\phi_\alpha^\dagger} \right] + V(\phi) + U(\mathcal{F}),$$

Performing an inverse Legendre transformation, we obtain the real Lagrangian (2.167).

Next we will verify the similarity transformation shown in section 2.5.2. We will not explicitly consider auxiliary terms in the quantisation procedure as it will not affect the similarity transformation as demonstrated above. The Lagrangian takes the form

$$\mathcal{L} = \sum_{\alpha=1,2} \frac{1}{2} D_\mu \phi_\alpha D^\mu \phi_\alpha - V(\phi, A_\mu), \quad (\text{D.14})$$

where the covariant derivative is defined as $(D_\mu\phi_\alpha)^a = \partial_\mu\phi_\alpha^a + e\epsilon^{abc}A_\mu^b\phi_\alpha^c$. The conjugate momenta are defined as $\Pi_\alpha^a := \delta\mathcal{L}/\delta\dot{\phi}_\alpha^a = (D_0\phi_\alpha)^a$. Performing the Legendre

transformation, we find

$$\begin{aligned}
\mathcal{H} &= \sum_{\alpha=1,2} \dot{\phi}_\alpha^a \Pi_\alpha^a - \mathcal{L} & (D.15) \\
&= \sum_{\alpha=1,2} [(D_0 \phi_\alpha)^a - e(A_0 \times \phi_\alpha)^a] \Pi_\alpha^a - \frac{1}{2}(D_0 \phi_\alpha)^2 + \frac{1}{2}(D_i \phi_\alpha)^2 + V(\phi, A_\mu) \\
&= \sum_{\alpha=1,2} \Pi_\alpha^a \Pi_\alpha^a - e(A_0 \times \phi_\alpha)^a \Pi_\alpha^a + \frac{1}{2}(D_i \phi_\alpha)^2 + V(\phi, A_\mu).
\end{aligned}$$

The similarity transformation will only affect the ϕ_2 field and its corresponding conjugate momenta

$$\phi_2 \rightarrow -i\phi_2, \quad \Pi_2 \rightarrow i\Pi_2. \quad (D.16)$$

Therefore the Hamiltonian transforms as

$$\eta H \eta^{-1} = \sum_{\alpha=1,2} (-1)^{\alpha+1} \Pi_\alpha^a \Pi_\alpha^a - e(A_0 \times \phi_\alpha)^a \Pi_\alpha^a + \frac{1}{2}(D_i \phi_\alpha)^2 + V(\phi, A_\mu). \quad (D.17)$$

The inverse Legendre transformation will map this Hamiltonian to (2.204).

Bibliography

- [1] C. M. Bender and S. Boettcher. Real spectra in non-Hermitian Hamiltonians having \mathcal{PT} symmetry. *Phys. Rev. Lett.*, 80:5243–5246, 1998.
- [2] J. Goldstone. Field theories with superconductor solutions. *Il Nuovo Cimento (1955-1965)*, 19(1):154–164, 1961.
- [3] F. Englert and R. Brout. Broken symmetry and the mass of gauge vector mesons. *Phys. Rev. Lett.*, 13(9):321, 1964.
- [4] P. W. Higgs. Broken symmetries, massless particles and gauge fields. *Phys. Lett.*, 12:132–133, 1964.
- [5] P. W. Higgs. Broken symmetries and the masses of gauge bosons. *Phys. Rev. Lett.*, 13(16):508, 1964.
- [6] G. S. Guralnik, C. R. Hagen, and T. W. B. Kibble. Global conservation laws and massless particles. *Phys. Rev. Lett.*, 13(20):585, 1964.
- [7] A. Fring and T. Taira. Goldstone bosons in different \mathcal{PT} -regimes of non-Hermitian scalar quantum field theories. *Nucl. Phys. B*, 950:114834, 2020.
- [8] A. Fring and T. Taira. Pseudo-Hermitian approach to Goldstone’s theorem in non-Abelian non-Hermitian quantum field theories. *Phys. Rev. D*, 101(4):045014, 2020.
- [9] A. Fring and T. Taira. Massive gauge particles versus Goldstone bosons in non-Hermitian non-abelian gauge theory. *arXiv preprint arXiv:2004.00723*, 2020.
- [10] A. Fring and T. Taira. ’t Hooft-Polyakov monopoles in non-Hermitian quantum field theory. *Phys. Lett. B*, 807:135583, 2020.

- [11] A. Fring and T. Taira. Complex BPS solitons with real energies from duality. *J. Phys. A Mathe. Theor.*, 53(45):455701, 2020.
- [12] F. Correa, A. Fring, and T. Taira. Complex BPS Skyrmions with real energy. *Nuclear Physics B*, 971(2):115516, 10 2021.
- [13] H. J. Ettliger and P. A. B. Dirac. The principles of quantum mechanics. *The American Mathematical Monthly*, 38(9):524, 11 1931.
- [14] J. von Neumann. *Mathematical Foundations of Quantum Mechanics*. Princeton University Press, 12 2018.
- [15] G. Gamow. Zur Quantentheorie des Atomkernes. *Zeitschrift für Physik*, 51(3-4):204–212, 3 1928.
- [16] A. J. F. Siegert. On the derivation of the dispersion formula for nuclear reactions. *Phys. Rev*, 56(8):750–752, 10 1939.
- [17] R. E. Peierls. Complex eigenvalues in scattering theory. *Proc. R. Soc. Lond. A. Math. Phys. Sci*, 253(1272):16–36, 11 1959.
- [18] N. Hatano, T. Kawamoto, and J. Feinberg. Probabilistic interpretation of resonant states. *Pramana - J. Phys*, 73(3):553–564, 2009.
- [19] E. Wigner. Normal form of antiunitary operators. *J. Math. Phys.*, 1:409–413, 1960.
- [20] F. G. Scholtz, H. B. Geyer, and F.J.W. Hahne. Quasi-Hermitian operators in quantum mechanics and the variational principle. *Ann. Phys*, 213:74–101, 1992.
- [21] J. Dieudonné. Quasi-Hermitian operators. *Proceedings of the International Symposium on Linear Spaces, Jerusalem 1960, Pergamon, Oxford*, pages 115–122, 1961.
- [22] M. Froissart. Covariant formalism of a field with indefinite metric. *Il Nuovo Cimento*, 14:197–204, 1959.
- [23] F. J. Dyson. Thermodynamic behavior of an ideal ferromagnet. *Phys. Rev.*, 102:1230–1244, 1956.

- [24] T. Marumori, M. Yamamura, and A. Tokunaga. On the “anharmonic effects” on the collective oscillations in spherical even nuclei. I. *Prog. Theo. Phys*, 31(6):1009–1025, 6 1964.
- [25] S.T. Beliaev and V.G. Zelevinsky. Anharmonic effects of quadrupole oscillations of spherical nuclei. *Nucl. Phys*, 39(C):582–604, 12 1962.
- [26] D. Janssen, F. Dönau, S. Frauendorf, and R.V. Jolos. Boson description of collective states. *Nucl. Phys. A*, 172(1):145–165, 1971.
- [27] A. Mostafazadeh and S. Ozcelik. Explicit realization of pseudo-Hermitian and quasi-Hermitian quantum mechanics for two-level systems. *Turk. J. Phys*, 30(5):437–443, 7 2006.
- [28] M. Znojil and H. B. Geyer. Construction of a unique metric in quasi-Hermitian quantum mechanics: Nonexistence of the charge operator in a 2×2 matrix model. *Phys. Lett. B Nucl*, 640(1-2):52–56, 8 2006.
- [29] D. P. Musumbu, H. B. Geyer, and W. D. Heiss. Choice of a metric for the non-Hermitian oscillator. *J. Phys. A Math. Theo*, 40(2):F75–F80, 1 2007.
- [30] M. S. Swanson. Transition elements for a non-Hermitian quadratic Hamiltonian. *J. Math. Phys*, 45(2):585–601, 2 2004.
- [31] P. Dorey, C. Dunning, and R. Tateo. Spectral equivalences from Bethe ansatz equations. *J. Phys.*, A34:5679–5704, 2001.
- [32] C. M. Bender, D. C Brody, and H. F. Jones. Complex extension of quantum mechanics. *Phys. Rev. Lett.*, 89(27):270401, 2002.
- [33] A. Mostafazadeh. Pseudo-Hermiticity versus PT symmetry: The necessary condition for the reality of the spectrum of a non-Hermitian Hamiltonian. *J. Maths. Phys.*, 43:202–212, 2002.
- [34] J. von Neumann and E. P. Wigner. Über merkwürdige diskrete eigenwerte. In *The Collected Works of Eugene Paul Wigner*, pages 291–293. Springer, 1993.
- [35] T. Kato. Perturbation theory for linear operators. (*Springer, Berlin*), 1966.
- [36] W. D. Heiss and A. L. Sannino. Avoided level crossing and exceptional points. *J. Phys. A Math. Gen*, 23(7):1167, 1990.

- [37] I. Papadopoulos, P. Wagner, G. Wunner, and J. Main. Bose-Einstein condensates with attractive $1/r$ interaction: The case of self-trapping. *Phys. Rev. A*, 76(5):053604, 11 2007.
- [38] H. Cartarius, J. Main, and G. Wunner. Discovery of exceptional points in the Bose-Einstein condensation of gases with attractive $1/r$ interaction. *Phys. Rev. A*, 77(1):013618, 1 2008.
- [39] R. Lefebvre, O. Atabek, M. Šindelka, and N. Moiseyev. Resonance Coalescence in Molecular Photodissociation. *Phys. Rev. Lett*, 103(12):123003, 9 2009.
- [40] R. Lefebvre and O. Atabek. Exceptional points in multichannel resonance quantization. *Eur. Phys. J. D*, 56(3):317–324, 2 2010.
- [41] O. Atabek, R. Lefebvre, M. Lepers, A. Jaouadi, O. Dulieu, and V. Kokoouline. Proposal for a laser control of vibrational cooling in Na(2) using resonance coalescence. *Phys. rev. lett*, 106(17), 4 2011.
- [42] M. Liertzer, Li Ge, A. Cerjan, A. D. Stone, H. E. Türeci, and S. Rotter. Pump-induced exceptional points in lasers. *Phys. Rev. Lett*, 108(17):173901, 4 2012.
- [43] W. D. Heiss and A. L. Sannino. Transitional regions of finite Fermi systems and quantum chaos. *Phys. Rev. A*, 43(8):4159–4166, 4 1991.
- [44] F. Leyvraz and W. D. Heiss. Large N scaling behavior of the Lipkin-Meshkov-Glick model. *Phys. Rev. Lett*, 95(5):050402, 7 2005.
- [45] W D Heiss, F G Scholtz, and H B Geyer. The large N behaviour of the Lipkin model and exceptional points. *J. Phys. A Math. Gen*, 38(9):1843–1851, 2 2005.
- [46] P. Cejnar and M. Heinze, S. and Macek. Coulomb analogy for non-hermitian degeneracies near quantum phase transitions. *Phys. Rev. Lett*, 99(10):100601, 9 2007.
- [47] H. Qin, R. Zhang, A. S. Glasser, and J. Xiao. Kelvin-Helmholtz instability is the result of parity-time symmetry breaking. *Phys. Plasmas*, 26(3):032102, 3 2019.

- [48] C.E. Rüter, K.G. Makris, R. El-Ganainy, D.N. Christodoulides, M. Segev, and D. Kip. Observation of parity-time symmetry in optics. *Nat. phys.*, 6(3):192, 2010.
- [49] A. Guo, G. J. Salamo, D. Duchesne, R. Morandotti, M. Volatier-Ravat, V. Aimez, G. A. Siviloglou, and D.N. Christodoulides. Observation of \mathcal{PT} -symmetry breaking in complex optical potentials. *Phys. Rev. Lett.*, 103:093902(4), 2009.
- [50] R. El-Ganainy, K. G. Makris, D. N. Christodoulides, and Z. H. Musslimani. Theory of coupled optical \mathcal{PT} -symmetric structures. *Opt. Lett.*, 32(17):2632, 9 2007.
- [51] K. G. Makris, R. El-Ganainy, D. N. Christodoulides, and Z. H. Musslimani. Beam dynamics in \mathcal{PT} symmetric optical lattices. *Phys. Rev. Lett.*, 100(10):103904, 3 2008.
- [52] S. Klaiman, U. Günther, and N. Moiseyev. Visualization of branch points in \mathcal{PT} -symmetric waveguides. *Phys. Rev. Lett.*, 101(8):080402, 8 2008.
- [53] S. Longhi. Bloch oscillations in complex crystals with \mathcal{PT} symmetry. *Phys. Rev. Lett.*, 103(12):123601, 9 2009.
- [54] C. M. Bender, K. A. Milton, and V. M. Savage. Solution of Schwinger-Dyson equations for \mathcal{PT} -symmetric quantum field theory. *Phys. Rev. D*, 62(8):085001, 2000.
- [55] C. M. Bender, D. C. Brody, and H. F. Jones. Extension of \mathcal{PT} -symmetric quantum mechanics to quantum field theory with cubic interaction. *Phys. Rev.*, D70:025001(19), 2004.
- [56] C. M. Bender, S. F. Brandt, J. Chen, and Q Wang. The \mathcal{C} operator in \mathcal{PT} -symmetric quantum field theory transforms as a Lorentz scalar. *Phys. Rev.*, D71:065010, 2005.
- [57] C. M. Bender, V. Branchina, and E. Messina. Critical behavior of the \mathcal{PT} -symmetric $i\phi^3$ quantum field theory. *Phys. Rev. D*, 87(8):085029, 2013.
- [58] A. M Shalaby. Vacuum structure and \mathcal{PT} -symmetry breaking of the non-hermetian $i\phi^3$ theory. *Phys. Rev. D*, 96(2):025015, 2017.

- [59] C. M. Bender, D. C. Brody, and H. F. Jones. Scalar quantum field theory with a complex cubic interaction. *Phys. Rev. Lett*, 93(25):1–4, 2004.
- [60] H. F. Jones and R. J. Rivers. Which Green functions does the path integral for quasi-Hermitian Hamiltonians represent? *Phys. Lett. A Gen. At. Solid State Phys*, 2009.
- [61] C. M. Bender, V. Branchina, and E. Messina. Ordinary versus \mathcal{PT} -symmetric ϕ^3 quantum field theory. *Phys. Rev. D*, 85(8):085001, 1 2012.
- [62] A. M. Shalaby. Effective Action study of \mathcal{PT} -Symmetry Breaking for the non-Hermitian $(i\phi^3)_{6-\epsilon}$ Theory and The Yang-Lee Edge Singularity. *Int. J. Mod. Phys. A*, 34(17):1950090, 10 2018.
- [63] A. M. Shalaby. Extrapolating the precision of the hypergeometric resummation to strong couplings with application to the \mathcal{PT} -symmetric $i\phi^3$ field theory. *Int. J. Mod. Phys. A*, 35(08):2050041, 3 2020.
- [64] O. O. Novikov. Scattering in pseudo-Hermitian quantum field theory and causality violation. *Phys. Rev. D*, 99(6):65008, 2019.
- [65] A. Dwivedi and B. P. Mandal. 2-Loop β Function for Non-Hermitian \mathcal{PT} Symmetric $i\phi^3$ Theory. *arXiv*, 12 2019.
- [66] A. Dwivedi and B. P. Mandal. Higher loop β function for non-Hermitian \mathcal{PT} symmetric $i\phi^3$ theory. *Ann. Phys*, 425:168382, 2 2021.
- [67] C. M. Bender, P. N. Meisinger, and H. Yang. Calculation of the one-point Green's function for a $-g\varphi^4$ quantum field theory. *Phys. Rev. D*, 63(4):045001, 1 2001.
- [68] H. F. Jones, J. Mateo, and R. J. Rivers. Path-integral derivation of the anomaly for the Hermitian equivalent of the complex \mathcal{PT} -symmetric quartic Hamiltonian. *Phys. Rev. D*, 74(12):125022, 12 2006.
- [69] H. F. Jones and R. J. Rivers. The disappearing Q operator. *Phys. Rev. D*, 75(2):025023, 12 2006.
- [70] A. Shalaby and S. S. Al-Thoyaib. Non-perturbative tests for the asymptotic freedom in the \mathcal{PT} -symmetric $(-\phi^4)_{3+1}$ theory. *Phys. Rev. D*, 82(8):085013, 1 2009.

- [71] H. F. Jones. Green Functions for the wrong-sign quartic. *Int. J. Theo. Phys*, 50(4):1071–1080, 4 2011.
- [72] C. M. Bender, V. Branchina, and E. Messina. \mathcal{PT} -symmetric φ^4 theory in $d = 0$ dimensions. *arXiv preprint arXiv:1501.00514*, 2015.
- [73] K. Symanzik. Small-distance-behaviour analysis and Wilson expansions. *Comm. Math. Phys.*, 23(1):49–86, 3 1971.
- [74] J. Alexandre and C. M. Bender. Foldy-Wouthuysen transformation for non-Hermitian Hamiltonians. *J. of Phys, A: Math, and Theor.*, 48(18):185403, 2015.
- [75] C. M. Bender, H. F. Jones, and R. J. Rivers. Dual \mathcal{PT} -symmetric quantum field theories. *Phys. Lett.*, B625:333–340, 2005.
- [76] R. J. Rivers. Path integrals for pseudo-Hermitian Hamiltonians. *Int. J. Theor. Phys*, 50(4):1081–1096, 4 2011.
- [77] J. Alexandre, P. Millington, and D. Seynaeve. Symmetries and conservation laws in non-Hermitian field theories. *Phys. Rev. D*, 96(6):065027, 9 2017.
- [78] J. Alexandre, J. Ellis, P. Millington, and D. Seynaeve. Spontaneous symmetry breaking and the Goldstone theorem in non-Hermitian field theories. *Phys. Rev. D*, 98:045001, 2018.
- [79] P. D. Mannheim. Goldstone bosons and the Englert-Brout-Higgs mechanism in non-Hermitian theories. *Phys. Rev. D*, 99(4):045006, 2019.
- [80] P. Millington. Symmetry properties of non-Hermitian \mathcal{PT} -symmetric quantum field theories. *J. Phys. Conf. Ser.*, 1586(1):012001, 2020.
- [81] J. Alexandre, J. Ellis, P. Millington, and D. Seynaeve. Spontaneously breaking non-Abelian gauge symmetry in non-Hermitian field theories. *Phys. Rev. D*, 101(3):035008, 2020.
- [82] J. Alexandre, J. Ellis, P. Millington, and D. Seynaeve. Gauge invariance and the Englert-Brout-Higgs mechanism in non-Hermitian field theories. *Phys. Rev. D*, 99(7):075024, 2019.

- [83] J. Alexandre, J. Ellis, and P. Millington. Discrete spacetime symmetries and particle mixing in non-Hermitian scalar quantum field theories. *Phys. Rev. D*, 102(12):125030, 2020.
- [84] J. Alexandre, J. Ellis, and P. Millington. \mathcal{PT} -Symmetric non-Hermitian quantum field theories with supersymmetry. *Phys. Rev. D*, 101(8):085015, 1 2020.
- [85] C. M. Bender and K. A. Milton. A non-unitary version of massless quantum electrodynamics possessing a critical point. *J. Phys. A. Math. Gen.*, 32(7):L87, 1999.
- [86] J. Alexandre, C. M. Bender, and P. Millington. Non-Hermitian extension of gauge theories and implications for neutrino physics. *J. High. Energy. Phys*, 2015(11):111, 2015.
- [87] J. Alexandre, C. M. Bender, and P. Millington. Light neutrino masses from a non-Hermitian Yukawa theory. *J. Phys. Conf. Ser*, 873(1):012047, 2017.
- [88] J. Alexandre, P. Millington, and D. Seynaeve. Consistent description of field theories with non-Hermitian mass terms. In *J. Phys. Conf. Ser*, volume 952, page 012012, 2018.
- [89] M. C. Medina, L. and Ogilvie, M. A. Schindler, and S. T. Schindler. Universality of pattern formation. *Phys. Rev. D*, 102(11):114510, 6 2019.
- [90] H. Raval and B. P. Mandal. Deconfinement to confinement as \mathcal{PT} phase transition. *Nucl. Phys. B*, 946:114699, 2019.
- [91] V. E. Rochev. Hermitian vs \mathcal{PT} -symmetric scalar Yukawa model. *J. Mod. Phys*, 07(09):899–907, 12 2015.
- [92] A. Beygi, S. P. Klevansky, and C. M. Bender. Relativistic \mathcal{PT} -symmetric Fermionic theories in $1 + 1$ and $3 + 1$ dimensions. *Phys. Rev. A*, 99(6):1–16, 2019.
- [93] J. Alexandre, N. E Mavromatos, and A. Soto. Dynamical Majorana neutrino masses and axions I. *Nucl. Phys. B*, 961:115212, 12 2020.
- [94] M. N. Chernodub, A. Cortijo, and M. Ruggieri. Spontaneous non-Hermiticity in Nambu–Jona-Lasinio model. *arXiv preprint arXiv:2008.11629*, 2020.

- [95] A. Felski, A. Beygi, and S. P. Klevansky. Non-Hermitian extension of the Nambu-Jona-Lasinio model in $3 + 1$ and $1 + 1$ dimensions. *Phys. Rev. D*, 101(11):1–10, 4 2020.
- [96] J. Alexandre and N. E. Mavromatos. On the consistency of a non-Hermitian Yukawa interaction. *Phys. Lett. B*, 807(3):135562, 8 2020.
- [97] T. Kanazawa. Non-Hermitian BCS-BEC crossover of Dirac Fermions. *J. High. Energy. Phys*, 2021(3):1–21, 2021.
- [98] A. Felski and S. P. Klevansky. Fermion and meson mass generation in non-Hermitian Nambu-Jona-Lasinio models. *Phys. Rev. D*, 103(5):056007, 3 2021.
- [99] T. D. Lee. Some special examples in renormalizable field theory. *Phys. Rev*, 95(5):1329–1334, 9 1954.
- [100] C. M. Bender, S. F. Brandt, J. Chen, and Q. Wang. Ghost busting: \mathcal{PT} -symmetric interpretation of the Lee model. *Phys. Rev.*, D71:025014, 2005.
- [101] A. M. Shalaby. Possible treatment of the ghost states in the Lee-Wick standard model. *Phys. Rev. D*, 80(2):025006, 7 2009.
- [102] P. D. Mannheim. Ghost problems from Pauli–Villars to fourth-order quantum gravity and their resolution. *Int. J. Mod. Phys. D*, (i):2043009, 9 2020.
- [103] B. Paul, H. Dhar, and B. Saha. Ghosts in higher derivative Maxwell-Chern-Simon’s theory and \mathcal{PT} -symmetry. *Phys. Lett. B*, 808:135671, 2020.
- [104] C. M. Bender, P. E. Dorey, C. Dunning, A. Fring, D. W. Hook, H. F. Jones, S. Kuzhel, G. Levai, and R. Tateo. *\mathcal{PT} Symmetry: In quantum and classical physics*. World Scientific, Singapore, 2019.
- [105] K. B. Datta. *Matrix and linear algebra*. Prentice-Hall of India New Delhi, India, 1991.
- [106] P. D. Mannheim. Antilinearity rather than Hermiticity as a guiding principle for quantum theory. *J. Phys. A. Math. Theor*, 51:315302(58), 2018.
- [107] Y. Nambu and G. Jona-Lasinio. Dynamical model of elementary particles based on an analogy with superconductivity. II. *Phys. Rev.*, 124(1):246, 1961.

- [108] S. Weigert. Completeness and orthonormality in \mathcal{PT} -symmetric quantum systems. *Phys. Rev. A*, 68(6):062111, 2003.
- [109] C. M. Bender and S. P. Klevansky. Nonunique \mathcal{C} operator in \mathcal{PT} quantum mechanics. *Phys. Lett. A*, 373(31):2670–2674, 2009.
- [110] A. Mostafazadeh. Pseudo-Hermiticity and generalized \mathcal{PT} - and \mathcal{CPT} -symmetries. *J. Math. Phys.*, 44:974–989, 2003.
- [111] A. Mostafazadeh. Pseudo-Hermitian representation of quantum mechanics. *Int. J. Geom. Meth. Mod. Phys.*, 7:1191–1306, 2010.
- [112] T. Frith. Time-dependence in non-Hermitian quantum systems. *arXiv:2002.01977, PhD Thesis, City, University of London*, 2019.
- [113] L. D. Landau. On the theory of phase transitions. *Ukr. J. Phys.*, 11:19–32, 1937.
- [114] T. Goldzak, A. A. Mailybaev, and N. Moiseyev. Light stops at exceptional points. *Phys. Rev. Lett.*, 120(1):013901, 2018.
- [115] M. Miri and A. Alu. Exceptional points in optics and photonics. *Science*, 363(6422), 2019.
- [116] A. Fring. \mathcal{PT} -Symmetric deformations of the Korteweg-de Vries equation. *J. Phys. A*, 40:4215–4224, 2007.
- [117] P Goddard and D. I. Olive. Magnetic monopoles in gauge field theories. *Rep. Prog. Phys*, 41(9):1357, 1978.
- [118] E. Corrigan, D. I. Olive, D. B. Fairlie, and J. Nuyts. Magnetic monopoles in $su(3)$ gauge theories. *Nucl. Phys. B*, 106:475–492, 1976.
- [119] M. K. Prasad and C. M. Sommerfield. Exact classical solution for the 't Hooft monopole and the Julia-Zee dyon. *Phys. Rev. Lett*, 35(12):760, 1975.
- [120] J. Arafune, P. G. O. Freund, and C. J. Goebel. Topology of Higgs fields. *J. Math. Phys*, 16(2):433–437, 1975.
- [121] E. B. Bogomolny. The stability of classical solutions. *Sov. J. Nucl. Phys. (Engl. Transl.); (United States)*, 24(4), 1976.

- [122] T. W. Kirkman and C. K. Zachos. Asymptotic analysis of the monopole structure. *Phys. Rev. D*, 24(4):999, 1981.
- [123] C. Adam, L. A. Ferreira, E. da Hora, A. Wereszczynski, and W. J. Zakrzewski. Some aspects of self-duality and generalised BPS theories. *J. High. Energy Phys*, 2013(8):62, 2013.
- [124] A. Cavaglia, A. Fring, and B. Bagchi. \mathcal{PT} -symmetry breaking in complex nonlinear wave equations and their deformations. *J. Phys. A*, 44:325201(42), 2011.
- [125] J. Cen and A. Fring. Complex solitons with real energies. *J. Phys. A: Math. Theor.*, 49(36):365202, 2016.
- [126] J. Cen, F. Correa, and A. Fring. Time-delay and reality conditions for complex solitons. *J. Math. Phys.*, 58(3):032901, 2017.
- [127] P. Kumar, A. Khare, and A. Saxena. A model field theory with $(\psi \ln \psi)^2$ potential: Kinks with super-exponential profiles. *arXiv preprint arXiv:1908.04978*, 2019.
- [128] D. Arrowsmith and C. M. Place. *Dynamical systems: differential equations, maps, and chaotic behaviour*, volume 5. CRC Press, 1992.
- [129] L. A. Ferreira, P. Klimas, A. Wereszczyński, and W. J. Zakrzewski. Some comments on BPS systems. *J. Phys. A Math. Theor.*, 52(31):315201, 2019.
- [130] W. D. Heiss. The physics of exceptional points. *J. Phys. A. Math. Theor*, 45(44):444016, 2012.
- [131] C. Adam, J. Sanchez-Guillen, and A. Wereszczyński. A Skyrme-type proposal for baryonic matter. *Phys. Lett. B*, 691(2):105–110, 2010.
- [132] C Adam, C Naya, J Sanchez-Guillen, R Vazquez, and A Wereszczyński. The Skyrme model in the BPS limit. In *The Multifaceted Skyrmion*, pages 193–232. World Scientific, 2017.
- [133] C. J. Houghton, N. S. Manton, and P. M. Sutcliffe. Rational maps, monopoles and Skyrmions. *Nucl. Phys. B*, 510(3):507–537, 1998.

- [134] E. Witten. Current algebra, baryons, and quark confinement. *Nucl. Phys. B*, 223:433–444, 1983.
- [135] T. H. R. Skyrme. A unified field theory of mesons and baryons. *Nucl. Phys.*, 31:556–569, 1962.
- [136] S. B. Gudnason. Exploring the generalized loosely bound Skyrme model. *Phys. Rev. D*, 98(9):096018, 2018.
- [137] C. Adam, K. Oles, and A. Wereszczynski. The dielectric Skyrme model. *Phys. Lett. B*, 807:135560, 2020.
- [138] P. Rosenau and J. M. Hyman. Compactons: Solitons with finite wavelength. *Phys. Rev. Lett.*, 70(5):564–567, 1993.
- [139] E. Bonenfant and L. Marleau. Nuclei as near BPS Skyrmons. *Phys. Rev. D*, 82(5):054023, 2010.
- [140] C. Adam, J. Sanchez-Guillen, and A. Wereszczynski. BPS submodels of the Skyrme model. *Phys. Lett. B*, 769:362–367, 2017.
- [141] F Bagarello and J. Feinberg. Bicoherent-state path integral quantization of a non-hermitian hamiltonian. *Ann. Phys*, 422:168313, 2020.
- [142] N. D. Mermin and H. Wagner. Absence of ferromagnetism or antiferromagnetism in one-or two-dimensional isotropic Heisenberg models. *Phys. Rev. Lett*, 17(22):1133, 1966.
- [143] C. Adam, C. Naya, J. Sanchez-Guillen, and A. Wereszczynski. Bogomolnyi-Prasad-Sommerfield Skyrme model and nuclear binding energies. *Phys. Rev. Lett.*, 111(23):232501, 2013.
- [144] L. A. Ferreira and L. R. Livramento. A false vacuum skyrme model for nuclear matter. *arXiv preprint arXiv:2106.13335*, 2021.
- [145] G. H. Derrick. Comments on nonlinear wave equations as models for elementary particles. *J. Math. Phys*, 5(9):1252–1254, 1964.
- [146] M Nakahara. *Geometry, topology and physics*. CRC press, 2018.